Future changes and signal analyses of climate means and extremes in the Mediterranean Area deduced from a CMIP3 multi-model ensemble

vorgelegt von

Gernot Vogt

aus München

Würzburg, Januar 2014

"Viewed from the distance of the moon, the astonishing thing about the earth, catching the breath, is that it is alive. The photographs show the dry, pounded surface of the moon in the foreground, dead as an old bone. Aloft, floating free beneath the moist, gleaming membrane of bright blue sky, is the rising earth, the only exuberant thing in this part of the cosmos. If you could look long enough, you would see the swirling of the great drifts of white cloud, covering and uncovering the half-hidden masses of land. If you had been looking for a very long, geologic time, you could have seen the continents themselves in motion, drifting apart on their crustal plates, held afloat by the fire beneath. It has the organized, self-contained look of a live creature, full of information, marvelously skilled in handling the sun. "

"Wenn man die Erde vom Mond aus betrachtet, ist das Erstaunliche, ja Atemberaubende, dass es dort Leben gibt. Die Aufnahmen zeigen im Vordergrund die trockene zerfurchte Mondoberfläche, die völlig tot wirkt. Darüber steigt die Erde empor: Sie schwebt zwischen der feuchten, glänzenden Membran des hellblauen Himmels, das einzige in diesem Teil des Kosmos, das den Betrachter in Hochstimmung versetzt. Wenn man lang genug hinschauen könnte, würde man das Gewirbel der großen, breiten Wolkenbänder sehen, die die halb verborgenen Landmassen verdecken und wieder enthüllen. Hätte man einen langen geologischen Zeitraum hingeschaut, hätte man erkennen können, wie die Kontinente sich bewegen und – während das Feuer darunter sie oben hält – auf ihren Krustenplatten auseinander treiben. Die Erde hat das zufriedene Antlitz eines Lebewesens, das sehr viel weiß und großen Geschick im Umgang mit der Sonne besitzt."

Lewis Thomas, (1974), *The lives of a cell*

Abstract

Considering its social, economic and natural conditions the Mediterranean Area is a highly vulnerable region by designated affections of climate change. Furthermore, its climatic characteristics are subordinated to high natural variability and are steered by various elements, leading to strong seasonal alterations. Additionally, General Circulation Models project compelling trends in specific climate variables within this region. These circumstances recommend this region for the scientific analyses conducted within this study. Based on the data of the CMIP3 database, the fundamental aim of this study is a detailed investigation of the total variability and the accompanied uncertainty, which superpose these trends, in the projections of temperature, precipitation and sea-level pressure by GCMs and their specific realizations. Special focus in the whole study is dedicated to the German model ECHAM5/MPI-OM. Following this ambition detailed trends and mean values are calculated and displayed for meaningful time periods and compared to reanalysis data of ERA40 and NCEP. To provide quantitative comparison the mentioned data are interpolated to a common 3x3° grid.

The total amount of variability is separated in its contributors by the application of an Analysis of Variance (ANOVA). For individual GCMs and their ensemble-members this is done with the application of a 1-way ANOVA, separating a treatment common to all ensemble-members and variability perturbating the signal given by different initial conditions. With the 2-way ANOVA the projections of numerous models and their realizations are analysed and the total amount of variability is separated into a common treatment effect, a linear bias between the models, an interaction coefficient and the residuals.

By doing this, the study is fulfilled in a very detailed approach, by considering yearly and seasonal variations in various reasonable time periods of 1961-2000 to match up with the reanalysis data, from 1961-2050 to provide a transient time period, 2001-2098 with exclusive regard on future simulations and 1901-2098 to comprise a time period of maximum length. The statistical analyses are conducted for regional-averages on the one hand and with respect to individual grid-cells on the other hand. For each of these applications the SRES scenarios of A1B, A2 and B1 are utilized. Furthermore, the spatial approach of the ANOVA is substituted by a temporal approach detecting the temporal development of individual variables. Additionally, an attempt is made to enlarge the signal by applying selected statistical methods.

In the detailed investigation it becomes evident, that the different parameters (i.e. length of temporal period, geographic location, climate variable, season, scenarios, models, etc…) have compelling impact on the results, either in enforcing or weakening them by different combinations. This holds on the one hand for the means and trends but also on the other hand for the contributions of the variabilities affecting the uncertainty and the signal. While temperature is a climate variable showing strong signals across these parameters, for

precipitation mainly the noise comes to the fore, while for sea-level pressure a more differentiated result manifests. In turn, this recommends the distinguished consideration of the individual parameters in climate impact studies and processes in model generation, as the affecting parameters also provide information about the linkage within the system.

Finally, an investigation of extreme precipitation is conducted, implementing the variables of the total amount of heavy precipitation, the frequency of heavy-precipitation events, the percentage of this heavy precipitation to overall precipitation and the mean daily intensity from events of heavy precipitation. Each time heavy precipitation is defined to exceed the 95th percentile of overall precipitation. Consecutively mean values of these variables are displayed for ECHAM5/MPI-OM and the multi-model mean and climate sensitivities, by means of their difference between their average of the past period of 1981-2000 and the average of one of the future periods of 2046-2065 or 2081-2100. Following this investigation again an ANOVA is conducted providing a quantitative measurement of the severity of change of trends in heavy precipitation across several GCMs.

Besides it is a difficult task to account for extreme precipitation by GCMs, it is noteworthy that the investigated models differ highly in their projections, resulting partially in a more smoothed and meaningful multi-model mean. Seasonal alterations of the strength of this behaviour are quantitatively supported by the ANOVA.

Kurzzusammenfassung

Bezüglich seiner sozialen, wirtschaftlichen und natürlichen Gegebenheiten ist der Mittelmeerraum eine Region, die in Anbetracht des zu erwartenden Klimawandels äußerst anfällig ist. Seine klimatischen Eigenschaften sind hoher natürlicher Variabilität, unterschiedlichen Antriebsmechanismen, sowie einer starken saisonalen Schwankung unterworfen. Zudem projizieren Globale Zirkulationsmodelle für diese Region aussagekräftige Trends für ausgewählte Klimavariablen. Diese Vorraussetzungen machen den Mittelmeerraum zu einem hervorragenden Studienobjekt für diese wissenschaftliche Arbeit. Auf der Basis der CMIP3 Datenbank ist das zu Grunde liegende Ziel dieser Arbeit eine detaillierte Untersuchung der Gesamtvariabilität und der damit einhergehenden Unsicherheit, die in den Projektionen der Globalen Zirkulationsmodelle und deren einzelnen Realisationen die Trends der Variablen Temperatur, Niederschlag und Druck überlagert. Besonderes Augenmerk liegt dabei auf dem deutschen Modell ECHAM5/MPI-OM. Für dieses Ziel werden Trends und Mittelwerte für aussagekräftige Zeitperioden berechnet und graphisch den Reanalysedatensätzen NCEP und ERA40 gegenübergestellt. Um quantitative Vergleiche zu ermöglichen werden die angesprochenen Datensätze auf ein gemeinsames geographisches Gitter von 3x3° interpoliert.

Der Gesamtanteil der Variabilität wird in seine Entstehungsquellen durch die Anwendung einer Varianzanalyse (ANOVA) aufgeteilt. Dies wird mit einer 1-Wege Varianzanalyse für einzelne Globale Zirkulationsmodelle und ihre Realisationen durchgeführt, wobei ein Anteil dem Signal entspricht, das in allen Realisationen vorhanden ist und ein Anteil dem Rauschen zugeordnet werden kann, das das Signal überlagert und unterschiedlichen Anfangsbedingungen des Modells geschuldet ist. Durch eine 2-Wege Varianzanalyse werden die unterschiedlichen Realisationen mehrerer Klimamodelle in eine Analyse eingebunden, wobei der Anteil der Gesamtvariabilität wiederum in einen gemeinsamen Signalanteil, einem Anteil des linearen Unterschieds zwischen den verschiedenen Klimamodellen, einem Interaktionskoeffizient und dem Rauschen aufgeteilt werden.

Die Anwendung dieser Verfahren wird detailliert ausgeführt, indem die Analysen auf jährlicher und saisonaler Grundlage für unterschiedliche Zeitperioden, nämlich 1961-1990 für den Vergleich mit den Reanalysedatensätzen, 1961-2050 als eine Übergangsperiode zwischen den Szenarien, 2001-2098 als reinen zukünftigen Betrachtungszeitraum und 1901-2098 um eine maximal umfassende Zeitperiode zu erhalten, betrachtet werden. Die statistischen Verfahren werden sowohl für regionale Mittelwerte als auch für einzelne Gitterpunkte berechnet. Für jede dieser Berechnungen werden die SRES Szenarien A1B, A2 und B1 herangezogen. Zudem wird der räumliche Ansatz der ANOVA ebenso durch einen zeitlichen ersetzt, wodurch die zeitliche Entwicklung der einzelnen Variabilitäten dargestellt wird. Des Weiteren wird durch gezielte statistische Methoden versucht, künstlich verstärkte Signale zu detektieren.

Durch die detaillierte Untersuchung wird offenkundig, dass die unterschiedlichen Randbedingungen (hier die Länge der Zeitperiode, der geographische Ort, die Bezugsvariable, die Saison, das Szenario, das Modell, etc…) eine entscheidende Rolle für das Ergebnis spielen, indem sie einerseits durch deren unterschiedlicher Kombination es sowohl verstärken als auch glätten können. Dies gilt sowohl für die Mittelwerte und die Trends als auch für die unterschiedlichen Partitionen der Variabilitäten, die wiederum die Unsicherheiten und das Signal beeinflussen. Während Temperatur starke Signale über alle dieser Randbedingungen aufweist, so zeigt sich für Niederschlag hauptsächlich ein starkes Rauschen, während für Druck eine sehr ambivalente Verteilung hervortritt. Dies wiederum beweist, dass dieser differenzierte Ansatz bezüglich der Betrachtung der Abhängigkeit dieser Randebedingungen unabdinglich in Klimafolgestudien und der Modellentwicklung ist, da diese Bedingungen auch Informationen über die Wechselbeziehungen im System beinhalten.

Schließlich wird noch die Entwicklung von Extremereignissen hinsichtlich der Niederschlagsmengen von Extremereignissen, der Häufigkeit der Ereignisse von extremen Niederschlagsmengen, dem prozentualen Anteil der Niederschlagsmenge aus Extremereignissen zu der Gesamtniederschlagsmenge und der mittleren täglichen Intensität von Niederschlagsextremereignissen untersucht. Hierbei wird ein Extremereignis als ein Ereignis definiert, das in seiner Menge oberhalb des 95.Perzentils der Menge der Gesamtereignisse liegt. So werden Mittelwerte dieser Variablen für ECHAM5/MPI-OM und über alle Modelle sowie deren Veränderungen zwischen ihren Mittelwerten aus den Zeiträumen der Vergangenheit 1981-2000 und den zukünftigen Perioden von 2046-2065 oder 2081-2100 gezeigt. Der Struktur dieser Studie folgend, wird wiederum eine ANOVA angewendet um eine quantitative Ermessung der Stärke der Veränderung im Erscheinungsbild von Extremniederschlagsereignissen über eine Vielzahl verschiedener Zirkulationsmodelle zu gewinnen.

Ungeachtet der schwierigen Tatsache, Extremniederschlagsereignisse aus GCMs abzuleiten, ist es erwähnenswert, dass die betrachteten Modelle stark in ihren Projektionen abweichen, was wiederum zu einem in einem gemäßigten und aussagekräftigerem Multi-Modell Mittelwert führt. Saisonale Unterschiede in diesem Verhalten können durch die ANOVA quantitativ belegt werden.

Table of Contents

List of Tables

List of Figures

List of Acronyms

ANOVA   Analysis of variance

AMO   Atlantic Multidecadal Oscillation

AOGCM   (coupled) Atmosphere-Ocean General Circulation Model

CMIP3   Coupled Model Intercomparison Project (phase 3)

DFG   Deutsche Forschungsgemeinschaft

EA   East Atlantic Pattern

EA/WR   East Atlantic/West Russian Pattern

ECMWF   European Centre for Medium-Range Weather Forecasts

EMP   Eastern Mediterranean Pattern

ENSO   El-Nino Southern Oscillation

GCM   General Circulation Model

GHG   Green House Gas

IPCC   Intergovernmental Panel on Climate Change

ITCZ   Intertropical Convergence Zone

KLIWEX-MED   Klimawandel und Extremereignisse im Mediterranen Großraum

MA   Mediterranean Area

NAO   North Atlantic Oscillation

NCAR   National Center for Atmospheric Research

NCEP   National Centers for Environment and Prediction

OECD   Organisation for Economic Cooperation and Development

PCMDI   Program for Climate Model Diagnosis and Intercomparison

PNA   Pacific North American Pattern

RCM   Regional Climate Model

SAM   South Asian Monsoon

SCAND   Scandinavian Pattern

SRES   Synthesis Report on Emission Scenarios

SST   Sea-surface temperature

SS   Sum-of-Squares

1   Introduction

Recent discussions of climate change stir mankind as one of the leading global controversies. Following the definition that climate change is reffering to a „..change in the state of the climate that can be identified (e.g., by using statistical tests) by changes in the mean and/or the variability of its properties and that persists for an extended period, typically decades or longer..." (IPCC 2012), the mentioned debate exhibits questions of the strength and range of the effects of climate change. Furthermore, it depicts the nature of the effects, the time period within these effects take place and finally also the spatially difference in the experience of future changes. Still, some sceptics and lobbyists declare conspiracies and challenge climate change in total, though the debated climate change is nearly completely proved and reasonable. So, the 4th IPCC (**I**ntergovernmental **P**anel on **C**limate **C**hange) assessment report propose the statement in 2007 that it is even „very likely that it [*the global climate change of the past 50years]* is not due to known natural causes alone". Besides, it is not the aim to find final evidences of climate changes in this study, it aims at a quantifying comparison of different climate simulations in a specific area.

1.1   Preface

The issue of climate change is relevant all over the globe. Nevertheless, GIORGI notes (2002a, p. 675): „Understanding and quantifying climatic changes at the regional scale is one of the most important and uncertain issues within the global change debate". This statement hits the main characteristic of the study at hand, comprising two fundamental aims.

As one should provide quantitative findings among the issue climate change, first of all the accompanying uncertainties have to be considered, quantified itself and consecutively accounted for in the final outcome of a changing climate. Thus, the first aim of this work is a detailed analysis and quantification of uncertainties, arousing by the employment of several **G**eneral **C**irculation **M**odels (GCMs), their specific realizations and their differences to each other. Though, GCMs are treated as old-fashioned in many scientific communities it must not be forgotten that GCMs still provide the groundwork for all downscaling assessments and uniquely encompass the whole globe in their simulations and projections with its energy and mass balances, disregarding the relative crude resolutions.

The second aim is the accompanying elucidation of projected climate change in a specific region of subcontinental scale. Two main reasons recommend the **M**editerranean **A**rea (MA) as area of investigation for this study. One motivation is provided by the scientific frame which already allocates huge expertise developed by several recent and ongoing research programmes and projetcs allowing advanced scientific exchange on the one hand. Nevertheless, the MA has not been in the climate research focus in the last century, as it was supposed to be (ULBRICH et al. 2006, GIORGI & LIONELLO 2008).

Furthermore many studies have only been conducted with an average assessment of the whole MA (e.g. GIORGI & MEARNS 2002, GIORGI 2002a, GIORGI 2002b) and/or without seasonal assessments or with focus on a particular meaningful season (TRIGO et al. 2006), whereat the different seasons exhibit strong differences. Still there are strong uncertainties in the projection of future courses of the Mediterranean climate. Accompanying more recent projects the underlying study aims to reveal spatially and temporally more detailed findings. Furthermore the opportunity was afforded to conduct the study at hand as a part of a comprehensive challenge to quantify the uncertainties of future climate projections. In this frame further studies accompany the underlying one, which have been accomplished using regional climate models or diverse assessments of statistical downscaling. The underlying study shall fit to the ones mentioned and complete this comprising approach by setting up an investigation across several GCMs developed by the the fittest climate institutions on the globe.

The second reason justifying the establishment of the MA as region of investigation accounts for its characteristics itself. Thus, when considering its specific social, economic and natural conditions and their highly interacting connections the MA may be one of the most interesting regions on earth in the sense of its behaviour to a designated global change. Furthermore in various former scientific results the MA is highlighted as so-called „hotspot" in terms of a climate change (GIORGI 2006). Still, particularly from the point of view from natural sciences the MA is uniquely, which will be discussed below. And finally some antecedent considerations lead to the conclusion that the climate change in the MA might offer a robust predictability concerning the signal or trend of change in relation to its uncertainties, whereat this topic shall be stressed in the latter chapters. The underlying study is embedded in a **D**eutsche **F**orschungs**g**emeinschaft (DFG) funded project called „**Kli**ma**w**andel und **Ex**tremereignisse im **Med**iterranen Großraum" (KLIWEX-MED) conducted by an equitable collaboration of the Institute for Geography at the University of Augsburg and the Institute for Geography and Geology at the University of Würzburg.

To put these aims into practice the study starts with two introducing chapters providing the groundwork for further progress by giving a short overview of the climatologic background in the MA at first and afterwards a discussion follows about the benefit derived from the usage of GCMs, while their advantages and shortcomings are pointed out in a description of their structures and operation principles. These chapters provide the essential tools for the subsequent interpretation of the mean values and trends in chapter 4. The results are derived from different datasets, variables and for specific time periods. At this point the fundamental methods and data have already been introduced and defined in chapter 3. These basics are sustained throughout the following chapters, when in chapter 5 a quantifying approach of a comparison between these models and the analysis of uncertainties are fulfilled. The next chapter is generally addicted to extreme events of precipitation concerning means and trends and a consequent application of the foregoing analyses of uncertainty on the different periods the extremes are computed in. In the final concluding chapter a roundup is conducted by a summary of the main findings and how

they bear upon former experiences completed with some hints of future need of research.

1.2 The Mediterranean Area - a physiogeographic and climatic presentation

To provide a lucid assessment of future projections in this area it is indispensable to address the physiogeographic and climatic conditions in the following chapter, which will be done in two paragraphs, where the first will give a short overview of physiogeographic conditions, e.g. topography, and the definition of the MA as the area of research in this study. The latter paragraph will offer an introduction about the Mediterranean climate in general and its steering elements from the global scale like teleconnections to the local scale e.g. given by local cyclogenesis to mountain barriers. This is essential in the proceeding of this study, as the fundamental tools for a comprehensive interpretation of trends and mean values is provided on the one hand. On the other hand this introduction gives first insight of natural variability of climate and its specific continuity, which is a main issue in this work.

1.2.1 Physiogeographic characterization

Drawing the borders of the MA is not as easy as it is supposed to be. A former rather misleading definition was the ocurrence of the olive tree. The olive tree mainly occurrs in coastal areas, but misses in higher altitudes and also in Egypt and Libya (ROTHER 1993). However to apply climate research it would be appropriate to consult a more climate-based definition of the MA.

Concerning radiative aspects the MA is located between the midlatitudes and the subtropics. The Mediterranean Sea as the geographical heart of this area is surrounded by continental areas with Europe in the north, Africa in the south and Asia in the east. In the West the Atlantic Ocean adjoins the Mediterranean Sea, where the narrow strait of Gibraltar (with a depth of 300m and a width of 14km), provides the exchange between the two oceans. However the Mediterranean Sea is a nearly complete enclosed ocean, though a second but even smaller exchange is given to the Black Sea. This is the first characteristic which makes the Mediterranean Area unique on the globe. The Mediterranean Sea also steers the regional water cycle, by dispensing more water by evaporation (934-1176mm/year) than gaining rainfall input (331-477mm/year), which is the case for every month (MARIOTTI et al. 2002), whereat the Black Sea, the rivers and the Atlantic Ocean supply the deficit. The close vicinity to the oceans subordinates this area to both continental and maritime air masses originating from both tropical and polar areas. Whereat, the Mediterranean Sea provides huge air humidity, which is reflected in overall relatively high precipitation amounts at observational stations, e.g. Beirut with up to 893mm or Nice with 862mm of annual precipitation. Hygric conditions are generally defined by the distance to the Atlantic Ocean, so the impact of the Atlantic Ocean is transferred by the Mediterranean Sea for approximately 4000km to the east (WEISCHET & ENDLICHER 2000). Consequently, besides the reduction

of precipitation within the latitudes from north to the south, it is also reflected from the west to the east by a diminished influence of the humid air-masses from the Atlantic Ocean. Average temperatures increase from northwest to the southeast, while continental conditions become more influential towards the Asian continent, while yearly temperature ranges still stay beneath 20°C (ROTHER 1993). The sea-surface temperatures, ranging between 12-27°C in the annual cycle, evoke stabilized atmospheric layers when they are cooler than the air temperature, which again enforces the subtropical high, while in winter the opposite takes place. In summer and winter temperature amplitudes are smoothed (WEISCHET & ENDLICHER 2000).

The morphologic situation varies strongly over the whole area. Gulfs, peninsulas, mountainous regions and isles of different dimensions are alternating over small distances. Ranges of mountains, e.g. the Pyrenees, the Alps, the Rhodopes, the Taurus Mountains and the Northern Anatolian Mountains define the Mediterranean climate as well, as they prevent the intrusion of cold air-masses from the north. Other orographic ridges like the Apennines, the Iberian Plateau or the Dinarides dissect the Mediterranean Sea evoking characteristic luv and lee climates, whereat the latter exhibits prominent instances with up to 4600mm annual precipitation in the Bay of Kotor or generally the west coast of the Levant with Beirut and Haifa and their counterparts of Damascus and Amman in the lee (WEISCHET & ENDLICHER 2000). In accordance with the hypsometric differences the climate conditions changes with the height above sea-level to cooler temperatures and thus snowfall occurs in these areas in winter. Accumulated snow coverages in mountainous regions provide natural resources of water being persistent into warmer and drier periods in the year and supply water capabilities for agriculture (e.g. Sierra Nevada for Almeria) and cities (e.g. Sierra de Gredos for Madrid or the Apennines for Rome), while albedo is increased furthermore. Though, frost periods are rather unusual and occur only in continental areas, in areas of higher altitude or in exceptional cases, which is confirmed by the 7°C isotherme, as it follows closely the northern coastal line of the Mediterranean Sea (WEISCHET & ENDLICHER 2000). Generally frost days are diminished towards the south. The overall warm and moderate temperatures expands the growing season over the whole year unless it is not affected by hygric conditions. These sharply fragmented area and heterogeneous land-sea distribution pattern with its peninsulas and isles makes it very difficult to generalize the region to homogeneous characterizations. For the reason of the database and a more or less given climatologic unity, the area of investigation (and thus the MA) is defined in this work from -20° to 45° longitude by passing the 0° meridian and 26° to 45° northern latitude (see 3).

1.2.2 The Mediterranean climate

The MA is located in a transition zone between the domain of the cyclogenesis in the zone of prevailing westerlies and the subtropical high pressure zone with its dry climate and the trades in the south. With different seasons the influence of both climatic factors alternates. Thus, main characterizations are the humid winters with moderate temperatures and dry and hot summers. Following KÖPPEN (1931) the Mediterranean climate is

categorized in the Csa and Csb climate, indicating temperatures in summer above 22°C in the first class and in the latter class slightly lower summer temperatures in the vicinity of the Atlantic Ocean and in mountainous areas. The wettest month in the cold season is defined to exhibit three times the precipitation of the driest month in the warm season. Anyway, this definition does not satisfy an explicit definition, as California or southwestern Australia exhibit similar conditions.

Seasonal characteristics are more pronounced in the north with wet and cool conditions and the south with dry and hot conditions. The latter one is subject to the descending branch of the Hadley-Cell, while the humid northern area is more subordinated to the west wind zone and thus inevitably influenced by the formation of the Azores High. The affecting interplay of the dipole between the Icelandic Low and the Azores High is defined as NAO (**N**orth **A**tlantic **O**scillation). An index of this dipole can be built between the normalized sea-level pressure of Lisbon and Stykkisholmur (HURRELL 1995), which is the hemispheric branch of the Arctic Oscillation. The seesawing effect of the two centres of action on each other exhibits also long term trends, besides the seasonal shifting of the Atlantic stormtracks. By the latitudinal moving of the Atlantic stormtracks during the year the MA is subordinated to a natural seasonal variability of precipitation, e.g. by a more facile propagation of cyclones to the eastern parts of the MA. This propagation is framed by subtropical highs over northeastern Africa being persistent over the whole year and the continental thermic low over Eurasia. Furthermore, positive NAO indices, i.e. a pronounced dipole structure between the two centres of action, are linked to negative precipitation anomalies in winter, predominantly in the western and southern partitions of the studied area (HURRELL 1995, XOPLAKI 2002, TRIGO et al. 2006, TRIGO et al. 2002). The relatively low amount of precipitation in western parts of the MA can be partly ascribed to a high pressure system located over the Bay of Biscay accompanying positive phases of the NAO (DÜNKELOH & JACOBEIT 2003, HURRELL 1995). The opposite holds for negative NAO indices (e.g. TRIGO et al. 2006, HURRELL 1995). The blocking phenomenon of NAO induced high pressure systems even expands on the continental areas (SCHERRER et al. 2006, BARRIOPEDRO et al. 2006), by e.g. a ridge located between the British Isles and Fennoscandia, which deflects cold air to the eastern Mediterranean, while Eastern Europe is provided with moderate temperatures. Besides the relation to the NAO and the routes of storms drifting eastward, blocking systems also affect the conditions of cyclogenesis in the Mediterranean, as sinking dry air-masses and high pressure generally evoke stable atmospheric conditions. The impact of mid-latitude variability is highest in winter (HURRELL 1995), while in summer tropical and subtropical steering elements become more influential (XOPLAKI 2002). The effect of the NAO declines from the west to the eastern Mediterranean and southward. Besides precipitation also impacts on temperature can be detected (XOPLAKI 2002, POZO-VAZQUEZ et al. 2001). E.g. TORETI et al. (2010) try to link a positive/negative NAO index in winter with warmer/cooler temperature in the north and cooler/warmer temperature in the south and east and for a negative NAO index vice versa (see also HURRELL 1995 and XOPLAKI 2002). Thus, for the Iberian Peninsula the reactions of warmer temperature on the NAO are stronger on positive phases, while the negative phases have warm impact on the remaining MA (POZO-VAZQUEZ et al. 2001, GOUBANOVA et al.

2010) and the Sahara (GIORGI 2002a). Generally in the total MA, a positive NAO index rather leads to higher temperature anomalies (GOUBANOVA et al. 2010). In the last decades of the 20th century the NAO index was rising leading to a northward shift of the stormtracks accompanied by southwestern winds (HURREL 1995). Consecutively, this evokes warmer and drier conditions in the MA. This could be particularly identified for precipitation in winter but also temperature exhibits some increase in winter and here also in the eastern parts (TRIGO et al. 2006). Long term affection of the NAO will thus have future impacts on the impinging of the Atlantic storms onto the MA and thus consequently have major impacts on both precipitation and, though to a lesser extent, on temperature.

Besides the NAO, being the first modes showing detectable influences on the Mediterranean climate, the **E**ast **A**tlantic Pattern (EA), as a respond to the NAO in greater heights, the EURASIA 2 Pattern or **E**ast **A**tlantic-**W**est **R**ussian Pattern (EA/WR) as a branch of the EA evoked by a drift of the EA towards northern Europe at approximately 750hPa and the EURASIA 1 Pattern or **Scand**inavian Pattern (SCAND) are addressed (ULBRICH et al. 2012, BARNSTON & LIVEZEY 1987). For precipitation the impact of the EA is less than that of the NAO exceptionally for special cases when the EA/WR is induced, whereat the positive indices of the latter can be related to a decrease of precipitation and lower temperatures in the southeastern MA, while in the western MA for temperature a negative correlation can be confirmed (KRICHAK & ALPERT 2005, XOPLAKI 2002). This is caused by anticyclonic conditions over western Europe and a trough over the Caspian Sea, whereat the impinging wet air-masses from the Atlantic are blocked (e.g. by subsidence of dry air masses in the west). An advection of cold air mass from the north generates and its reaction with warm sea-surface temperatures evokes cyclonic and wet conditions in the eastern MA (XOPLAKI 2002). Furthermore, the EA accounts remarkably for temperature variability in the western MA, as cold air intrusions occur. They may be evoked by a pronouncing effect of a high in the vicinity of the British Isles and a cyclonic system in the south in strong negative phases of the EA and the NAO (MAHERAS et al. 1999). Negative pressure anomalies within the interplay of an anticyclonic centre over Fennoscandia and a trough over the vicinity of the Iberian Peninsula represent the negative phase of the SCAND mode and vice versa, leading in the positive mode to precipitation amounts higher than normal in the central MA by predominant southerlies and south-westerlies. Furthermore cyclogenetic conditions are provided over Italy and the luv-sides of the mountain ridges with an east-west orientation (XOPLAKI 2002, WEISCHET & ENDLICHER 2000). While the impact of the already mentioned patterns on temperature is proven, the effect of the SCAND is mainly confined on precipitation (XOPLAKI 2002). Besides the thermically induced and seasonal alternating pressure conditions over Eurasia, in winter the steering of these macroscale patterns becomes prevalent, when the radiatively induced pressure gradient between midlatitudes and subtropics effects stronger westwinds. In summer other steering factors prevail.

HATZAKI et al. (2007) identify a teleconnection which is referred as **E**astern **M**editerranean **P**attern (EMP). An interaction between the eastern MA and the northern Atlantic is induced by predominating cyclonic activities over central Europe in winter and autumn, leading in the positive phase of the EMP to

warming in northwestern Europe and enhanced precipitation in the eastern MA. It is noteworthy that in the negative phase above-average temperatures occur in Greece.

With the Mediterranean Oscillation a similar mode is described by CONTE, GIUFFRIDA & TEDESCO (1989) which defines the difference of sea-level pressure between the eastern and western part of the MA. This is predominantly evoked by a northern and western rise of sea-level pressure, which again is related to the NAO (DÜNKELOH & JACOBEIT 2003, TRIGO et al. 2006). Further patterns have been identified, e.g. the North Sea-Caspian pattern (KUTIEL & BENAROCH 2002).

Besides the extratropical teleconnections also tropical circulation modes affect the MA. This holds, particularly for the **E**l-**N**ino **S**outhern **O**scillation (ENSO) (ALPERT et al. 2006). It occurs by a modification of the Walker cell, e.g. during El-Nino, which in turn may lead to a weakening of the Atlantic Hadley cell again having impact on the southern MA (RODO 2001). Furthermore El-Nino events can cause a modification of subtropical and mid-latitude jet streams by a significant warming of central and eastern pacific sea surface temperatures combined with a heating of the adjacent atmosphere. Then the teleconnection between the **P**acific **N**orth **A**merican pattern (PNA) and the NAO is enforced by a consecutive shifting of Rossby-waves and jet streams providing eventually enhanced migration routes for low pressure systems. Still, affection of Rossby-waves by sea-surface temperature is particularly evident during La-Nina periods. Anyway, this variabilities lead to modifications of the NAO, a consecutive deviation of normal cyclone tracks and thus to a change of expected temperatures and precipitation (MARIOTTI, BALLABRERA-POY & ZENG 2005) (as described above). One further famous instance in the eastern Mediterranean on precipitation is an assumed link of the dislocation of the eastern Mediterranean jet stream of 50-100km to the south during El-Nino years, which leads to an enhanced precipitation in Israel in winter. However, this association only appears in the recent observations, probably evoked by an enhanced frequency of El-Ninos in the last decades (TRENBERTH & HOAR 1997). Also, in the western MA in spring, particularly for the region of the Iberian Peninsula, a coherence of ENSO and precipitation can be confirmed. Here, the precipitation rises during autumn about 10% antecedent to the ENSO maximum and declines in the following spring to up to 50% (MARIOTTI, ZENG & LAU 2002, ALPERT et al. 2006). Even for summer increasing values of precipitation could be found by SEUBERT (2010). During the La-Nina phenomenon winter precipitation declines over the southwestern MA, due to a northward shift of low pressure tracks (POZO-VAZQUEZ et al. 2005). However, GIORGI (2002a) found a negative correlation of precipitation anomalies between the MA and the northern part of South America with CRU data (NEW, HULME & JONES 1999/2000). Still, the correlation coefficient is low and a possible temporal shift, accounting for triggering delay, is not included in GIORGI´s general approach (2002a). So POZO-VAZQUEZ et al. (2005) or MARIOTTI, ZENG & LAU (2002) suggest that the transmission of El-Nino impacts to the MA is delayed by approximately 3 months. Furthermore, El-Nino leads to high pressure areas over the western Mediterranean, whilst La-Nina effects rather depressions (LAITA & GRIMALT 1997). As HALPERT & ROPELEWSKI 1992 and RODO 2001 describe an occurring cooling over the western Mediterranean Sea, which

is evoked by an El-Nino event and consecutively caused atmosphere-ocean interactions, also affections on temperature are involved by ENSO. Still, as ENSO affects the climate conditions in the MA with dependency on season and the stage of action of the specific El-Nino phase with probably delay of several months the quantitative extractions of these impacts are complicated (ULBRICH et al. 2012). Though decadal changes of this teleconnection are evident as well, relations between El-Nino and rainfall over northern Africa disappeared in 1931-1960 (KNIPPERTZ et al. 2003). This may be due to the mentioned interconnection of the NAO. ALPERT et al. (2006, p. 156) state that "The ENSO influence appears more relevant at interannual timescales than the NAO effect". Nevertheless, the unforeseeable NAO already constrains the predictability of Mediterranean climate to a few months. However, the seasonal steering mode for the MA is the NAO, which is also affected by the ENSO itself, e.g. by the above-mentioned interplay of the ENSO and the PNA. Overall, one can conclude that the impact of ENSO on the MA is not well understood today and further research indispensable (ALPERT et al. 2006, XOPLAKI 2002).

A further tropical system linked with the climate variability in the MA is the **S**outh **A**sian **M**onsoon (SAM). Sea-level pressure varies by the steering of the South Asian Monsoon to lower values in summer in Asia Minor, which builds a counterpart to the Azores High and to increasing pressure over the Middle East, which evokes the dry Etesian winds from the north (ULBRICH et al. 2012, WEISCHET & ENDLICHER 2000). These pressure anomalies are accompanied with a positive correlation of temperature anomalies. Whereas a stepwise delay of the onset of the south Asian Monsoon is identified. This shifts the decrease of pressures towards the summer months, evoking in consequence an overall falling of pressure values (XOPLAKI 2002) in the eastern MA from early summer towards midsummer (ALPERT et al. 2006). SEUBERT (2010) identified a negative correlation between Indian summer Monsoon and northeastern MA precipitation amounts. Also in the southeastern MA a descending branch, which is associated with dry and warm atmospheric conditions accompanied by developments of desertification, is caused by an enforcement of the intensity of the SAM and here particularly by a future strengthening of the SAM (XOPLAKI 2002). Finally, further studies have been fulfilled to identify possible relations between temperature and snow coverages and the SAM (XOPLAKI 2002), which also can be linked to the Etesian winds being again induced by the remote steering of the Monsoon (ZIV, SAARONI & ALPERT 2004). Again in winter the impact of the NAO is predominant, besides occasional polar outbreaks caused by the Asian winter Monsoon (ALPERT et al. 2006).

Also the African Monsoon seems to be linked with Mediterranean climate variability, as BALDI et al. 2006 identified negative correlations in summer. Wet and cool conditions in the MA are coinciding with negative precipitation anomalies in south western Africa, while hot and dry summers are accompanied with a strong Monsoon in Africa. An eastern extension of the Azores high and/or SST (**s**ea-**s**urface **t**emperatures) anomalies may cause this phenomenon (SEUBERT 2010, BALDI et al. 2006). Again ENSO seem to bear responsibility on this linkage (SEUBERT 2010). Furthermore a relation between the African Monsoon and the South Asian Monsoon is identified by RAICICH, PINARDI & NAVARRA (2003), who analyse the pressure pattern over the Mediterranean as its linkage.

Thus it becomes evident that none of these teleconnections are unaffected from each other. In the dynamical global climate system they rather overlie themselves in enforcing or weakening each other, again having once more impact on the next teleconnection. That is one crucial point making climate projections that difficult. Efforts have been made by e.g. SEUBERT (2010) to facilitate this comprehensively coupled system, so she found a mode, e.g. comprising the ENSO and the Indian Monsoon. Still, the MA is distinctly induced by several kinds of teleconnections with different sources (ULBRICH et al. 2012).

Located at a western continental border the MA is certainly subdued to the impact of cyclones defining the weather and thus climate conditions. The antecedent paragraphs provide the background for this passage, as e.g. the characteristics of the NAO have strong impact on the cyclones advected to the MA (NISSEN et al. 2010). As already mentioned above, the location of the highest cyclone-track density is shifted towards northern latitudes during positive phases of the NAO, while cyclogenetic preconditions are enhanced during negative phases. Similar results can be found for the EA/WR, as with its positive phase a reduction of cyclones is caused for particularly the central northern and the northwestern MA comprising Italy and the adjacent ocean. In opposite enhanced cyclones occur near the Levant during these conditions. Less impact is caused by the SCAND leading during its positive phase to a small but significant increase of cyclones in the western and eastern Mediterranean basin and a southward shifting of the polar jet and finally to a complicated interaction of suptropical and polar jets (ULBRICH et al. 2012, NISSEN et al. 2010). Further impact is evoked by the characteristics of the Red Sea Trough, which clearly affects the orientation and direction of jet streams in the upper and lower troposphere.

Still, large-scale steering elements are not the exclusive mechanism allocating cyclones, as the occurrence and severity of cyclones is also dependent of the land-sea distribution, the sea-surface temperatures, the topography and finally the alignment of baroclinic levels. With turbulences or strong wind shears, cold air intrusions might enter the troposphere. Under these preconditions and convection schemes, driven by specific stream characteristics, the requirement for cyclogenesis is fulfilled. In turn this naturally influences the precipitation regime in the eastern MA. Concerning the seasonal variability, with anticyclonic conditions in summer, generally stable atmospheric conditions by relatively cool sea-surface temperatures and the low pressure gradients between the subtropics and the midlatitudes the affection of west winds is marginal. Thus, the account of autochthone cyclogenesis in the MA, e.g. in the Gulf of Lyons or the Gulf of Genoa (see below) is accented. In the transitional and cold seasons the interaction between warm air masses of the MA and cold air masses advected from the Atlantic may provide preconditions for the development of strong Mediterranean storms (TRIGO, BIGG & DAVIES 2002). Particularly in the colder seasons the impact of cyclones is increasing. These systems might not only be the source of the synoptic dynamics over the Atlantic. They also originated from Africa and many of them also develop as autochtonous systems over the Mediterranean Sea, being short-lived and much smaller than their Atlantic counterparts. However, these cyclones provide rain, wind and storms and accompany storm surges (ULBRICH et al. 2012). Cyclogenesis is

stimulated in lee sided regions of orographic ridges, by baroclinic conditions generated by the land-sea contrast and generally by the Mediterranean Sea being warmer and providing more humidity, energy and unstable conditions than the surrounding land masses in winter. This defines three primary cyclogenetic areas with the lee of the Atlas ridge in the transitional seasons, the Gulf of Genoa and the proximity of Cyprus. Particular the latter ones remain stable regions of cyclogenesis throughout the whole year, whereas the vertical deepening of the trough is fastest by cyclones generated in the vicinity of Genoa. Here, the advection of cold air-masses by taking the path of the Rhone-Saone is supplied permanently. The baroclinic effect and the lee effect particularly become important in winter, when further cyclogenetic areas are the Aegean Sea, the Adriatic Sea, the Ionean Sea, the Tyrrhenian Sea, the Baleares and the Iberian Peninsula, the Algerian Sea and the Black Sea (ULBRICH et al. 2012, WEISCHET & ENDLICHER 2000).

With respect to the water shortage in the MA, discussed in 1.2.4, these cyclones bear responsibility for the prevalent water supply. E.g. for Israel the Cyprus cyclones from November to March account for around 70% of the annual precipitation sum and for 50% of the precipitation variability in winter (ULBRICH et al. 2012). Negative aspects are the storm surges, e.g. as these ones generated by the Genoa cyclones strongly affect the northern coast in the Adriatic Sea by the propagation of oceanic waves along the northwest – southeast orientation of the Adriatic Basin. However, the generation of storm surges or waves depends on cyclone tracks, whereas these are mostly located on a southern track with east-west axis. In spring the short living cyclones from the southern Mediterranean coastline and northern Africa become predominant. The so-called Sharav cyclones are born in the lee of the Atlas and enforced by the delay of the warming of the Mediterranean Sea in contrast to the North African deserts. Overall their moisture content is rather low as they originate from the Sahara. Still, they induce hot and dry conditions often associated with dust-storms at their cool front (ULBRICH et al. 2012). It is assumed that the radiative effect of aerosols of these storms being blown northward by southerly winds into the Mediterranean region counts enormously, as these winds even may be enforced by the high over the central Mediterranean Basin and a low over the British Isles. So, the Mediterranean dust transport is found to reach higher altitudes than Atlantic dust transport. Finally, though cyclonic activity is pronounced in the transitional seasons, favourite conditions are found for the genesis of Saharan Lows or cyclones generated in the south of the Atlas in the summer months, while these cyclones are moving eastward to Egypt and Israel. Exceptionally, a high over Libya circumvents eastward propagation of these lows and provides an extension of dust clouds into the western part of the Mediterranean. Salt particles and anthropogenic or industrial aerosols from central Europe perfect the complexity of the typical climate of the MA (ALPERT et al. 2006).

Besides the lee of mountaineous barriers, further small scale processes, which are hard to model due to the high relief energy, the heterogeneous land-sea contrast or the diversified vegetation coverage, superimpose the synoptic steering elements, e.g. by the immense moisture source supplied by the Mediterranean Sea or the mountain barriers restraining mesoscale air masses (see above).

The strong orographic heterogeneity creates windsystems with unique modifications. Besides that wind is also generated by large-scale steering, as e.g. pressure anomalies and associated gradients, convective situations are responsible for local wind systems and are hard to capture and generalize. A noteworthy wind system is the Sirocco. It is generated by a low pressure system over northern Africa, inducing south-easterly wind from Africa onto the Mediterranean Sea. This dry and hot wind may be conveyed over the Adriatic Sea comprised by the surrounding mountain ridges of the Apennines and the Dinaric Alps. Storm surges, swollen by this wind, may affect the northern Adriatic coasts and adjacent cities, e. g. Venice (LIONELLO et al. 2012). Depending on country or culture these continental and tropical winds are also called Chili, Ghibli, Leveche, Solano and Kamsin (WEISCHET & ENDLICHER 2000).

The Bora is a down-slope wind, streaming from the Dinaric Alps into the Adriatic basin. Although the Bora may be enforced by pressure patterns like a southwestern trough or a northeastern anticyclone, its typical pattern and distribution is generated by local factors e.g. the three-dimensional strength of the impinging wind on the mountains, the angle of the income, the vertical and horizontal distribution of the mountain ridges, the temperature and the moisture (GRISOGONO & BELUSIC 2009). By gaps in the zonal mountain barrier in the north (see 1.2.1) canalized wind systems like the Mistral, which affects the Gulf of Lion with cold air advection, develop. Canalized winds can also be found within the Strait of Gibraltar called Levanter or the Tramuntana in Catalonia or Maestrale in Italy. Further winds are the Sharkiya, Vardaris over Macedonia, Libeccio, Vandevales, etc… (LIONELLO et al. 2006b). Many of these winds interact with land/sea wind systems.

Finally, abnormal hot or cool temperatures may be enforced or eased by these interactions, while local or seasonal preconditions may also strongly affect these temperatures. So, droughts in winter and spring can lead to extreme high temperatures in summer, as latent heat cannot be removed by a high effective evaporation.

Among large-scale steering and oceanic impacts, land-sea interactions, topographic barriers, exposition, natural aerosols also snow cover extensions (VAN DEN BESSELAAR, KLEIN TANK & VAN DER SCHRIER 2010), vegetation, (CLAUSSEN 1998, FOLEY et al. 1998), or natural and anthropogenic aerosols and further short-scale and local factors modulate the trigger effects on temperature and precipitation.

1.2.3 Discussion of natural variability of Mediterranean climate

It is referred to this alteration of climate conditions evoked by these mentioned steerings (except the anthropogenic aerosols) as natural variability playing a role on annual and decadal scales. A continuative discussion of the definition of variabilities is provided in chapter 2. GIORGI (2002a) assesses extents of these variabilities for precipitation and temperature and sets them into context with other sub-continental regions. For brevity these analyses referring to variabilities could not be conducted within this study in chapter 4, why

precedently GIORGI´s findings from 2002a are presented to round up the addressed mean values and trends. The yearly interannual range of variability amounts for temperature is about 1.5°C, with highest amplitudes in winter. For precipitation it amounts 40% (30% in WEISCHET & ENDLICHER 2000) of the average precipitation, whereat highest interannual variability is shown in summer, as convective processes steer this climatic element. Besides some Australian regions, northern Africa exhibits highest interannual and interdecadal variability of precipitation in all seasons (GIORGI 2002a). In the MA, for temperature specific modes of variability lasted in many cases longer than three years in the last century, showing a higher impact of multi-year variability than interannual variability. Concerning anomalies according to interannual variability only a few occurrences (of about 8) lie beyond or above the 90th percentile for precipitation and temperature in winter. In summer extreme variability occurs even rare. Thus, also extreme variability is rather less in the Mediterranean concerning different sub-continental areas over the globe (GIORGI 2002a). Referring on anomalies of natural variability the Mediterranean Area correlates significantly with Greenland and adjacent northern territories and southern South America in temperature, while precipitation anomalies are related to northern Asia. Of course positive correlations of temperature anomalies are found to adjacent sub-continental regions (GIORGI 2002a).

For summer anomalies of temperature and precipitation can be correlated negatively with a significance at a level of confidence of 99%, which can simply be associated to cloudy conditions during rainy periods diminishing the incidence of solar radiation and the replenishment of soil moisture evoking cooling heat fluxes off the surface and vice versa. This mechanism becomes predominant in summer, when local fluxes became the main steering instead of synoptic advective patterns (GIORGI 2002a).

Many studies relevant to natural variability have been consulted. Further and more detailed insights can be obtained by the study of FERNANDEZ, SAENZ & ZORITA 2003, which deals with the variability of atmospheric moisture and the studies of MAHERAS et al. (1999) and MAHERAS & KUTIEL (1999), who investigate temperature anomalies in the MA. In both studies the focus lies on crucial variables and their relations to large-scale air masses.

GIORGI & LIONELLO (2008) discuss that a general warming is in line with enforced natural variability. This might particularly hold for the precipitation by an enhanced moisture capacity within warm air and the expected intensification of the hydrologic cycle under warmer conditions. In turn temperature variability can be attributed to the precipitation variability again because of the herewith associated change in energy budgets on surfaces. So, variability of temperature is closely related to precipitation in the warm season.

1.2.4 Vulnerability

Due to the moderate, warm or even high temperatures, the availability of water and thus of precipitation is the most crucial aspect. Precipitation occurs in a high seasonal, yearly and spatial variability. Particularly the southern MA, where the demand on water is higher than the annual precipitation (ROTHER

1993) is highly vulnerable to water shortage (LIONELLO et al. 2006a). These regions are mostly economically dependent from its agricultural productivity and autonomy. The crop yield suffers from the variability of precipitation and the temperature change within the subsequence of seasons, e.g. by droughts or water shortage, while a shift in annual mean values of temperature and precipitation is assumed to lead to minor yield losses only (RÖTTER & VAN DE GEIJN 1999). Anyway, the relative dry and hot climate conditions in the summer season lead to high stress for plants. But also low precipitation amounts in winter and spring are specifically associated with yield losses. River discharge is not equally distributed over the year and many of the characteristics of several streams are torrential outflow rates, while also smoothing refillments of rivers in summer by melting of glaciers are missing. So, e.g. the Guadalquivir or the Bradano exhibit variabilities in the discharge of about 1:100 (ROTHER 1993). Furthermore, storage capacities of the ground are relatively weak, caused by early deforestation in the ancient world, leading to a drying out in summer, while in winter higher precipitation amounts cannot be collected by the soil. Consequently, severe rainfall during the wetter seasons also has negative impacts on plants as e.g. fields are drowned, fertile soil is eroded and pedogenesis is impeded (XOPLAKI, MAHERAS & LUTERBACHER 2001). Thus, special focus is dedicated to meteorological extreme events like intense precipitation and time-persistent rainfall as they may cause floods and landslides. Also, in this regard several regions are very vulnerable due to their narrow agricultural utilizable spaces, the mountainous areas or their vicinity to the coast. The last-mentioned areas may be also strongly affected by probably intensifying storm ocurrence and amplification of waves. Particularly the sea-level rise in the Adriatic Sea leads in an already very vulnerable region again to enormous pressure on Venice. However sea-level rise or storm surges are not only dedicated to cyclones or wind-storms but also associated with air-pressure variability (TSIMPLIS & JOSEY 2001). With respect to hydrology and agricultural preconditions the situation even gains more severity due to the high population density in this sensitive ecosystem (LIONELLO et al. 2006a). As it has been highlighted the MA is thus strongly vulnerable by the externe influences of a designated climatic change and the accompanying circumstances. That is the most important reason why the underlying project of the detection of uncertainties in climate change projections is located in the MA.

1.3   Discussion

   The MA is located in a transitional region between the subtropics and the midlatitudes with broad seasonal alternation with hot and dry summers and mild and wet winters. As shown in this chapter the Mediterranean climate is evidently originated by the impact of macroscale atmospheric patterns, where the most important is the NAO, which generally evokes during its positive/negative mode warmer and drier conditions in the north/south and cooler and wetter conditions in the south/north. These teleconnections gain main influence in the cooler seasons. The importance of macroscale forcings is even emphasized as it has e.g. been tried to correlate wave heights of different Mediterranean Sea regions during different seasons with the NAO, EA/WR and the SCAND (PINO, LIONELLO & GALATI 2010).

Their steering is accompanied by the typical orographic features, the oceanic circulations and generally by the Mediterranean Sea, and other local assigning factors as snow cover, albedo, soil moisture, land-sea interaction, vegetation characteristics, etc., leading e.g. to superpositions by the mentioned natural noise and to a temporally and spatially highly heterogeneous and complex interplay with each other. This interplay must not be assumed to be fixed in temporal or spatial dimensions, particularly not in the case one of the participating factors is modulated, e.g. by progessively emitted greenhouse gases and consecutive temperature increases. Thus, the Mediterranean climate is highly sensitive with its local steering components, e.g. cyclones, to the large-scale steerings from mid-latitudes and tropics.

Considering these facts the MA with its interesting physiogepgraphic preconditions is thus uniqueley providing an interesting frame to conduct climatologic studies. Furthermore, by the complexity and sensitivity of its climate the MA may be particularly affected by changing conditions in future, which is aggravated by its high social, natural and economic vulnerability and the weak ability for the landscapes to regenerate.

Still, one should not forget that the Mediterranean climate itself has global impacts by e.g. the linkage between the African and the Asian Monsoon or the Mediterranean outflow in the Atlantic Ocean and thus being a steering element of the thermohaline circulation (ULBRICH et al. 2006).

2   The usefulness of GCMs to assess man-made climate change

The present chapter outlines the advantages concerning the application of climate models with its constraints, e.g. the problems inherent with the confined temporal and spatial resolutions, complex dynamic processes which are not completely understood today or the issue of limited computational facilities. Finally, the inevitability of the employment of climate models is highlighted with a definition of uncertainties according to climate modelling, which are handled quantitatively in consecutive chapters.

2.1   Foregoing consideration

In history of mankind experimental designs have always been a beloved possibility to discover deepest secrets of nature. Meanwhile one has to reassess this methodology as experiments had left the insularity of the probation in many disciplines. One must definitely ask- if the experiment is still safe. For sure the comparison with tests of nuclear bombs or experiments with genetic engineering are far-fetched but they had already become reality and might affect our system much more than we dare to think about. The same problem arises with the "experiment" of the climate change, as climate is much too complex to copy it in an enclosed laboratory to conduct isolated experiments. Of course the global experiment mankind started by means of emitting CO_2 into the atmosphere is a very exciting one and will provide the correct results in future periods of observations. But on the other hand it would be very impudent to start the overview of the data when it might be already too late to adapt to a possibly changing climate, since the following impacts might be a rising sea-level, harvest losses, spreads of diseases, etc. Furthermore, the way might be irreversible. In history comparable climate changes have not been recorded so it is not possible to draw any conclusions about this project in future. Finally, it is irresponsible to await this changed climate (CUBASCH & KASANG 2000). A second planet Earth does not exist.

2.2   Complexity of Climate

The natural climate system can be separated in several subsystems - consisting of the atmosphere, the cryosphere, the biosphere, the land surface with its pedosphere and lithosphere and the hydrosphere. Climate conditions are generated by the diversified interactions of these subsystems. These internal processes take place on various temporal and spatial scales and exhibit different times of reaction (JACOBEIT 2007), which enhances the complexity of their reciprocal interaction.

These complex internal interaction of these subsystems is affected by external processes (e.g. volcanic eruptions, solar activities, orbital parameters or anthropogenic emissions affecting the transmissivity of the atmosphere,

which again induces changes in the balance of energy) and steered by boundary conditions (e.g. topographic and orographic features like land-sea distribution or mountain ridges, which are determined by tectonic processes, roughness of the land-surface, vegetation, soil, ice coverage, seasonal and latitudinal solar irradiation). The evoked permanent shifts in climate (JACOBEIT 2007) can be documented in records of paleoclimate (ABRANTES et al. 2012, LUTERBACHER et al. 2006, JONES & MANN 2004). Thus climate cannot be defined as constant condition or a static value but rather more as a variable subordinated to continuing changes (JACOBEIT 2007).

The shifts in climate conditions can be described as variability or changes. Internal variability denotes the interdecadal or decadal shifts, which are evoked by the interaction of internal processes and exhibit cycles, e.g. the sequences of the ENSO, the NAO, the thermohaline circulation being e.g. subject to atmospheric modifications or the AMO (**A**tlantic **M**ultidecadal **O**scillation). Further internal climate variability may be induced by the characteristics of the cryosphere. By fixed external processes and fixed boundary conditions this internal variability can be simulated by climate models, though the phases and magnitudes of these events are not captured yet and the results of several models are not concordant. Furthermore, GCMs are able to reconstruct the observed climate trends by the neglection of internal variability but with the comprehension of boundary conditions and external processes (ANDRONOVA & SCHLESINGER 2000). A climate change is existent, when a long term shift is evident, which e.g. occurred in the transition of the last ice age into the Holocene. Nevertheless, this change might also be a deflection within a continuing cycle. Still, these developments may be concealed by short time variability being subject of external and internal processes. As the effects of internal interactions and external forcing superimpose each other the resulting signal needs to be decomposed. For this the forcing boundary conditions, the extent of the external steering and the interaction of the internal interactions have to be known. These internal factors are not only affecting climate individually but also have effect on each other, which in turn leads to an impact on climate. These processes take place in a mostly nonlinear interaction.

Furthermore, these internal processes are dynamically subdued to climatic shifts itself, which for instance may affect the magnitudes of the NAO (JACOBEIT et al. 2001, JACOBEIT 2007), or may cause a cession of the thermohaline circulation by a warming of SSTs and an enforced freshwater input, whilst a possible enhanced frequency of El-Nino events would detain this development by prolonged dry periods over Western Europe. As these relations of the dynamical processes might not be fixed in a proceeding change of climate one refers to nonstationarities (SUMNER et al. 2003). Further dynamical feedbacks are given by the coupling of temperature, ice or snow and albedo evoking a warming over arctic regions up to 7.5°C (MEEHL et al. 2007, CUBASCH & KASANG 2000), the fertilising effect of carbon on plants, the temperature dependant dissolving ability of oceans of trace matters (particularly carbon), or the photosynthetic ability of vegetation or phytoplankton, where the latter one is enhanced by lower temperatures (JACOBEIT 2007). Besides carbon cycles vegetation also steers albedo and local water balances (GANOPOLSKI et al. 1998, CLAUSSEN 1998). A seasonal instance of dynamical feedbacks may be the coupling of reduced precipitation, causing a

decrease in soil moisture content, which in turn leads to a diminishment of latent heat convection and thus to an increase of surface temperature (ROWELL & JONES 2006) in the European summer heat-wave of 2003 (STOTT, STONE & ALLEN 2004). So, as one can see, the natural feedbacks are not really known and thus hard to capture in climate simulations.

The fundamental question of climatology is to detect and to distinguish these manipulating elements with their effect in magnitude and impact on other variables. Only if a long-term trend can be significantly distinguished from the summarized high frequent, decadal and interdecadal processes (i.e. broad scale circulations, which are mentioned above) and their signals the term climate change is appropriate. Single events like the European heat summer in 2003 are thus no explicit indication of climate change (JACOBEIT 2007).

Changing climate may be a continuously process but the former condition also may become instable, in the case that conserving thresholds are trespassed.

Concerning the recent warming most external processes seem to play only a minor role as the change of orbital parameters occurs in too long periods (i.e. 22,000 a -100,000a). Also the solar impact, although the knowledge about this steering is rather sparse, is supposed to be at 0,5°C only in the last 3 centennials (CUBASCH et al. 1997) and volcanic eruptions show an ambivalent result on change.

Another external process is induced by anthropogenic impact, besides other actions like the shaping of the surface. It is the emission of particles and GHGs (**G**reen **H**ouse **G**ase**s**), which leads to a change of biogenic climate by a change of vegetation, the formation of specific local climate conditions (e.g. urban climate), to a cession of stratospheric ozone, air pollution, which affects stress on the animate world and to a change of atmospheric transmissivity and thus to a change of the energy balance. While the emission of particles evokes mostly cooling, the emission of GHGs enforces the greenhouse effect (apart from sulphur dioxide which reacts by atmospheric chemical processes and is in turn transformed into sulphur aerosols (CUBASCH & KASANG 2000). The greenhouse effect is a natural process detaining partially long-wave radiation leaking into space relative to the incoming short-wave radiation from the sun. This process lifts global temperature of about 30-33°C permitting the appearance of life. By an additive anthropogenic emission of GHGs into the atmosphere this relation may be shifted towards an accentuated detaining of energy outstream, leading to global warming. Some GHGs are e.g. water vapour, methane, fluorochlorinated hydrocarbons, tropospheric ozone, nitrous oxide and carbon dioxide. The concentration of the latter one has increased from 280ppm up to 380ppm since industrialization (JACOBEIT 2007). Considering temperature, the 1990ies were the warmest decade in the last millennium. Since the beginning of the 20th century, temperature exhibits an increase of 0.6° C, which happens in the last 10,000 years in an uniquely short time (CUBASCH & KASANG 2000). Although variations of about 10°C have been reconstructed, there is no evident source demonstrating an already happened comparable increase within such a short time period in history.

Consecutively, the scientific community is more or less uniquely supposing an influence of anthropogenic GHG emissions on the climate, i.e. at first a rise of global temperature and secondary an impact on the planetary circulation with its hydrological connections, like distribution, frequency and amount of precipitation. Though physically experiments and theorems clearly support this influence, an effective detection of anthropogenic climate change induced by e.g. GHGs could not been given yet (CUBASCH & KASANG 2000, (VON STORCH, GÜSS & HEIMANN 1999, PAETH 2007). This is due to the fact, that climate change occurs permanently in the history of earth and climate models have great uncertainties between each other, e.g. even the averaged global warming is projected to occur between 1.8°C and 4°C (IPCC 2007, p 13) as its best estimate. But, the main argument may be, that natural internal climate variability like the chaotic and nonlinear behaviour of large-scale flow interactions in the oceans or the atmosphere superimposes external affections (PAETH & HENSE 2002). These variabilities overly the long term climatic change driven by anthropogenic emissions and thus lead to considerable problems distinguishing natural variability from long term forcing. It is evident that this holds particularly for smaller periods. A possible method of a scientific detection of a significant impact of a certain steering element like increasing emissions of GHGs could be the optimal fingerprinting (HASSELMANN 1997), as it has been applied by PAETH & HENSE (2001) or PAETH & MANNIG (2013).

However CUBASCH & KASANG found (2000) with a probability error of 5%, that the warming of 0.4°C from 1966-1998 is not attributed to natural variability.

2.3 General Circulation Models (GCMs)

For detection of the elements steering climate and inducing climate change, one needs knowledge about the development of climate elements in future. Despite one does not know the exact future course of climate one has the possibility to simulate the reality in present and future in a dynamic, statistic and deterministic way with models GCMs. This is a powerful and relatively fast and low-cost approach– and maybe also the only one (see.2.1) - given by computer facilities to prove climate change with the employment of clearly defined forcing scenarios. GCMs are realized from a chosen year in the past continuing until a few hundred years in future. The consecutive chapter concerns the construction of the operating climate models while it outlines the inherent uncertainties of their employment. Concerning the underlying study it is helpfully to distinguish "inter-model" and "intra-model" uncertainty.

2.3.1 Inter-model uncertainty

In this chapter the underlying processes of operating climate models are described. "Inter-model" uncertainty is handled synonymously to the discrepancies of two or more different GCMs to each other.

2.3.1.1 Discretization and Parametrization

The physical theorems of conservation of mass, momentum and energy are fundamental for climate models. A GCM couples the mentioned components and tries to simulate their processes in a realistic 3-dimensional way, with its variables, e.g. moisture, salinity, etc…

Physical laws are implemented in GCMs by the following differential equation (1)

$$ 1) \qquad \frac{\partial E}{\partial t} = f(t, \vec{v}) , $$

with ∂E as change of a certain characteristic in the system within the infinite short time interval ∂t as function of time and the spatial exchanging medium, e. g. fluid streams, which are defined by the variables density, i.e. salinity in oceanic matters, pressure and temperature. In the atmosphere the streams of vapour and liquid water have to be distinguished as the levels of energy are specific. Consecutively, formula (1) describes the changing conditions at each specific location, which is again linked by formula (1) with other locations. Thus, an interacting network is defined (PAETH 2007). Dependent on the time-step the variable E changes, as shown in formula (2).

$$ 2) \qquad E_{t+1} = E_t + \Delta t \cdot f(t, \vec{v}) . $$

This formula is discretised in 3-dimesional units with a certain horizontal and vertical length (spatial discretization) and in temporal units (temporal discretization), i.e. only calculated in spatial and temporal discrete sections defining the temporal and spatial resolution of the model (PAETH 2007). Conventional horizontal resolutions are e.g. T21 which is a spectral unit and describes a spatial area of about $250,000 km^2$. Latitudinal and longitudinal resolution is mostly realized spectrally, an exception is given by the UKMO models (e.g. HadAM3 with 3.75°x 2.5° or about 400x280km) (POPE et al. 2000), (VON STORCH, GÜSS & HEIMANN 1999). The borders of the vertical layers are defined in heights whereupon biggest vertical differences of the specific parameters are expected to depict the most appropriate model of the atmosphere. Thus the vertical discretization is not equally distributed like the horizontal discretization. In the atmosphere the layers with their borders are expressed with their geopotential heights, whereupon a number of about 15 layers with a height of 100m-10km (dependant on the level) has been practicable. Ocean models which are coupled with climate models compute with about 11 layers (VON STORCH, GÜSS & HEIMANN 1999). The higher the spatial resolution of a model is, the shorter should be the time interval. While for a T21 model an interval of 40 min may be sufficient, a model with a doubled precise resolution (T42) has four times the number of spatial units and needs at least a twice precise resolution, i.e. 20min. This discretization is inevitable concerning the limited skills of computer power to run GCMs projecting climate over the whole earth for many climatologic variables in a quite complex physical and statistical behaviour and calculating the interaction of these variables in a

very high temporal resolution within minutes for a total simulated time period of about 300 years.

However, these spatial and temporal units have been resolved to higher and more precise units in latest history due to enhanced computational power. In this study the spatial cells have a length and width of about 100km-200km with reasonable time-steps of 3-5min. (PAETH 2007, ULBRICH et al. 2006). With the aim to comply with these requirements only the most powerful computers have the ability to run climate models.

Despite enhanced possibilities of computer power, this necessity of discretization is a big constraint of GCMs, as principally all the dynamical processes are depicted by the equations on the one hand, but on the other hand every variable is used in this equations with an averaged value as all the different characteristics in the considered unit are combined, e.g. the coverage of clouds, the coverage of sea-ice, vegetation characteristics, albedo, water storage capability, etc… . Topographical height is also averaged over this discretization steps. Consecutively, small topographic features like mountain ridges or land-sea contrasts having a resolution of less than the discrete unit become indistinct or simply vanish. But in the MA these subscale contrasts may be distinct (see 1.2.1). Hence local climate effects, e.g. heavy rainfall or cyclones (ULBRICH et al. 2006), and the feedbacks of the forcing of an emission scenario cannot be described in an appropriate way by GCMs at this resolution (GIORGI & FRANCISCO 2000b). Overall, subscale features, processes or movements cannot be depicted (VON STROCH, GÜSS, HEIMANN 1999).

That is why these subscale processes, as e.g. irradiation, deep convection, sea-ice dynamics, cloud physics, snow, soil moisture, condensation, fluid movements or subscale orographic features are given by parameters or parameterization schemes, i.e. terms depicting the net-effect of the unresolved processes. These parameters are often found by a combination of statistic, empiric and deterministic functions of small scale models. It is obvious that particularly empirically found equations need to be validated for all seasons, locations and situations, before they are implemented in the GCM. Furthermore, empirically found parameterization schemes might not be appropriate for future climate conditions with e.g. higher concentrations of atmospheric green house gases.

This parameterization P affects the climatic field E at a certain time t within the time Δt and the function given in equation (1), described in formula (3):

$$3) \qquad E_{t+1} = E_t + \Delta t \cdot f(t, \vec{v}) + P$$

Not only subscale processes are described by parameterizations. There are also many components or processes, which are relatively hard to capture as the numeric knowledge about them is sparse, e.g. atmospheric transmissivity. Another famous instance are convective transports, molecular heat diffusion or turbulent heat fluxes, which are rather less in their averaged vertical transport. Though, neglecting them would lead to higher surface temperature in the simulations (VON STROCH, GÜSS, HEIMANN 1999).

Particularly the turbulent fluxes are depicted in a deterministic approach, where the relations between known variables are used to obtain these turbulences. Here, an exchange of a specific fluid with its characteristics of momentum, energy and mass is conducted for every time-step between two discrete units. The amount of this exchange mainly depends on the height above the boundary layer (e.g. the surface), the speed(-direction) of the fluid, the layer specific differences of horizontal movements and the temperature gradient between the exchanging layers (VON STROCH, GÜSS, HEIMANN 1999).

Convection schemes describe a redistribution of energy or energy carriers. It occurs on scales of only few km in horizontal dimension but it is the driving mechanism of hemispherical phenomenona like the Hadley-Cell, as convective cells exchange moist into several km height within short time. Former parameterizations completely exchanged the different layers, in the case of higher mass in the upper layer. However modern GCMs are equipped with cloud models providing convection, cloud development, cloud physics and condensation. Again the cloud model needs to make parameterizations as well (VON STROCH, GÜSS, HEIMANN 1999).

A further problem after the calculation of the characteristics within each discrete spatial and time unit is exchanges between these units. These are rather unknown but may be deviated on large scales with the specific equations of fluid movements, current conditions and equations of mass balances of each individual unit. This becomes rather complicated on the scale of relatively high resolved spatial and temporal units. In addition to the general parameterizations this is one of the most serious constraints of GCM, leading to difficulties in the closure of the equations (VON STROCH, GÜSS, HEIMANN 1999).

These processes and features offer the opportunity to adjust climate models to expected results by the tuning of these parameters. This may enlarge the knowledge about these processes in turn but its impact on the modelling should be investigated precisely, as particularly parameterization may be a strong source of errors.

Finally, the boundary conditions (see 2.2) have to be defined. With the combination of several models the problem arises that the models have to be fitted to each other. Subscale models do not usually match with the requirements and results of the main model. That is why one model has to be adjusted, which can be done with the tuning of some parameters, being in turn a source of uncertainty and errors.

2.3.1.2 Coupling of models

For current GCMs the overall climate system is distinguished in subsystems and thus into several models, up to date for atmosphere and the ocean (AOGCM – coupled **A**tmosphere-**O**cean **G**eneral **C**irculation **M**odel). In near future the climate system may be represented by further couplings of specific models for e.g. land-surface and its vegetation (CLAUSSEN 1998, FOLEY et al. 1998). Particularly the latter one is quite complicated. An interesting study has

been conducted by DÜMENIL GATES & LIESS (2001), who simulate different climate courses by varying the vegetation in the MA. Results of deforestation are a reduction of precipitation and a consecutive decrease of evaporation and eroded soils, having less soil-moisture capacity. A change in precipitation amounts may also affect soil weathering and thus shifts in rain water chemistry, which is prevalent to any Saharan dust input in Spain (AVILA, QUERALT-MITJANS & ALARCON 1997). However, the implementation of cycles of matters, e.g. the carbon, with its sources and sinks is another challenge. A sink of global carbon circulation may be the sinking of death zooplankton to the sea floor. Favourable environment for phytoplankton and thus zooplankton is essentially dependant by the supply of calcium and other nutrients. As these processes are small-scaled and not completely understood, today parameterizations and presumptions have to be made to model the cycles of matter approximately (see 2.3.1.1).

These mentioned models are interacting with each other. Here the implementation of the sub-systems gets increasing complexity. For instance, the ocean was refined from its first simple design of a swamp ocean by means of a wet surface with a certain temperature supplying evaporation to an elaborate agglomeration of interactions by energy balances, deep circulation, wind impulse, salinity, horizontal energy transports, vertical layers and convections, and thus annual cycles of sea surface temperatures. Consecutively, single ocean models have been coupled with atmospheric models interacting by means of precipitation, evaporation, wind and irradiation, reflection and sensible heat fluxes. In the next steps sea ice modules and land surface modules have been introduced communicating again with already interdependent schemes concerning e.g. albedo, soil moisture and rivers. Biological, chemical and physical processes, e.g. photosynthesis or the dissolve of organic matters, are influencing these subsystems again and connect them with each other.

The next difficulties GCMs are faced with are the different timescales in which the processes are taking place in the subsystems. So local weather can be assigned from seconds to hours (coalescence, clouding, rain), while ocean currents are e.g. on monthly scales, internal variability can be expressed in decadal and interdecadal periods and glacier fluctuation or deep water currents take place in centuries or even millennia. These components, which are differently changing in time, have to be coupled in a realistic way. That is why discretised temporal steps for e.g. oceans last from 1 to several days.

Another point may be the positive or negative feedback of the subsystems to each other. With positive/negative feedbacks one would predict an augmentation/abatement of climate change (see 2.2) (VON STORCH, GÜSS & HEIMANN 1999).

However, by the combination of models, systematic errors also affect other subsystems and are hard to capture. A famous instance is the sensitivity of plants on the fertilizing effect of carbon. If a vegetation model correctly simulates this sensitivity, which has been found by observed reactions and former amounts, in reality the reactions and thus the cycles of matter within the atmosphere and the ocean might be wrong (VON STORCH, GÜSS &

HEIMANN 1999), as these are modified by enhanced anthropogenic carbon emissions in future.

With the coupling of autonomous models the new global systems may reach other equilibrium states resulting in worse simulation results than before, e.g. disappearance of sea ice. This is attributed to the new forcing, as e.g. the ocean model is forced by wind of the atmospheric model, while the atmospheric model receives evaporation restrained by the oceanic model. For long simulations this problem has been encountered by flux adjustment (VON STORCH, GÜSS & HEIMANN 1999). However, these adjustments or tunings are the source of further uncertainty. Fortunately the latest generation of models, used in this study, are able to perform without the help of these adjustments. GIORGI (2002b) found also in a comparison in the UKMO models (with the antecedent HadCM2, which performs with flux adjustments, and the up to date HadCM3) that no strong differences in the quality of their projections can be found (further investigation is done by GORDON et al. (2000) who showed only a minor model drifting and persistent temperatures developments of the sea-surface).

In the case of a comparison of different GCMs, the individual specifications respective to their couplings, parameterizations and discretizations might lead to a different response on a certain forcing. For instance some of these differences are investigated in detail by SON et al. (2008) who analyse the role of ozone recovery in models on the development of ENSO during the south-hemispheric summer or by SHINDELL et al. (1999) who compute the impact of different vertical resolutions on the extratropical atmospheric circulation patterns.

2.3.2 "Intra-model" uncertainty

Concerning several simulations of one specific GCM, also discrepancies will develop, originating from different initial conditions a model is fed with at the start of the simulation.

2.3.2.1 Initial conditions

Another aspect is that each climate model produces an internal variability itself. The reasons are the unknown initial conditions the model is started with. At the temporal starting point t=0 an initial value has to be assigned for every variable in every discrete unit. These data are hardly available for today but definitely unknown in most cases for former centuries the models are started in, e.g. soil moisture for all globally units, pressure in all vertical layers or precipitation over sea-surfaces.

To provide these initial conditions a reasonable dataset is generated by an interpolation and an application of correlating algorithms on the few known data, filling the spatial and temporal gaps of missing data and even providing fields of thitherto not observed elements. The homogeneous temporal and spatial grid of data is implemented into the GCM. Nevertheless, these methods of data assimilation or data development by the deduction from other data induce high

uncertainties, which again may cause strong impacts on the modelled results themselves (see e.g. 3.3).

To challenge this problem GCMs are set up for several times with different initial conditions, which are mostly originating from the inherent uncertainties of the generation of these data. It is referred to these modelled realizations as an ensemble of one specific model in the further progress. Therefore it is indispensable to maintain a specific scenario over all these simulations to be able to account for the impact of these different initial conditions. As the retention of the characteristics in the atmosphere is relatively short, one can characterise these different simulations as completely randomized and independent samples of climate taking temporally and spatially effect presented in one climate model (STORCH & ZWIERS 1999, VON STORCH, GÜSS & HEIMANN 1999).

By means of the nonlinearity of these systems, e.g. phase transitions of water, and the complicated equations, e.g. describing fluid components of atmospheric or oceanic streams the choice of initial conditions might have impact on the results, although above they have been defined as randomized. That is why the discrepancies between the ensemble-members could be a measurement of the accuracy of the overall projection (VON STORCH, GÜSS & HEIMANN 1999).

Depending on the complex interactions of the internal processes one may ask whether there are several possible states of our current climate determined by boundary conditions and by external forcing but affected by randomly operating internal feedback or different initial conditions (JACOBEIT 2007). Due to the nonlinearity of the equations the different initial conditions and the parameterizations have strong impact on the goodness of the results of the climate models. As these relatively small tunings may lead to extreme differences in the results, compare the calculation of the deterministic chaos of May (e.g. in VON STORCH, GÜSS, HEIMANN 1999 on p.88), a climate model is not able to make predictions. In this study the terminus projection is applied. This high nonlinearity of interacting climate elements also affects weather forecasts and constrains them to a maximum prediction length of 1-2 weeks (GIORGI & FRANCISCO 2000b). Besides this description, this phenomenon is also known as butterfly effect. However detailed studies about this phenomenon found that the results are mainly shifted in their phases but less in their amplitudes or magnitudes. That is why means and extremes are mainly unaffected in the consideration of time periods of sufficient length. Thus, climate projections are assessable (VON STORCH, GÜSS & HEIMANN 1999). This is evident when many of these processes are averaged. The frequency distribution of the averaged signal has the shape of a Gaussian bell curve. Nevertheless, the averaged curve is temporarily independent and contains no predictability, the so-called white noise. The recalculation of the parameters is impossible in most times. That is why it is particularly hard to obtain the parameters in natural systems where different initial conditions complicate this numerical mathematical approach (VON STORCH, GÜSS & HEIMANN 1999).

2.4   External uncertainty by SRES scenarios

The models have been driven by different assumptions about the global development implemented in different greenhouse gas forcing scenarios. In these forcing scenarios different atmospheric greenhouse gas (GHG) concentrations, mainly Carbon and Sulfur Dioxide, while there are also scenarios for e.g. Methane, CFCs, etc…, are implemented in response to pre-defined emissions, which are estimated on anticipated courses of technological progress, future population growth and environmental awareness (NAKICENOVIC et al. 2000). External variability like volcanic eruptions or solar activity are neglected to separate the human contribution on the natural climate with its inherent variability (see 2.2). This is another aspect to evite the term of "predictions" and to denote climate simulations as projections or sensitivity studies, hence they do not refer to reality (PAETH 2007).

It is noteworthy that not only carbon emissions are included in these scenarios. Also assumptions are made on sulphur emissions, which in turn may impede surface warming by the development of aerosols showing higher absorbing characteristics on short-wave radiation than on long-wave terrestrial radiation (CUBASCH & KASANG 2000). The decrease of global average temperature during the mid of the 20th century is due to sulphur aerosols. At least in industrialized countries enhanced catalysing techniques reduced the emissions of sulphur afterwards.

The presumptions made on the human future reaction are manifold, which lead to a considerable number of different scenarios comprising some uncertainty. Thus, in the **S**ynthesis **R**eport on **E**mission **S**cenarios (SRES) several (meanwhile about 40 different scenarios (PAETH 2007) of these storylines have been introduced by the IPCC, which embrace a broad range of probable future conditions. Each scenario is treated as equally probable (NAKICENOVIC et al. 2000). The most familiar scenarios are A1, A2, B1 and B2 with its subdivisions (table 2.1).

In our study we apply our investigations on the IPCC emission scenarios A1B, A2 and B1, following closely the choice of the 4th IPCC report (MEEHL et al. 2007, p.755) for the 21st century. This selection of scenarios nearly reflects the range of all IPCC scenarios, where B1 can be allocated to the lower end of this range with a CO_2 concentration of about 550ppm at the end of the 21st century. A proceeding change to a service society is anticipated with the use of clean and sustainable energy sources. The global system is depicted by a social, ecologic and economic network. Within the A2 scenario a world of only local economical and technological development and huge regional discrepancies is assumed, while population increases persistently in developing countries, which finally leads to a CO_2 concentration of 850ppm in 2100. Some sort of a compromise offers the A1 scenario, with quick economical growth, the use of new and efficient technologies and a decline of population after a peak in the middle of the 21st century. Regionally discrepancies in development are eliminated by intercultural exchange and schoolings. The "B" is indicating that a balance between fossil and renewable energy sources is employed, effecting a more moderate course for this scenario based on rather adverse/endurable anticipations by the A1FI/A1T scenario. The A1FI scenario projects an increase

of atmospheric CO2 concentration to up to 1000ppm at the end of the 21st century, which is the level of the Mesozoic concentration, 65 million years ago. With the A1B scenario a CO_2 concentration of about 700ppm will be reached (GIORGI & LIONELLO 2008; NAKICENOVIC et al. 2000). Further details, also with B2, which is not used in this study and which will lead to a CO_2 concentration of about 620ppm at 2100, are shown by table 2.1. The former IS92a scenario, which describes a future carbon emission located between the A2 and the A1B scenario, has been withdrawn from recent studies as the sulphur emissions have been estimated as too high (PAETH 2007).

SRES Scenarios		Orientation	
		Ecologic	Economic
Globalisation	Global	B1 (decline of population after peak in the mid-century, resource efficient technologies, global solutions of economic, ecologic and social sustainability)	A1(b) (decline of population after peak in the mid-century, b represents a balance between fossil and non fossil energy sources)
	Regional	B2 (emphasis on sustainability → only local success, persistent increase of population but lower than A2)	A2 (ecological development is spatially fragmented, persistent increase of population)

Table 2.1: Principal segmentation of the main SRES scenarios (NAKICENOVIC et al. 2000).

Considering temperature, the different forcings of the scenarios project an increase of the global averages, while the uncertainties are large, as the B1 scenario evokes the lowest likely increase with 1.1°C and the A1F1 projects a maximal likely increase of 6.4°C for a specific GCM (IPCC 2007, p.13).

However, recently the SRES scenarios have been criticized for different reasons, e.g. as they are definitely not equally possible, while an unbalanced choice of scenarios is applied for many studies (GARNAUT et al. 2008). Furthermore, the "worst-case" scenario A2 is supposed to be still too optimistic in case of future economical growth. This is due to the non-OECD (**O**rganisation for **E**conomic **C**o-operation and **D**evelopment) countries, being generally classified to developing or transition countries, which account for up to 85% of global emission since 2000, while this rate has been at roughly 30% in the late 1970s. This is associated to a stronger reliance on coal (particularly in China), which has a higher potential on CO_2 emission, than oil or gas. For OECD countries the increasing trend is declining. Furthermore, the energy used relatively to GHG emission declines in the transition and developing countries (GARNAUT et al. 2008).

Though it is not the aim of this study, this problem is noteworthy and a critical verification of the reliability of the scenarios associated with the aim of the specific study is suggested. So, in the underlying study, the primary perspective is not the assessment of future climate conditions in the Mediterranean Region for policy makers but the dealing with uncertainties, whereas a comprising range of scenarios is applied. Nevertheless, this also permits a trustful future projection for the Mediterranean Area, as the applied scenarios are still the most influential and thus capable forcings in climate change science (GARNAUT et al. 2008).

For the 20th century control runs the forcing has been conducted by observed GHG and aerosol emissions (20c3m scenario).

2.5 Handling of uncertainties

2.5.1 Dynamical and statistical downscaling

To compensate the shortcomings of crude GCM resolutions and the consecutively concealed variability of climate variables affected by subscale features, several methods have been developed to downscale this global climate projections. One possibility is to nest a regional model into the global model (GIORGI & MEARNS 1999). This regional model is realized on a certain region with a relatively high resolution and so may capture typical regional influences and characteristics in a better way (GIBELIN & DEQUE 2003). At its borders the regional model permanently yields the input variables simulated by the forcing GCM. Unfortunately the above mentioned uncertainties produced by the GCM will be transferred to the RCM. An interesting example is given by PAXIAN et al. (2011), who try to quantify the influence of the NAO on the trends of climate elements, which are projected for the future with the Regional Climate Model REMO (JACOB et al. 2001, JACOB et al. 2007) and the driving GCM ECHAM5/MPI-OM. Firstly, they found, that its impact on trends is quite large and secondly, that the trends are to a higher amount correct after distracting the impact of the NAO, which in turn means, that the NAO, in this case simulated by ECHAM5/MPI-OM, is not well represented. By forwarding the boundary conditions from the GCM into the adjacent areas of the RCM, some crucial aspects affecting the area covered by the RCM, developed in these marginal areas, may be underrepresented (LIONELLO et al. 2006b). So, there is lack in the skill for the nesting methods for employing regional climate models (RCMs) in GCMs over the MA (ALPERT et al. 2006). Still, the problem of discretization and parameterization is also evident in RCMs. Besides REMO (JACOB et al. 2001, JACOB et al. 2007), well known and frequently applied RCMs are e.g. HIRHAM (CHRISTENSEN et al. 1996), GKSS (STEPPELER et al. 2003) or SMHI (JONES & REID 2001). Many of them have been applied for the MA within the PRUDENCE project (CHRISTENSEN, CARTER & GIORGI 2002).

Another promising method is the statistical downscaling (WILBY et al. 1998) as fulfilled within the KLIWEX-MED project group in Augsburg. Here a statistical relation is built up between "known" fields (predictors) and the "unknown" field of interest (predictand). Underlying statistical methods for these relations may be multiple (linear) regressions (HERTIG & JACOBEIT 2008a), Generalized Linear Models (HERTIG et al. 2013a), neuronal networks (HEWITSON & CRANE 1996), model output statistics (GLAHN & LOWRY 1972), canonical correlations (HERTIG & JACOBEIT 2008a) or a weather generator (PAETH & DIEDERICH 2010). The most valuable predictors must be selected carefully, as they also affect each other (multicollinearity), are dependant on season, area and are subordinated to the downscaling approach. E.g. HERTIG & JACOBEIT (2008a) recommend the implementation of 1000hPa and 500hPa geopotential heights in combination with specific humidity for the modelling of precipitation in the MA by a canonical correlation analysis. But still in the case of an elaborate choice of

predictors, the occasional missing of important boundary conditions (e.g. soil moisture as predictor for temperature) must not be underrated

A substantial disadvantage is the presumption of the stability of the found relations between predictor and predictand, as these may not necessarily be valid in future under changing climate conditions and its thus affected internal variability. GIORGI 2002a found by an analysis of standard deviations an increase of 30year variability in the MA for precipitation in winter and a decrease for temperature and precipitation in summer, which can be interpreted as a kind of nonstationarity. Another instance for nonstationarities is discussed by GOUBANOVA et al. 2010. HERTIG & JACOBEIT (2008a) e.g. account for the problem of the nonstationarities by employing a 5 year training period, where the statistical relation is found, for 10 consecutive times (50years), enabling the analyses of the alteration of these regressions. Furthermore a large and deliberate number of predictors should provide a more robust result (HERTIG & JACOBEIT 2008a).

Irrespective of all regionalisation techniques one must not forget that the groundwork is still provided by GCMs. So they are responsible for an adequate projection of decadal and interdecadal climate variability of climate variables and features for the RCMs and on the second hand for an accurate simulation of the impact of a designated climate change on the features of interest (LIONELLO et al. 2006a). TRIGO & PALUTIKOF (2001) investigate GCMs and varying downscaling methods. A further possible approach is the application of high resolution GCMs with the constriction of the analyses on specific time slices to reduce the computational costs (CUBASCH et al. 1995, CHRISTENSEN & CHRISTENSEN 2003). Following this idea, for the underlying work the extremes built up of daily values (also generating a huge amount of data) are analysed by the consideration of specific time-slices.

2.5.2 Underlying Approach

According to the spatial uncertainties, former GCM studies of future climate change have been done in a rather integral way for the average MA, as it facilitates computational costs, enables the possibility of facile comparisons to other regions and may diminish complexity in processing algorithms, e.g. interpolation procedures (e.g. GIORGI 2002b, GIORGI & MEARNS 2002). In the underlying study spatial patterns will be analysed as well, as it primarily accounts for the problem of uncertainties dedicated to individual simulations by considering different models and their different simulations. These models are set up with different parameterization schemes and different discretizations. Consecutively, the simulated climate can be interpreted as randomly possible climate conditions.

With a Monte Carlo approach an ensemble of simulations is created of one GCM which allows to proof different variables and if these variables are rather affected by the external forcings or dominated by the internal variability implemented in the model.

Heterogeneous parameterization schemes are implemented by the different models. To cope with this source of uncertainty different models are analysed by means of some sort of a probabilistic approach. The highly different modelling approaches inherent in the specific models is an advantage in this multi-model approach providing enhanced accuracy in the interpretation of the common signal out of various projections.

That is why it makes sense to compare different climate models with each other. So a range of climate projections and the mean climate projection can theoretically be developed. One will also experience that some results of some climate models seem to be more reasonable than the results of another one. Also some models might differ strongly from the multimodel-mean, while others reproduce their simulations really close to that multimodel-mean. However it is not possible to conclude about the quality of one model´s performance respectively to other models in this way even if the considered model seems to simulate the past time periods in comparison to the observations quite well. The questions arising are surely: Which model is the best? Is one model better than another? Which is correct? Is any model actually correct?

Unfortunately these questions cannot be answered precisely, as even a model which seems to simulate rather strange results might have some correct approaches and thus might simulate specific features more realistic than other models.

The task of this work is to separate the amount of variability of the anthropogenic emissions from the partition of the impact of model characteristics, parameterizations and resolution differences and intra-model uncertainties. This is done within all the models and over a linear combination over all the models and their individual simulations. Despite that it is not the aim to distinguish and to define the sources of intra-model or inter-model variability from each other in a quantitative way. The impact of the anthropogenic emissions is subordinated to the scenarios of the IPCC (NAKICENOVIC et al. 2000) and will be investigated in chapter 4 concerning the long term trend given by all the simulations and models.

As it is discussed above, the nonlinearity of the climatic processes, the unknown initial conditions and the different parameterizations lead to a deterministic chaotic result. In this study the opportunity is offered to average many of these different results given by different climate models with their different parameterizations and their multiple realizations accounting for various initial conditions as their actual values are unknown. With the investigation of the means and the frequencies a good fitting and thus trustful analysis is applied. Shifts in phase of the different simulations and temporal analyses should be treated with care. Furthermore, one has to keep in mind that parameterization is changing within time, as for instance atmospheric transmissivity is affected by enforced greenhouse gas emissions. These processes may enforce or decrease the results and consecutively lead to trends within longer time periods

Additionally other equations may be influenced indirectly leading to positive or negative feedbacks, which again may run into a new equilibrium.

2.6   Benefit from GCMs

First of all, the models provide consistent long time data-series without any spatial or temporal gaps. The short time slice of climate observations can not fulfil these requirements, as the observational records have not been long enough and there are often data vacancies in space and time series. Many of the characteristics and relations within the climate of the MA, illuminated in 1.2.2, have been assessed with the dynamical help of modelling and its statistical analyses. Nevertheless, results of climate models have to be evaluated with observational data in order to assess some sort of reliability when crossing the passage to future data.

GCMs are also used to understand more characteristics of the natural variability of climate and its physical processes (VON STORCH, GÜSS & HEIMANN 1999, PAETH 2007). This is arranged by the separation of features influencing the climate, e.g. by deliberate masking of some features like the anthropogenic emissions, and helps to identify their role in this arrangement of processes (STOTT et al. 2000). A possible consequence might be a distinct identification of the most crucial forcing feature nowadays. Natural variability affecting climate, as e.g. volcanic eruptions or variability in solar radiation, are neglected to separate anthropogenic climate change (see above).

Finally, today the use of numerical models of the climate system is the most valuable instrument for the assessment of the behaviour of future climate in global, regional and local scales (RANDALL et al. 2007). And, not at least because of this fast and low-cost approach, it is an indispensable tool to assess the accompanied possible problems, e.g. sanitary, food security, political and economical aspects, affecting the earth and humanity (PAETH 2007).

Principally there is a restriction in quality and in the amount of all possible conditions, as simulations and projections are constrained in the specific temporal and spatial resolutions of climate models and their parameterizations and are assessed in an approximate way with fundamental presumptions.

Thus one has to keep in mind that climate models are not able to make climate predictions as it would imply detailed forecasts of future conditions. The claim on climate models is rather the projection of general future conditions, e.g. increasing temperature in the climate means in sensitivity studies. Atmospheric short-term conditions have to be analysed in the context of average conditions in at least 30 years (as defined by the WMO). Consecutively, these models project the statistics of the weather and whether these statistics are changing. This is assigned to atmospheric processes being a highly nonlinear system which leads to the obvious problem that weather forecasts are constricted in their accuracy on one or two weeks. Climate models are aiming to detect atmospheric features, changes and variabilities at the order of seasonal, monthly, yearly, decadal or centennial timescales.

In pursuance of GIORGI & FRANCISCO (2000a&b) the uncertainties of the projection of a GCM develop out of three sources:

  1.)   Different forcing scenarios

30

2.) Different GCMs with the specific parametrizations, discretizations and couplings

3.) Different individual simulations of one specific GCM with its initial conditions evoking various results in the simulations by the nonlinearity of the numeric assessment of the internal climate variability

These three sources, making the results of GCMs relatively unpredictable need to be decoded, as they may be quite effective (VON STORCH, GÜSS & HEIMANN 1999). In further chapters point 2.) will be referred as "inter-model" uncertainty and point 3.) will be referred as "intra-model" uncertainty. This catalogue of uncertainties has also been applied by KITTEL, GIORGI & MEEHL (1998).

Further points in this numeration may be the assessment of subscale processes (GIORGI & MEARNS 1991) or the application of RCMs GIORGI & MEARNS (1999). This is not the aim of this study and consecutively, barely resolved processes have to be analysed with care. In this study, embedded in KLIWEX-MED, the aim is to analyse different GCMs with their uncertainty. A new goal can be defined by studies of the uncertainties concerning the nesting of several RCMs (DEQUE et al. 2005). However, as outlined above, this approach is far more complicated as this uncertainty is subordinated to other uncertainties, e.g. GCMs, and thus requires much higher computational and financial efforts. Thus, the analyses of GCMs should be considered as fundamental and antecedent, at which the CMIP3 database (**C**oupled **M**odel **I**ntercomparison **P**roject (phase 3) (see 3.1) provides one modern data collective. On the sub-continental scale (the area of investigation is defined in 3.1.1) GCMs with their specific resolutions are supposed to give reliable estimations of the course of climate conditions (GIORGI 2002a).

Among other studies (e.g. KITTEL, GIORGI & MEEHL 1998; GIORGI & FRANCISCO 2000a & b) concerning sub-continental assessments of climate conditions by GCMs, this study provides a framework with the depiction of inherent uncertainties for other applications like downscaling assessments, as it has been done within the KLIWEX-MED project or for the study of DEQUE et al. (2005), who introduce the application of different RCMs as further source of uncertainty.

It is very hard to account for these uncertainties as research for a better understanding of natural processes is still needed, being aware that mankind will never gain omniscience, being simply restricted by the Heisenberg uncertainty principle. Furthermore, to asses impacts of different resolutions may single-handedly cause enormous computational and labour costs. Although, such studies have been fulfilled meanwhile (GIBELIN & DEQUE 2003, MERKEL & LATIF 2002).

Still, one can finally suggest, that climate models are the best tool to assess a probable climate change in the future.

3 Databases and primary processing

This chapter deals with the sources providing the data utilized in the following study. The first part describes the basic treatments for the data from the GCMs considering the utilization of monthly data in detail. Some constraints prohibited the imprudent acceptance of all the data. These constraints are highlighted and the arguments of a following preselection specified. Furthermore, the fundamental processing of the data by e.g. choosing periods, seasons or interpolation strategies is defined and basic methods of statistical processings are depicted. Chapter 3.2 describes the modifications in the processing of daily data derived by GCMs, while the basic processing is sustained. Afterwards the reanalysis data are introduced and alterations in their treatment described as well.

Out of all the data we extract the monthly means of the variables temperature [C°], precipitation [mm] and sea-level pressure [hPa]. This choice can be justified by different reasons. First of all, temperature should be directly affected by an enhanced green-house effect, based on the physical understandings of the solar radiation balance (e.g. PAETH & HENSE 2002). Secondly, precipitation is strongly affected by large-scale circulation patterns, storm tracks, vapour fluxes and can thus highlight model errors concerning these features and reflect the overall model accuracy over a certain region (GIORGI & FRANCISCO 2000b, PAETH & HENSE 2002). Sea-level pressure is a spatially less heterogeneous field, but might provide possible explanations for the distribution of temperature and precipitation values in seasonal and spatial aspects. Furthermore, for research on climatic impact studies these variables have priority in investigation as particularly precipitation and temperature directly affect the socio-economic conditions (LIONELLO et al. 2006a). Finally, these variables have been investigated in numerous studies concerning a similar ambition (e.g. GIORGI & FRANCISCO 2000b, GIORGI 2002a).

3.1 General Circulation Models

A worldwide approach has been done from about 20 working groups, who calculated several climate simulations and projections for the 20th and 21st century and even beyond by running General Circulation Models (GCMs), which have been considered for the fourth Assessment Report (4AR) of the Intergovernmental Panel on Climate Change (IPCC) (RANDALL et al. 2007).

In this study it is referred to this data, which is obtained from the WCRP CMIP3 Multi-Model dataset at the **P**rogram for **C**limate **M**odel **D**iagnosis and **I**ntercomparison (PCMDI) (http://www-pcmdi.llnl.gov/). The whole dataset consists of the data of 24 different GCMs and is of public access. The reader is kindly referred to this website to obtain further information of the participating GCMs.

This systematic dataset is of unexampled quality and extensiveness and can be addressed as state of the art in the recent climate research (GIORGI &

LIONELLO 2008). Table 3.1 depicts the models of the CMIP3 database with the name and the country of the developing institute and the describing reference.

Model	Reference	Country/Institute
BCCR-BCM2.0	FUREVIK et al. 2003	Norway/Bjerknes Centre for Climate research
BCC-CM1	CSMD 2005	China/Beijing Climate Center
CGCM3.1 (T47)	MC FARLANE et al. 2005	Canada/Canadian Centre for Climate Modelling and Analyses
CGCM3.1 (T63)		
CNRM-CM3	SALAS-MELIA et al. 2005	France/Meteo France - Centre National de Recherches Meteorologiques
CSIRO-MK3.0	GORDON et al. 2002	Australia/Commonwealth Scientific and Industrial Reserach
CSIRO-MK3.5	GORDON et al. 2010	Organisation (CSIRO) Atmospheric Research
ECHAM5/MPI-OM	ROECKNER et al. 2003	Germany, Max Planck Institute of Meteorology
ECHO-G	LEGUTKE & VOSS 1999	Germany & Korea/Meteorological Institute of the University of Bonn, Meteorological research Institute of the Korea Meteorologial Administration (KMA), and model and data group
FGOALS-g1.0	WANG et al. 2004	China, National Key Laboratory of Numerical Modeling for Atmospheric Sciences and Geophysical Fluid Dynamics (LASG)/Institue of Atmospheric Physics
GFDL-CM2.0	GFDL GAMDT 2004	USA/U.S. Departement of Commerce/National Geographic and Atmospheric Administration (NOAA)/Geophysical Fluid Dynamics Laboratory (GFDL)
GFDL-CM2.1		
GISS-AOM	RUSSELL et al. 1995	USA/National Aeronautics and Space Administration/ Goddard Institute for Space Studies (GISS)
GISS-EH	SCHMIDT et al. 2006	
GISS-ER		
INGV-SXG	SCOCCIMARO et al. 2007	Italy, Instituto Nazionale di Geografisica e Vulcanologia (INGV) and Numerical Applications and scenarios Division (CMCC)
INM-CM3.0	ALEKSEEV et al. 1998	Russia, Institute for Numerical Mathematics
IPSL-CM4	HOURDIN et al. 2006	France/Institut Pierre Simon Laplace
MIROC3.2 medres	K-1 Model Developers 2004	Japan/Center for Climate System Research (University of Tokyo), National Institute for Environmental Studies, and Frontier Research Center for Global Change (JAMSTEC)
MIROC3.2 hires		
MRI-CGCM2.3.2	YUKIMOTO et al. 2006	Japan/Meteorological Research Institute
NCAR-CCSM3	COLLINS et al. 2006	USA/National Center for Atmospheric Research
NCAR-PCM	WASHINGTON et al. 2000	
UKMO-HadCM3	GORDON et al. 2000	UK/United Kingdom Meteorological Office, Hadley Center
UKMO-HadGEM1	STOTT et al. 2006	

Table 3.1: Overview of the General Circulation Models depicted in the CMIP3 database with their reference and developing institutions and countries.

To reveal a closer look onto the dataset table 3.2 exhibits information on the introduced models concerning their spatial resolution, atmospheric height and the number of simulations fulfilled in specific scenarios as provided by the CMIP3 database. Colour-shaded models or simulations exhibit errors or cannot comply with fundamental requirements of this study, why these specific simulations/models have not been involved. The reasons for this are different, as e.g. the BCC-CM1 has already been withdrawn by the CMIP3 database as the forcing had been erroneous (http://www-pcmdi.llnl.gov/). Yellow shading is due to a too crude spatial resolution. Green shading is very specific and occurred during the processings and prohibited the further utilization of mentioned simulations as e.g. 10 years are missing in the data. The glosses in

the table provide detailed information. The confinements diminishing the overall dataset are considered in detail in the consecutive chapters.

Model	Resolution	Top of Atmosphere	Simulations per scenario			
			20c3m	B1	A1B	A2
BCCR-BCM2.0	2.81° x 2.81°/ T63	25hPa	1	1	1	1
BCC-CM1	1.87° x 1.87°/T63	25hPa	withdrawn because of erraneous SST forcing			
CGCM3.1 (T47)	3.75° x 3.75°/T47	1hPa	5	4	5	5
CGCM3.1 (T63)	2.81° x 2.81°/T63	1hPa	1	1	1	0
CNRM-CM3	2.81° x 2.81°/ T63	0.05hPa	1	1	1	1
CSIRO-MK3.0	1.87° x 1.87°/T63	4.5hPa	3	1	1	1
CSIRO-MK3.5	1.87° x 1.87°/T63	4.5hPa	1	1	1	1
ECHAM5/MPI-OM	1.87° x 1.87°	10hPa	4	3	4	3
ECHO-G	3.75° x 3.75°	10hPa	5	3	3	3
FGOALS-g1.0	2,81° x 3°/T42	2.2hPa	3	3	3	0
GFDL-CM2.0	2.5° x 2°	3hPa	3	1	1	1
GFDL-CM2.1	2.5° x 2°	3hPa	3	1	1	1
GISS-AOM	4° x 3°	10hPa	2	2	2	0
GISS-EH	5° x 4°	0.1hPa	5	0	4	0
GISS-ER	5° x 4°	0.1hPa	9	1	5	1
INGV-SXG	1.12° x 1.12°	10hPa	1	0	1	1
INM-CM3.0	5° x 4°	10hPa	1	1	1	1
IPSL-CM4	3.75° x 2,5°	4hPa	2	1	1	1
MIROC3.2 medres	2.81° x 2.81°/ T42	30km	3	3	3	3
MIROC3.2 hires	1.12° x 1.12°/ T106	40km	1	1	1	0
MRI-CGCM2.3.2	2.81° x 2.81°/ T63	0.4hPa	5	5	5	5
NCAR-CCSM3	1.4° x 1.4°	2.2hPa	9	8	7	5**/***
NCAR-PCM	2.81° x 2.81°	2.2hPa	4	4*	4	4***
UKMO-HadCM3	3.75° x 2.46°	5hPa	2	1	1	1
UKMO-HadGEM1	1.87° x 1.24°	39,2km	1	0	1	1

Table 3.2: GCMs with their spatial resolution and their atmospheric height. In the columns on the right the number of realizations depending on the considered scenario is depicted, as they are available in the CMIP3 database (yellow: neglected models because of their spatial resolution, red: withdrawn models by CMIP3, green: erroneous data by processing).

*for NCAR-PCM in the B1 scenario the realizations 1 and 4 are starting not before 2200 respectively 2100 and are thus located out of bounce considering the applied periods.

**for run5 the 2070ies are missing

***erroneous by processing, as realizations 1-4 experience a crack (offset) to the 20c3m scenario for sea-level pressure

As table 3.2 indicates, there are more or less realizations per model per scenario. The number of these realizations is not unique across all models and all scenarios and for some categories there is not even one realization available. Some others have been realized for several times per scenario, which will be referred to as an ensemble in the further study.

The model ECHAM5/MPI-OM, will be treated in more detail, as it is also crucial in the other subprojects being part of the KLIWEX-MED project, e.g. it is the model, where REMO is nested in, or as the arrangement for the statistical downscaling procedures. For brevity ECHAM5/MPI-OM will be denoted as ECHAM5 in the following.

3.1.1 Area of investigation and interpolation procedure

The final field of investigation covers the area from 45° to -20° in longitude by passing the 0° meridian and from 26° to 45° northern latitude. The area ranges from the Alps in the North to the North African countries in the south and from the Iberian Peninsula in the West to the countries of the Middle East. Furthermore, a great partition of the Eastern Atlantic Ocean is included with the intention to take its affection into account. This is close to former studies in the Mediterranean region (e.g. GIORGI & FRANCISCO 2000a&b, KITTEL, GIORGI & MEEHL1998) to facilitate comparisons.

To facilitate the analysis between the different GCMs an interpolation on a 3x3° grid has been conducted. This provides the option to compare different grid-cells (in total 184) between the simulations as they are subject to different resolutions (see table 3.2), besides the integral assessment, which is also conducted in this study with the aim to present general features for a more comprehensive perception. The 3x3° grid was chosen as compromise, to preserve a respectively high spatial resolution on the one hand and not to give the illusion of a much higher spatial resolution as actually available on the other hand. Interpolation for temperature and sea-level pressure has been conducted with a biquadratic spline function which fits a second order polynom to the data. The resulting value is adjusted by the computation of the value of the nearest old grid-cell and the gradients to the adjacent zonal, meridional and diagonal grid-cell. For precipitation this was not possible, as negative precipitation values would occur after the interpolation (particularly in low precipitation regions with adjacent high precipitation amounts, e.g. arid zones in Africa in vicinity to the Atlas or the Atlantic Ocean). So with the inverse distance weighting a nearest neighbour method was used. The nearest four older grid-cells have been selected and with a weighting by their distance to the new grid-cell, defined by the cosine, the average has been computed and allocated to the new grid-cell. It is noteworthy that this method performs also as a low pass filter by smoothing original vaules.

Consecutively, the interpolation procedure is the source of further uncertainties affecting the upcoming analyses. A famous instance may be the different discretization schemes with an individual resolution and representation of land-sea contrasts. These specific features, which result in a heterogeneous reproduction of climatic fields are smoothed out and mixed with the filtering effect of the spatial interpolation (GIORGI & FRANCISCO 2000b). Within the framework of the underlying study there was no possibility to account for this problem. However, coastal grids are few and thus it is assumed that this and other subscale effects should be low, besides some smoothing of the values. Still, the comparison is more or less illustrative for NCEP/NCAR, ERA40 and the climate models with their individual specific resolutions as the grid-cells might be out of phase to each other concerning e.g. coastal vicinity which might be expressed differently as ocean cells or land-surface by another dataset. In turn this e.g. may lead to higher or lower temperatures. At least in the regional means of the whole area of interest this disturbing phenomenon should be negligible. Further studies on the impact of different resolutions have been conducted by GIBELIN & DEQUE 2003 or MERKEL & LATIF (2002), who found

a significant enhance of reliability by GCM simulations through a more detailed resolution (T42 to T106) for circulation dynamics.

In order to minimize these shortcomings and the affection by too efficient spatial errors evoked by the interpolation procedure an antecedent choice of the models to be utilized has been fulfilled by disregard of models with a spatial resolution coarser than 3° in both latitude and longitude. Consecutively, 8 models (CGCM3.1 (T47), ECHO-G, GISS-AOM, GISS-EH, GISS-ER, INM-CM3.0, IPSL-CM4 and UKMO-HadCM3) have been neglected, which are highlighted in a yellow frame in table 3.2. The disadvantage of a diminished number of models has been taken into account within this compromise to avoid too strong spatial perturbations. With table 3.2, one can draw following exemplary conclusion after the foregoing selection: For the 20c3m scenario, there are 16 models with totally 44 realizations and 9 models with several members, which are varying in their number dependant on the specific model.

3.1.2 Time periods

In table 3.2 only transient simulations are described, which means that to every future realization a specific control realization precedes on which the future realizations are developing associated with their specific forcing scenario (B1, A1B, A2). A schematic view is given by figure 3.1, taking ECHAM5 for example for precipitation.
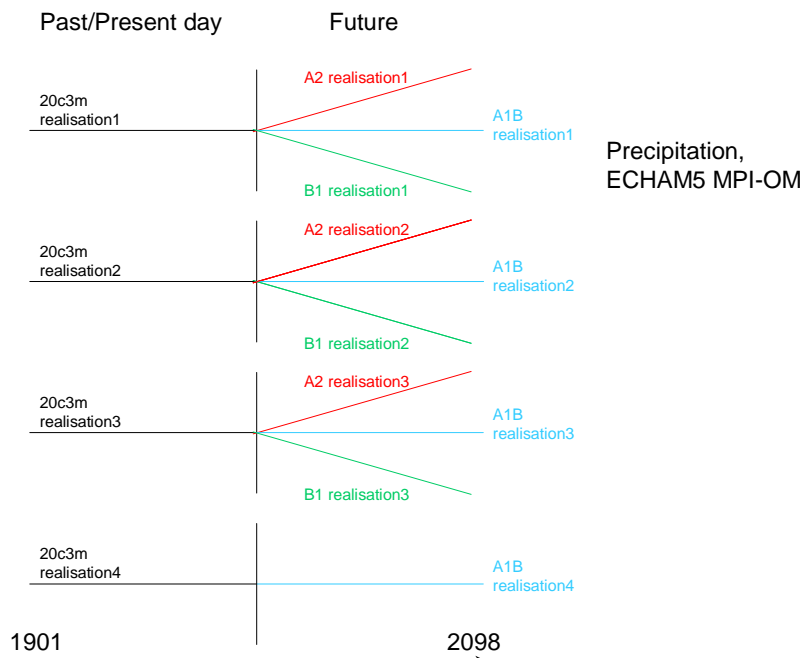
Figure 3.1: Scheme of the courses and combination of different realizations for ECHAM5 for precipitation.

For former times (ca. the 20th century) all runs are forced by the 20c3m scenario which feeds the models with measured CO_2 and aerosol emissions (GIORGI & LIONELLO 2008; NAKICENOVIC et al. 2000). To keep consistency in the realization periods, the considered overall time period was chosen from 1901-2098. This time slice allows an investigation with a maximum number of models, as most of the models have been realized in this period. Furthermore, it previously has been assumed, that nearly 200 years allow an adequate length for desired analytical issues. However, this period also enables the study to analyse control runs and future projections separately. Consecutively, periods of investigation are chosen for 1901-2098, for 2001-2098, for 1961-2050 and for 1961-2000 in order to have a time slice with maximum length, to investigate the future period, to have a transient time slice and to have a time slice which only concerns the reference periods by the 20c3m scenario. The latter one is chosen, as the reanalysis data become more reliable in later periods, see beneath (KISTLER et al. 2001, GIOGI 2002a). This relatively short period is still chosen to last at least for 40 years, to capture effects of decadal internal variability and to avoid sampling errors (FRANCISCO & GIORGI 2000b). Particularly GIORGI 2002a shows the necessity of the choice of time slices of more than 30 years in terms of natural multidecadal variability with the CRU dataset of NEW, HULME & JONES 1999/2000. Within his total integration period from 1901-1998, GIORGI 2002a shows a standard deviation of about 40% for temperature and precipitation mean values in average 30-year time windows from the nearly centennial year mean. The differences between 30-year averages amounts still less than 5% of each variable (precipitation or temperature). On the other hand it is not the intention to extend the temporal period until natural variability is less effective in maybe a centennial period, while man-made impacts by emitting carbon mostly become active in the second half of the 20th century (MOBERG et al. 2006). As many studies already discuss (e.g. GIORGI 2002a), it matters highly which time-period and length is covered by the trend calculation.

In consecutive chapters the data is concerned to yearly and seasonal averaged analyses, whereas the seasons are defined as winter (December, January, February), spring (March, April, May), summer (June, July, August) and autumn (September, October, November), as it already has been done in former studies, e.g. GIOGI 2002a&b. Please note that the winter calculation is conducted with the December mean from the year before. This may lead to discrepancies by comparisons to the overall year, as the whole year data is built from January to December and e.g. the seasonal sums of precipitation cannot be summed up and compared to the whole year sum.

3.1.3 "Cooking Recipe"

After the interpolation, one has several initial files containing monthly values for every grid-cell of one specific realization of one specific model in one scenario of the considered climatic field. The consecutive processing has been conducted as follows:

The "cooking recipe" displays the general processing methods in terms of averages and trends. Later methods being not that common, are described in detail in the specific chapters.

1) Calculation of the different seasons (as already indicated):

Year (January until December)

Spring (March, April, May)

Summer (June, July, August)

Autumn (September, October, November)

Winter (December, January, February)

This is done for all scenarios, all variables and all realizations.

2) Separation in the mentioned time periods (as already indicated):

1901-2098 to comprise the total time-slice

1961-2000 to assess data for the 20c3m runs

1961-2050 to have an analyse of a transient period

2001-2098 to only account for the future.

Again this is done for all scenarios, all seasonal and yearly classifications, all variables and all realizations.

3) Building up ensemble-means:

In the cases, a model is represented by several realizations, the ensemble-mean is built by the average of the number of the different realizations. If there is only one realization for one scenario and one variable, this simulation is defined to be representative for the model. Still the ensemble-means are dependant on the specific scenario, all seasonal and yearly classifications, all variables and the specific period. The number of ensemble-members varies with the scenario.

4) Building up multi-model means:

The ensemble-averages and the models with one realization as well, are averaged to the multi-model mean. Thus the multi-model mean is not weighted by a specific number of realizations associated with the specific models. The reader is early advised that another different multi-model mean has been built by the computation of only the models having more than one realization. This is done in order to conduct the ANOVA, which is introduced in chapter 5. Again this is done with respect to scenario, all seasonal and yearly values, variables and the specific period. It must be specified that the number of models accounting for this multi-model means varies with the scenario, as well as the number of individual realizations. For the ANOVA utilized in the chapter of the extremes (6.3), every realization of every model has been applied to compute the average, with no respect to ensemble-means, thus a weighting of models is at hand.

5) Building of regional means

All results of steps 2), 3) and 4) are subject to an averaging over all grid-cells. Every grid-cell has been weighted equally to compute a mean over the whole region of investigation. The dependence on scenario, seasonality, variable and the specific period is persistent.

6) Temporal average

Each regional mean out of 2), 3), 4) and 5) is averaged over the time resulting e.g. in one final value for data out of 5). This is conducted for every scenario, season or yearly average, variable and period.

7) Building of time-slices

For the period from 1901-2098 all results from step 5) have been subject to a calculation of a sliding mean. Like a smooth pass filtering a certain period is averaged and shifted by yearly steps throughout the whole period of 198 years. The specific mean value is projected on the median year of the integration period. Consecutively, the total length of time is shortened by the length of the averaging period minus 1. This procedure is done twice, once for a 30-year averaging period and secondly for a 60-year averaging period. Once again this is done with respect on scenario, seasonality, variable and of course for multi-model means, ensemble-means and individual realizations.

8) Calculation of trends

Out of the steps 2), 3) and 4) the trends have been computed. This climate changes can be induced by external forcing, e.g. by GHG emissions. It is noteworthy that these trends can be hidden by interdecadal natural variability, e.g. the NAO (see 1.2.2, GIORGI 2002a) or interannual variability, though the latter is considered as negligible, as the integration period of 40 years, i.e. 1961-2000, is chosen as relatively long.

The trends are calculated with a linear regression by means of the least square fit method. Formula (4) describes the least square fit line.

$$4) \qquad Y = bx + a \, ,$$

where Y is the value of the variable and x the number of the annual timestep. The regression coefficient or the slope b is calculated by the ratio of covariance and variance (formula (5)):

$$5) \qquad b = \frac{\sum_{i=1}^{I} \left(x_i - \overline{x} \right) \left(y_i - \overline{y} \right)}{\sum_{i=1}^{I} \left(x_i - \overline{x} \right)^2} \, ,$$

where y represents the variable and x represents the year on the abscissa with i=1,…,I annual timesteps. While a (intercept of axis) is calculated by formula (6).

$$6) \qquad a = \overline{y} - b\overline{x} \, .$$

The coefficicient of determination B is computed by formula (7):

$$7) \qquad B = r^2 = \left(\frac{\sum_{i=1}^{I}\left(x_i - \overline{x}\right)\left(y_i - \overline{y}\right)}{\sqrt{\sum_{i=1}^{I}\left(x_i - \overline{x}\right)^2 \sum_{i=1}^{I}\left(y_i - \overline{y}\right)^2}} \right)^2 .$$

The trend is tested by the application of a t-test with the 0-Hypotheses:

H_0: κ=0

H_A: κ≠0,

where no dependency from Y on X is given when κ=0. With H_0 the statistical test value is given with formula (8).

$$8) \qquad t = \frac{B_{yx}}{S_B} \qquad df : I - 2,$$

where B_{yx} is the estimator from Y to X given by formula (7) and S_B is the "standardized" error of b, given by equation (9):

$$9) \qquad S_B = \frac{\sqrt{S_y^2(I) - B_{yx}^2 S_x^2(I)}}{S_x(I)\sqrt{I-2}} ,$$

where S_x and S_y are the variances of the data of Y and X with its length I. Significance is tested with a two-tailed t-test at the 95% confidence level. The trends are computed individually for each scenario, each seasonal and yearly categories, each variable and in the specific period.

9) Calculation of regional trends

Analogously to 5) all trends have been averaged over all grid-cells, indicating an overall mean-trend over the investigated area, where scenarios, seasonal and yearly categories, variables and periods are persistent.

10) For further investigation within the chapter of the 2-way ANOVA (5.5) a normalization procedure has been executed on the regional means out of the individual realizations resulting out of step 7). More information on this normalization procedure is provided in 5.5. Afterwards for these normalized individual realizations step 3) and 4) have been repeated, followed by step 7).

3.2   Specifications on daily GCM data

For the calculation of the precipitation extremes, daily data have to be applied. These are also derived from the CMIP3 database depicted in the diagram of figure 3.2.
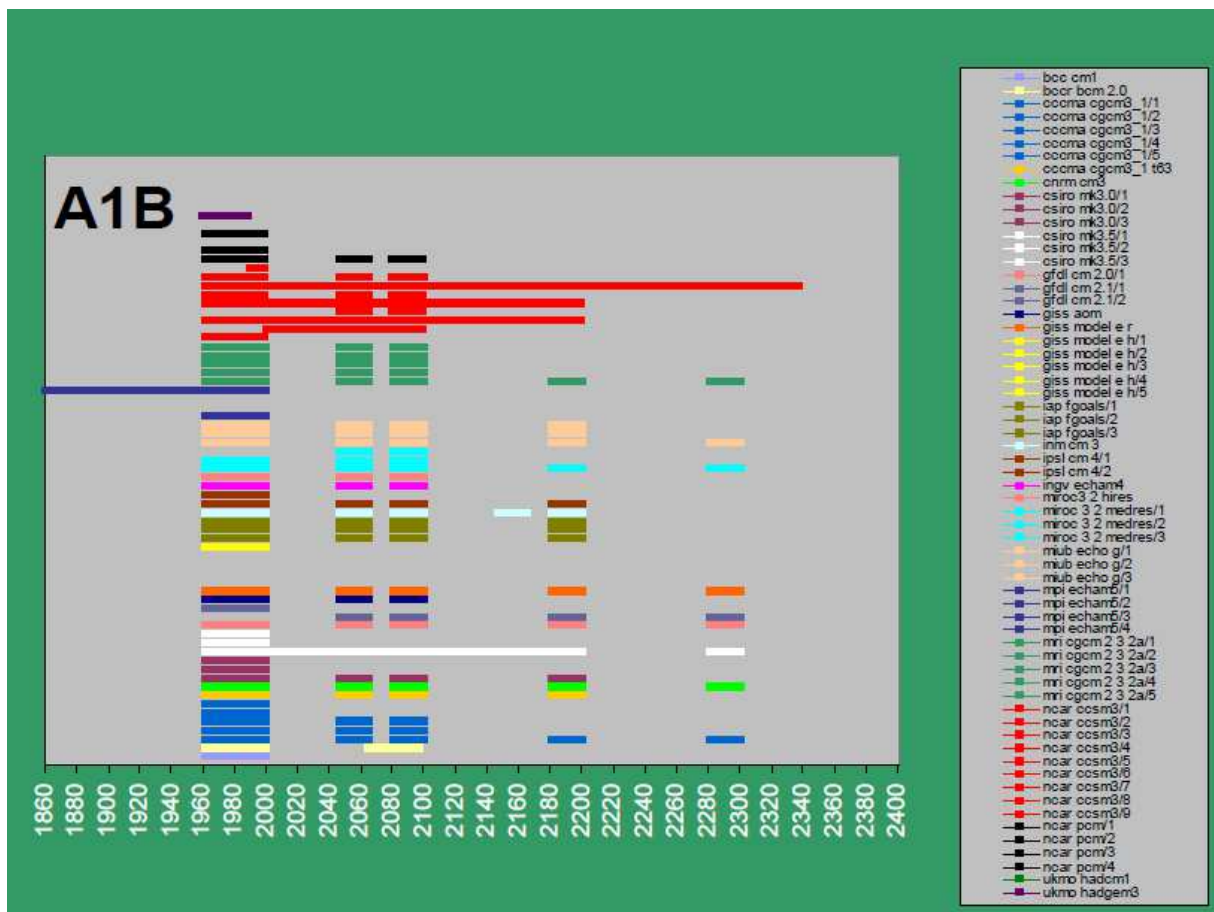
Figure 3.2: Supply of daily precipitation data for the 20c3m scenario and the sequential A1B scenario by the CMIP3 database by the different realizations dependant on the time.

The realizations displayed in the legend, but not figured in the plot directly, have been placeholders dedicated for attempts with other scenarios (not

shown). An investigation of scenarios besides the A1B has been discarded finally as for A1B the maximum number of realizations is available. Again, the foregoing selection considering the resolution of the models applied for the monthly data is persistent leading to the discard of several models. Also the requirement of equal time periods diminishes the amount of models available. To gain the maximum number of realizations the application of the years of 1981-2000 as reference period and 2046-2065 and 2081-2100 are determined (compare figure 3.2). Unfortunately these short time periods of at least 20 years might be disturbed by natural variability (see 2.2 and 2.6 and the consecutive chapter). Nevertheless, this compromise has to be committed to preserve the uncertainty dedicated to a maximum range of realizations. As it easily can be seen, these requirements can not be fulfilled by models, for which only projections are provided in one of the two periods, i.e. UKMO-HadGEM1, GFDL-CM2.1 (with essentially two different runs, one representing the future and the other reflecting the reference period), BCC-CM1, realization 3 by MIROC3.2 medres, realization 1, 2, 4 and 9 for NCAR-CCSM3 and finally the realizations 2 and 4 for NCAR-PCM.

Model	Realizations in the A1B scenario for precipitation
CGCM3.1 (T63)	1
CNRM-CM3	1
CSIRO-MK3.0	1
CSIRO-MK3.5	1
ECHAM5/MPI-OM	1,2,3
FGOALS-g1.0	1,2,3
GFDL-CM2.0	1
MIROC3.2 medres	1,2
MIROC3.2 hires	1
MRI-CGCM2.3.2	1,2,3,4,5
NCAR-CCSM3	3,5,7

Table 3.3: Utilized 22 realizations for the calculation of percentiles.

As ECHAM5 plays a crucial role for this study, daily data of 3 realizations have been directly obtained by demand from the operating Max-Planck Institute in Hamburg. Other realizations are provided with an insufficient length of one of the specific periods, i.e. BCCR-BCM2.0, and by reasons of the missing year 2100 the realization 6 and 8 of NCAR-CCSM3 and unfortunately also realization 1 of NCAR-PCM, which completely discards the model finally. Table 3.3 reflects the remaining models with their 22 realizations finally used for the derivation of extremes. A detailed description of the computation of the percentiles is given in chapter 6. For brevity the investigation of overall yearly findings is discarded, with the intention to preserve a more detailed analyses of the different seasons.

Trends are simply calculated by the differences of the temporal averages of two time periods, while the following building of ensemble-means/trends and multi-model means/trends is given by 3) and 4) of the cooking recipe for

monthly data. Still, the dependency to grid-cells, periods and seasons are sustained within the multi-model datasets.

3.3   Reanalysis datasets

The goal of assessing future climate with GCMs implies to employ observation data of former atmospheric conditions in order to have a more or less adequate possibility to compare the results of GCMs with the observations in the so-called control periods. For this intention, two sets of reanalyses data are used.

Reanalysis data "is the analyses of past observational data using a fixed, tried and tested data assimilation system" (UPPALA et al. 2005, p. 2969). This leads to a combined estimation of the state of the atmosphere at specific time-steps being assessed from observations and background knowledge of the atmosphere. The observations consist of different measurement methods and variables, being spatially and temporally not equally distributed in the majority of cases and contain specific errors and specific amounts of accuracy. The background knowledge is modelled in short range forecasts of about 6h and calculated from the observations and again the former background assessments of the atmosphere. This is necessary to achieve a comprehensive dataset, which is complete in terms of the domain, time and meteorological fields. Thereby 6h cycles of reanalyses sequences are developed consisting of a statistical combination of individual initial states given by the atmospheric background and observations and again of values from the observational network. Thus the data are developed from a dynamical and physical modelling part and dynamical physical relationships to observations are given by error statistics. That is why the spatially and temporally density of the observational network has great impact on the performance of the reanalysis dataset (UPPALA et al. 2005).

Shortcomings accompanied with this method are deficiences within the statistical aggregation of background and observation data or the modelling of the background itself. These introduced biases or even trends can prohibit conclusions on climate change or studies of long-term variability. However, many errors could be identified and corrected by expertise knowledge about reanalysis settings. Setting up assimilation algorithms lead to further improvements of these reanalysis datasets (UPPALA et al. 2005).

The first "reference set" utilized in the underlying study is a reanalysis dataset by a cooperation project of NCEP (**N**ational **C**enters for **E**nvironment and **P**rediction) and NCAR (**N**ational **C**enter for **A**tmospheric **R**esearch), shortly referred to NCEP in the following. The measurement techniques range from rawinsondes and satellites to surface stations collecting data of e.g. pressure, humidity, temperature, wind speed and precipitation. With the aim of generating a homogeneous and transient grid over the whole globe a model is developed, adjusting and computing missing values of some fields by physical or statistical relationships with further variables (KISTLER et al. 2001, UPPALA et al. 2005).

The result is a comprehensive data set containing transient values of surface temperature and precipitation among further variables like rotational wind or geopotential heights. Particular temperature is a relatively reliable value as mainly station data with direct measurements have been utilized for this assessment. While temperature in upper atmosphere is declared as a class A variable, precipitation is less trustable and only denoted with a C rating, as it is derived by modelling assessments and thus completely dependant of other variables and their assimilations being in turn accompanied by uncertainties. Even the surface near temperature is only rated with B, as the model orographics are divergent to the real surface conditions as response to the model-specific spatial resolution and thus surface values are only secondarily implemented. Additionally surface temperature is also modelled by heat fluxes and their parametrizations in the model. Altogether, this also provides high uncertainties concerning surface temperature. Furthermore, by mistake wrong snow cover data have been used for the years from 1974-1994, which has greatest impacts in autumn and spring. With its moderate climate it is decided to use NCEP though, as snow cover impact may be negligible in the MA, except for some north eastern and elevated regions. KISTLER et al. (2001) figure out that the main impacts are experienced over the US and Canada. Compared to other reanalysis data NCEP shows the highest RMS error to satellite data for precipitation over the northern hemisphere between 20°-80° over both, ocean and land surfaces.

Thus, caution is recommended by using this data and with ERA40 a second reanalysis dataset is consulted, which was developed by the **E**uropean **C**entre for **M**edium-Range **W**eather **F**orecasts (ECMWF). Likewise to the NCEP data also the ERA40 data was built from an aggregation of several observation-methods like satellites, buoys, stations, radiosondes, etc... Again, within time, the observation methods to the total amount of observations changed with e.g. an increase of satellites and a general increase of the utilization of remote sensing instruments accompanied by a decrease in the use of radiosondes from the late 1980s onward, although the latter reached a higher accuracy. Anyway, new techniques like buoys can easily compensate the closure of former stations like fixed ocean weather ships. Still, shortcomings are evident by e.g. incomplete data like flight pressure levels from airports before 1973 or lack of station data prior to 1967, which is e. g. reflected in temperature, humidity and soil moisture values. Data of snow coverage is not existent in early years and thus similar to NCEP not properly trustable. Also for ERA40 surface air temperature is affected by the issue of snow coverage (see above), as also improvements between ERA40 and ERA15, the precedent dataset, are shown, when the parametrization of snow-albedo is enhanced for ERA40. These improvements include higher horizontal and vertical resolutions, more observation stations and a stronger implementation of satellite data, by comprising direct measurements. Furthermore, atmospheric fields have been widened by an introduction of ocean-wave analysis and ozon. This improvement can also be stated for the eastern Mediterranean regions. Likewise to NCEP it must be stated, that also within the ERA40 data temperature is a product of an interpolation procedure connected with a modelled atmospheric background and thus not only derived from in situ measurements. For further readings on ERA40 on data coverage, accuracy and reliability the reader is kindly referred to UPPALA et al. (2005).

Several approaches can be used to assess the reliability of reanalysis datasets. Examples are the calculations of short range forecasts from the reanalysis data and check the accuracy of these forecasts. Others may be the comparison of simulated variables with measured variables, or the assessment of global mass balances from reanalysis, or even the comparison to other reanalysis datasets. The NCEP results are approved as they are e.g. already interpreted in former studies (e.g. MARIOTTI, ZENG & LAU 2002; FERNANDEZ, SAENZ & ZORITA 2003). Also XOPLAKI et al. (2004) achieve a good relation of NCEP and about 300 stationary observation series applying a 4-year running mean filter on both datasets in the last 50 years of the 20th century with a coefficient of correlation of about 0.78. KISTLER et al. (2001) nevertheless showed relative good agreement of NCEP reanalysis data of surface temperature and station-data. Figures with global and tropical spatial means indicate slight underestimations of NCEP, particularly in the last decade of the 20th century of about up to a half degree in the global mean. Besides NCEP, also ERA40 has proven its applicability many times in numerous studies, e.g. in LIONELLO et al. (2006b).

Main specifications of these two reference datasets are displayed in table 3.4.

	Spectral resolution	Horizontal resolution	Vertical resolution
ERA40	T159	2.5°x1.9°	60 vertical levels
NCEP	T62	1.875°x1.92°	28 vertical levels

Table 3.4: Main specifications of ERA40 and NCEP data.

Consecutively, one can state that reanalysis datasets are also equipped with errors, being diminished by more comprehensive measuring systems, an increasingly spatial and temporal coverage of measuring systems and by the building of temporal and spatial means, as erroneous data are smoothed out (GIORGI 2002a). Whereupon both, NCEP and ERA40, have been interpolated onto a 3x3° grid to fit with the developed model grid. This should reduce highly resolved errors. Furthermore, temporal and spatial averages are computed by means of the "cooking recipe" 5) and 6). Herewith the common time periods from 1961-2000 are employed, although NCEP is available from 1948 onward (1957 for ERA40). The reason for a shorter period is that earlier times are afflicted with greater uncertainties associated with the inevitable problems of less observation stations, the heterogeneous spatial distribution of these stations, etc… (KISTLER et al. 2001).

For observations it is difficult to assess meaningful trends, as the measurement changed during time and the earliest data are affected by high uncertainties (see above). Although, for qualitative comparisons the trends of the reanalysis data have been calculated by 8), followed by 9) of the "cooking recipe".

However, the uncertainties are highest within regions of temporal and spatial sparse coverage of measuring systems, e.g. in mountainous areas, over sea

surfaces or in deserts. Still, by embracing two different sets of observations this study copes some amount uncertainty.

4   Means and Trends in the Mediterranean Area

Although the increase of GHG concentration is homogeneously distributed in the atmosphere and will consecutively affect temperature everywhere, the projected warming on global average is not homogeneously distributed over the earth surface, as climate originates from a mixture of further forcing effects like e.g. aerosols, land-use change, orographic steerings, coastal vicinities or last but not least simply the impact of short-time natural variability (e.g. CUBASCH & KASANG 2000). It is needless to say, that this also is the case for other fields like precipitation or sea-level pressure, as e.g. temperature is a steering element for the general circulation with its impact on precipitation and the capacity of water content in the atmosphere (Clausius-Clapeyron relationship, e.g. FREI et al. 1998, DEQUE, MARQUET & JONES 1998). As outlined in 1.2 the MA is a highly complex region with its typical characteristics, which cannot be catered by analyses in global contexts (GIORGI 2006). This already becomes evident in global maps of the IPCC (MEEHL et al. 2007, p. 767), where the trends of temperature, sea-level pressure and precipitation are depicted for summer and winter.

The primary objectives of this chapter are to provide an insight on the projected mean and trends over the models with respect to the reanalysis data, which allows at least qualitative information about the models´ ability to represent former climate conditions, supposing correctness of the reanalysis data. Nevertheless, it is a general problem to compare models´ projections with observations or reanalysis. At least by the missing correctness of the past observations the evaluation of the models suffers problems. Furthermore, biases to models evoke, due to specific locations of observation stations the reanalysis data are reassessed with, clearly affecting temperature or precipitation when the station is on the top of a mountain or in a luv- or lee position, as climate models can not account for these small topographic issues. Also urban stations may reflect a warmer climate disturbed by anthropogenic heat clusters. However, it is quite interesting to compare observed trends with the trends out of the simulations of the GCMs. If the model shows this trend also, confidence in the model to adequately reproduce long-term climate changes will be provided.

For a first view on the course of GCMs and their reproduction of past climate with a comparison of reanalysis data spatial means and trends for the period of 1961-2000 are calculated for each simulation for temperature, precipitation and sea-level pressure. Multi-model-means and ensemble-means for ECHAM5 are opposed to similarly computed reanalysis data, i.e. NCEP and ERA40. Finally, out of this regional means and trends are built and comprehensively illustrated. All the computation has been done in a seasonal and yearly approach. Individual realizations are not shown for brevity in this chapter as a detailed analysis of their individual course is followed in chapter 5.

A closer description of these data is found in chapter 3. For a closer view on the data setup, the ensemble-means and the multi-model mean table 3.2 provides information, whereat always the maximum number of available

simulations/models has been utilized, following the idea of e.g. REIFEN & TUOMI (2009), that a multi-model mean of maximum number of realizations and models comprises the maximum possibilities of future climate developments, though this dataset deviates from the dataset of the ANOVAs (see 5). The methods of the calculation of the means and trends are found in the "cooking recipe" in chapter 3.1.3.

Afterwards same analysis is conducted for the future periods of 2001-2098 with different scenarios with the intention to provide a future projection of climate conditions developing in the MA. The figures depicted in this chapter contain maps, which are structured consistently by illuminating the assessed means in the left column and the calculated trends in the right column. The rows indicate the overall year values and the yearly sequence of seasons from top to bottom, i.e. spring, summer, autumn and winter.

4.1   Reference Period (1961-2000)

At first the period of 1961-2000 is investigated in more detail with two fundamental aims. At first it is important to gather some insight on the different behaviour of the models in the simulation of climatic conditions, which already took place. These already experienced climatic conditions allow the comparison with the simulated results of the models.

4.1.1 Temperature

Although Mediterranean temperature is not such a highly variable unit than precipitation, e.g. GIORGI 2002a assesses the interannual variability over the whole year of about 0.25°C by the standard deviation, it is strongly dependant on several perturbations by e.g. land-sea interactions, regional conditions or of course large-scale steering (ALPERT et al. 2006, TRIGO et al. 2006). Highest interannual variability is found in winter with up to 0.6°C. Interannual variability can be enforced by snow-ice cover feedbacks, whereas colder regions than the MA should be affected more strongly (GIORGI 2002a).

By starting with the reanalysis data NCEP, in the left column of figure 4.1, one clearly recognizes the seasonal cycle of temperature having maximum values in summer (middle row) and coldest in winter (lowest row), while autumn (fourth row) exhibits slightly higher temperatures than spring (second row). The north-south gradient with warmer values in the south is common to all seasons. Lowest values can be found in the northeastern parts southern to the Caucasus with about 4.7°C in the annual mean and slightly above -6°C in winter. Hottest values are reached with slightly above 35°C in Sahara and the continental areas of the Syrian and Arabian Desert (~34°C) in summer. The difference between water surfaces and land-surfaces clearly becomes evident.

The NCEP dataset describes a warming trend (right column of figure 4.1) in the MA, being particularly pronounced in summer in the northeastern regions, with up to roughly 2.5°C over northern Spain and Israel, but being also evident

in other seasons and consecutively still significant (black dots) over most regions for the whole year (first row). Over the total year the countries at the southeastern coast of the Mediterranean Sea are affected strongest by the heating, where the trend shows significance. Nevertheless in the colder seasons NCEP also reveals strong cooling patterns attaining nearly -5°C in eastern Turkey with maxima in winter. The cooling area over Saharan regions is persistent over all seasons and reaches significance in the results for the whole year.
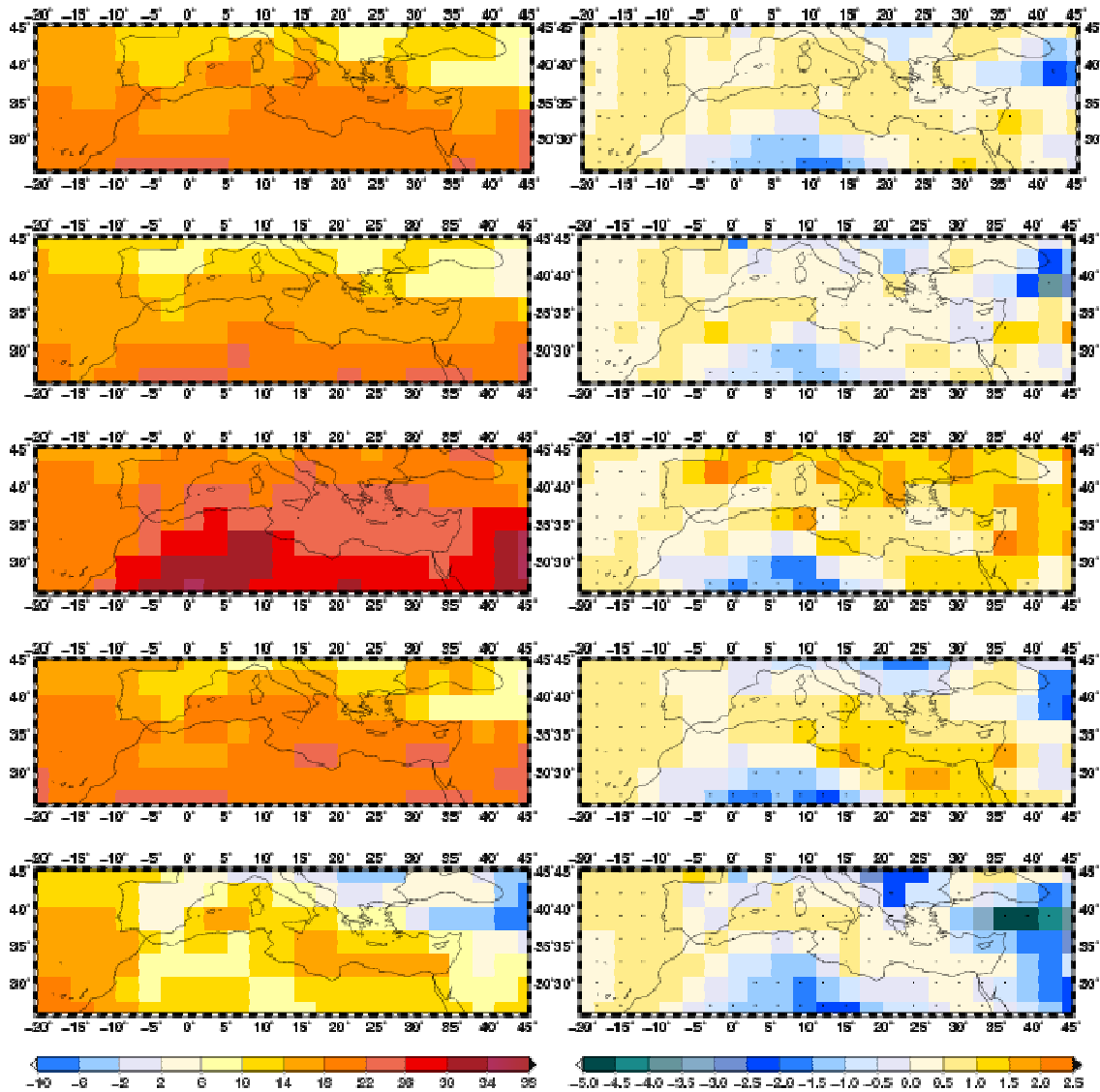
Figure 4.1: Interpolated NCEP means (left column) and NCEP trends (right column) for temperature [°C] in the period of 1961-2000. Rows indicate the season from top to bottom year, spring, summer, autumn and winter. Black dots in the trend figures represent significance at the α=5% level.

In addition to the NCEP results the means and trends of ERA40 are displayed in figure 4.2. The latter data exhibits (1.82°C in the regional average for the year) warmer temperature values than NCEP. This is persistent over each season and nearly holds for every region. The spatial pattern is in notable agreement between these two reanalysis data.

Compared to NCEP an accentuated warming in summer is not that evident. Still the seasons of strongest warming remain summer and autumn. While winter does not reflect a similar magnitude of cooling in ERA40. Still the yearly warming trend of 0.45°C (0.15°C in NCEP) on spatial average is apparent. The trends of ERA40 show distinct differences in their spatial distribution to that of NCEP, as it is somehow shifted to the west. Consecutively, the significant negative trend over the Saharan region is not visible in the ERA40 data as it is depicted as one of the regions with the strongest signal exhibiting significant positive trends within this period. The northeastern part of the Mediterranean is subordinated to cooling processes having maximum values in winter, which is analogous to NCEP but not significant in most of the grid-cells. Overall, for both NCEP and ERA40, in the east of our study area it becomes more difficult to assess temperature changes.

Figure 4.2: *Interpolated ERA40 means (left column) and ERA40 trends (right column) for temperature [°C] in the period of 1961-2000. Rows indicate the season from top to bottom year, spring, summer, autumn and winter. Black dots in the trend figures represent significance at the α=5% level.*

The ensemble-means of the realizations 1-4 of ECHAM5 in figure 4.3 capture well the seasonal cycle. Overall the pattern is well reproduced by the GCM, while it shows a more smoothed northeast distribution of temperature values than the observations. The values are more reminding of the NCEP data, as they exhibit the coldest values of all the three data sets.

Concerning the trends one can see that (right column of figure 4.3) only in spring the northern MA and in winter some western areas experience a slight decrease of temperature, which is not established by the reanalysis data. However, with 0.48°C the spatially and seasonally averaged trend the magnitude of warming is near to the reanalysis, while strongest warming is also simulated for summer. Despite the reanalysis data, ECHAM5 indicates a more homogeneous spatial distribution of the trends in figure 4.3. The trend is significant in most cases, although it does not reach the high absolute positive or negative values as the reanalysis data do. The east/west contrast shown in ERA40 and NCEP is not reproduced.
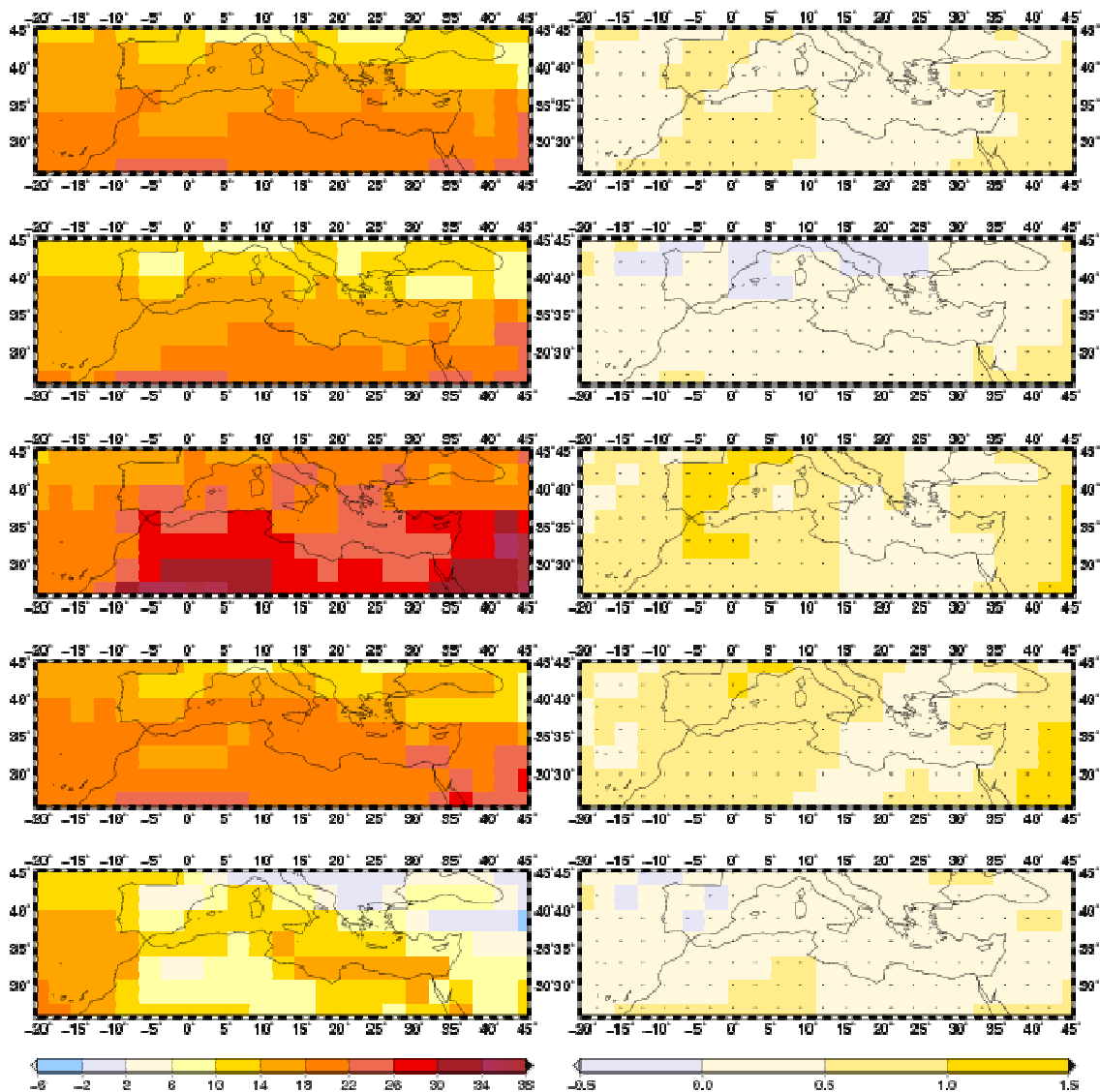
Figure 4.3: Interpolated ECHAM5 ensemble-means (left column) and ECHAM5 ensemble- trends (right column) for temperature [°C] in the period of 1961-2000. Rows indicate the season from top to bottom year, spring, summer, autumn and winter. Black

dots in the trend figures represent significance at the α=5% level.

The seasonal cycle of temperature (figure 4.4, left column) with the hottest to the coldest seasons from summer to autumn, spring and winter is still found in the multi-model mean indicating the good performance of the models in representing the seasonal specific temperature. The multi-model mean shows the most homogeneous pattern of all members of this data group. This is due to the filtering effect of the averaging method. Special features of individual models with their specific simulations and again their individual projected values are smoothed out. That is why horizontal bands of equal temperature are predominant, sometimes following the land-sea distribution. Only in winter the relatively cool continental part of northwestern Africa is spared out. It is noteworthy that ECHAM5 is close to the multi-model mean concerning the spatial pattern and the absolute values, which in turn implies that the differences of ECHAM5 and the reanalysis apply also for the multi-model-mean and the reanalysis data.

In the right column of figure 4.4 the trends of the multi-model-mean are depicted. Still, highest warming occurs in summer with largest magnitudes in the east following the reanalysis data with NCEP in particular and the central north of Africa, which rather recalls the information given by ERA40. Small indications of cooling, as e.g. shown by ECHAM5 in the colder seasons, vanish by the effect of averaging. Significant warming trends of about 1°C are given over large parts of the region. Regional characteristics captured by individual models are lost.
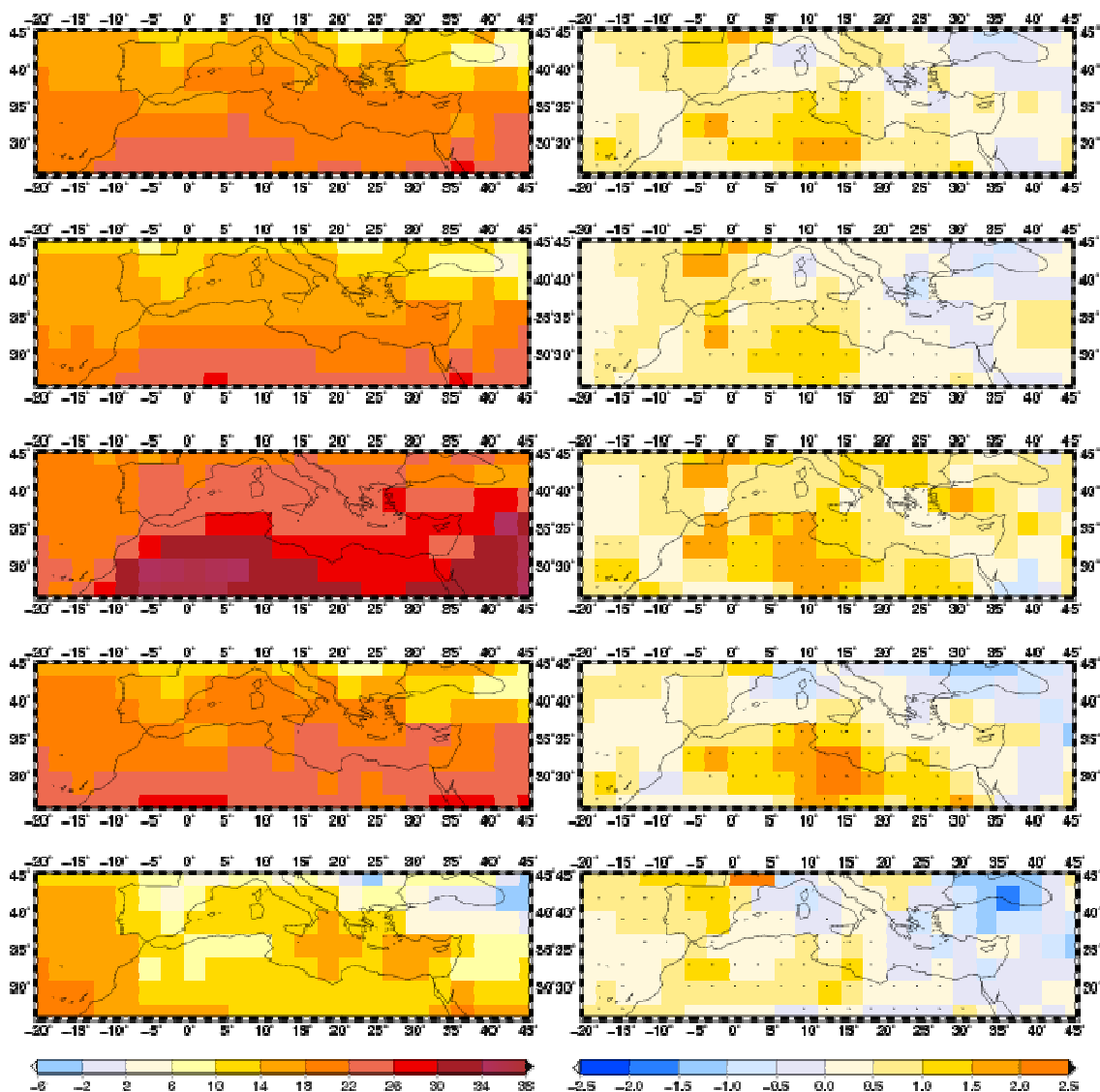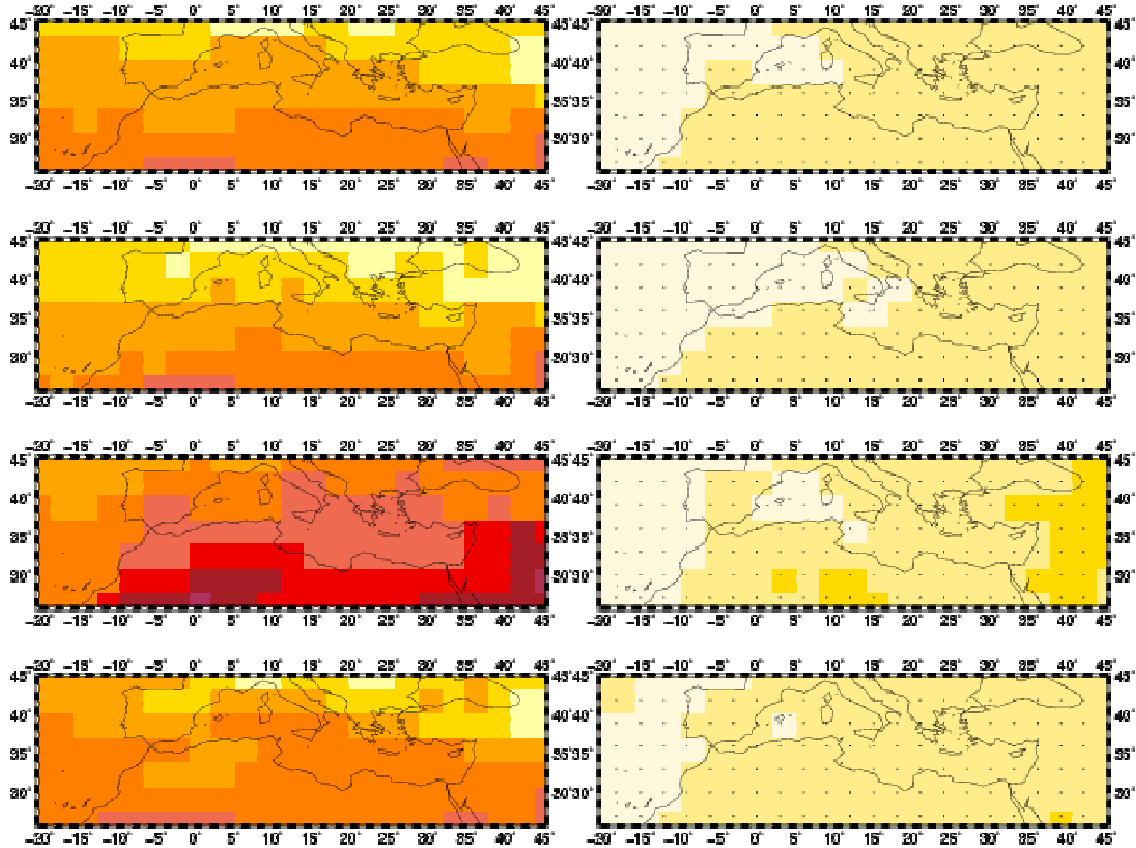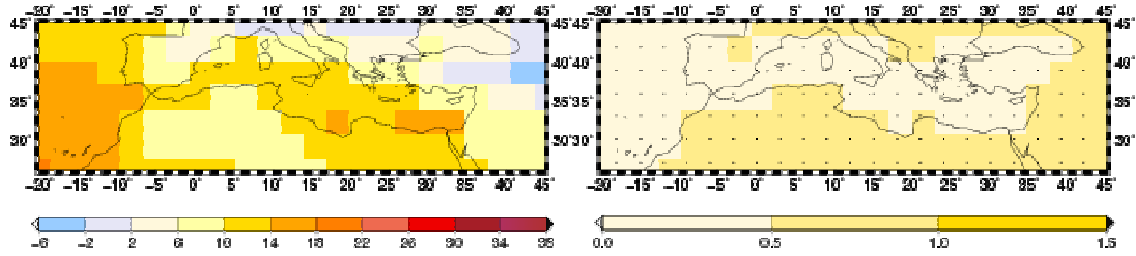
Figure 4.4: Interpolated multi-model means (left column) and multi-model trends (right column) for temperature [°C] in the period of 1961-2000. Rows indicate the season from top to bottom year, spring, summer, autumn and winter. Black dots in the trend figures represent significance at the α=5% level.

Temperature Mean 20c3m 1961-2000
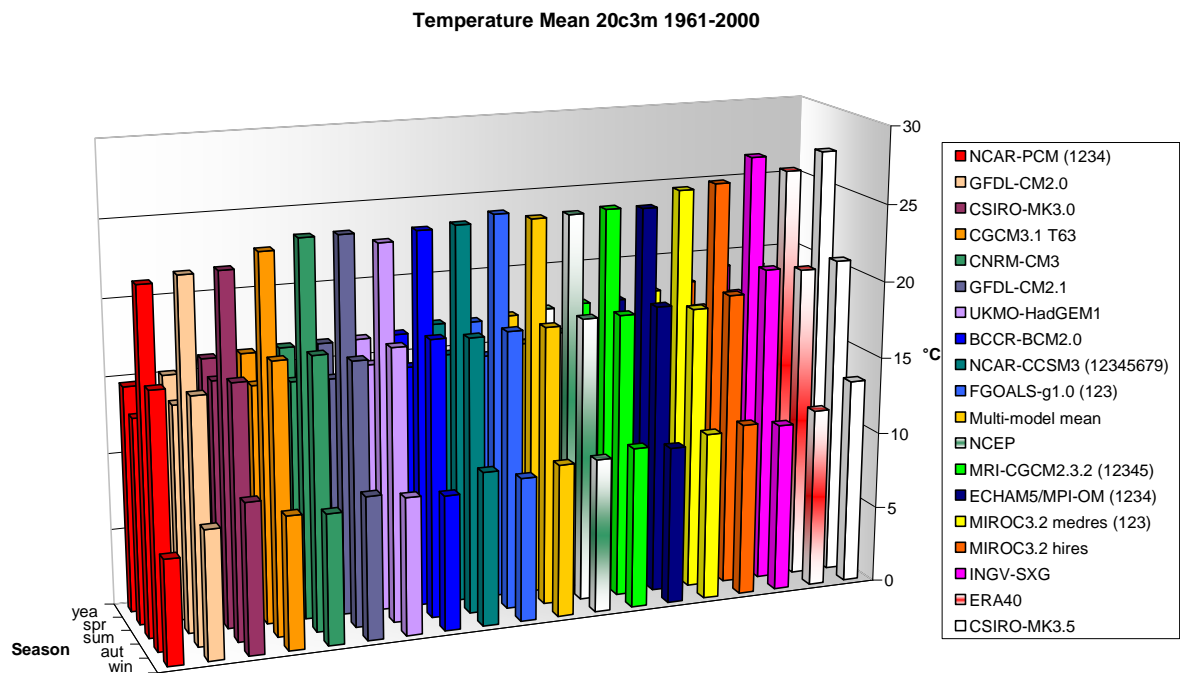
Figure 4.5: Regional temperature means [°C] of GCMs (20c3m) and reanalysis data for the specific seasons computed for the period of 1961-2000.

Concerning the multi-model mean and the averaged reanalysis data the difference is 1.4°C in spring (below 1°C in the other seasons, and roughly 1.2°C for the whole year). Definitely the models match better in winter than in summer. However each model shows an apparent seasonal cycle.

In figure 4.5, the cooler part of the models setting up the multi-model mean are beyond the gap of the two reanalysis data sets. Thus, one can easily state that the warmer partition of the models seems to be more realistic, while 5 models are located within the bias of the reanalysis data. However, the models fit quite well with the reanalysis data, particularly with respect to the bias between NCEP (17.34°C yearly average) and ERA40 (19.15°C). As the models are sorted by their yearly averages only CSIRO-MK 3.5 is a mite hotter than both of the reanalysis data. Consecutively, though the possibility for NCEP is existent of being too cold, the NCEP reanalysis data shows a high agreement to the multi-model-mean for the MA as figure 4.5 illustrates. Still, the NCEP data

are far beneath the ERA40 reanalysis data. A possible explanation of a supposed general underestimation of the temperature by the models in winter may be the recent neglection of flux adjustments in several models, leading to a failure in a warmer adaption of sea-surface temperatures, which would lead to a more moderate surface temperature in the air particularly in winter (see also the spatial maps in figures 4.1-4.4) (GIORGI 2002b). However, the distribution of models with the implementation of flux adjustment cannot explain the alignment of the models in figure 4.5. The spread between the models accounts up to 5.5°C for the year.

Compared to the reanalysis data the models differ in the magnitudes of the trends and the seasonal distribution (figure 4.6), whereas the reanalysis show a distinct difference of maximum increases in summer and the other seasons. In most of the models the warming is equally distributed over all the seasons. Differences between the various datasets may be explained by a mismatching topography. So, for reanalysis data height has been used as predictor for the assessment of temperature. In the models the resolution and thus the topographic features are different as already mentioned in chapter 2.3.1.1. These features are averaged resembling in a not adjusted temperature to height instead of to the reanalysis data. For precipitation this problem should be negligible, as precipitation furthermore depends on luv-/lee effects, convection, etc…, and thus should not be related directly with height (GIORGI & FRANCISCO 2000b). Disregarding the NCEP data in winter, all members depict a rising trend, varying from 0.25°C to nearly 1.1°C. GIORGI 2002a explains his findings of strong positive CRU trends with snow-cover or ice albedo feedback in winter. If this holds true the negative NCEP trend depicted in figure 4.1 becomes rather doubtful as KISTLER et al. (2001) describes the NCEP data as erroneous concerning the data of snow coverage, which affects the modelled temperature values, as already discussed in chapter 3.3.

Temperature Trend 20c3m 1961-2000
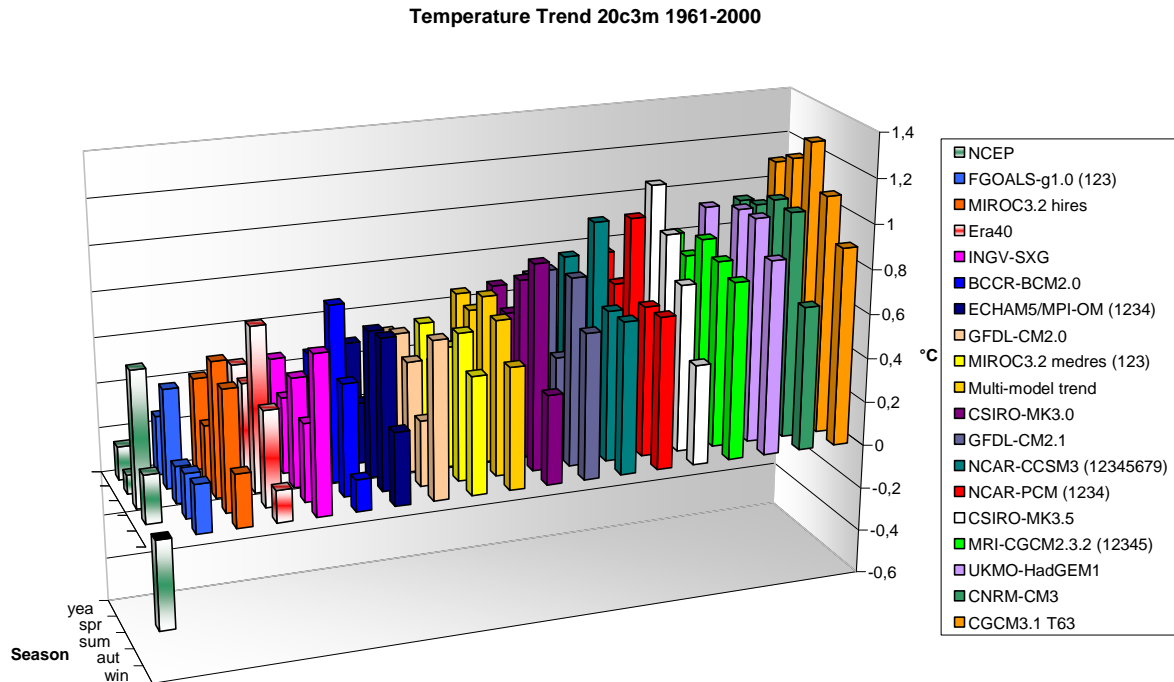
Figure 4.6: Regional temperature trends [°C] of GCMs (20c3m) and reanalysis data for the specific seasons computed for the period of 1961-2000.

4.1.2 Precipitation

Precipitation is one of the most important climate parameters as it is not only one of the main characteristics in the definition of local climatic conditions (e.g. KÖPPEN 1931). Furthermore, it strongly affects socio-economic (e.g. agriculture) and environmental (e.g. vegetation) systems (GIORGI 2006). "Precipitation patterns are the most evident limiting factor for human activities and natural ecosystems in the Mediterranean. If climatic change produces quantitative or qualitative alteration of rainfall patterns, human communities and natural ecosystems can be irreversibly damaged." (LUTERBACHER et al. 2006, p. 40). Its frequency and total amount determines the benefit of irrigation systems, hydroelectric power generation or water supplies, which holds for most of the Mediterranean countries (COSTA, SANTOS & PINTO 2012, TRIGO et al. 2006). GIORGI 2002a estimates an interannual variability of up to 5% over the whole year and up to 15% in summer. This former result is rather surprising as the variability in the cold season should be more pronounced as the impact of large-scale circulation patterns, i.e. particularly the NAO, (see 1.2.2), become predominant with their own high variability itself then. In summer the interannual variability is steered by convective effects being forced e.g. by evaporative activities see also 1.2.2. As described in several studies, the global distribution of precipitation trends is heterogeneous with a projected future increase in the tropics and higher latitudes (PAETH 2007, MEEHL et al. 2007). Regionally, the shift in precipitation amounts is due to a modification of synoptic circulation patterns affecting jets, storm routes or Monsoon teleconnections (GIORGI 2002a). E.g. by an enforcement of tropical steering circulations a further decrease is projected in the already relative arid subtropics (PAETH 2007). For

local assessments of small scale conditions the thermical structure of the atmosphere has to be considered. Generally, one has to expect an increase of precipitation by a thermal induced amplification of the atmospheric moisture content and a consecutive enforcement of the hydrological cycle (GIORGI 2002a).


Figure 4.7: Interpolated NCEP means (left column) and NCEP trends (right column) for precipitation [mm] in the period of 1961-2000. Rows indicate the season from top to bottom year, spring, summer, autumn and winter. Black dots in the trend figures represent significance at the α=5% level.

One can clearly extract the specific seasonal variation of the precipitation in figure 4.7 from NCEP. The main part of the yearly precipitation amount occurs in the colder season from October to March while in winter, i.e. from December to February precipitation is most and thus about three times higher than the precipitation amount in summer. This is e.g. associated with the track of Atlantic low pressure systems defined by the NAO (see 1.2.2). The relatively high precipitation amounts in winter are followed by the intermediate rainfall in spring and autumn when the impinging of the storms on the European continent with their high precipitation magnitudes migrates northward. In summer the

precipitation amount is lowest. However, the contributions of spring and autumn are considerable, while in summer particularly the countries in the south of the MA suffer droughts, often accompanied with heat periods resulting in pronounced arid conditions. This water shortage is only counteracted by rare storms or convective rain (TRIGO et al. 2006). Besides the seasonal cycle a latitudinal distribution is evident, i.e. the amounts decrease from north to the south, to the arid zones and deserts in northern Africa. The Red Sea Trough, mentioned in chapter 1.2.2 rarely effects precipitation as the trough is located in lower atmospheric layers surrounded by dry air and overlayed by a high pressure system preventing rising and cooling of air masses. After interpolation the topographically generated precipitation maxima are rather crude but still identifiable, evoked e.g. by convective processes and their implementation of topographical modelling, e.g. in the vicinity of the Alps, the Atlas or the Balkans GIORGI, BI & PAL (2004a/b). Levante particularly in summer suffers high aridity because of sinking air masses (ULBRICH et al. 2012). It is noteworthy again that the yearly values are not the sum of the four other seasons, as winter is calculated for DJF, i.e. the two months of the consecutive year, while the yearly values account for the specific calendar year.

For NCEP the decrease in winter precipitation is strongest compared to the trends in other seasons. Hence, the total year precipitation trend is considerably affected by the winter reduction. The NAO being linked to winter precipitation in the MA exhibits a trend towards a strong positive NAO index (HURRELL 1995), consequently identifying one reason for the decrease of precipitation (see 1.2.2). Considering the spatial pattern, particularly in the northern-central of the MA, over Mesopotamia, the Balkans, the Ligurian Sea, and the Central of the Iberian Peninsula, considerable drying is found, which is affected with maximum amplitudes with up to -785mm. In winter the drying belt shifts meridionally to the south.
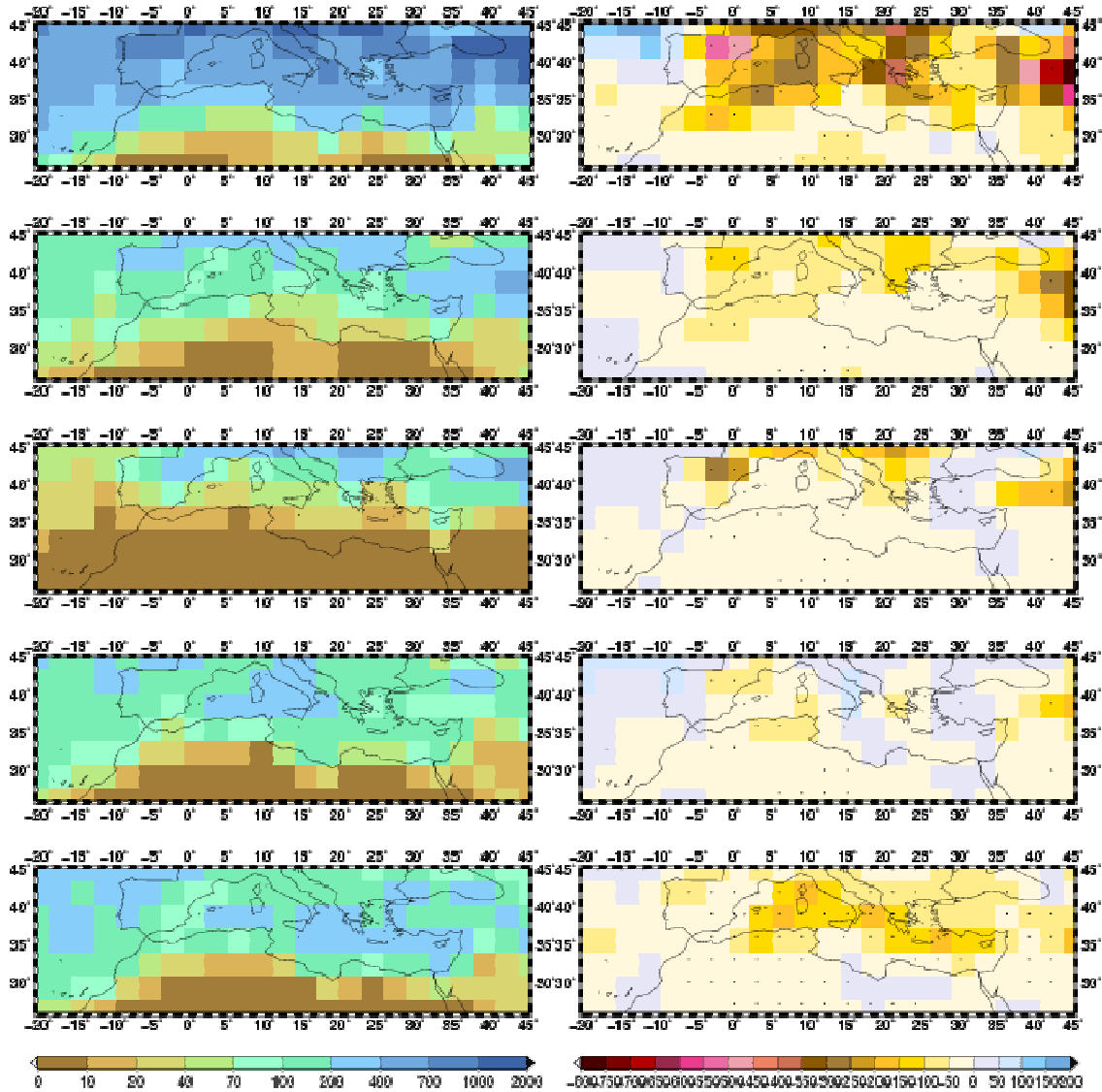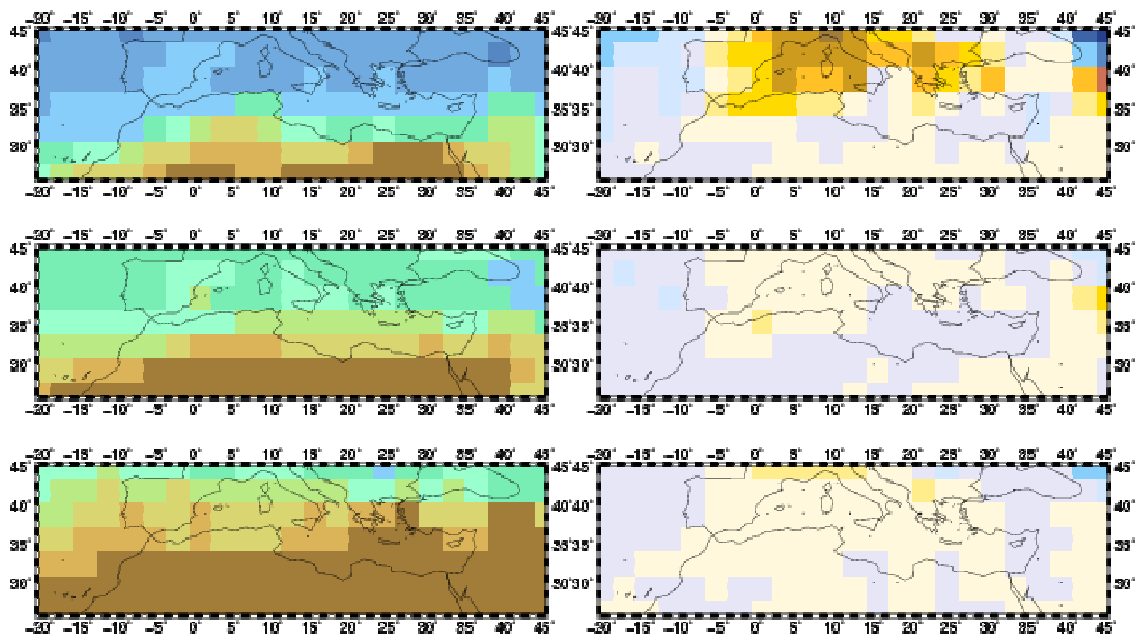
Figure 4.8: Interpolated ERA40 means (left column) and ERA40 trends (right column) for precipitation [mm] in the period of 1961-2000. Rows indicate the season from top to bottom year, spring, summer, autumn and winter. Black dots in the trend figures represent significance at the α=5% level.

The means of ERA40 show a similar seasonal cycle to NCEP in figure 4.8, though they behave slightly drier in the overall amounts. This is illustrated by a northward orientation of the precipitation belts in ERA40 compared to NCEP. Still in the northern regions the yearly amounts of precipitation does not exceed 1000mm in ERA40. Aside from the north-south discrepancy which is shifted by season, for ERA40 a west-east difference can also be established by means of the eastward drifting storm patterns leaving major parts of precipitation at the western and western coastal areas, e.g. the northwestern of the Iberian Peninsula.

For ERA40 the decreasing trend in winter is lower than for NCEP. Though significant drying is only found in winter and over the whole year and here predominantly over the northern regions, the overall values indicate a slightly prevailing drying. A decrease of precipitation can also be found in autumn, while spring exhibits no clear changes in future precipitation, which is in contradiction to the NCEP values. At the northwest and northeast borders an increase has been depicted, which is in agreement with NCEP for the Atlantic regions, while over the regions south to the Caucasus it contrasts the NCEP data. Again, strongest decrease is located over the western Mediterranean Sea.
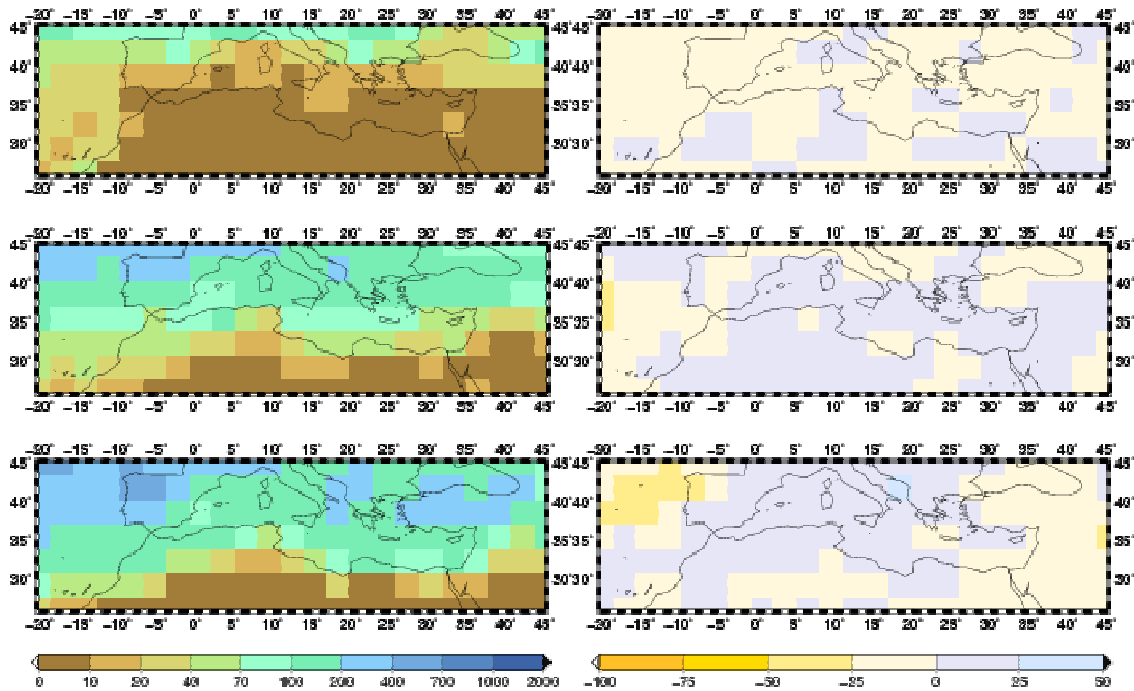
Figure 4.9: Interpolated ECHAM5 ensemble-means (left column) and ECHAM5 ensemble- trends (right column) for precipitation [mm] in the period of 1961-2000. Rows indicate the season from top to bottom year, spring, summer, autumn and winter. Black dots in the trend figures represent significance at the α=5% level.

ECHAM5 captures the seasonal cycle and the total amounts of precipitation quite well (figure 4.9), while it shows slightly wetter conditions over all seasons compared to ERA40. This holds particularly for the Atlantic regions. In the colder seasons the maxima of precipitation are rather located in the western of the MA, while in other models and in NCEP, maxima are frequently located over eastern regions. Consecutively, ECHAM5 combines the amounts of NCEP with the reasonable spatial distribution of ERA40. Compared with the observations, for the ECHAM5 results there is a higher matching in their distribution than for the results of most of the other models, i.e. most models are too wet, particularly in the southwestern regions, which holds e.g. for MIROC3.2 hires, CNRM-CM3 or CGCM3.1 (T63) – not shown). Further models are not mentioned here, as detailed analyses concerning these issues within more meaningful periods are applied later.

ECHAM5 (illustrated in figure 4.9- right column) does not reproduce analogous seasonal distributions of the trends indicated within the reanalysis data and shows positive and negative evolutions of precipitation in the end of the 20th century throughout the seasons.

Whereat, only small trends, rejecting any significance at the 95% level of confidence, are shown with the exception in winter over the Atlantic Ocean. Over most regions ECHAM5 even predicts an insignificant increase of precipitation. One should keep in mind that the ensemble-mean shown here, is built up of 4 different realizations with different initial conditions. Thus, a filtering happened to individual high or low trends, which are specific to the considered realization. By deducing a drying process over the northern parts of the MA from ERA40 and from NCEP ECHAM5 can not reproduce this pattern. However,

different spatial accounts for trends are inherent to most simulations (e.g. UKMO-HadGEM1, MIROC3.2 hires, etc… – not shown). Even some models reflect a positive trend over the period from 1961-2000 (e.g. CSIRO-MK3.5 – not shown). Regarding ECHAM5, one can see strongest reductions of precipitation over the Iberian Peninsula especially in winter and spring.
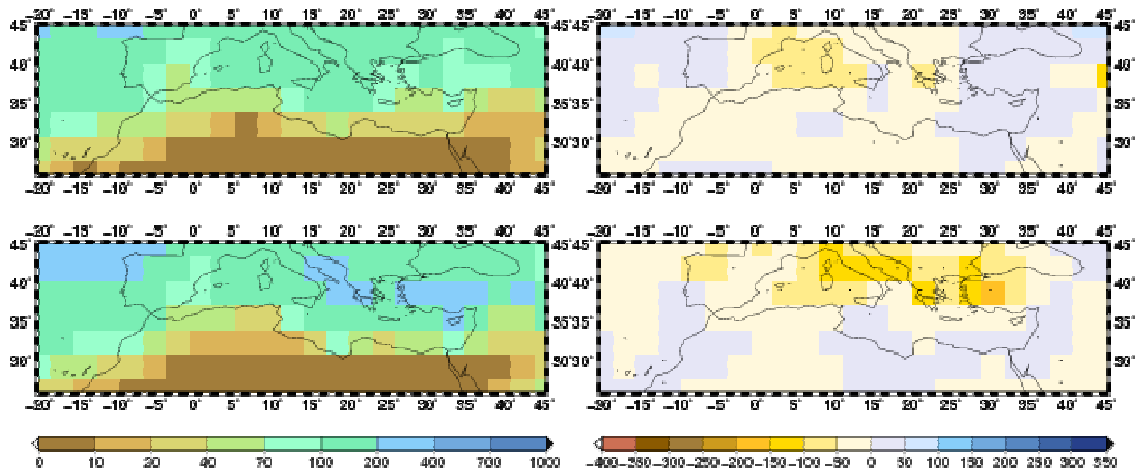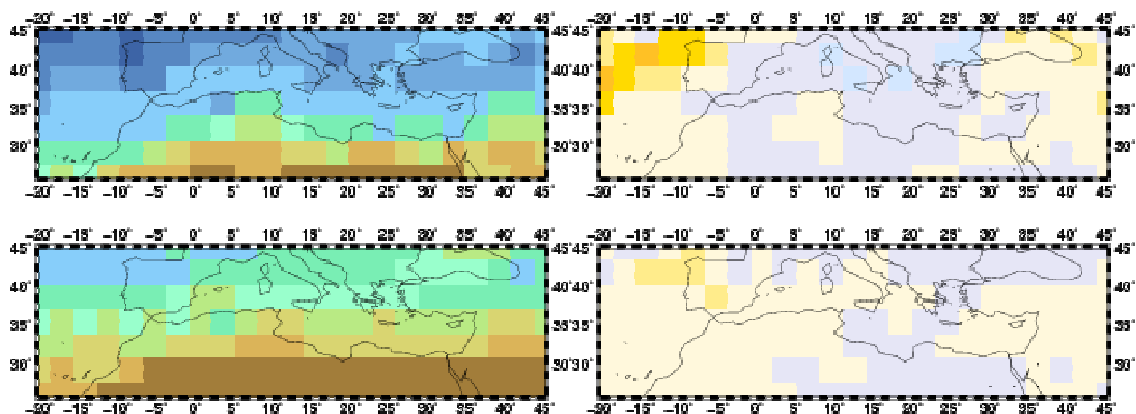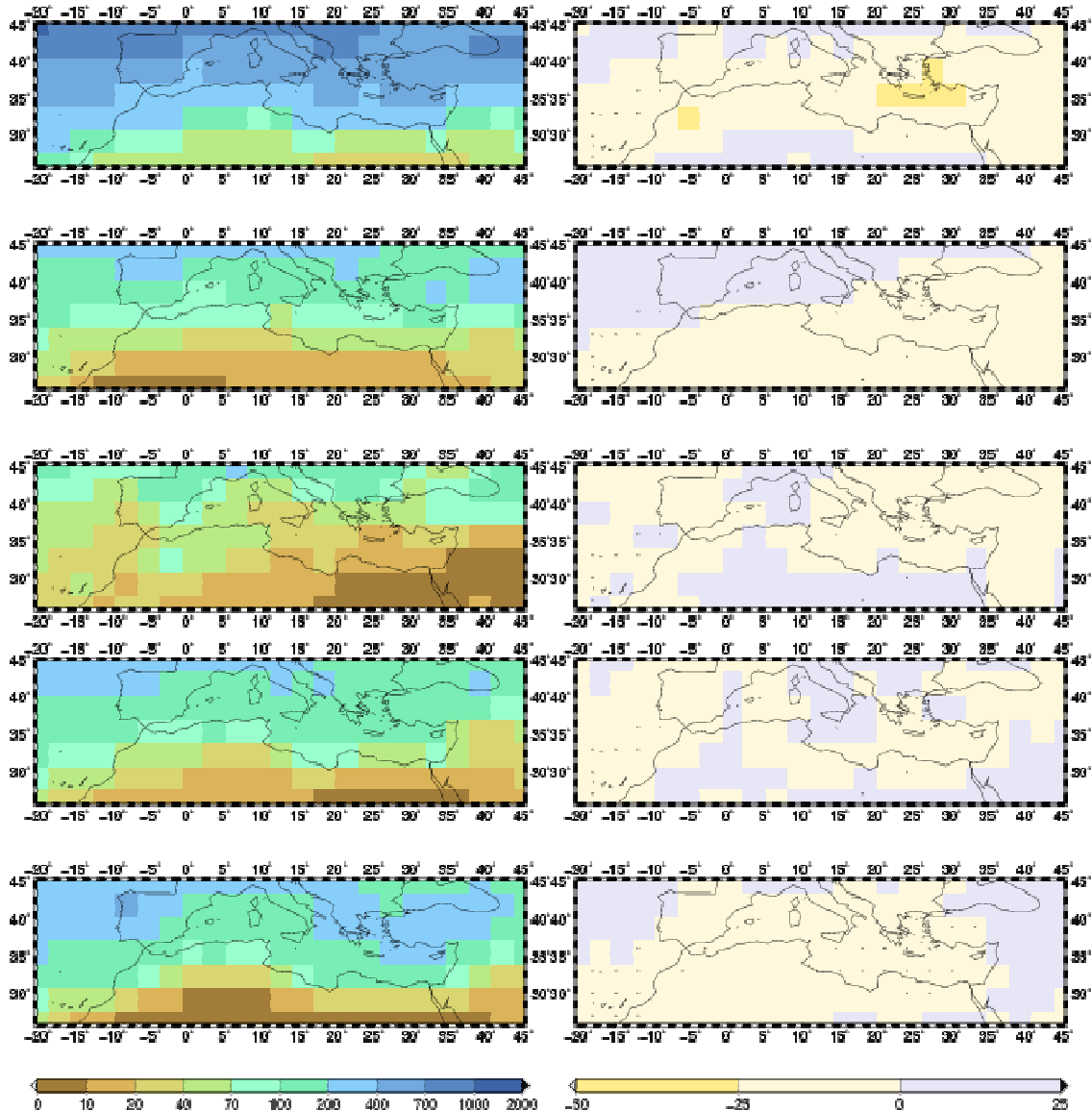

Figure 4.10: Interpolated multi-model means (left column) and multi-model trends (right column) for precipitation [mm] in the period of 1961-2000. Rows indicate the season from top to bottom year, spring, summer, autumn and winter. Black dots in the trend figures represent significance at the α=5% level.

Compared with the observations, the GCMs also capture the seasonal cycle of precipitation amounts following principally on the seasonal behaviour of the NAO (see 1.2.2). Also, spatially the broader pattern can be reflected by the GCMs. Particularly in winter the models agree to the observations with the drying over the Mediterranean with discrepancies over Turkey. Also, in autumn higher agreement is reached over southern France and the Alps. In summer the differences between the multi-model mean and the other data are highest. While ECHAM5 simulates precipitation in relation to the reanalysis data in a

quite good performance, the multi-model overestimates precipitation particularly over the southwest of the area of investigation (particularly for NCEP as reference). As discussed in chapter 1.2.2, summer precipitation in the MA is primarily steered by convection and thus strongly dependant on the model specific parametrization schemes. Nevertheless, this overestimation of summer precipitation is noteworthy, while the impact of ECHAM5, which is also included in the illustrated mean, on the multi-model mean is superimposed. The overestimation of the precipitation by ECHAM5 over the Northern Atlantic is abated in the multi-model mean with exception in summer.

As introduced by the section dealing with the ECHAM5 trends, the models behave differently in matters of the reproduction of the trends. Thus, similar to ECHAM5 the multi-model mean can also not show a distinct seasonal distribution of trends. Also spatial patterns are not interpretable, as these are consequently smoothed (see figure 4.10). Still a trend is visible, which is slightly decreasing in total, partially documented by significance.

Precipitation Mean 20c3m 1961-2000
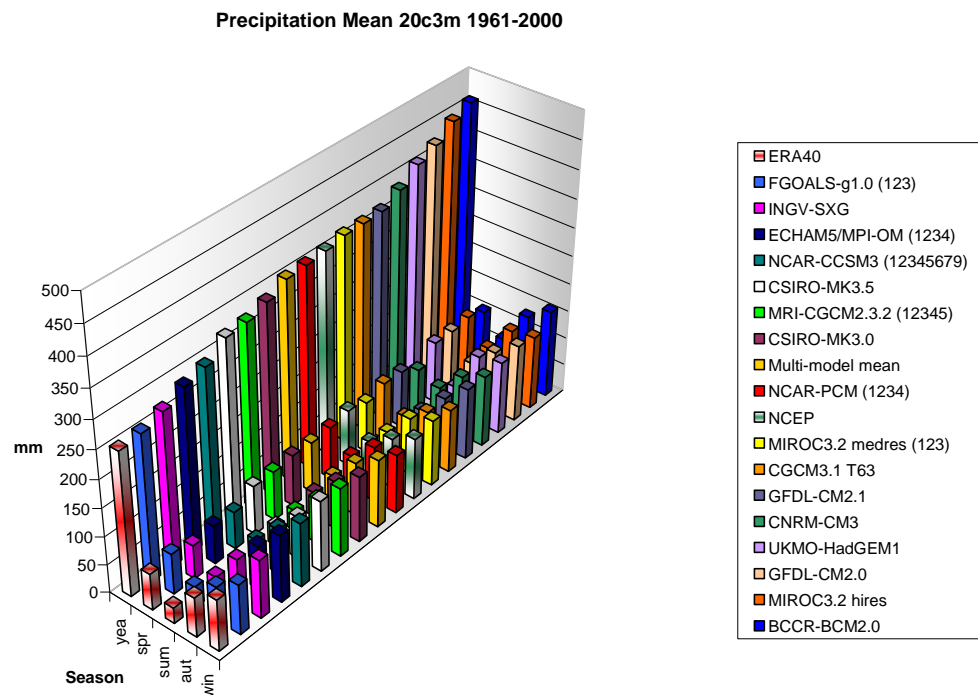
Figure 4.11: Regional precipitation means [mm] of GCMs (20c3m) and reanalysis data for the specific seasons computed for the period of 1961-2000.

In figure 4.11 the spatial average means are sorted by their yearly sum. Again the two reanalysis datasets exhibit a large bias to each other (about 100mm in the yearly average) implying the difficulty in the analysis of precipitation with its high temporal variability. Most models are found somewhere between the reanalyses, where also the multi-model mean is located in this range. Only in summer in the south and western Mediterranean the values are overestimated with 40-70%, which might be dedicated to the generally small amount of precipitation at this season and these regions. Though pronounced differences in magnitude are partially obvious, the reproduction of the seasonal cycle by every model is encouraging, whereat, concerning the total amounts, some

models predict a higher precipitation in autumn than in spring, while some vice versa. However, this also applies for the reanalysis data, where NCEP shows marginally higher precipitation in spring.
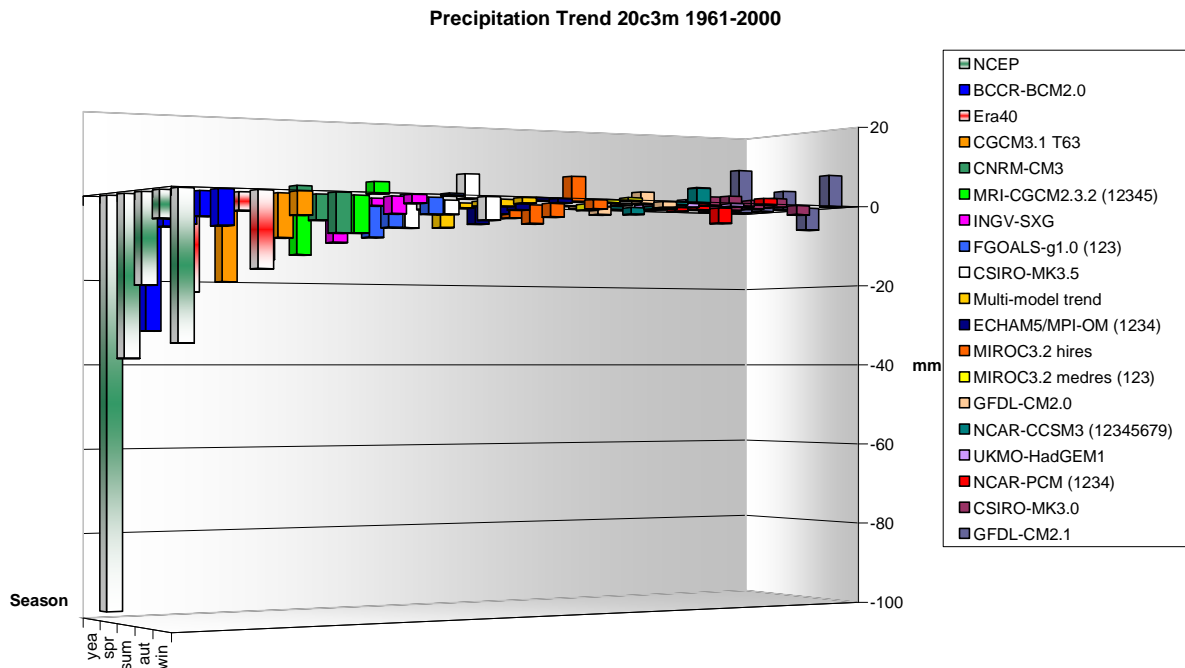
Figure 4.12: Regional precipitation trends [mm] of GCMs (20c3m) and reanalysis data for the specific seasons computed for the period of 1961-2000.

The precipitation trends are illustrated in figure 4.12. A differentiation of seasonal dependency of trends is not possible. Compared to temperature (figure 4.6), the direction of the trends is two-sided with a very strong decrease by NCEP, mainly in spring and winter. The latter is also reproduced by ERA40 but with only about 50% of the NCEP magnitude. Hence, the NCEP reduction of precipitation with its spatial pattern in figure 4.7 is outstanding. No distinct trend is evident in the multi-model mean confirming the former studies (e.g. GIORGI 2002a, GIORGI & LIONELLO 2008), and the denotation above about the different behaviours of the models. Still the total tendency of all the models (reflected in the multi-model mean) is in accordance to the reanalysis, presenting a decreasing trend over most seasons and thus most pronounced in the total year. This decrease is steered by few models with mainly CGCM3.1(T63) (-8.1mm over the year) or CNRM-CM3 (-5.9mm over the year), where also the strongest decrease is found in winter and thereby confirming reanalysis data.

4.1.3 Sea-level pressure

The third climatic field investigated in this study is sea-level pressure, as pressure is one of the most fundamental elements of weather and climate. Though it is actually indiscernible for human beings in their daily or hourly variations, it clearly affects other variables like temperature, precipitation or

winds by interacting relationship (LUTGEN & TARBUCK 2007). E. g. the *Ideal Gas Low* describes its direct relation to temperature with the help of the gas constant. In contrast to geopotential heights indicating constant pressure charts, sea-level pressure is a constant height chart denoting the pressure on a generalized height, i.e. sea-level derived by the mean sea level. It has been developed to facilitate comparisons between several observation stations located on different altitudes (AHRENS 2000).

The IPCC (2007, p. 767) illustrates a general rise of sea-level pressure over the oceanic surfaces. In winter an eastward extension of the Azores High is demonstrated, which may show responsibility for the decrease of precipitation by blocking the westerly winds and the accompanied moist air from the Atlantic Ocean (PAETH et al. 2007).

Figure 4.13: Interpolated NCEP means (left column) and NCEP trends (right column) for sea-level pressure [hPa] in the period of 1961-2000. Rows indicate the season from top to bottom year, spring, summer, autumn and winter. Black dots in the trend figures represent significance at the α=5% level.

For sea-level pressure the borders and the gradients give more information than the analysis of the absolute values. In a large-scale aspect the Mediterranean shows a trough, which can hardly be depicted in the illustrated section. So the mean pressure is shown again for NCEP (figure 4.13) and the other data members and depicted within an explicit range of hPa.

In the summertime the eastern Mediterranean exhibits relatively low pressure, which is part of a trough comprising the regions between southern Turkey and the Aegean Sea and the Persian Gulf, named the Persian Trough (with slightly above 1000.7hPa). The trough extends through the warm period of the year and also manifests in the yearly mean. The Azores high counteracts to this trough building a remote link over the African continent also affecting the eastern MA (ULBRICH et al. 2012). Thus, the western part is defined amongst others by blocking actions of an Atlantic dipole pattern extended in east-west axis suppressing the westerly streams of cool and moist air from the Atlantic to the MA. Furthermore, this pattern is self-energizing with the warming of the Mediterranean Sea. In autumn the gradient of sea-level pressure between Africa and the MA allows the assumption that the African Monsoon accounts for the trough located slightly south of the investigated area at nearly 15-20° northern latitude. This gradient is also attributed to the Red Sea Trough entering the MA from the eastern side and which is built up by the mountains on the eastern coast of the Red Sea (ZIV 2001, KAHANA et al. 2002). Still in winter its occurrence is perceivable in the reanalysis data, where NCEP also captures the negative sea-level pressure anomalies concerning the Cyprus Low, discussed in chapter 1.2.2 (ULBRICH et al. 2012). Also the Eurasian cold continental high-pressure zone is reflected well.

At first the reader is kindly adverted to the different scales of trends for models and reanalysis data in the following figures, as for the latter the scale is doubled to account for highest changes. Concerning the total year the MA suffered an increase in pressure for NCEP. This increase is mainly located near the eastern coast of the Black Sea, while seasonally highest positive trends are found in winter. Significance is found over eastern and southern regions where in the latter the positive trend counteracts the low pressure system over Africa. Particularly in winter the rise of sea-level pressure may be interpreted as an eastward extension of the Azores High. Furthermore, an increase of the Mediterranean Oscillation is noticeable by an increase of primarily western and central northern pressure in winter. In winter most of these trends are significant with up to 9.9hPa over the southern coast of the Black Sea and nearly 6.1hPa in the north.
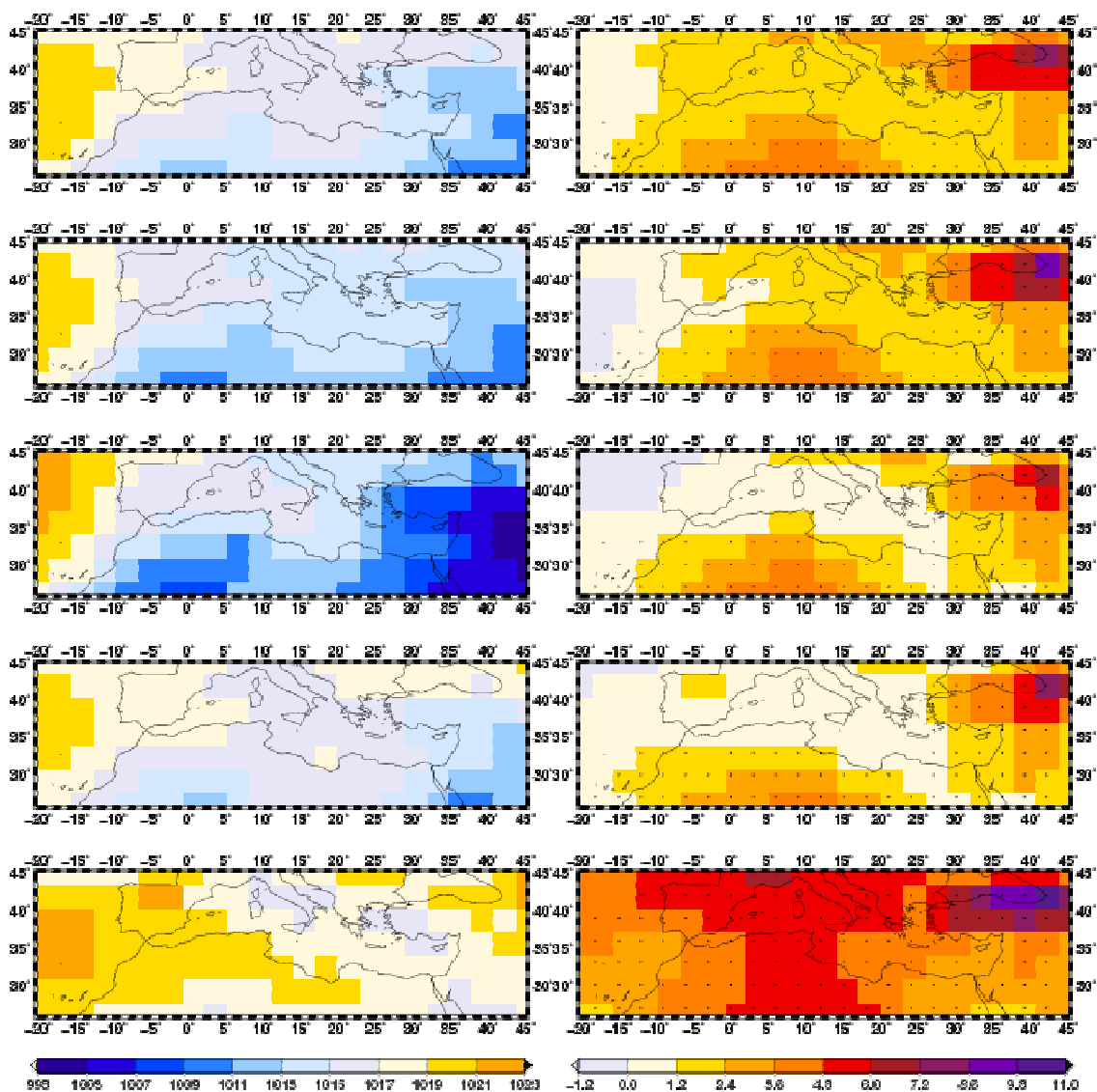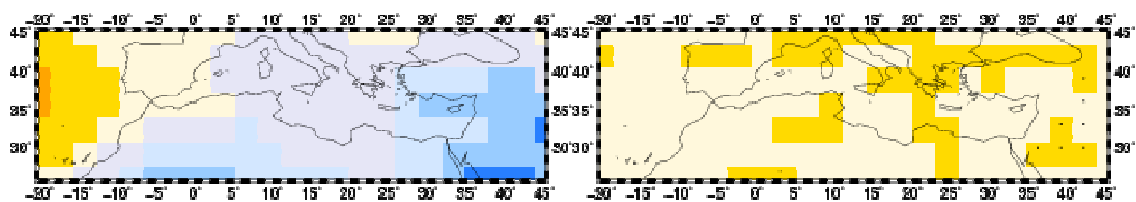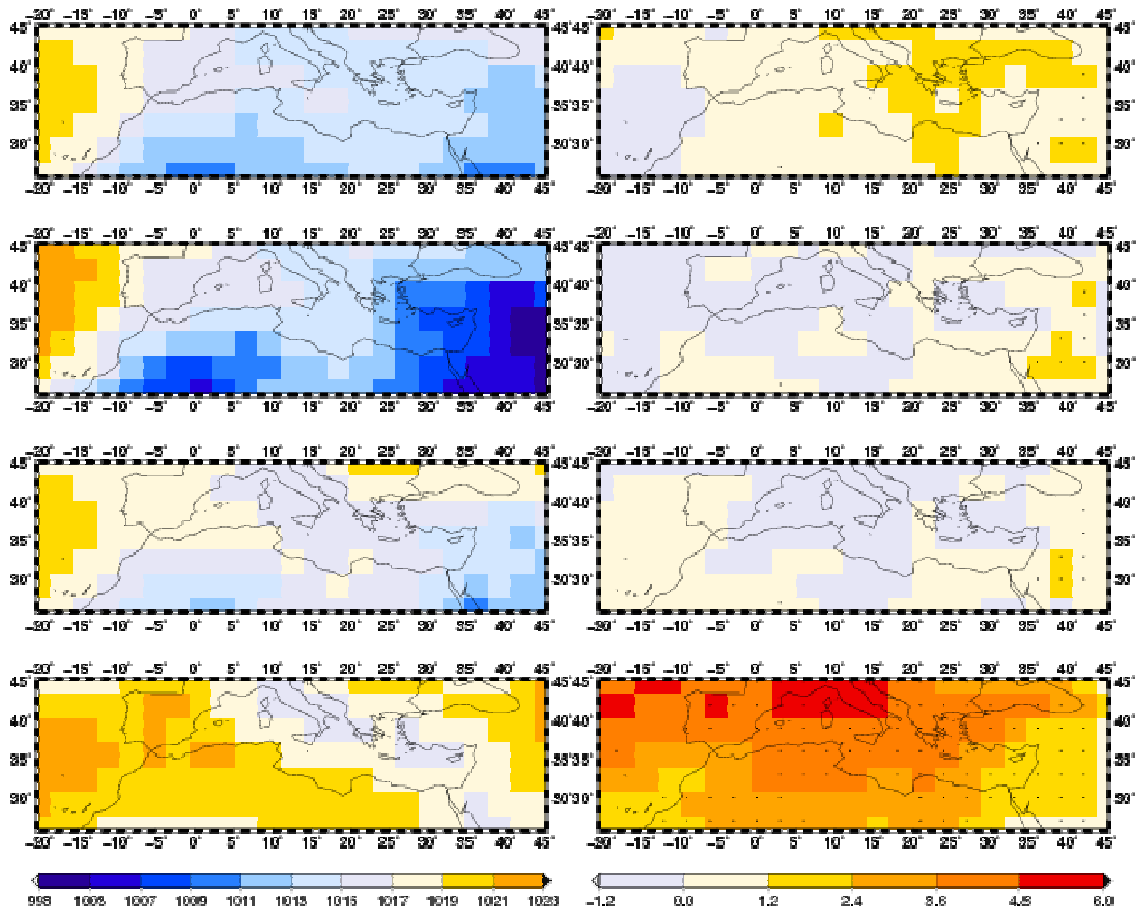
Figure 4.14: Interpolated ERA40 means (left column) and ERA40 trends (right column) for sea-level pressure [hPA] in the period of 1961-2000. Rows indicate the season from top to bottom year, spring, summer, autumn and winter. Black dots in the trend figures represent significance at the α=5% level.

According to NCEP most features can also be found in the ERA40 data (figure 4.14). This holds particularly for the Persian Trough in summer, the Red Sea Trough and the Saharan Low in autumn and even the Cyprus Low in winter. Accordingly the reanalysis are in agreement in the seasonal cycle and the spatial pattern. Also the magnitudes are in an encouraging consistency.

While NCEP shows an increase of sea-level pressure over all seasons, this phenomenon is confined on winter for ERA40 with highest values in the north with up to 5.67hPa, which fits to the NCEP values (see figure 4.13), while in the warmer seasons even a slight decrease without significance is visible. Still in spring in the eastern regions a rise is described. With the prevailing winter trends this leads to an overall increase of sea-level pressure in the total year, which is indeed partially significant though it is weaker than the NCEP values. However, agreements between the two reanalysis data concerning the trends are generally low.
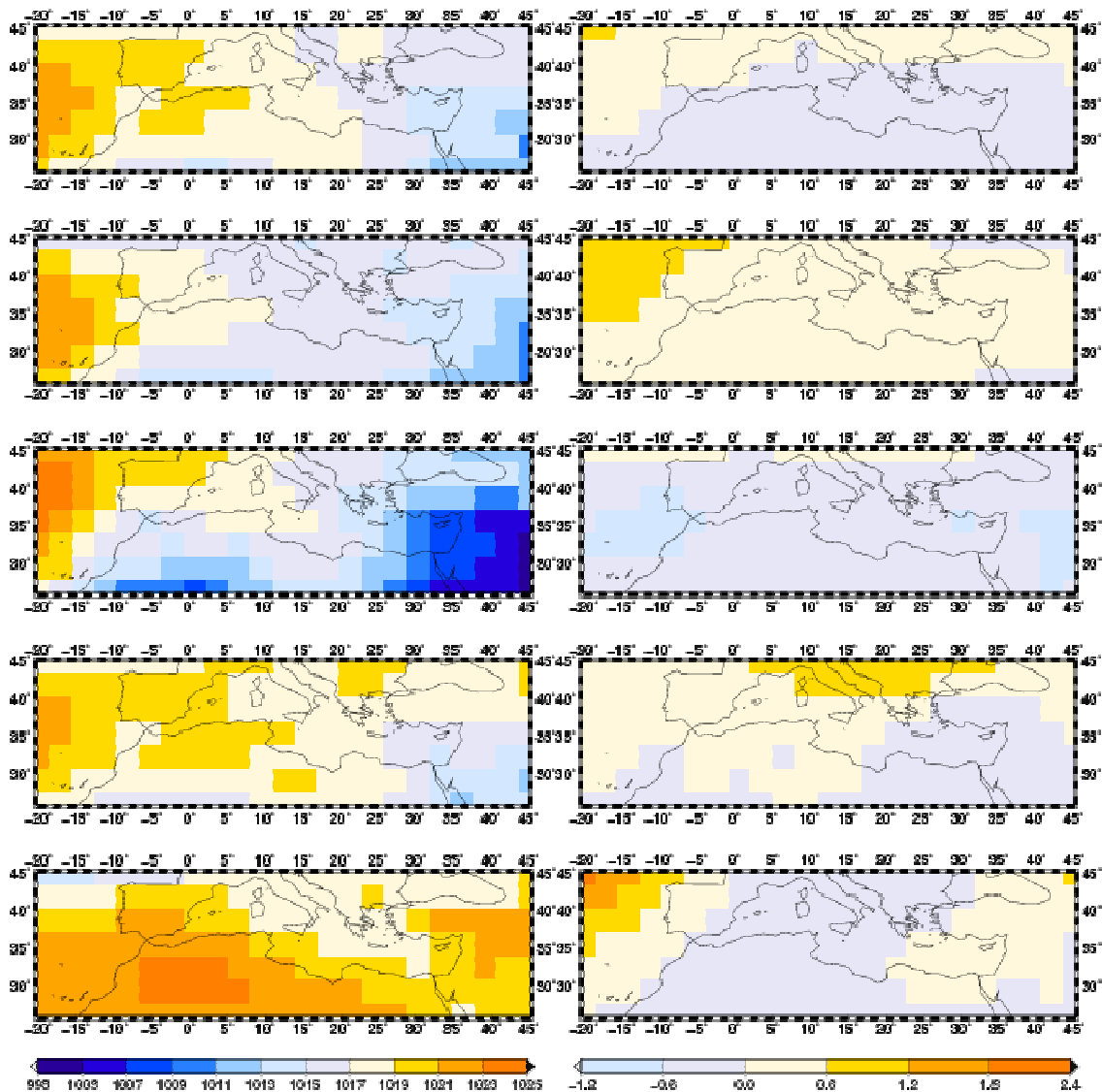
Figure 4.15: Interpolated ECHAM5 ensemble-means (left column) and ECHAM5 ensemble- trends (right column) for sea-level pressure [hPa] in the period of 1961-2000. Rows indicate the season from top to bottom year, spring, summer, autumn and winter. Black dots in the trend figures represent significance at the α=5% level.

Again ECHAM5 reproduces a distinct seasonal cycle (figure 4.15). Thus, the Persian Trough, clearly shown within the reanalysis data, is also well captured by ECHAM5. Also, the southern low pressure systems over Africa are evident. Smaller features as the Cyprus Low are not visible in the ECHAM5 simulations. This Cyprus Low is interesting, as some models reproduce this feature (e.g. MRI-CGCM2.3.2 or FGOALS-g1.0). The relatively high pressures over the Atlantic have a farer extension into the MA, while the northern part of Africa also shows slightly too high values in winter (with roughly 1024.63hPa).

ECHAM5 does not reproduce any trends illustrated by the reanalysis data. This is notably evident in the total year when ECHAM5 models a decrease of pressure of nearly the whole area, whereat all simulated changes are relatively small and not significant. One still has to keep in mind, that the legend is twice the distance for the models than for the reanalysis data concerning the trends.

This holds for the majority but not for all of the models (e.g. CGCM3.1 (t63) fits notably well with NCEP or ERA40 trends particularly in winter).
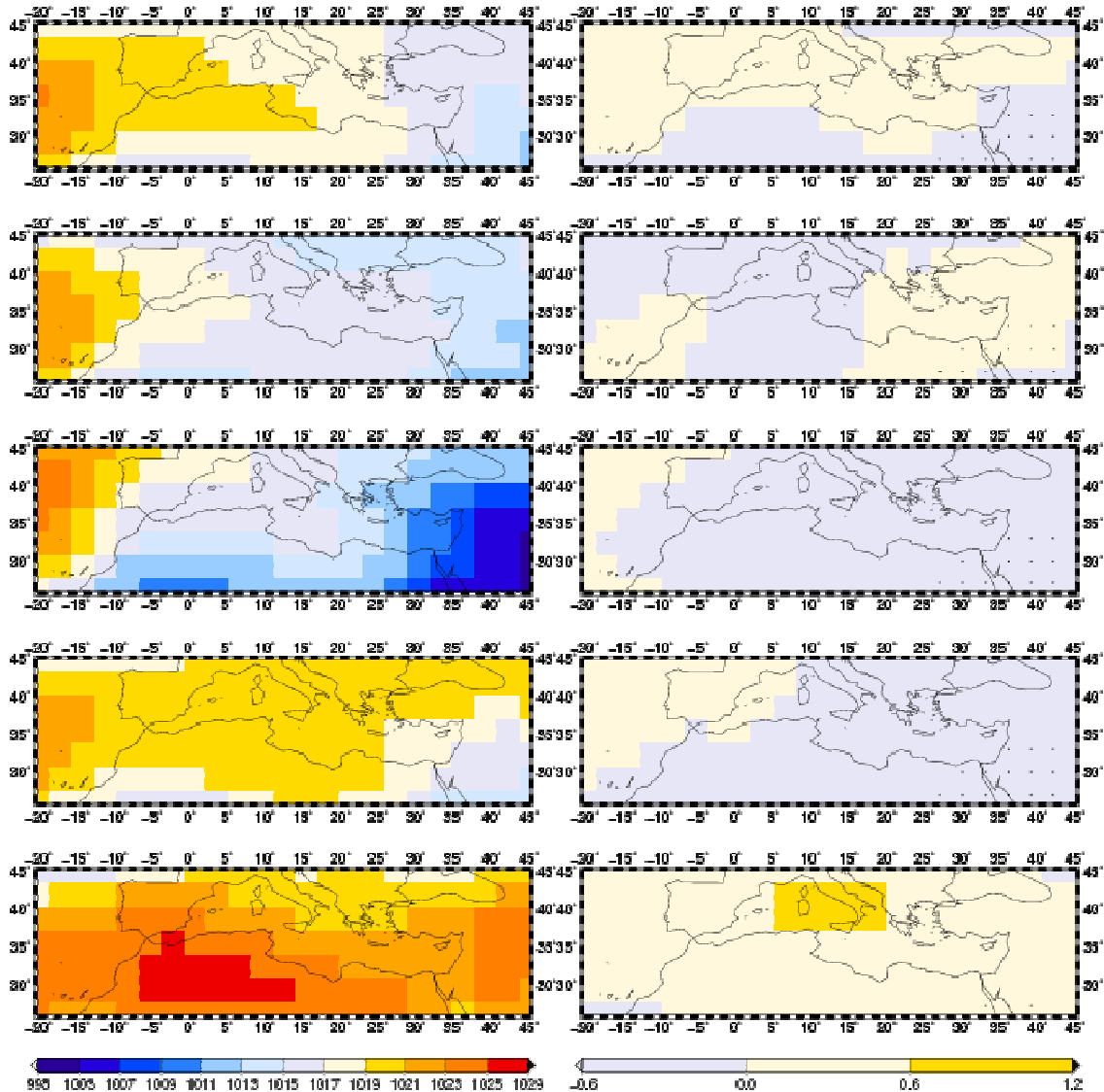
Figure 4.16: Interpolated multi-model means (left column) and multi-model trends (right column) for sea-level pressure [hPa] in the period of 1961-2000. Rows indicate the season from top to bottom year, spring, summer, autumn and winter. Black dots in the trend figures represent significance at the α=5% level.

In figure 4.16 the models show an evident seasonal cycle with the distribution and the magnitudes of the sea-level pressure. Still the Persian Trough with its western branch of the Saharan Trough is persistent over the averaging of all models and consecutively well reproduced by most climate models. The same holds for the Red Sea Trough and the Saharan Low in autumn. While the Cyprus Low and its related features are finally not even suggestive. Compared to ECHAM5 and the reanalysis data, all the models exhibit in their mean higher values in winter (1021.87hPa). To ECHAM5 the multi-model mean fits well with the geographical distribution, though the multi-model mean indicates more extreme magnitudes in the extreme seasons (with 1026.21hPa in winter over the Sahara) than the model of the MPI. Generally the sea-level pressure is overestimated by the multi-model mean compared to the reanalysis, which also

69

holds for ECHAM5, though not with that extent. This indicates, that ECHAM5 is closer to the reanalysis than the average of climate models.

Neither any patterns with their magnitude, direction or distribution of the reanalysis data nor of ECHAM5 are reproduced by the average trend of all models (right column of figure 4.16) indicating indirectly the high uncertainty concerning sea-level pressure. For instance increase of sea-level pressure does not exceed 0.72 hPa, while NCEP depicts nearly 9.9hPa (see above). Concerning the overall year, the sparse increasing structures of the NCEP data are substituted by slightly decreasing values, which also show significance. This is due to continuous slight decreases over nearly all seasons, which are not existent in the reanalysis, at least not in NCEP. Thus, a seasonal separation of trends is not possible. As the multi-model mean hardly shows strong trends, a high discrepancy over the models is expected.

Sea-level pressure Mean 20c3m 1961-2000
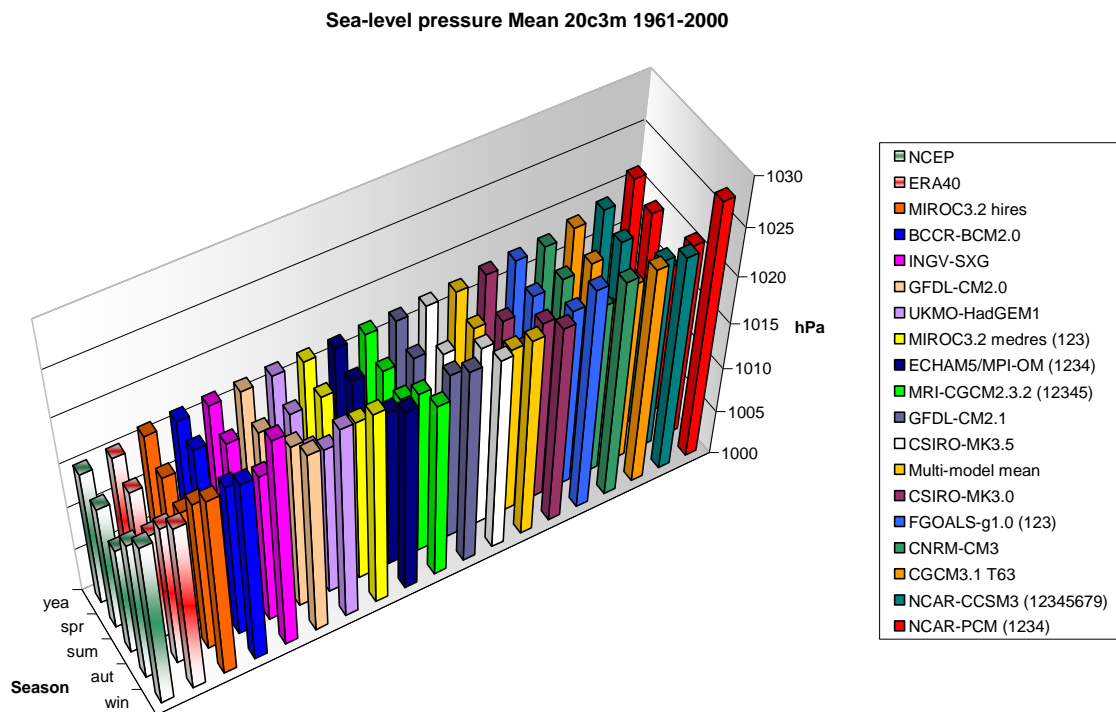
Figure 4.17: Regional sea-level pressure means [hPa] of GCMs (20c3m) and reanalysis data for the specific seasons computed for the period of 1961-2000.

Figure 4.17 depicts an overview over all the data members. In the spatial averages the reanalysis are close to each other, forcing all the models to overestimate them. With its encouraging resolving of spatial patterns (not shown) and the average values MIROC 3.2 hires is one of the most promising GCMs concerning sea-level pressure. However, the spreads between the models are huge, particular with respect to NCAR-PCM, showing extremely high values (1021.3hPa over the year and 1027.8hPa in winter compared to 1019hPa in winter for ERA40). These high values of NCAR are above all others in all seasons and thus strongly affect the multi-model mean, being shifted to the right side of the figure, where models with higher seasonal averages are depicted. Again, the seasonal cycle is uniquely reproduced by all models

matching the reanalyses with highest values in winter and lowest values in summer.
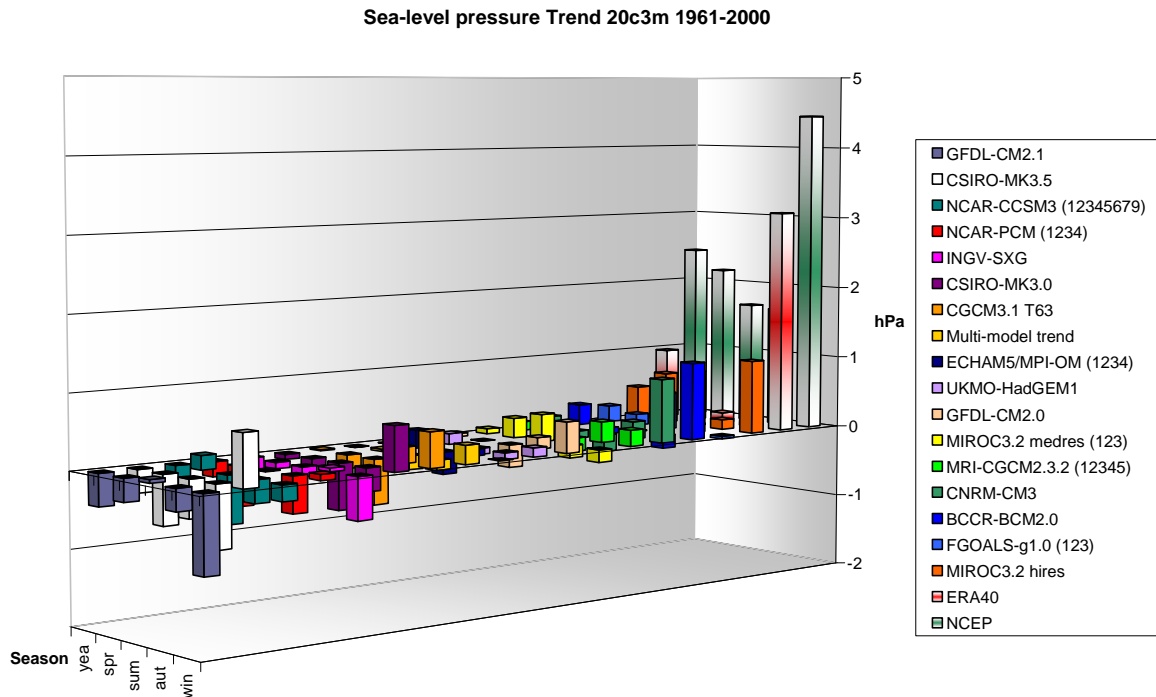
Figure 4.18: Regional sea-level pressure trends [hPa] of GCMs (20c3m) and reanalysis data for the specific seasons computed for the period of 1961-2000.

After the strong differences in the spatial maps between the trends of the reanalysis data, ECHAM5 and the multi-model mean (right columns in figure 4.15 and 4.16), one expects the differences in the individual trends given in figure 4.18. This overview prohibits the assumption of any seasonally independent development of sea-level pressure. Furthermore, the positive trend depicted by NCEP (with up to 4.5hPa in winter) and ERA40 (3.08hPa) cannot be reproduced by the models, though some show increases winter. The suitable operating MIROC 3.2 hires, concerning the mean values, shows slight increasing trends in all seasons as well. For many models no distinct trends are evident, transplanting the multi-model mean somewhere in the middle of figure 4.18 with its trends around zero, prohibiting any statement.

4.1.4 Integration to other studies

For temperature the MA suffered strong warming in the last 40 years of the 20th century. Strongest warming can be found in the western parts. In summer the warming is highest being reproduced by most of the models and is reflected in the multi-model mean, which also shows a reasonable range of warming, as it lies between the range of both reanalysis data sets. GIORGI utilized (2002a) CRU observation data (NEW, HULME & JONES 1999, 2000), which allowed spatially detailed analyses and found a spatially average trend of 0.75°C warming in the MA. This is preferably evoked from the last decades of the 20th century depicting the strongest increases in the whole century with maximum

amplitudes for summer of about 1°C-2°C, while also the increase of temperatures in winter exceed the total year trend. These results for the cold season can not be affirmed by the analyses of ERA40 (figure 4.2) or NCEP (figure 4.1), as particularly the NCEP data exhibit negative trends for winter, while the concordant strong summer warming is prevailing over all the other seasons.

GIORGI (2002a) attributes his strong positive trend in winter to the snow-cover or ice albedo feedback (see 4.1.1) in winter. If this holds true, the negative NCEP trend depicted in figure 4.1 becomes rather doubtful, as KISTLER et al. (2001) describe the NCEP data being erroneous concerning the data of snow coverage affecting the modelled temperature values (see 3.3). However, the comparisons to GIORGI´s study of 2002a are hard to draw, as in the underlying approach only the last 4 decades of the 20th century are investigated and trends of climate variables do not necessarily behave linearly (TRIGO et al. 2006). Besides the different integration periods, the investigated area has not the same extend. Finally, GIORGI (2002a) restricts his study on land surfaces and the CRU (NEW, HULME & JONES 1999, 2000) data has a spatial resolution of 0.5°x0.5°. Nevertheless, the yearly resulting trends (in figures 4.1 and 4.2) of the reanalysis data confirm GIORGI´s findings in 2002a. Furthermore, several different authors identified a warming in the MA by the end of the 20th century (e.g. TORETI et al. 2010). Already GIORGI, BI & PAL (2004a) found the pronounced summer warming, which is primarily located in the western Mediterranean region and which is rather depicted by ERA40 than by NCEP. Also XOPLAKI (2002) addresses an east/west contrast in her study analysing observation data series. By means of intermittent cooling in the east, overall trends are harder to detect there, which is also reflected in the underlying study. In winter there is a slight overestimation by the simulations while in the other seasons simulations lie beneath the observations (GIORGI & LIONELLO 2008). GIORGI & LIONELLO (2008) based their study on the differences on projected values forced by A1B scenario of 2071-2100 and the 20c3m reference forcing 1961-1990. Their composition of the multi-model mean is deviating from that one consulted here. PARRY et al. 2000 also utilized a multi-model mean with a differing model-choice with up to 5 GCMs until the 2080s. The fitting of the underlying results to the mentioned study is well and again the highest increase of temperature can be attributed to the summer-season. The slightly deviating setting of the multi-model mean provides an explanation for the only small discrepancies in the amounts of trends to this study. Besides the differing choice of models over the other studies, in all cases summer suffers highest temperature increases. GIORGI (2002b) also found an underestimation of HadCM3, a model discarded in the underlying study, of about 2°C in winter and the total year, while summer matches quite well. A slight underestimation is also represented in his multi-model mean and thus in most of the models. Still, the models reproduce the means in their spatial and seasonal distribution well.

Concerning average precipitation in the MA, NCEP shows a marginally higher humidity than ERA40. The CRU dataset illuminated by GIORGI (2002a) depicts for the last century a trend of –5% in winter and in the whole year, while summer shows slight increases. This confirms the seasonal trend distribution of the underlying study, though no increase can be found here. A decrease of precipitation is reflected in the last 40 years of the 20th century. Significance is

only given in winter for NCEP, where the downward trend is highest, particularly in the eastern MA. Opposite signals, as indicated in other studies (TRIGO et al. 2006, XOPLAKI 2002, GAO, PAL & GIORGI 2006), are located in the western part of the studied area or the Alps in winter, can not be confirmed and are more attributable to the high spatial heterogeneity. In agreement with further studies the strong overall downward trend is also dominant in spring and winter (HERTIG & JACOBEIT 2008a). Besides the negative trend in summer, ERA40 shows higher agreement to GIORGI´s study of 2002a. But distinctive trends are also rare in his study. However, as already mentioned, the studies are hard to compare, which even more holds for precipitation. At this point the reader is kindly referred to the huge spread between ERA40 and NCEP, see figure 4.11. Generally, the GCMs tend to overestimate precipitation. Also in the study of GIORGI & LIONELLO (2008) underestimation of precipitation is not higher than 20% for the whole Mediterranean region. Additionally for HadCM3, GIORGI (2002b) analysed an overestimation of precipitation of about 25% in summer, while in winter and the total year the model fits quite well with the CRU data. A seasonal distribution of average precipitation is well reproduced, whereupon also latitudinal gradients are persistent. The decrease of precipitation given by most of the models is also described by JACOBEIT, DÜNKELOH & HERTIG (2007), who found a prevailing decrease of precipitation in winter and spring in their study, while in autumn some slight increases are detected. Also seasonal differences in trends are mentioned in several studies but there is still scope to quantify the knowledge of interannual cycles their amplitude and its designated change (TRIGO et al. 2006). This seasonal distribution would mainly apply for NCEP, though there is no increase in this data. The drying in the control periods represented by ECHAM5 has its strongest reductions of precipitation over the Iberian Peninsula in the colder seasons. Though no significance can be assessed, this coincides with PAREDES et al. (2006), who found major drying in March over the Iberian Peninsula by applying a relationship to the NAO index. The spatially heterogeneous distribution of the trends (by the different models), which has been mentioned, is also proved by the HadCM3 results given by GIORGI (2002b). The resulting low common trend of the multi-model mean is also attested by LIONELLO & GIORGI (2008). They also describe the general uncertainty of GCMs in reproducing analogous trends.

The relative high pressure of ECHAM5 over the northern part of Africa in average respectively to the reanalysis data is already mentioned by a former study of HODSON & SUTTON (2008) who made their assessments from 1951-1994. This high pressure overmatching the reanalysis in winter is even reflected in the yearly map of figure 4.15 and reproduced by many models, as it can be seen in the multi-model mean which is also reported by GIBELIN & DEQUE (2003). Still the GCMs agree in the seasonal cycle and the spatial distribution of the mean values. The trends and here the amounts cannot be reproduced by the GCMs in this period. A seasonal and spatial distribution with mainly increases in winter and in the south is neither reproduced by the individual model ECHAM5 nor by the multi-model mean. Overall, the model ensemble rather neglects any trends, besides demonstrating differences to each other, which is in contrast to the increasing trends of the reanalysis data.

4.2   Future Period (2001-2098)

In this chapter, the models described in chapter 4.1 are analysed by illustrating their means and trends in the future from 2001-2098. The period of 98 years reveals a longer period than the 40 years of the control period and thus in particular the future period provides an appropriate basis for the interpretation of the results obtained by the statistics in the subsequent chapters.

4.2.1 Temperature

Regarding ECHAM5 in figure 4.19, one recognize a considerable warmer mean temperature for 2001-2098 simulated with the A1B scenario than illustrated in figure 4.3 for 1961-2000 (~2°C for the overall year). The pattern of the relative temperatures stays mainly the same, with e.g. highest temperatures over the deserts (40.5°C in summer). The smallest differences can be found in winter and spring over the eastern and central northern regions, as it has been indicated by the low trends in figure 4.3. Consecutively, summer and autumn suffer most changes, being conducive on the warming of the total year. An interesting feature is the changes in the gradient from the different seasons to each other, whereat e.g. the differences between summer and winter are now closer to each other with about 0.7°C. Still the seasonal cycle is reasonably reproduced.

A distinct warming can be seen in the right column of figure 4.19 illustrating the trends for the different seasons. Lowest temperature increases are found over the sea and here mainly over the Atlantic Ocean, while even here rise of temperature exhibits a warming of around 3°C in many cases. Over the Mediterranean Sea the increase of temperature reaches higher values but still not the magnitude of land surfaces. Here the temperature increase is in most cases not beneath the 3.5°C threshold concerning the yearly values. This mitigating effect of the ocean is present to all seasons, which also confirms the findings of GIORGI & LIONELLO (2008). Considering seasonal differences, the future trends continue with strongest temperature increases in summer with rates up to 7.89°C in Macedonia accompanied by likewise temperature increase over Spain, northwestern Africa and the southeastern borders of our research area. The transition seasons show lower rates of warming, while lowest rates are illustrated in winter, where analogous to spring the Iberian Peninsula is spared out with maximum values. Concerning the whole MA still the southeastern and southwestern regions are affected most, combined with the central north, which is in winter particularly affected with maximum temperature increase of about 4.85°C. In figure 4.19 all trends are significant by α = 5%, indicated by black dots within the grid-cells. Following closely the illustration of the results for the reference period, again the multi-model mean is highlighted in figure 4.20, subordinated to the same period and the same scenarios as it has been applied to ECHAM5.

Figure 4.19: Interpolated ECHAM5 ensemble-means (left column) and ECHAM5 ensemble- trends (right column) for temperature [°C] in the period 2001-2098 in the A1B scenario. Rows indicate the season from top to bottom year, spring, summer, autumn and winter. Black dots in the trend figures represent significance at the α=5% level.

Analogously to ECHAM5 the multi-model mean also shows higher temperature values in the average future climate, which holds for every season. The already mentioned smoothing effect of the averaging algorithm of the individual models is evident again, evoking latitudinal belts, which sometimes also follow the coastlines. Considering the seasonal distribution highest warming is found for summer, with highest temperature in the southeastern region of the area of investigation (slightly above 38°C), while values beneath -1.6°C vanished. Only in the transition seasons the illustrated trends (in figure 4.4) are supposed to account for this developed mean. The mean of all models (figure 4.20) shows similar results to the ECHAM5 model, which is also included in the multi-model mean shown here. Totally the multi-model mean seems to be colder than the ECHAM5 model, which is confirmed in the figure 4.23 illustrating the seasonal spatial means, identifying ECHAM5 as one of the warmer models in the group of the multi-model mean.

Though the smoothing effect of the multi-model mean, still strong significant warming with up to 4.82°C is displayed, strongly following the ECHAM5 pattern with e.g. highest warming in summer with the Iberian Peninsula, the Near East and Algeria. Also the highest warming over Macedonia can be found again in the multi-model mean, where it is also enforced by the high ECHAM5 value. Lowest trends are illustrated in winter over the Iberian Peninsula counteracting with the strong warming in summer. Still the Iberian Peninsula belongs to the regions affected most by rising temperature. Overall the warming is slightest in winter also in agreement with ECHAM5, but still being not inconsiderable, as it is with ~2.7°C far above of hottest summer warmings in the control period (~0.72°C) for the Mediterranean average in the multi-model mean. Generally, warming trends are more pronounced over the land areas, which may amongst others be caused by the impact of snow - cover - albedo feedbacks in winter. Still it is lowest in winter, being consistent to ECHAM5 (figure 4.19).
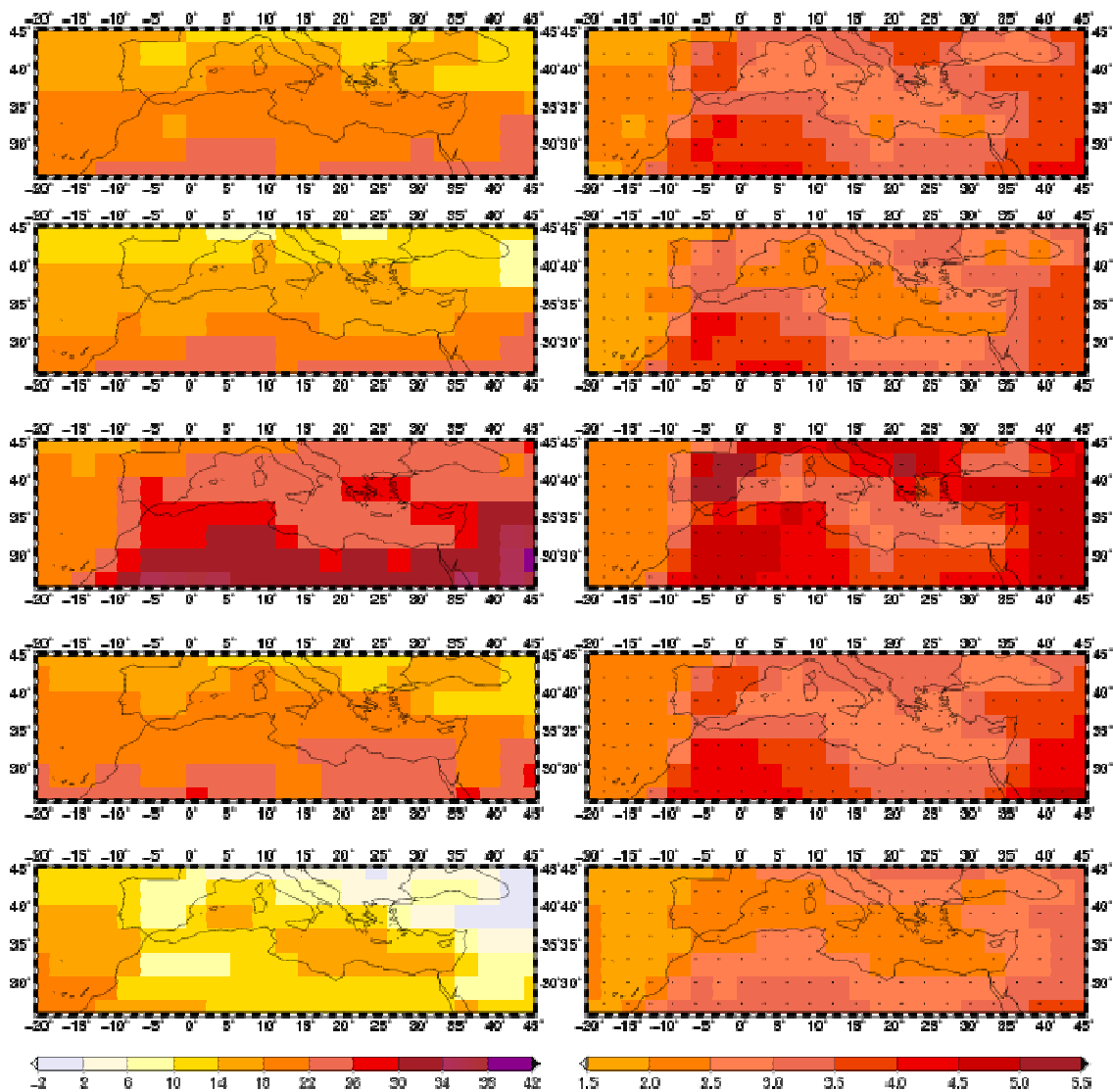
Figure 4.20: Interpolated multi-model means (left column) and multi-model trends (right column) for temperature [°C] in the period 2001-2098 in the A1B scenario. Rows indicate the season from top to bottom year, spring, summer, autumn and winter. Black dots in the trend figures represent significance at the α=5% level.

These projections are attributed to the A1B scenario, leading to considerable warming, though this scenario is located somewhere in the middle of the applied SRES scenarios in this study (see 2.4). The trends of the B1 scenario (left side) and the A2 scenario (right side) are shown for ECHAM5 in figure 4.21 for the extreme seasons, i.e. summer and winter, and the overall year. Dependant on the strength of the specific forcing scenario, it is evident that the more carbon is emitted, the stronger is the temperature increase. That is why in summer the temperature increase even exceeds the 8°C threshold in A2, while in the B1 scenario highest warming is still in summer and over Macedonia, but with a maximum of 4.9°C evidently lower. Still the B1 trends are significant and above the trends found in the control period (figure 4.3). Apart from the differences shown by the magnitudes of the trends, the substitution of the scenario has little effect on the spatial pattern. Also the seasonal distribution of the trends stays the same. Thus, the distribution of the trend for spring and autumn is not shown, as it is analogous to the A1B scenario, but with the typical amplitudes of the A2 or the B1 scenario. Consequently, the comparable A1B scenario can be assigned to somewhere in between these two scenarios.
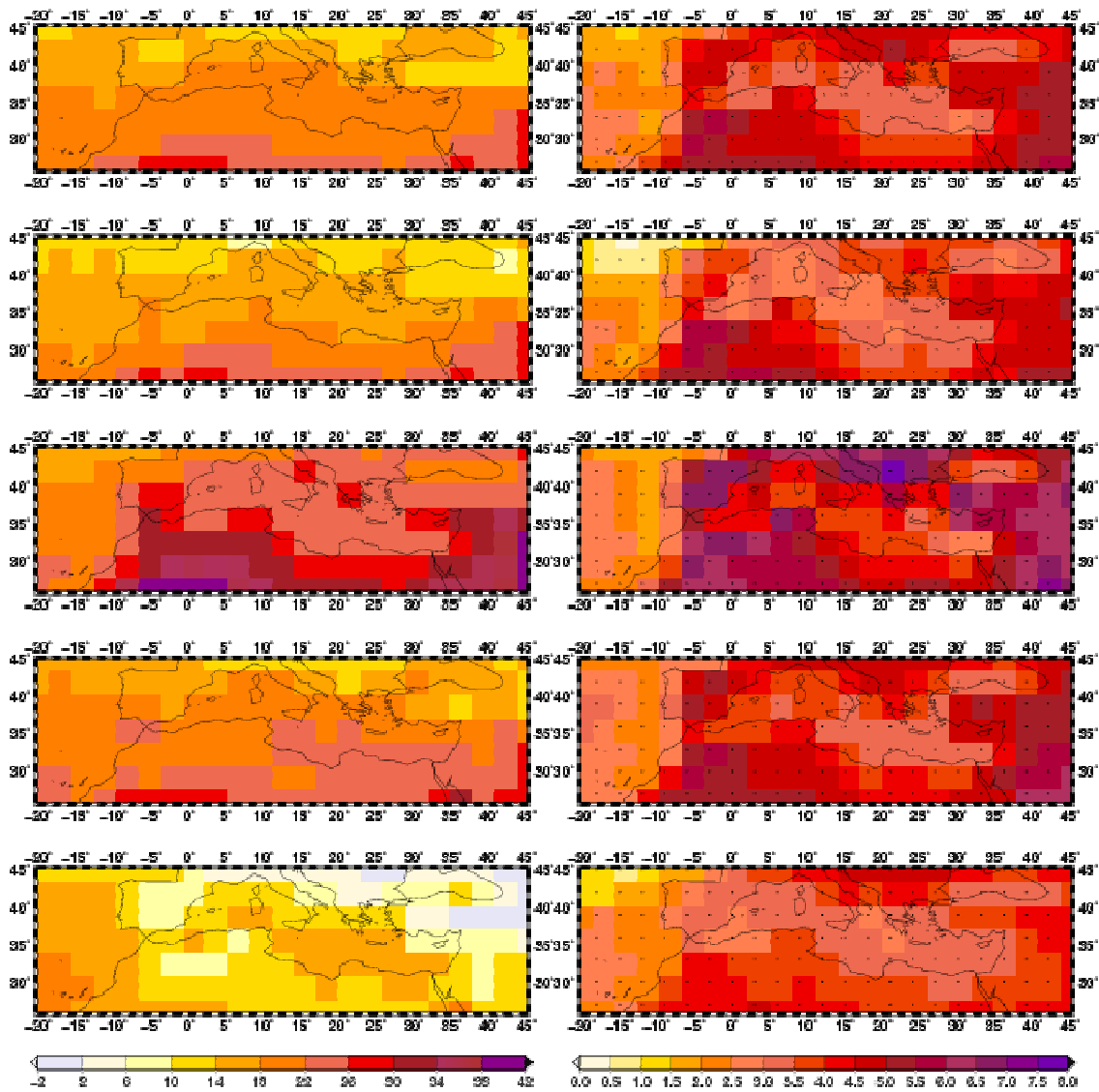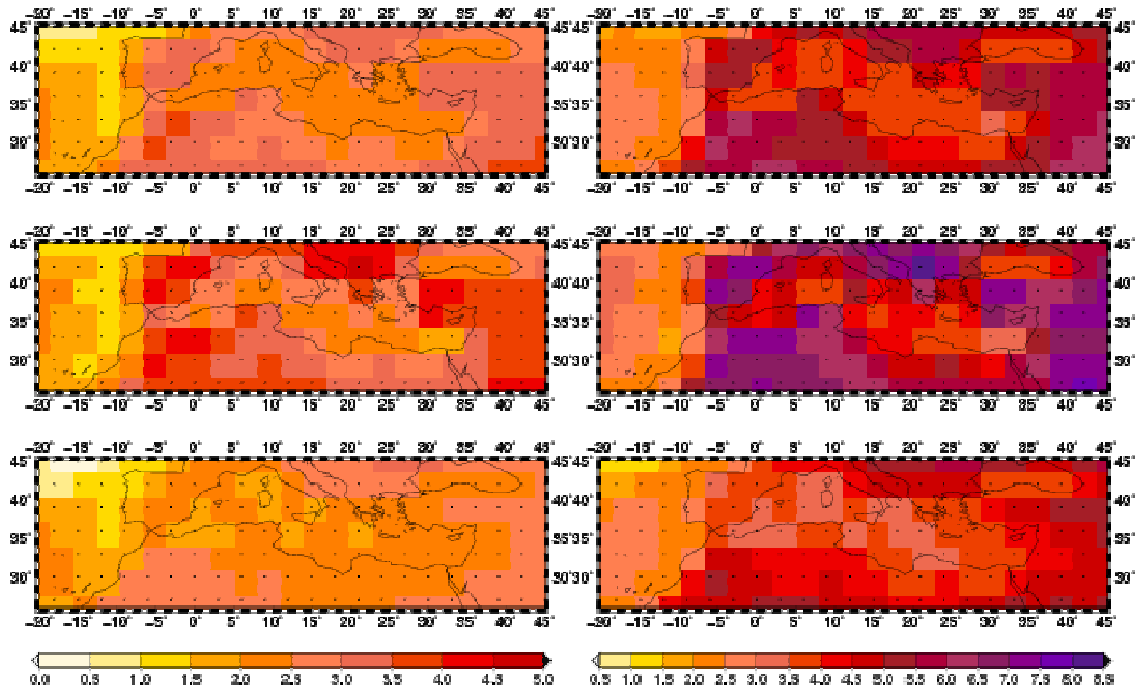

Figure 4.21: Interpolated ECHAM5 ensemble trends for B1 (left column) and A2 (right column) for temperature [°C] in the period 2001-2098. Rows indicate the season from top to bottom year, summer and winter. Black dots represent significance at the α=5% level.

For the multi-model mean figure 4.22 shows the trends in the scenarios B1 and A2. The medium impacts of the A1B with its comprising scenarios B1 and A2 are demonstrated again, besides the already observed feature of the smoothing phenomenon, leading to lower warming rates in every season. Again the land-sea surface distribution is reflected in the pattern of the warming amplitude, being most evident in summer in the A2 scenario. In winter, again demonstrating lowest warming, the separation of spatially differences is more difficult, holding particularly for B1 (0.2-3.3°C). Also the land-sea gradient in the warming trend becomes stronger with an increase of emissions.

Associated to ECHAM5 one can finally state that there is neither a shift in seasonal cycles, nor a change in the spatial pattern of values, evoked by a change of the scenarios. There is no necessity to behave this way for the models, as, first of all the forcing is not treated linearly within the model equations and, secondly this might further be disturbed by the composition of the model-ensembles and the multi-model mean.
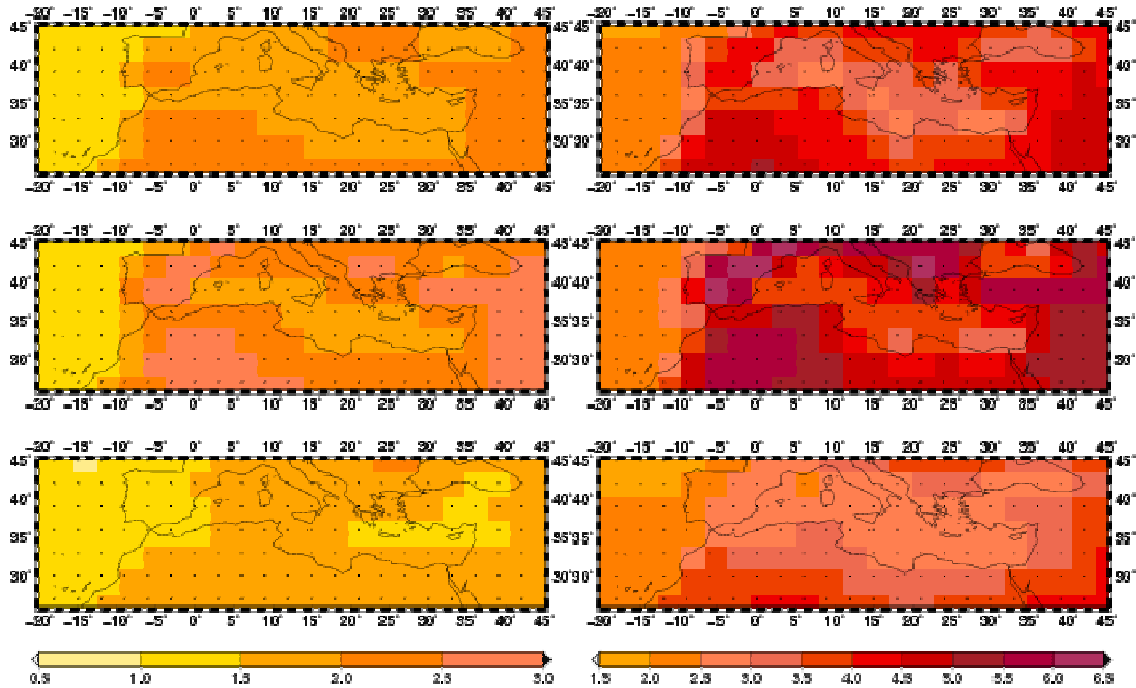
Figure 4.22: Interpolated multi-model trends for B1 (left column) and A2 (right column) for temperature [°C] in the period 2001-2098. Rows indicate the season from top to bottom year, summer and winter. Black dots represent significance at the α=5% level.

To elucidate the behaviour of the different models used, figure 4.23 shows the seasonally and spatially averaged mean temperatures over the whole MA for the specific models in 2001-2098 for the A1B scenario. It is noteworthy that for temperature in this scenario the most models have been available (see table 3.2), which leads to the most comprehensive analysis in this study associated with the highest potential of investigating uncertainties. The models in figure 4.23 are in the same order like the ones in figure 4.5, facilitating a comparison with each other and thus indicating their bias between their two means in the specific periods. As one can see in figure 4.23 the models show a huge spread in their annual mean temperature ranging from 16.3°C of NCAR-PCM to nearly 22.1 °C of the Australian model CSIRO-MK3.5. The individually introduced model ECHAM5 is slightly warmer than the average, indicated by the multi-model mean, which stands narrow above 19°C. Thus, demonstrated with the multi-model mean, a rise of the mean temperature can be observed, as for the former period 17.1°C are simulated. This higher mean is represented by all of the analysed models. Also for future periods the models clearly capture the annual cycles.

Figure 4.23: Regional temperature means [°C] of GCMs (A1B) for the specific seasons computed for the period of 2001-2098.

Compared to figure 4.6, in figure 4.23 a stronger trend can be recognized being subject to greenhouse gas emission scenarios, which now have serious impacts on temperature by their enhanced strength and their longer time period (98years compared to 40years, where the trend is computed) to evolute. For the total year, the trend of the multi-model mean stands at 3.2°C (compared to 0.65°C in 1961-2000). Now, the models again are in the same order as in figure 4.6 giving qualitative evidence about their changing compared to 1961-2000. So ECHAM5 and MIROC3.2 hires demonstrate a strong trend in relation to the former period, while the models, which already experienced a strong temperature rise from 1961-2000, show a tendency for smaller trends. Please note, that the latter models overestimated the former trend by the comparison with the reanalysis data. In the A1B scenario, the absolute values exceed 3.8°C in summer taking the multi-model mean as reference. It can be stated, that all models show the highest trend in summer, while winter exhibits the lowest rising temperature, making a seasonal dependency, as it has been described in chapter 1, evident.

Temperature Trend A1B 2001-2098
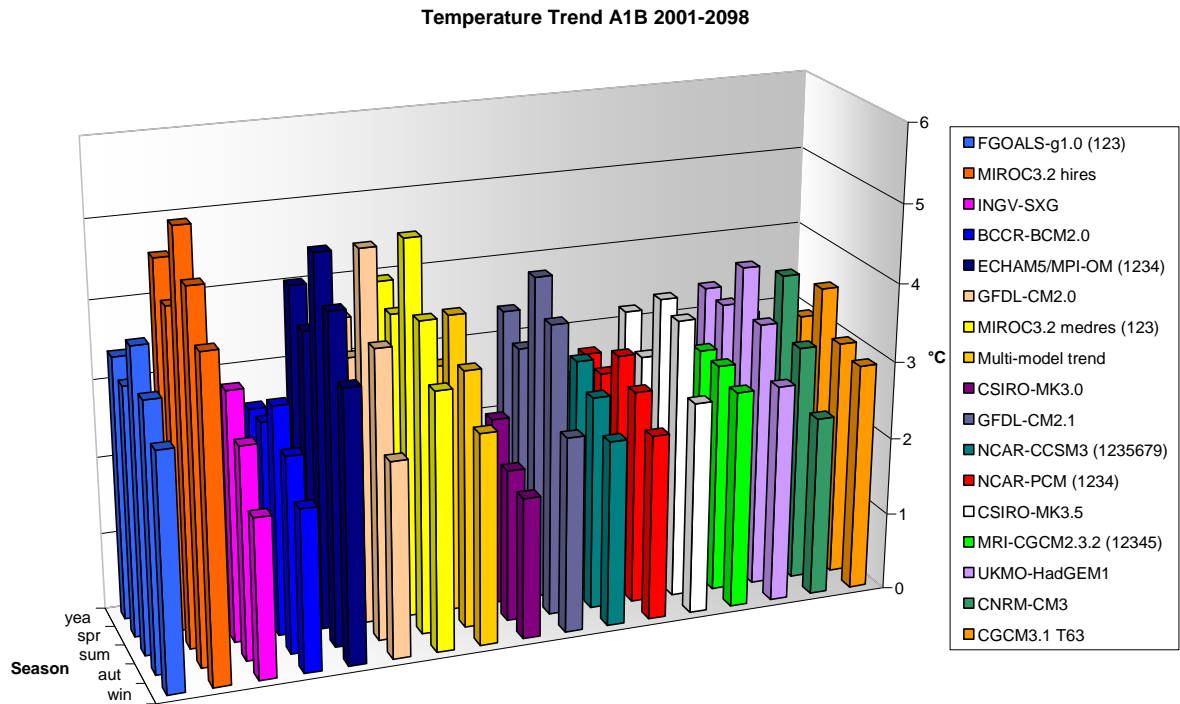
Figure 4.24: Regional temperature trends [°C] of GCMs (A1B) for the specific seasons computed for the period of 2001-2098.

This seasonal dependency is smoothed for the B1 scenario, illustrated in figure 4.25, which exemplarily can be seen by NCAR-PCM. Though, the multi-model mean still shows highest warming in summer (with up to 2.1°C). This indicates the mitigation of the temperature rise. Nevertheless, MIROC3.2 hires shows a warming exceeding the 3°C mark in the total year. This is astonishing but reasonable as one should think about the temperature increase of already 5.2°C in summer in the A1B scenario for the same model (figure 4.24). Unfortunately, this model is not available for the A2 scenario, where trends generally are highest (figure 4.26).

Temperature Trend B1 2001-2098
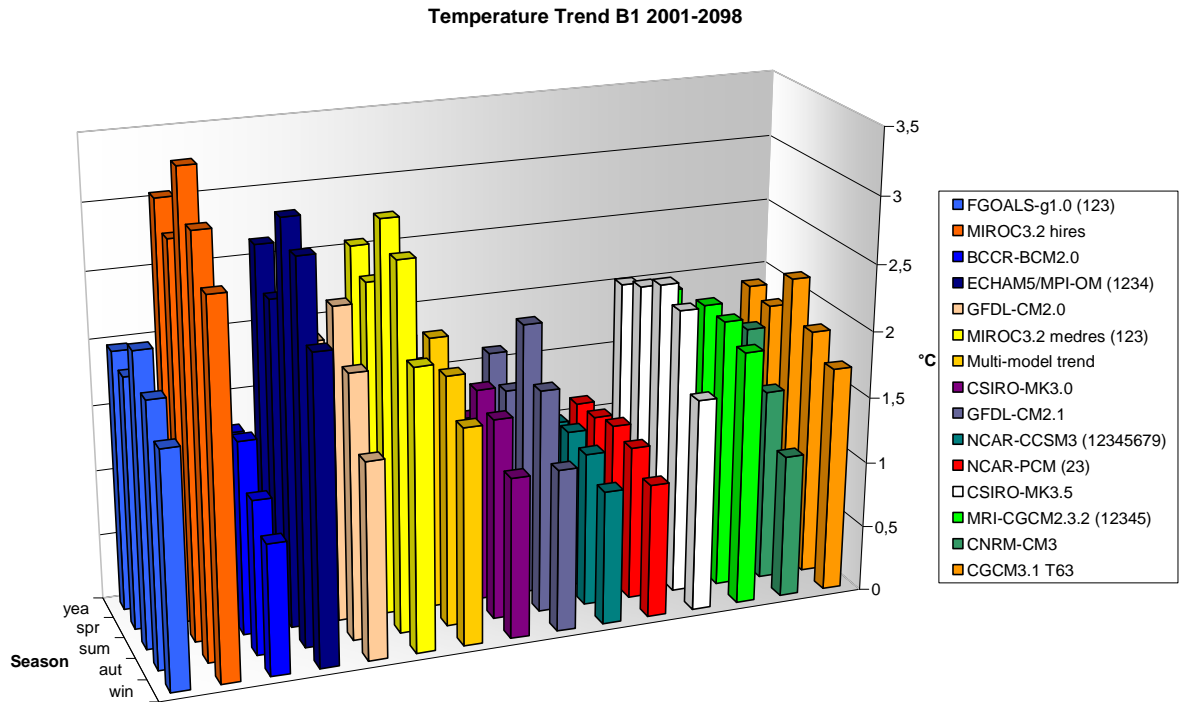
Figure 4.25: Regional temperature trends [°C] of GCMs (B1) for the specific seasons computed for the period of 2001-2098.

In A2 highest trends are shown. These occasionally even exceed the 5°C warming mark in summer in few models with a maximum value modelled by MIROC3.2 medres (5.4°C). Here ECHAM5 is one of the hottest models, while the multi-model mean still shows moderate warming in relation to the strong forcing scenario. Still many models show a rise of temperature of at least 4°C in the warmer seasons. Again it can be stated, that seasonal differences are pronounced most, when trends are highest. Furthermore the spatial maps are confirmed, concerning an increasing trend by a strengthening of the forcing, with B1 as the lowest to A1B and finally A2 with maximum magnitudes.
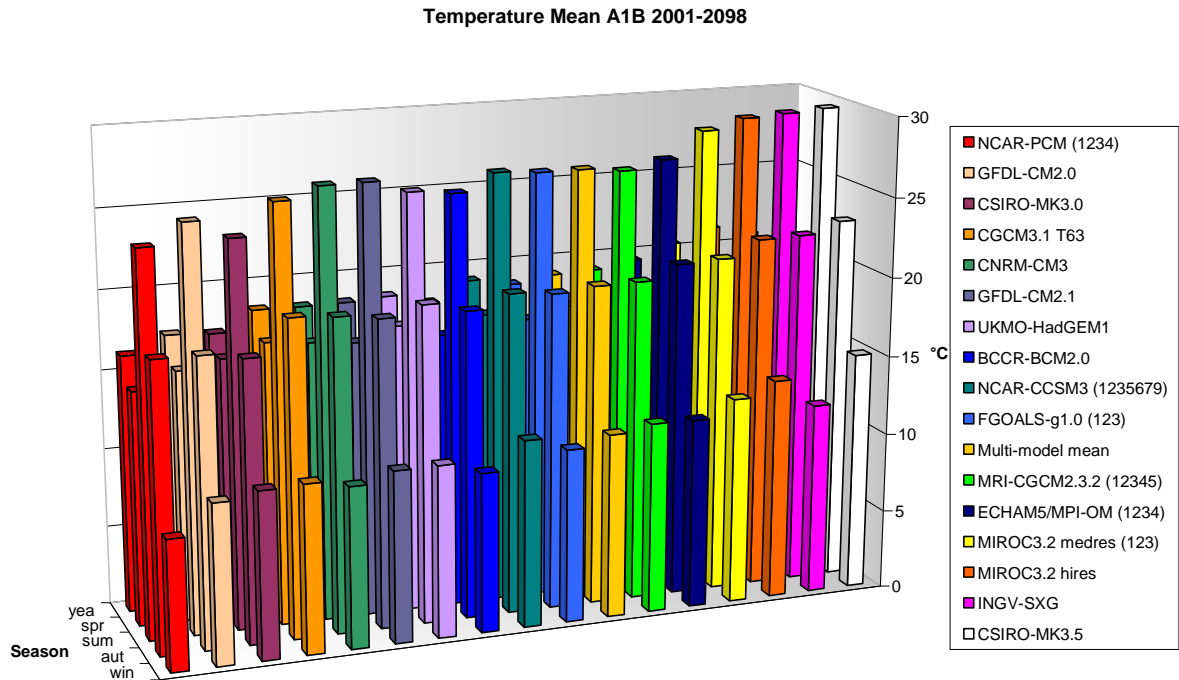
Temperature Trend A2 2001-2098
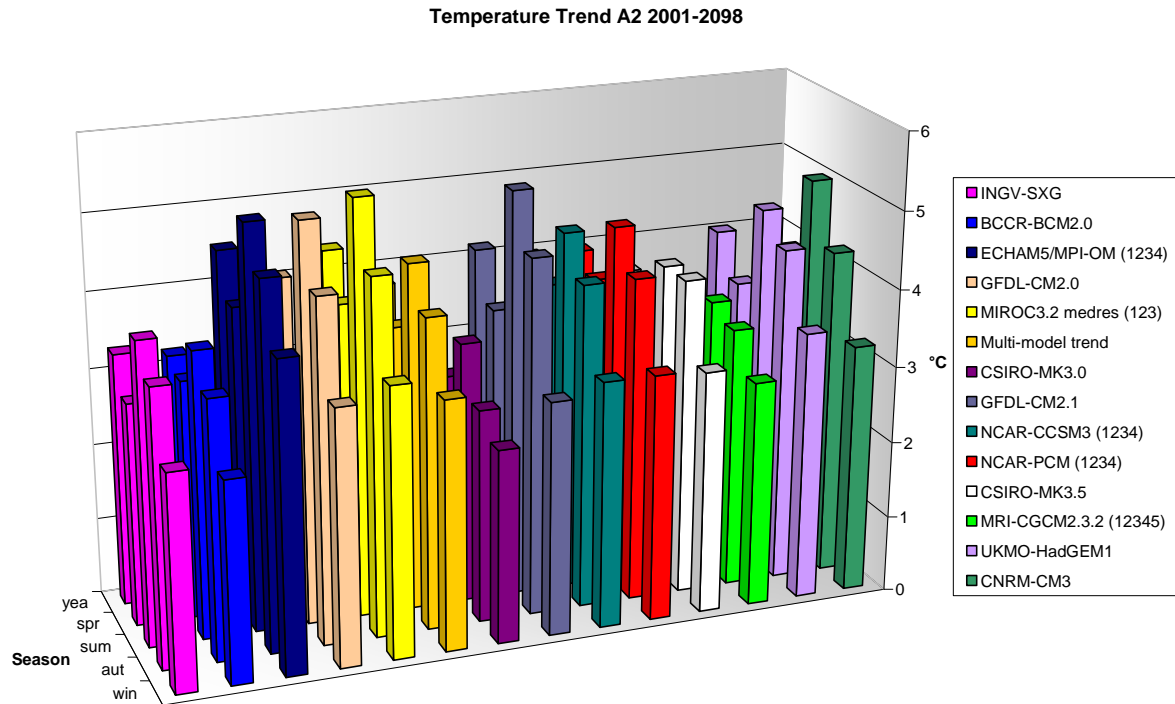
Figure 4.26: Regional temperature trends [°C] of GCMs (A2) for the specific seasons computed for the period of 2001-2098.

One still has to keep in mind, that the shown figures illustrate only mean values of climate models, being defined by several realizations. Therefore extreme temperatures, probably given by only one simulation, are filtered. The same holds for the single climate models concerning the multi-model mean. And finally, in the figures 4.23-4.26 spatial means are shown, averaging the values from the Atlantic, the Alps, Africa, etc…, which complicates the overall conclusion, as none of these individual regions is representative for the whole of the Mediterranean region. And thus, lower and of course also higher warming trends for some regions and simulations are lost in the averaging methods (compare the Macedonian region simulated by ECHAM5 in summer in the A2 scenario in figure 4.21). Nevertheless, one should be aware that every(!) model projects a rise in temperature in future independent of the scenario or season. For the future period the degree of warming even seems to become stronger.

4.2.2 Precipitation

To keep consistency to temperature the consideration of ECHAM5 in the A1B scenario for precipitation takes place first. Compared to the figure illustrating the years 1961-2000, in figure 4.27 one observes now drier conditions becoming evident by a northward shift of brownish colours, while the latitudinal belts are remaining. Notably this can be stated for summer, where the grid-cells with 0-10mm are reaching the northern coasts of the Mediterranean Sea. Lowest changes in the mean are shown during the rainy season in winter, which next to temperature again points out the stronger affection of summer conditions by

climate change. In any case the summer difference, shown in figures 4.27 and 4.9, takes effect on the total yearly precipitation, although the total precipitation amount is relatively low in the warm seasons. The pattern of the mean precipitation for 2001-2098 is not suggestive by the spatial trends computed for ECHAM5 in the control period (1961-2000).

Trends for ECHAM5 for the future period (2001-2098) are reflected in the right column of figure 4.27. In winter slow increases (without significance) are detectable in the northern part of the MA, which can be explained by the behaviour of the NAO and the increasing north-south pressure gradient (see below). But in most cases the figures indicate a drying trend, attesting the left panel of general drier conditions. This trend of drying seems to be shifted from north to the south with the hotter to the colder seasons. Strongest drying is detected over the eastern Mediterranean Sea in winter. Considered the total year the Iberian Peninsula, Macedonia, Albania and Turkey and the Eastern Mediterranean Sea suffer highest precipitation decreases of more than -182mm, which is in many cases more than doubled compared to figure 4.9. The development of this seasonal structure is not indicated in ECHAM5 trends of former periods (figure 4.9, while it brings the similar trend patterns of the reanalysis data to mind, where also the drying in winter prevails over the other seasons).
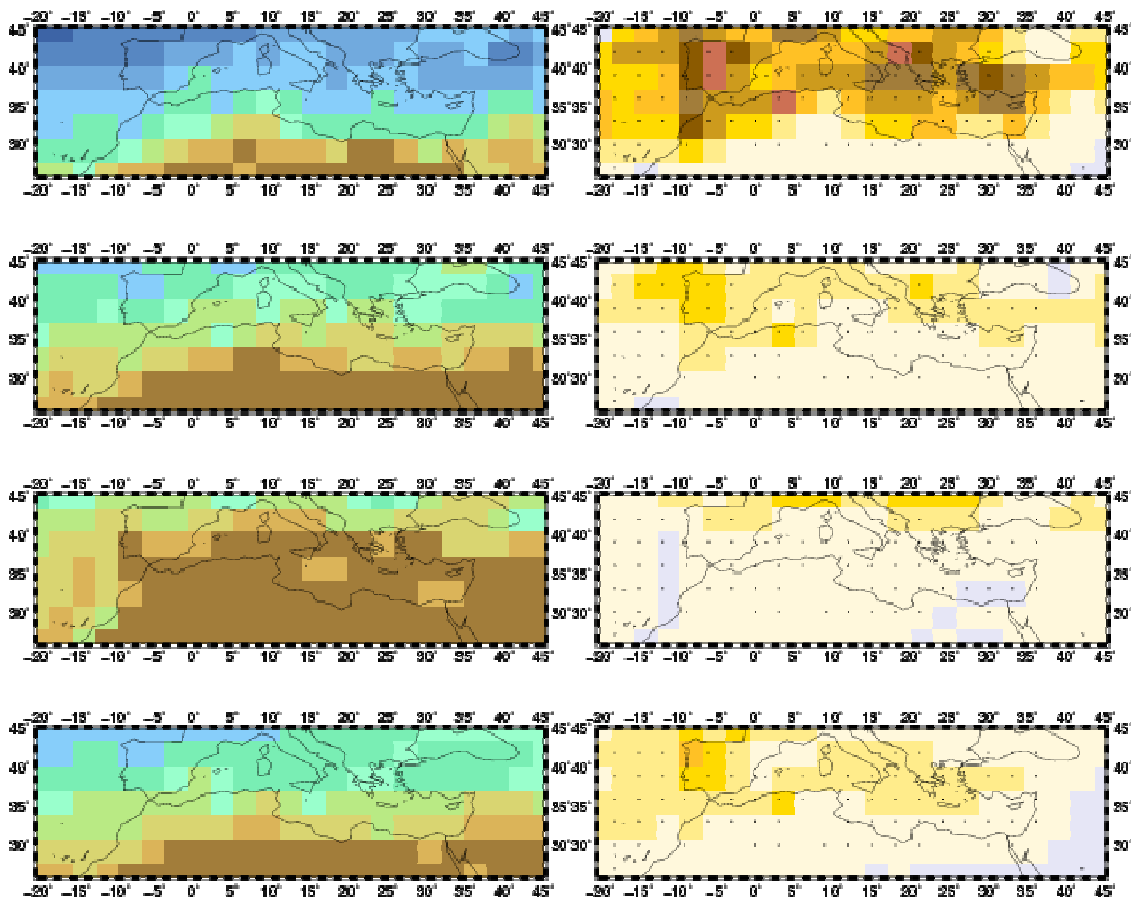
Figure 4.27: Interpolated ECHAM5 ensemble-means (left column) and ECHAM5 ensemble- trends (right column) for precipitation [mm] in the period 2001-2098 in the A1B scenario. Rows indicate the season from top to bottom year, spring, summer, autumn and winter. Black dots in the trend figures represent significance at the α=5% level.

Also the multi-model mean shows next to ECHAM5 slightly lower precipitation amounts (figure 4.28) compared to the period of 1961-2000 (figure 4.10). Nevertheless, the changes in amounts and patterns are small. Also in future conditions the multi-model mean illustrates a distinct north-south orientation of the distribution of precipitation with an evident seasonal cycle. Compared to the multi-model mean the driest areas, being located in the southeastern quarter of the map in summer, are again extended to the west by ECHAM5, which follows the findings of the control period. Again the multi-model mean is much wetter than ECHAM5, e.g. over central Italy with nearly 130mm.
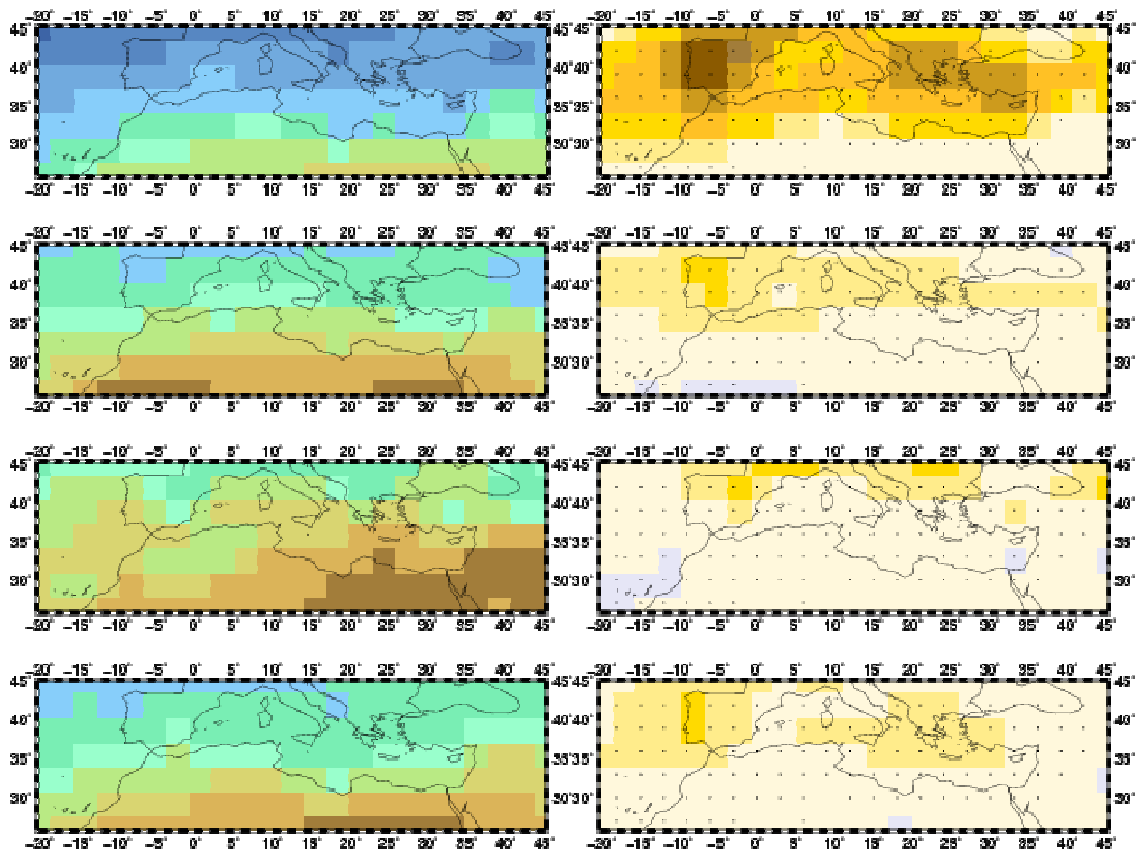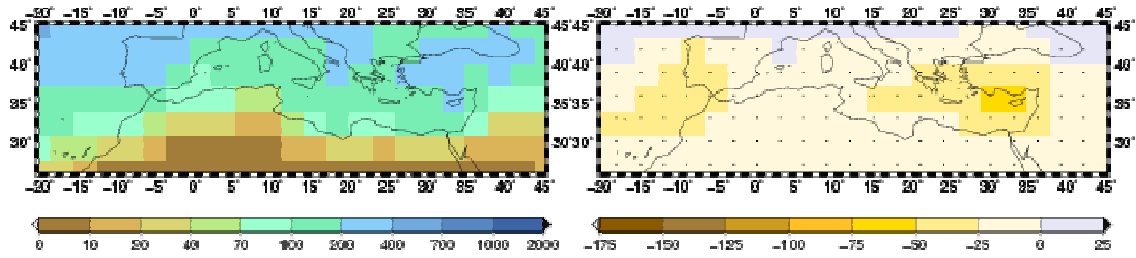
Figure 4.28: Interpolated multi-model means (left column) and multi-model trends (right column) for precipitation [mm] in the period 2001-2098 in the A1B scenario. Rows indicate the season from top to bottom year, spring, summer, autumn and winter. Black dots in the trend figures represent significance at the α=5% level.

The multi-model mean trend affirms the statement of ECHAM5. Decreasing trends of total precipitation are projected, showing their maximum in the northern regions during the hot seasons (-63mm), while this drying area is shifted to the south during the colder seasons. In winter and autumn the already mentioned dipole of drying develops, which is located over the Eastern Mediterranean Sea and the western Iberian Peninsula and the Moroccan coast. This double spot is echoed in the total year precipitation trend, resulting in two hot spots of drying: the Iberian Peninsula (-173mm) and western Turkey with the Aegean Sea, Greece, Macedonia and Albania (~-123mm). In winter, the projected wetting in the north of the area of investigation is not predominant in that season, which is the reason for the overall reduction. Nearly all trends are significant, except the results for northern Africa in the south of the area of investigation. The clear patterns, which cannot be found in the control period, indicate a higher agreement of the models to each other than in the last decades of the 20th century.
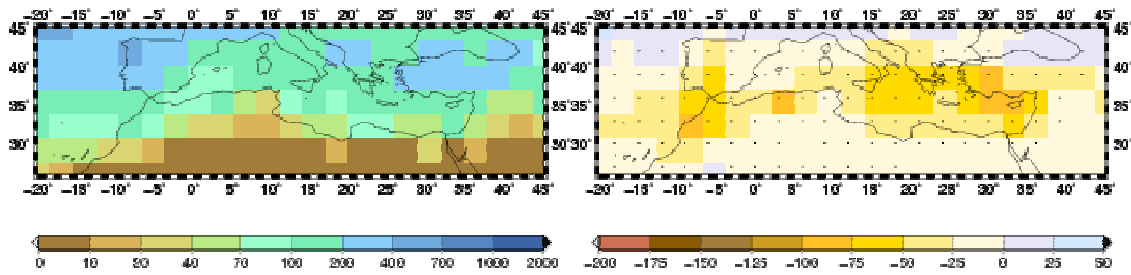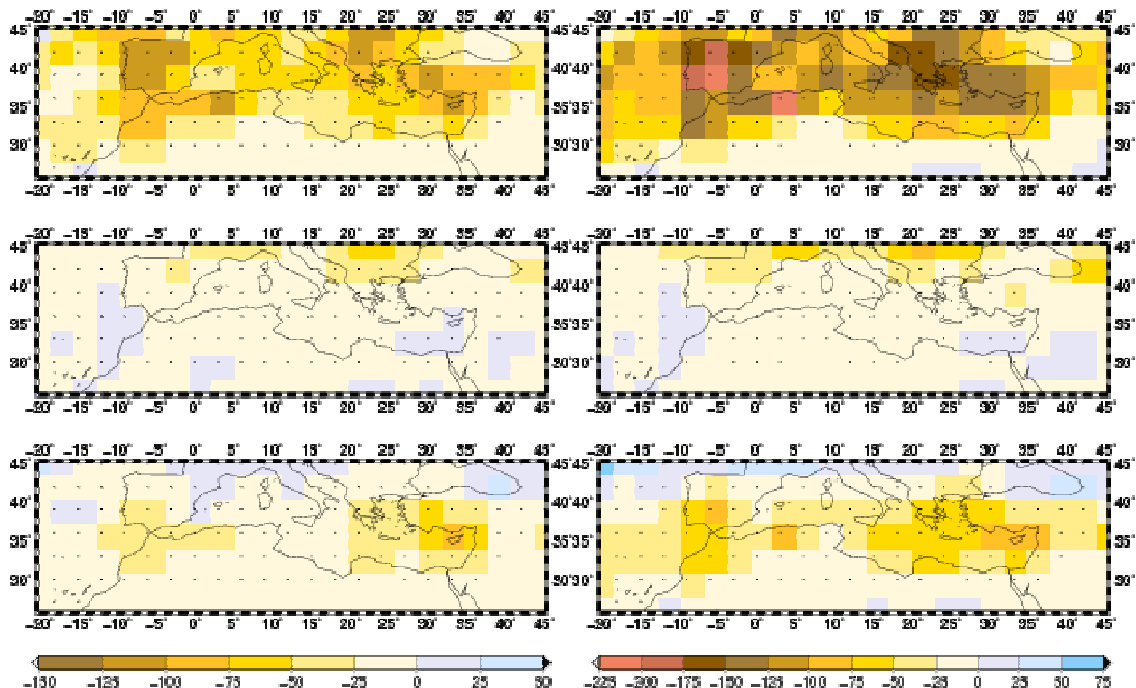

Figure 4.29: Interpolated ECHAM5 ensemble trends for B1 (left column) and A2 (right column) for precipitation [mm] in the period 2001-2098. Rows indicate the season from top to bottom year, summer and winter. Black dots represent significance at the α=5% level.

In figure 4.29 the scenarios of B1 and A2 are opposed again for the extreme seasons and the total year, now for precipitation modelled by ECHAM5. One quickly perceives the stronger reduction of precipitation accompanied with a stronger forcing, when also figure 4.27 is involved to that consideration. Consecutively, most distinct trends can be found over the total year for the A2 scenario over the South of Spain with minus -221.5mm while B1 depict lower trends. The pattern of the dipole develops stronger within the A2 scenario. While in B1 the increase of precipitation in the north of the MA is also not that attestable, as it has already been for ECHAM5 and the multi-model mean in the A1B scenario. Nevertheless, for all scenarios, even for the most admissible scenario of B1 strong significant decreases are modelled by ECHAM5, with up to 126 mm.
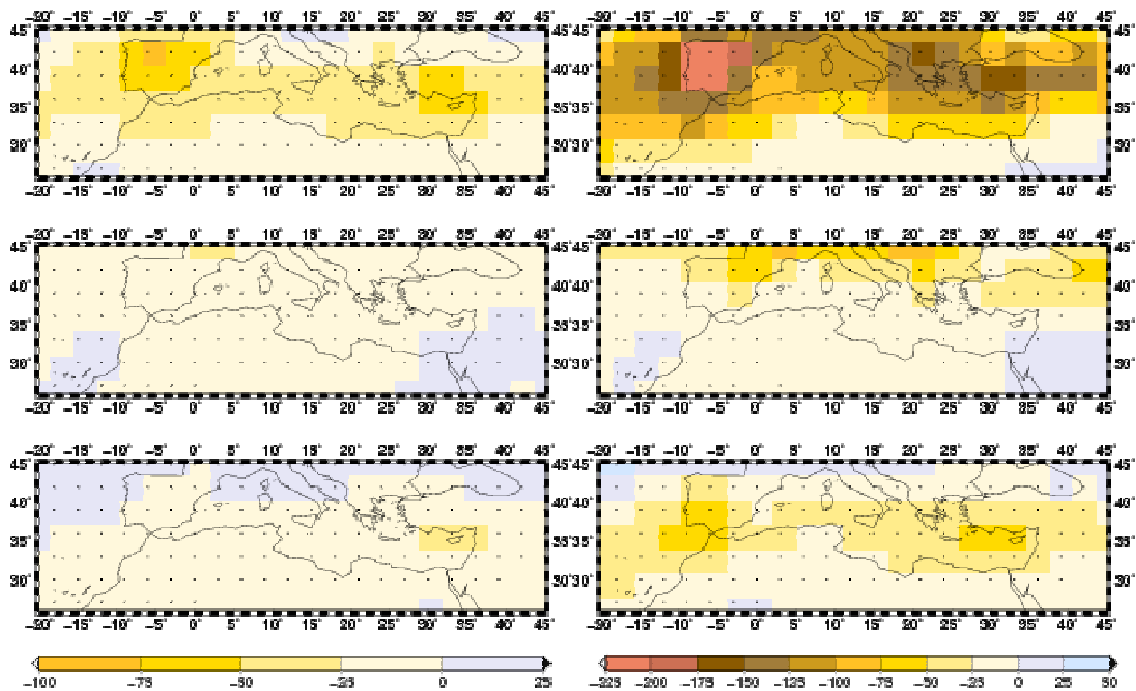
Figure 4.30: Interpolated multi-model trends for B1 (left column) and A2 (right column) for precipitation [mm] in the period 2001-2098. Rows indicate the season from top to bottom year, summer and winter. Black dots represent significance at the α=5% level.

Concerning the seasonal distribution and the overall statements similar maps to figure 4.29 are shown in figure 4.30 for the multi-model mean. An analogous pattern is seen for the A2 scenario compared to the A1B scenario in figure 4.28, while distinct trend distributions vanish for the B1 scenario. Nevertheless the B1 scenario matches to the stronger scenarios by the yearly map and the herein shown dipole pattern with its most severe trends over the Iberian Peninsula and Asia Minor. Particularly for the regions of northwestern Spain and the north of Portugal, the negative trends are associated with decreases in spring and autumn (not shown). The yearly negative trend of more than -46mm over Greece is confined on the two stronger scenarios. In contrast, the increasing trend of precipitation in the north of the area of research is also reflected within the B1 scenario and with up to 7.7mm strongest near the northeastern boundary. Furthermore, its extension to the south is biggest. The most impressing negative trends are found over the Iberian Peninsula in the A2 scenario with up to minus -217mm, slightly beneath the maxima of ECHAM5.

Figure 4.31: Regional precipitation means [mm] of GCMs (A1B) for the specific seasons computed for the period of 2001-2098.

   To gain a better estimation about the models reproduction of future precipitation conditions, the precipitation means of the applied models in the A1B scenario are shown (figure 4.31). Their relative magnitudes to each other can easily be analysed in comparison to their former distribution, as the sequence is the same of figure 4.11. MRI-CGCM2.3.2 and GFDL-CM2.1 suffered relative strong abatement of precipitation, where the first one is now the model with the lowest yearly precipitation amount. Lower reduction is inherent to the NCAR models (with ~ –11mm for the overall year in PCM and ~ –13mm for the overall year in CCSM3. General higher decrease is reflected in the multi-model mean (~ -35mm in the overall year). The range of this total precipitation means between MRI-CGCM2.3.2 and BCCR-BCM2.0 is with about 200mm extremely high. As already mentioned, ECHAM5 belongs to the drier models, showing an average mean of nearly 250mm in the total year. The seasonal dependency is preserved by every model.

   This seasonal dependency is still noteworthy, as the trends in figure 4.32 do not show this seasonal distribution, as some model indicate highest reductions in the intermediate seasons, while others like INGV-SXG project highest drying for winter. Only MRI-CGCM2.3.2 and NCAR PCM show light increases in winter of a few mm. Besides them, all(!) models over the period from 2001-2098 indicate a decrease of precipitation in every season. The multi-model trend reaches a decrease of 50.1mm over the total year. ECHAM5, already indicated as a model with relatively strong drying effects, still shows smaller trends than models from the GFDL, which project trends of above 100mm. Compared to the

control period, one has to conclude, that all the models have a stronger basis concerning the magnitudes and the direction of negative courses.

Precipitation Trend A1B 2001-2098
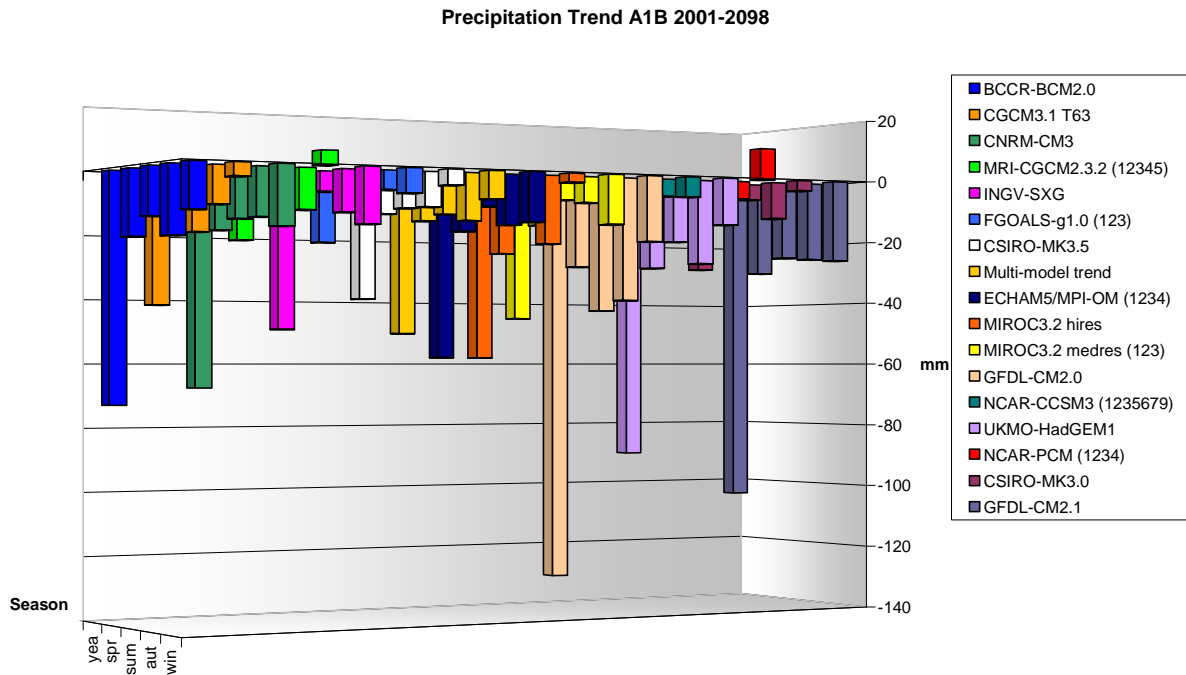
Figure 4.32: Regional precipitation trends [mm] of GCMs (A1B) for the specific seasons computed for the period of 2001-2098.

These two GFDL models even show a strong decrease over the moderate B1 scenario (figure 4.33) reaching nearly 40mm. Here the BCCR-BCM2.0 shows highest decreases. Irrespective of the model, all trends show a fewer decrease of precipitation in B1 compared to the A1B scenario. NCAR-PCM even states an increase of precipitation over a few mm in the overall year. The winter increase given by MRI-CGCM2.3.2 is compensated by the general negative trend throughout all the other seasons and results towards no distinct trend considering the total year. An interesting feature is the relative strong reduction of summer precipitation by GFDL-CM2.0, which is already indicated in figure 4.32. Other models show highest reductions in spring (e.g. GFDL-CM2.1) or winter (e.g. FGOALS-g1.0). These examples again prohibit a detectable seasonal distribution of the trends. Concerning the multi-model mean strongest reduction is found in autumn, like in figure 4.32. Regarding the B1 scenario as desirable for the future course of emissions, the decrease of precipitation projected by the multi-model mean is beneath the trends of the NCEP data shown in figure 4.12.

Precipitation Trend B1 2001-2098
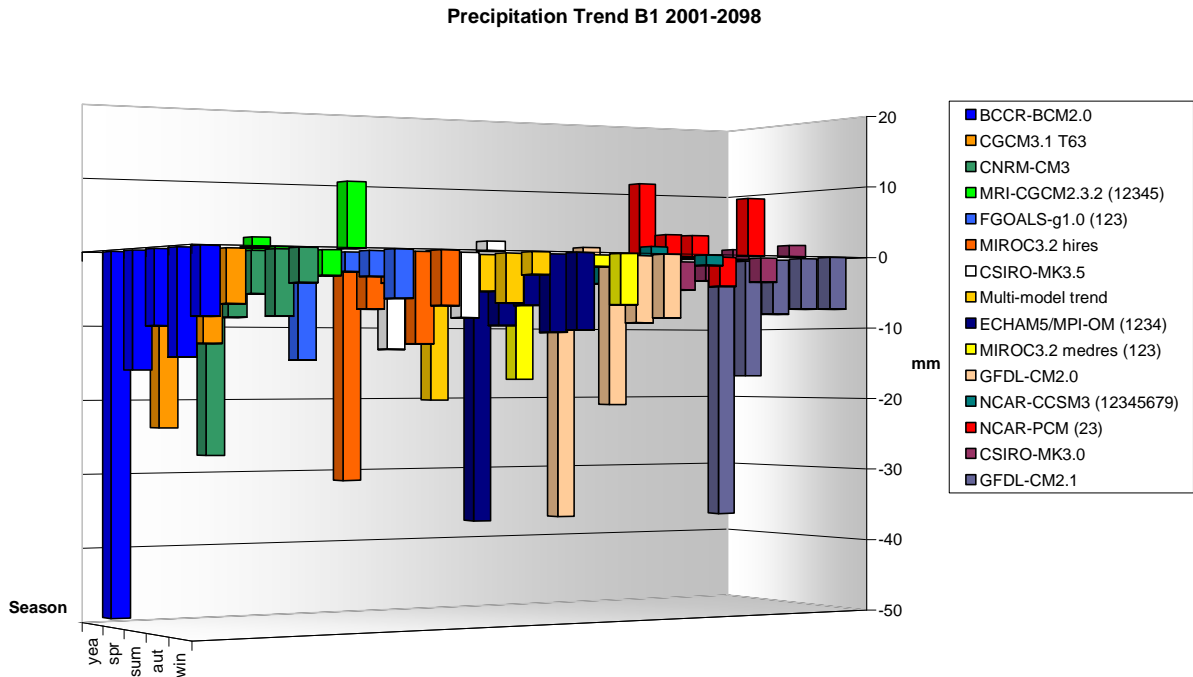
Figure 4.33: Regional precipitation trends [mm] of GCMs (B1) for the specific seasons computed for the period of 2001-2098.

Analysing the results given by the application of the A2 scenario (figure 4.33), the thitherto considerable results of the A1B scenario are surpassed. Also, the positive trend in winter, projected by NCAR-PCM, is nearly vanished taking the course from B1 over A1B to A2. While the multi-model mean still illustrates highest decreases in autumn, a distinct seasonal dependency of the trends cannot be distinguished. Although the amplitude of the decrease is highest over all models in the A2 scenario (with the maximum negative trend given by GFDL-CM2.1 with nearly -144mm, which has overtaken GFDL-CM2.0), the discrepancy between the models is extremely high, which already could be seen for the other scenarios. Still the average trend depicted in the multi-model mean for the overall year does not exceed the -67mm threshold, whereat this is about three times the trend of ERA40 in figure 4.12 for the whole year, though.
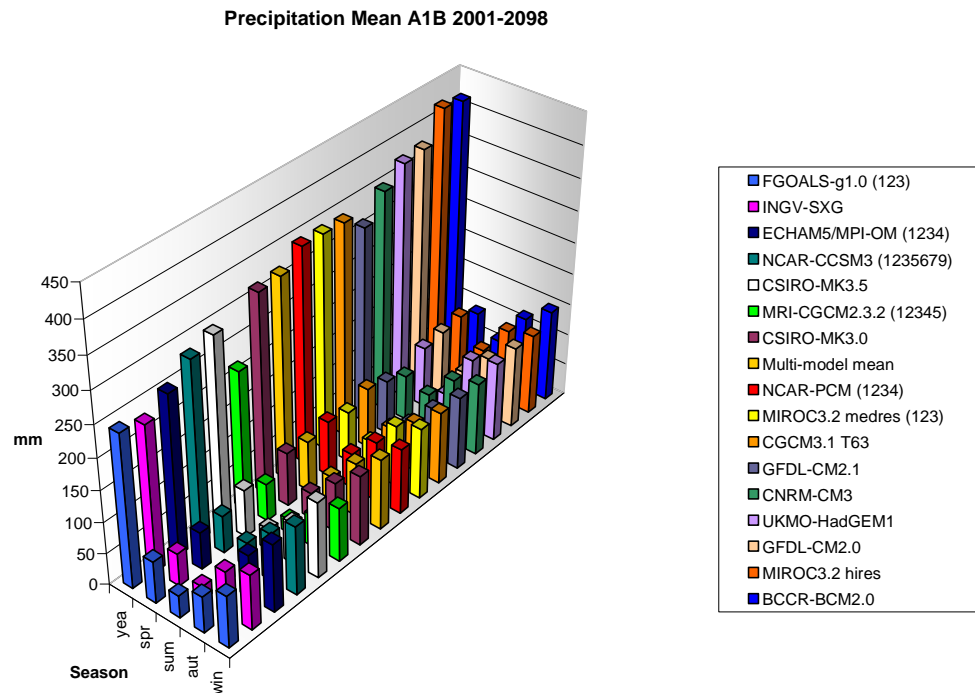
Precipitation Trend A2 2001-2098
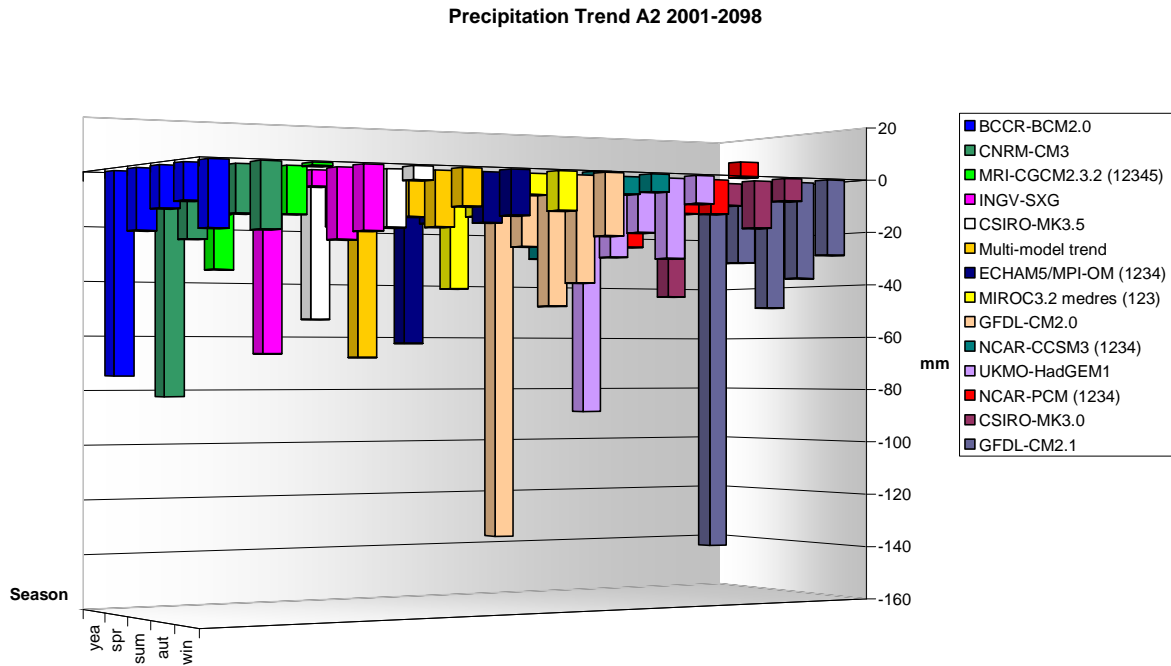
Figure 4.34: Regional precipitation trends [mm] of GCMs (A2) for the specific seasons computed for the period of 2001-2098.

4.2.3 Sea-level pressure

Figure 4.35 in the left panel illustrates the ensemble-mean values of the ECHAM5 simulations 1,2,3 and 4 in the average for the period 2001-2098 for sea-level pressure. While the overall pattern and the seasonal behaviour look relatively similar to the control period, an eastward extension of higher pressures can be established in the intermediate seasons (e.g. the branch of almost 1019 hPa in spring). A further difference to the control period (figure 4.15) is the pronounced and extended patterns considering the centres of low pressures (particularly in summer) or of high pressures. Particularly in winter the anticyclonic structure is enhanced over Jordan, Saudi-Arabia and the northeastern Africa (with up to 1025.4hPa), which has not been evident in the trend calculated for the control period of 1961-2000, as this has been too weak in its amplitude (figure 4.15).

The right panel of figure 4.35 shows the linear trend calculated in the period from 2001-2098 in the A1B scenario. With the exception of winter this trends shows no relation to the depicted trends of the reanalysis data, as illustrated in figures 4.13 and 4.14. Furthermore, compared to figure 4.15 within the control period, the different patterns have nothing in common, whereat in the future period more significant trends are evident. For the overall year this holds mainly for significant decreases of pressure in the south of the area of research (roughly up to -1hPa over the Red Sea), which is mainly associated with the reduction of sea-level pressure in the warmer seasons. While in winter an increase of pressure with up to 2.78hPa is significant over the centre of the MA. This increasing is obviously started in autumn and prolonged until spring, where

significance is missing. However this trend is superimposed by the reduction in summer, prohibiting significant conclusions for the overall year.
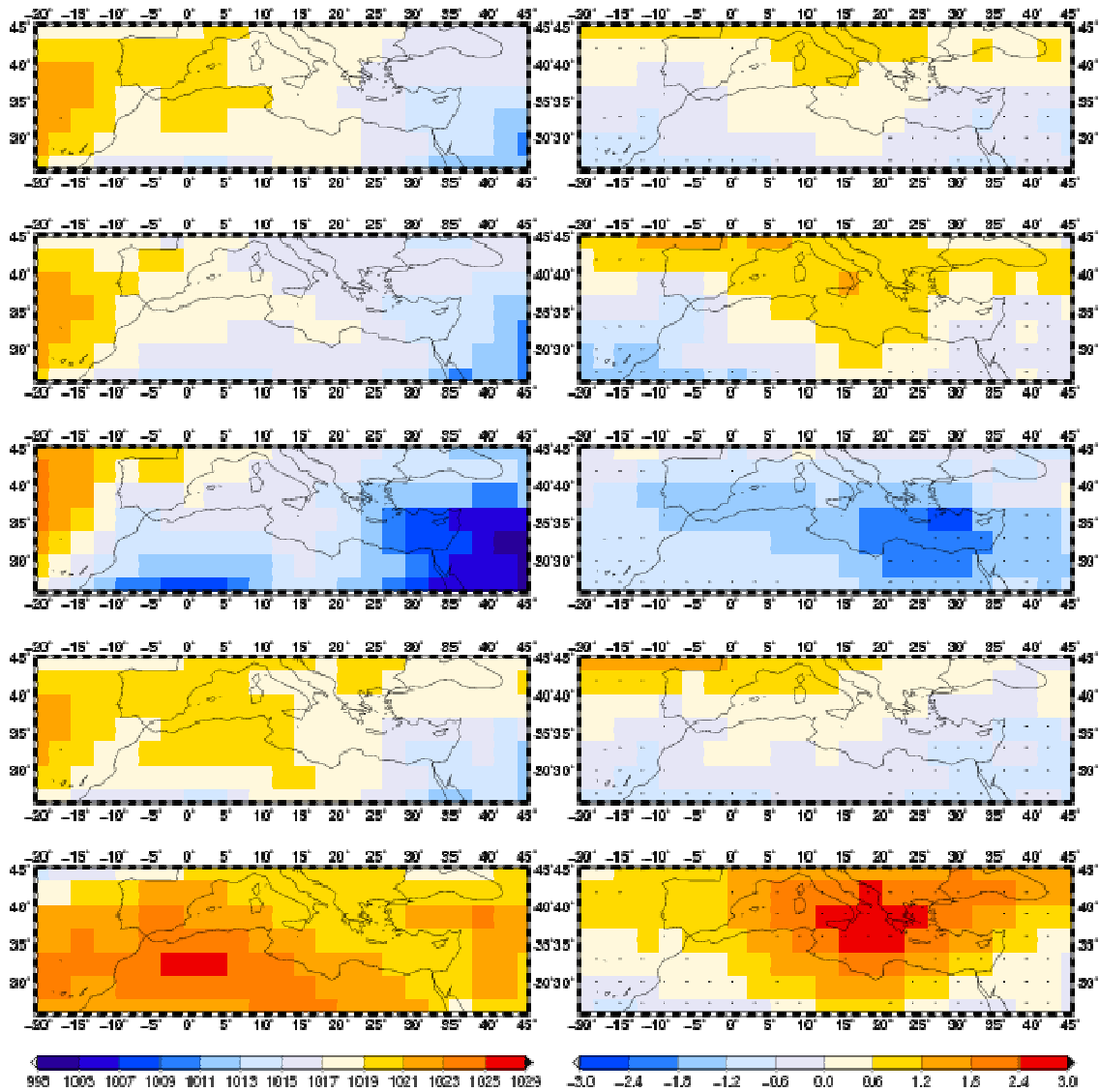
Figure 4.35: Interpolated ECHAM5 ensemble-means (left column) and ECHAM5 ensemble- trends (right column) for sea-level pressure [hPa] in the period 2001-2098 in the A1B scenario. Rows indicate the season from top to bottom year, spring, summer, autumn and winter. Black dots in the trend figures represent significance at the $\alpha=5\%$ level.

The results of the single model ECHAM5 are also reflected in the multi-model mean (figure 4.36) concerning the pattern and the seasonal behaviour. Nevertheless, the discrepancies of ECHAM5 to the multi-model mean are of the same kind in future as in the control period. This again holds for the exceeding values in the centres of the pressure cells in winter (the high pressure over northeast of Africa with 1026.8hPa) or the amplified extension of e.g. the Red Sea Trough in summer. Local features, which have not been distinct in the control period are not depicted in future also. This holds for other models as well (not shown). Compared to the control period, the sea-level pressure is higher in the total year with a displacement of the lower pressures to the east, which is mainly due to the increases in winter and autumn, and the smaller

counteracting of the decrease in summer. This development has not been indicated by the trends in 1961-2000, except by some small significant values describing a future extension of the southeastern trough (figure 4.16).

Still this development is reflected in the trends from 2001-2098 (right column of figure 4.35). The multi-model mean confirms the change in the rising means by an increase of sea-level pressure over the centre in the MA enhancing an anticyclonic stream of winds. During all seasons except summer the sea-level pressure rises from the eastern of the Atlantic spreading via the northern boarders of the area of investigation to the centre of the Mediterranean area. For summer, a distinct decrease of sea-level pressure is also evident in the multi-model mean. Compared to ECHAM5, most of the trends have a lower magnitude (1.85hPa over central MA in winter) but show significance. Again, ECHAM5 shows a high agreement on the spatial reproduction of trends by the multi-model mean.
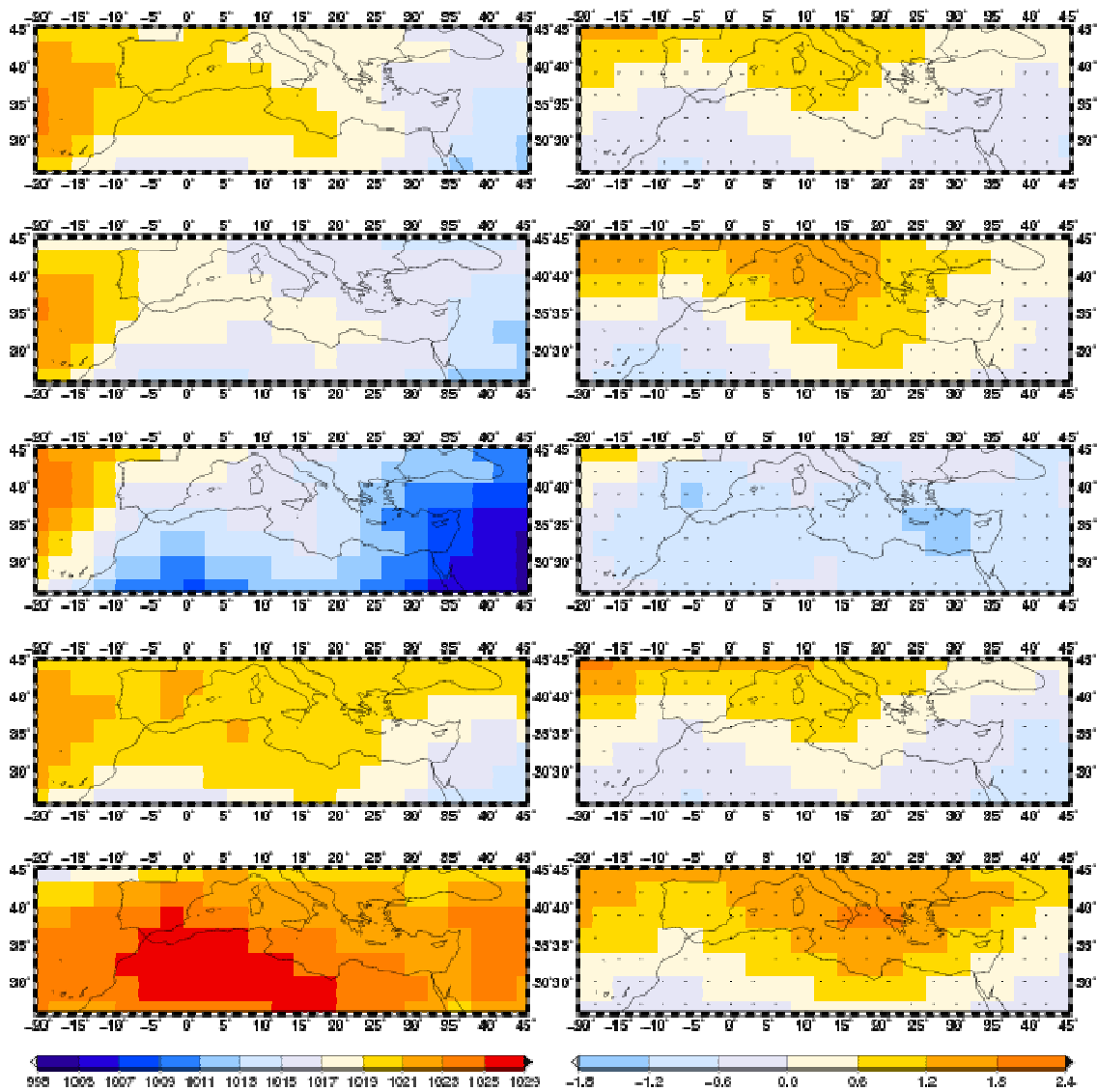
Figure 4.36: Interpolated multi-model means (left column) and multi-model trends (right column) for sea-level pressure [hPa] in the period 2001-2098 in the A1B scenario. Rows indicate the season from top to bottom year, spring, summer, autumn and winter. Black dots in the trend figures represent significance at the α=5% level.

By confronting the different scenarios with each other for ECHAM5 in figure 4.37, it becomes evident, that next to temperature and precipitation also the strength of the sea-level pressure trends is defined by the scenario. Furthermore, it is apparent that the values in the extreme seasons are intensified by the trends of the pressures, as for the A2 scenario, summer experiences a decrease of -2.7hPa, while winter undergoes an increase of nearly 3.1hPa (B1 -1.29hPa and 1.80hPa respectively). This enhanced potential of seasonal discrimination becomes not evident by the investigation of the yearly values, indentifying the necessity of a seasonal assessment of future climate analyses. This holds for every scenario. Consecutively, the change in magnitudes or potential changes in patterns by a change of scenarios underlie seasonal shifts. A spatial shift is the pronounced southern extension of increasing magnitudes over the year.
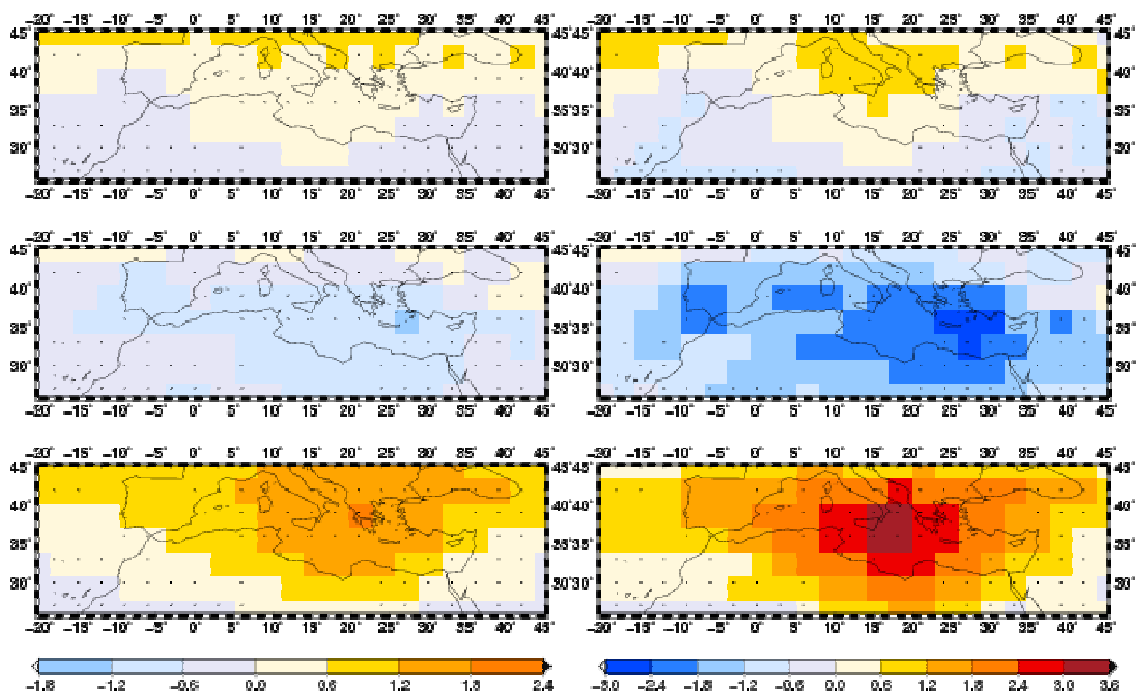
Figure 4.37: Interpolated ECHAM5 ensemble trends for B1 (left column) and A2 (right column) for sea-level pressure [hPa] in the period 2001-2098. Rows indicate the season from top to bottom year, summer and winter. Black dots represent significance at the α=5% level.

Besides the reproduction of the already known patterns and seasonal cycles, main differences can be found in the multi-model mean in the overall year with a stronger northern increase in the A2 scenario compared to ECHAM5 (1.68hPa over all the models compared to 0.95hPA in ECHAM5), while in the B1 scenario the multi-model mean drops behind ECHAM5 in the reproduction of positive trends in the north (figure 4.38). Consecutively in A2, other models seem to be stronger affected by an enforcement of emissions. The positive trend in A2 in the north for the overall year is explained by the considerable positive trend contributions in autumn (not shown), while the trend magnitudes in the extreme seasons are smoother compared to ECHAM5 and partially smoother to other models (compare figures 4.40, 4.41 and 4.42 below). Again, it is mainly the amplification of the values which is resulting by a substitution of the scenarios.
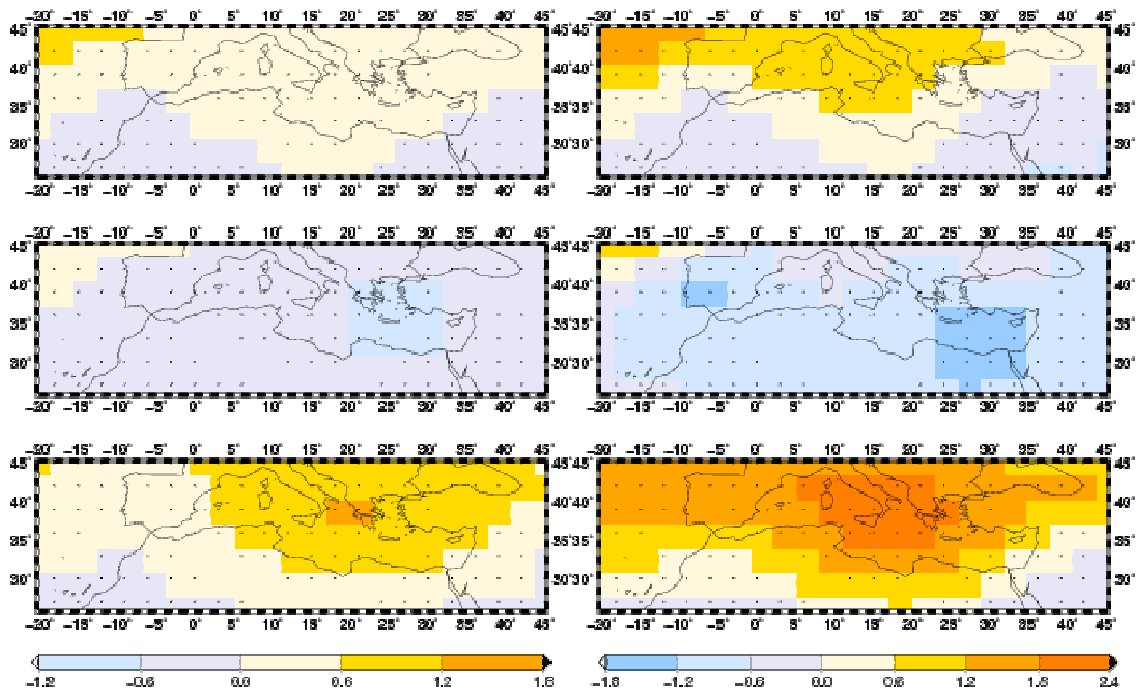
Figure 4.38: Interpolated multi-model trends for B1 (left column) and A2 (right column) for sea-level pressure [hPa] in the period 2001-2098. Rows indicate the season from top to bottom year, summer and winter. Black dots represent significance at the α=5% level.

Figure 4.39 illustrates only small changes in the mean compared to figure 4.17 out of the control period. While many models exhibit nearly no changes (e.g. the GFDL models), other models show slight increases (e.g. BCCR-BCM2.0). The already relative high values of NCAR-PCM (with about 1021.7hPa in the total year) are persistent in the future. Some models also show negative courses like the GISS AOM (neglected), where the results are rather doubtful, as no distinct seasonal cycle can be distinguished. This cycle is inherent to the other models, showing highest pressures in winter. Consecutively, the seasonal cycle is reflected in the multi-model mean allowing a comprehensive estimate of the behaviour of all the models.
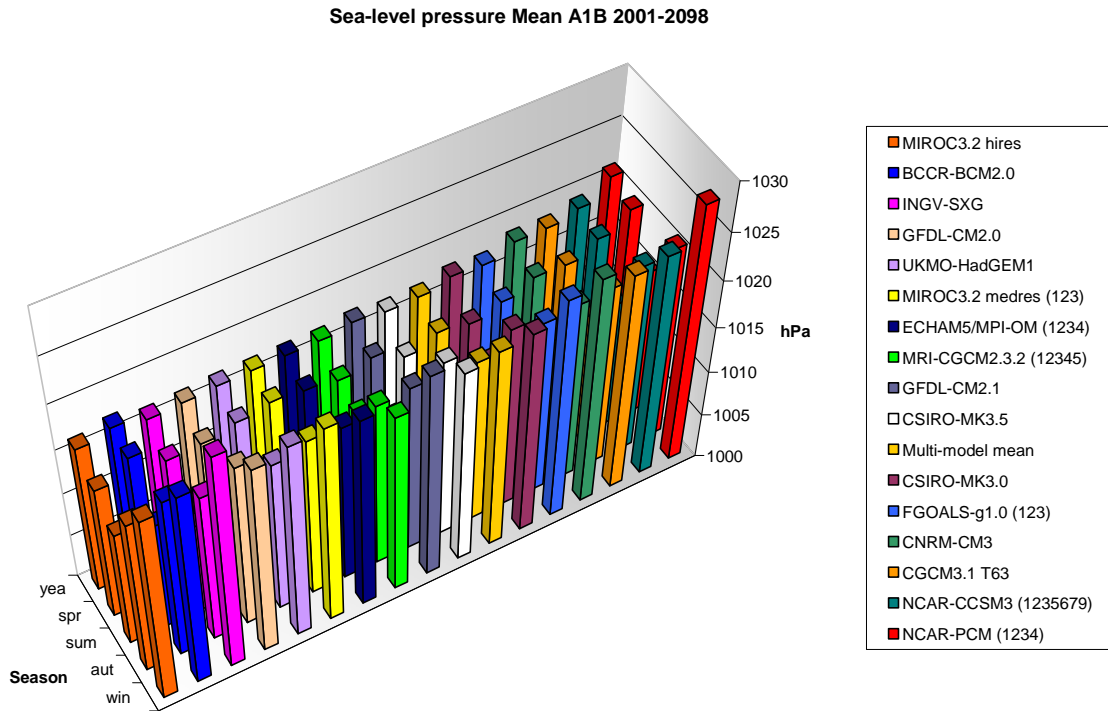
Figure 4.39: Regional sea-level pressure means [hPa] of GCMs (A1B) for the specific seasons computed for the period of 2001-2098.

Analogously to the 20c3m control runs, the appearance of the trends of the individual models is heterogeneous (figure 4.40). The reader is kindly advised on the persistent sequence of the models to figure 4.18. Consecutively, the strong differences between these two periods of models like GFDL-CM2.1 (with 0.65hPa in future for the overall year) or FGOALS-g1.0 (-1.1hPa in the year) become prominent. In fact a seasonal dependency is given by the consideration of summer and winter in the multi-model mean, though many models (e.g. CSIRO MK3.5) even not project the relatively strong increase in winter (e.g. figure 4.36). The well matching of ECHAM5 with the multi-model mean, which has already been mentioned in the comparison of figure 4.18 is confirmed.
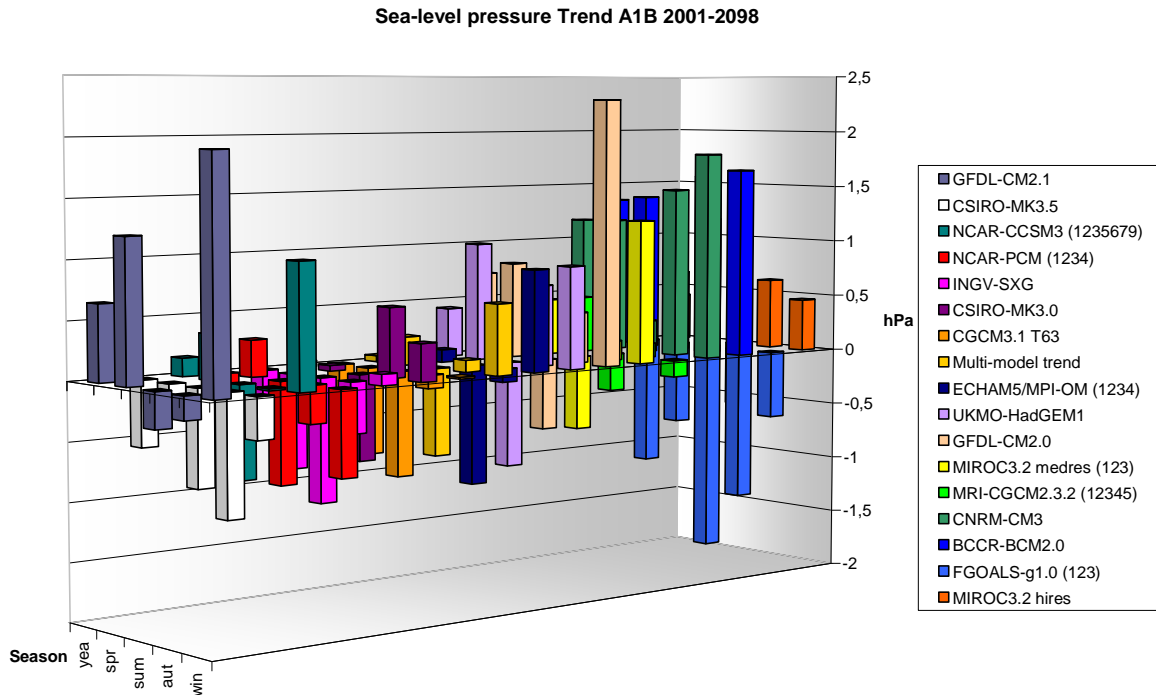
Figure 4.40: Regional sea-level pressure trends [hPa] of GCMs (A1B) for the specific seasons computed for the period of 2001-2098.

Concerning the B1 scenario, illustrated in figure 4.41, again the lower amplitudes compared to the trends depicted in 4.40 are evident. Thus, increasing trends are depicted as being lower. Nevertheless, as there are developments with opposite signs, as mentioned above for the A1B scenario, now tendencies of enhanced rising sea-level pressures in winter become evident, though the scenario has lower GHG emissions (MIROC3.2hires with 0.45hPa in A1B and 0.8hPa in B1). With opposite sign the same holds for NCAR-PCM. This is not expectable by a simplified assessment with one model or analyses of multi-model means and again highlights the necessity of a comprising approach with the focus on discrepancies and agreements over the specific models. The multi-model mean and ECHAM5 behave in the regional average as anticipated by the spatial maps in figure 4.35 and figure 4.36 respectively 4.37 and 4.38 and their seasonal cycles. I.e. Echam5 depicts a growing positive trend by the enforcement of the forcing scenario of 0.87hPa in A1B and 0.63hPa in B1 in winter.

Unfortunately the MIROC3.2hires model has not been available for the A2 scenario (table 3.2), prohibiting an analysis of its course on the A2 forcing (figure 4.42). In contrast to all findings, NCAR-PCM depicts a stronger negative trend by the pronounced forcing in winter (-0.72hPa in A2, -0.72hPa in A1B and -0.46hPa in B1). Still one should be aware, that the transient course from the 20c3m scenario onwards the NCAR realizations are disturbed, as described in the annotations to table 3.2. In this case, though the future development is separated from the control period, these models have not been neglected. Overall, this confirms again the different affections on sea-level pressure by a rising GHG concentration in the atmosphere by specific models. With respect to these different reactions of models the impact on the multi-model mean might

96

be balanced, showing no clear dependency in magnitudes. This non-expectable behaviour is already mentioned within the transverse interpretation of the multi-model mean with ECHAM5 under different forcings. Therefore, seasonal behaviour should be assessed with care.
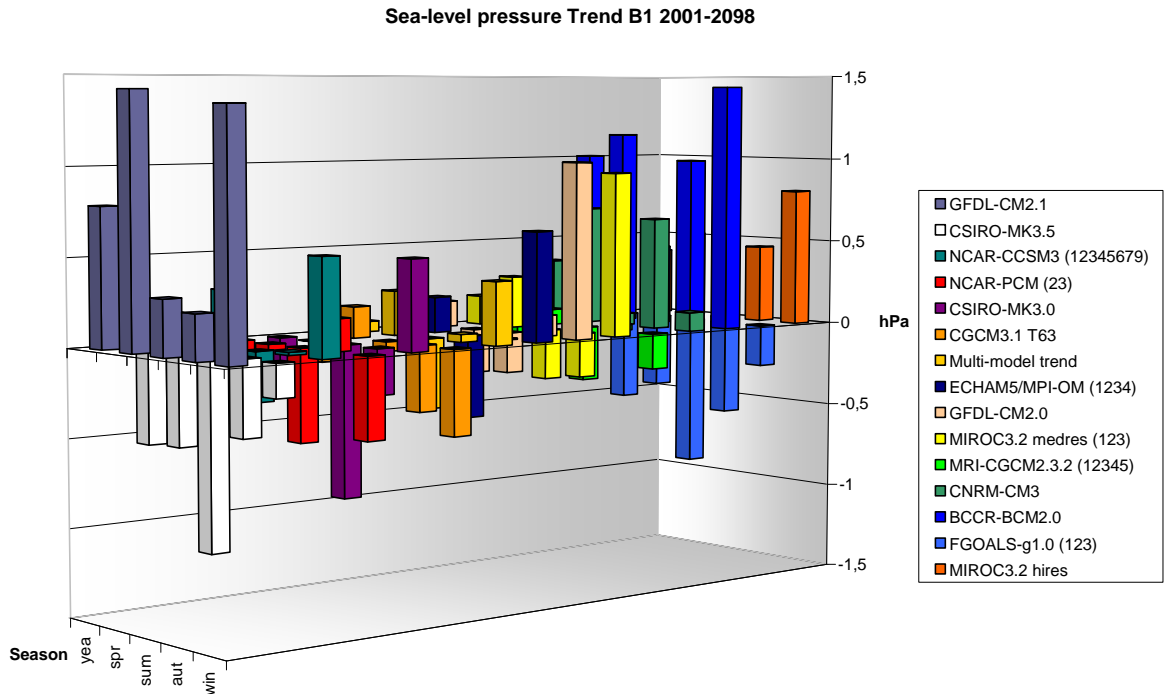
Figure 4.41: Regional sea-level pressure trends [hPa] of GCMs (B1) for the specific seasons computed for the period of 2001-2098.
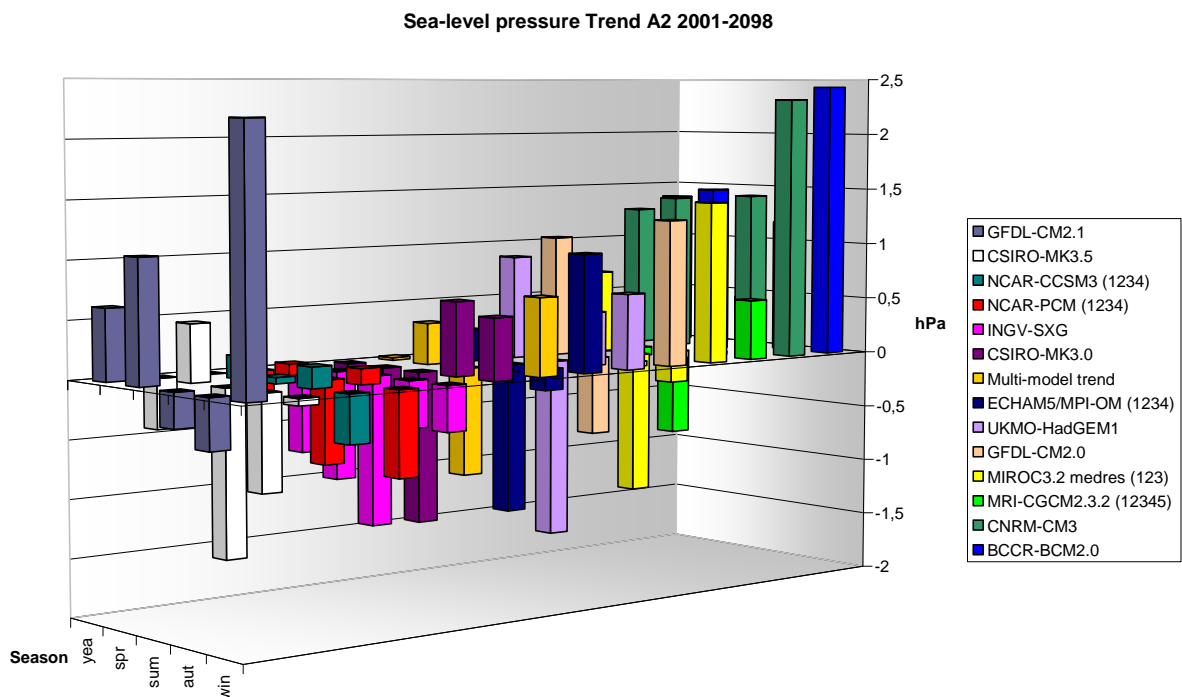
Figure 4.42: Regional sea-level pressure trends [hPa] of GCMs (A2) for the specific

seasons computed for the period of 2001-2098.

4.2.4 Integration to other studies

Besides the analyses of temperature, precipitation and sea-level pressure in the past (4.1.4), also many assessments have been accomplished for future projections.

Concerning temperature, the results of the multi-model mean and the individual models are in agreement with former studies conducted by e.g. PARRY et al. (2000) or GIORGI & LIONELLO (2008). Both found highest warming in summer with about 4.6°C for the A1B scenario (GIORGI & LIONELLO 2008) and 6-7°C in the A2 scenario (PARRY et al. 2000), which is somewhere beneath the results of the underlying study. Already 2000(a) GIORGI & FRANCISCO find with the HadCM2 model a future warming of up to 5°C in summer and in the strongest forcing, while in the other 3 applied scenarios the warming of up to 3°C is rather equally distributed over the seasons with lowest increase in winter (3.1°C in the A1B scenario by GIORGI & LIONELLO (2008) and 4-5°C in the A2 by PARRY et al. (2000)), being slightly above the results shown in the underlying study. Overall, the results of the study at hand are well accordant in magnitude of warming to nearby studies and its seasonal distribution (e.g. GIBELIN & DEQUE (2003)). Furthermore, the patterns of the trends are consistent over different scenarios, with a modification in their magnitudes. However, this is a non-constraining result, as the different scenarios do not behave linearly with their course of GHG emission and even if they did, the GCMs would not treat these emissions linearly. Anyway, the strongest warming is accompanied with strongest emissions, which can be attested by different former studies (e.g. GIORGI & LIONELLO 2008). Still for B1 most of the trends are significant. Also findings of the spatial distribution of warming are in agreement of former findings, where e.g. GIORGI & LIONELLO (2008) state that the warming in future is about 1°C higher over land-surfaces than over the ocean. In winter and spring GIORGI & LIONELLO (2008) found analogously highest warming over continental areas up to 4-5°C, which may be associated with a reduction of snow cover, predominantly occurring in the east. In autumn the warming is more equally approtioned than in spring (GIORGI & LIONELLO 2008).

Generally, trends of precipitation show decreasing amounts for future periods. Certainly, the underlying results reflect the findings of GIORGI & LIONELLO 2008, who also analyse drying trends of a slightly differing multi-model mean. They show a more pronounced drying in summer (about 40%), while in the transition seasons a reduction of rainfall accounts up to 25% in spring and 15% in autumn. Also within the study of GAO, PAL & GIORGI 2006 lowest drying is evident in autumn, where they even find some increases. Moreover, these results confirm former findings of GIORGI & FRANCISCO 2000a, as they find with the former model HADCM2 a stronger decrease of precipitation in summer than in winter up to 35%, dependant on scenario. For summer there are far more studies documenting consistency of a decreasing precipitation in the MA over several approaches and models, confirming the results of the study at hand (ULBRICH et al. 2006, PARRY 2000, GIORGI, BI & PAL 2004b,

RÄISÄNEN et al. 2004, GIBELIN & DEQUE 2003). Still, some former results are differing in the results, particularly for winter, as e.g. DEQUE et al. find (1998) increasing winter precipitation trends of about 30% with a CO_2 doubling scenario for the whole MA.

Concerning higher spatial distribution GAO, PAL & GIORGI 2006 experience a precipitation increase in winter in the northwestern Mediterranean area, which is explained by enforced wind velocities and accompanied resolved upslope effects on luv sides of mountain ridges (GAO, PAL & GIORGI 2006), which applies only partially in the underlying study as these processes cannot be resolved. Within the studies of GIORGI & LIONELLO (2008) and GAO, PAL & GIORGI (2006), the regions of drying are particularly located in the south, while the difference between north and south is especially in winter intense. Confirming these findings, also in this study the reduction of precipitation is latitudinally shifted with the seasons. Also in the north GIORGI & LIONELLO (2008) and GAO, PAL & GIORGI 2006 notice nearly no change in precipitation amounts except slight increases south of the Alps of about 5%. So, compared to GCMs, spatially higher resolved studies progressively find also areas with trends of increasing precipitation, which can be due to small scale thermodynamic activities (particularly in summer) and orographic features (GAO, PAL & GIORGI 2006). Though, with a statistical downscaling method (see 2.5.1) the study of HERTIG & JACOBEIT (2008a) confirms the findings of a prevailing decrease of precipitation. Particularly in the transition seasons they link these reductions with circulation patterns of different geopotential heights applying the B2 scenario. With a more detailed spatial resolution their results project a predominant decrease in the southern and eastern regions in summer and in the transitional seasons for northern and western regions, while the latter also experience an increase in winter (HERTIG & JACOBEIT 2008a). Nevertheless, followed studies exhibit other geographical patterns of trends concerning precipitation in summer, while the precipitation reduction in winter for the east is confirmed (HERTIG et al. 2013a). This is already discussed in the study of 2013a and demonstrates the complexity of a spatially detailed investigation of future precipitation development. Still the cold season remains difficult to assess, as in winter the studies at hand differ mainly in the representation of the latitude of the initiating drying (GAO, PAL & GIORGI 2006, GIORGI & LIONELLO 2008). The dipole structure of figure 4.28, is also reproduced in their studies, while their illustrated drying pattern is somehow shifted to the south. Besides the increase in the Alps, in the study of GIORGI & LIONELLO (2008) main reduction is located over mountain ridges, e.g. the Atlas, the Iberian Peninsula and the Balkan, which is neither confirmed by GAO, PAL & GIORGI 2006 nor in the underlying study. Also a higher irregularity of positive and negative trends across the seasons in the eastern MA cannot be confirmed in the underlying assessment. Contradictorily to the course of temperature, precipitation decreases more slightly over the sea, despite the assumed increase of evaporation due to higher temperatures and consecutively the higher moisture content. In any case, the geographical location of the Mediterranean Sea also has great influence on this and might explain this conflict. Another study of ULBRICH et al. 2006 shows annual drying patterns by RCMs forced by three different GCMs with maxima over the Iberian Peninsula extending to southwestern France and over north eastern land-masses. Overall the hot spots of drying are consistent with results of former studies, e.g.

ULBRICH et al. 2006 also when using an older GCM or SANCHEZ et al. (2004) or GAO, PAL & GIORGI (2006) applying an RCM. Finally, one should be aware, that at least in total (figures 4.32-4.34) a reduction of precipitation is evident and described by several studies.

Concerning the different scenarios of the different studies, strongest drying is found for the A2 scenario in summer, while particularly in winter the drying, evoked by the A1B forcing, is roughly stronger than that projected within the A2 scenario. As expected the B1 scenario shows lowest drying amounts in all seasons.

The strong drying trend in summer and here in the western areas is accompanied with an enforcement of anticyclonic conditions in the atmosphere (PAL, GIORGI & BI 2004) in the study of GAO, PAL & GIORGI 2006, which cannot be confirmed within the sea-level pressure field by the GCMs. Generally, for sea-level pressures nearby studies differ strongly in their future projections, which is obviously dedicated to their specific approaches or to the choice of model. In winter GIORGI & LIONELLO (2008) figure out an elliptically stretched increase of anticyclonic circulation, evoking a northward shift of allochthonous cyclones and thus stable conditions with again lower probability of cyclogenesis (see 1.2.2). This is close to the underlying results, while GAO, PAL & GIORGI (2006) can confirm this results with RegCM3 in winter. For summer/spring and autumn the study of GIORGI & LIONELLO (2008) exhibits decreases/slight increases with patterns resembling to the results presented above. Temperature and precipitation are clearly in line with the depicted pattern of sea-level pressure changes (GIORGI & LIONELLO 2008).

4.3   Conclusion

As the outlined results of means and trends are crucial for the comprehension of the antecedent chapters the conclusion provides, besides the detailed round-up, a synoptical aggregation of the three variables of investigation by describing their interplay and development in the context of the complex climate system. Therefore this synopsis partially follows up the integration to other studies in chapter 4.1.4. On the other hand, it can be proved, to which extent the knowledge about Mediterranean climate depicted in chapter 1.2 can be reproduced by the data in this study. An overall recapitulation is finally handled in chapter 4.3.2, where temporal courses of spatial averages are consulted.

4.3.1 Synopsis

Naturally, temperature is dependant on precipitation and coincidentally associated by pressure patterns, while of course precipitation and sea-level pressure are related to each other. Consecutively, the interactions of these variables are manifold and cannot be simply derived by mentioned instances. The most evident development is the increase of temperatures, whereat the warming of temperature clearly affects other variables, as wind, sea-level pressure or precipitation, by e.g. inducing atmospheric and oceanic circulation,

which itself initiates cyclogenesis and thus precipitation events or simply by increasing moisture capacities in warm air masses.

Besides the mentioned trend of temperature and precipitation, GIORGI & LIONELLO (2008) denote an anthropogenic signal not to be dominant before 1980. Thus, a perturbation by natural variability of this trend needs to be accounted for (see 2.2). Unfortunately at least for the reanalysis, the applied period of 40years is relatively short, as the impact of interdecadal variability (e.g. the NAO) has strong impact on climate in the MA (chapter 1.2.2). HURRELL (1995) analysed an overall strong positive trend of the NAO index for winter in the last 15 years of the 20th century, which turned into a decrease since the millennium change (OVERLAND & WANG 2005), while models tend to project rising indices (e.g. PAETH et al. 1999, PAETH & POLLINGER 2010). So, for winter the drying may be notably related to the rising behaviour of the NAO, bypassing storm tracks impinging from the Atlantic into the MA to the north, which in turn leads to a reduction of the transport of moist air asses from the Atlantic into the Mediterranean basin (HURRELL 1995), while the precipitation over northern and Central Europe is growing bigger (ULBRICH et al. 2006). This effect on the northern MA also becomes evident by diverse studies, as e.g. PAXIAN et al. 2011 try to quantify the impact of the NAO, and e.g. ECHAM5. It is naturally pronounced in winter with the seasonal alteration of storms in the mid-latitudes and lower subtropical influences. But also the increase of the pressure gradient postulated by global analysis of GCMs (MEEHL et al. 2007) simultaneously causes enhanced western winds with cyclogenesis leading to pronounced precipitation events and storms in the northern regions of the area of interest in winter (PAETH 2007). On the other side, the northern low pressure pole of the NAO is shifted westward inducing an eastward extension of the Azores High and thus pronounced blocking activity over the eastern Atlantic, which also detains storms entering the European coast (seen e.g. in figure 4.13 for NCEP) and is an additional reason for the decrease of precipitation (SCHERRER et al. 2006, BARRIOPEDRO et al. 2006). Because of natural and interdecadal variability, a rising index of the NAO is not solely evoked by heightened carbon concentrations in the atmosphere (PAETH et al. 2007). However, the reproduction of the NAO is hard for models. Still there are huge discrepancies in modelling oscillation indices, leading at least to mistakes by the estimation of trends inherent to natural variability (PAETH et al. 1999). Consecutively, an assessment on the models´ ability of the reconstruction of reasonable NAO cycles has to be done first. Still, many modelling approaches indicate an enforcement of these cycles or similar circulation indices in the next century (PAETH et al. 1999, PAETH & POLLINGER 2010).

Further temperature and precipitation variability is evoked by the EA (BARNSTON & LIVEZEY 1987) and the East Atlantic/West Russian pattern leading particularly in the southeastern MA to a decrease by turning the predominant north-westerly winds to enforced continental northern winds. These transport less wet air masses in the last decades of the 20th century (KRICHAK & ALPERT 2005, see also 1.2.2). An adjacent decrease of precipitation is shown neither in the reanalysis data (figures 4.7 and 4.8), nor in the models (figures 4.9 and 4.10). Although NCEP (figure 4.7) exhibits some continental reduction, which is overlapped by very strong reductions of

precipitation in total. Further analyses with NCEP data, precipitation variability and atmospheric modes are given by FERNANDEZ, SAENZ & ZORITA in 2003. Still, a similar phenomenon can be evoked by the simple eastward extension of the Azores High, which induces the blocking of the advection of moist Atlantic air masses into the Central Mediterranean Basin and a deflection to higher latitudes (see above). Further complexity in the affection of southeastern Mediterranean winter precipitation is added by the interplay of the African and Asian Monsoon and their shifting dimensions (ZIV, SAARONI & ALPERT 2004, BALDI et al. 2006). Particularly the latter one is supposed to trigger the decrease of sea-level pressure in summer by a stepwise shift of the onset of the rainy period (ALPERT et al. 2006). The complexity of climate variability and its relation to mentioned teleconnections and further steering modes, e.g. the Mediterranean Oscillation (CONTE, GIUFFRIDA & TEDESCO (1989) or the Hadley Cell (RODO 2001) has been already discussed in chapter 1.2.2.

The reduction of the southern precipitation in winter furthermore is associated by a reduction of local Mediterranean cyclogenesis (LIONELLO et al. 2006b, PAREDES et al. 2006) and by the corresponding growth of anticyclonic conditions, which, on the one hand advects dry air masses from east being likewise responsible for the precipitation decrease. E.g. this phenomenon is depicted in the lowest row of figures 4.29 and 4.30 and is favourable for stable atmospheric conditions on the other hand again (GIORGI, BI & PAL 2004b, XOPLAKI 2002, GIORGI & LIONELLO 2008), as shown in the lowest map in the right column in figures 4.35-4.38. ULBRICH et al. (2006) generally suggest to place the responsibility for precipitation e.g. in different cyclone statistics. NEELIN et al. (2006) show, that this is particularly true in the vicinity of zones of tropical convection. But also in summer the increasing sea-level pressure, translocated to the north, induces the shift of the drying area towards higher latitudes, which is, though the small section of the studied area, for ECHAM5 conceivable. A little more information about this phenomenon is given by the multi-model analysis in figure 4.30, which reflects the trends of ECHAM5 authentically. A reduction of the intensity of cyclones, e.g. in the Gulf of Genoa, over the Aegean Sea and the Turkish mountain ranges, leads to a further decrease of precipitation in summer, shown by SOMOT (2005). The reduction of precipitation is generally in line with the development of sea-level pressure.

Moreover, the decreasing pressure in summer in southeastern Turkey for future periods may lead to the weak increase of precipitation at the coast of Egypt. This can be confirmed again by the study of GIORGI & LIONELLO, who (2008) found very similar patterns and underlined these with conforming trends of 500hPa heights. The precise position of the Cyprus Low and the Red Sea Trough define the direction of the wind and thus the moist advection to the Levant. E.g. by a rather western position of the Red Sea Trough sand from the Saudi Arabian or Iraqi Deserts may be transported with the dry and hot south-easterly winds to the Levant (ULBRICH et al. 2012).

A reason for temperature rise in winter is given by MAHERAS et al. (1999), who explain a certain amount to low sea-level pressures in the western MA, as this constellation induces warm streaming from Africa to the eastern MA. However, though being a frequent atmospheric situation, a decrease of sea-level pressure in the southwestern MA can not be verified by the analysis.

Though, in winter the reanalysis here show a relative lower increase to other regions, while the models even show a slight decrease (figures 4.13 – 4.16). Anyway, this holds only for the reference periods. Still, a distinguishable east-west contrast mainly in winter is not detectable. For summer, one discerns the highest increase of temperatures, which might directly be related to the effect of GHGs or local steering, as teleconnection patterns like ENSO and NAO become more predominant in winter (see 1.2.2). Also, the reduction of precipitation in summer can be attributed to a decrease in soil moisture (GIBELIN & DEQUE 2003), being in turn a positive feedback of rising near-surface temperatures (ULBRICH et al. 2006). Furthermore, an enforced warming of land-surfaces, relative to the warming of sea-surfaces, might affect the transport of relative humidity and diminishes the precipitation over continental areas (ROWELL & JONES 2006). Concerning orographic steering of precipitation, GAO, PAL & GIORGI (2006) defines it as mean effective in summer, when convective elements become predominant. Additionally, GIORGI & LIONELLO (2008) ascribe only a slight effect in the change of precipitation amounts in the Alps.

4.3.2 Temporal courses of the realizations and reanalysis

To give some further insight of the temporal courses of realizations given by models providing multiple realizations, they are depicted by figure 4.43 for the A1B scenario. For brevity only the annual values and the extreme seasons concerning the amounts of the considered variables are shown, which is winter and summer.

103
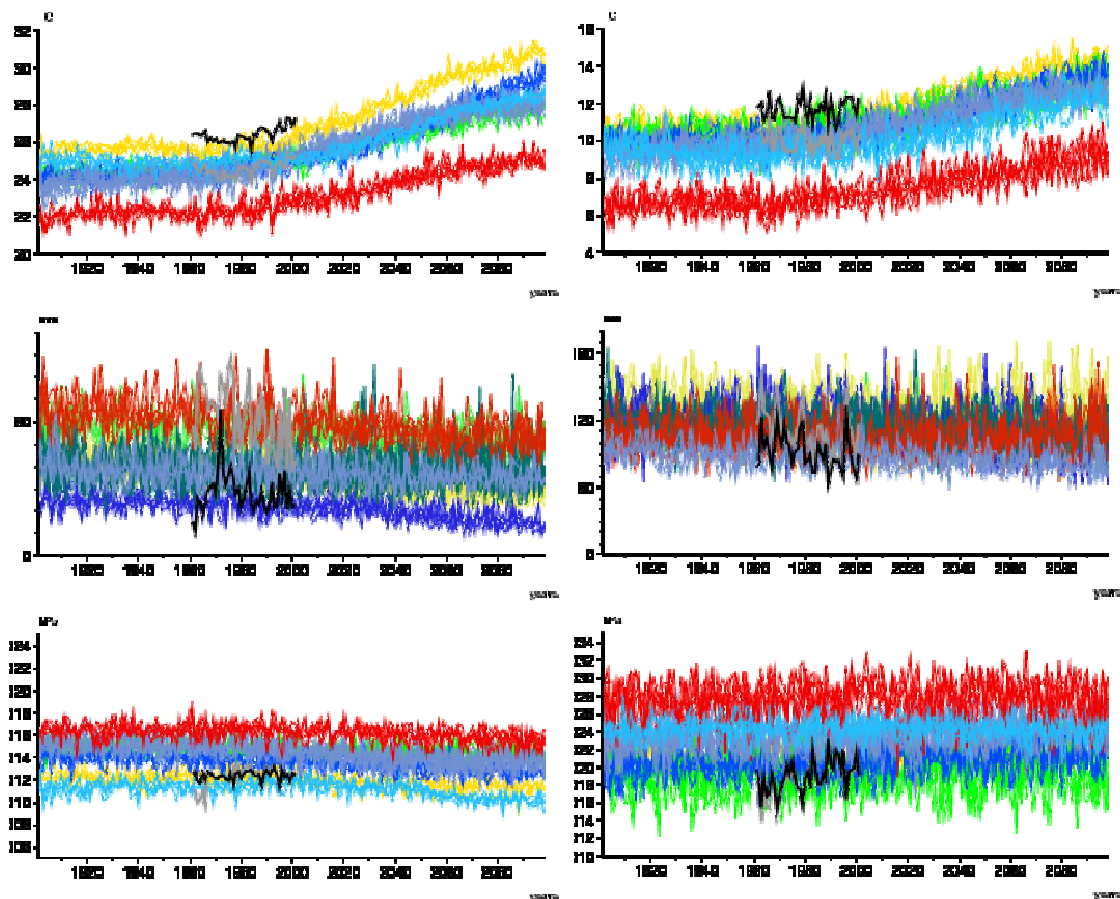
Figure 4.43: Temporal courses in the A1B scenario of temperature [°C] upper row, precipitation [mm] middle row and sea-level pressure [hPa] lower row for the realizations of the models providing ensembles. For colours of the models see legend of e.g. figure 4.42. Grey/black lines exhibit the reanalysis data by NCEP/ERA40. Left column: summer, right column: winter.

One can clearly indicate the rising development for temperature in winter and summer, where in the latter season the increase is pronounced. This increase is depicted by all models. Furthermore, the reanalysis data are illustrated for the period, they have been investigated in. The discrepancy between them is in evidence, while some models develop between this gap. General studies in literature deal with the issue of the reproduction of natural variability by the models, with results of an underestimation of natural variability by the models compared to observations This can particularly be seen in the first decades of the 20th century, when anthropogenic forcing is still rather small (GIORGI 2002b). This reveals a certain lag of GCMs in reproducing natural variability. Considering future periods, where this phenomenon might still be evident, the reason for this may be the missing implementation of other external forcings in the SRES scenarios like volcanic eruptions (chapter 2.4) (PAETH 2007). Still the spread between the models is greater than the discrepancy between the reanalysis datasets, with the outlying NCAR-PCM at the colder end of the dispersion in summer and winter and FGOALS-g1.0 at the upper boundary in summer. Besides the dispersion the figure also gives some idea of the natural variability, derived from the different initial conditions of the different realizations. The qualitative overview permits first interpretations, that is natural variability is less than the dispersion introduced by different modelling approaches concerning discretizations and parametrizations, i.e. developed by different GCMs. The more temporally or spatially detailed the analysis becomes, the more the discrepancies between the different data become evident. Consecutively, biases between the regional averages are small, which holds particularly for the means and here for temperature and precipitation. With the intention to investigate these fields, there are also only small differences between the means of two individual models (i.e. averaged realizations), which in turn may (but not necessarily) pretend and strengthen the plausibility of each single dataset with all its shortcomings.

The seasonal cycle is reproduced well by models and the multi-model mean concerning the reanalysis data. Also the spatial distribution of the magnitudes of the mean values is depicted adequately by every data for every field. Attention must be paid that individual grid-cells are analysed this way, which leads to a mandatory comparison. Although one should not forget, that these individual grid-cells hardly give evidence about the actual climate conditions representative for an averaged region. Spatially detailed trend patterns cannot be reproduced by the models in the reference period. Overall, the trends show higher discrepancies in the different datasets. Highest agreement is reflected for temperature, where warming is evident in all datasets, in the annual average and here primarily for summer with a seasonal distribution, which holds for the reference period and the future. For temperature only NCEP shows a decrease of temperature and then for winter.

Considering precipitation in the second row (figure 4.43), this natural or internal variability is pronounced in winter, while the model dispersion is higher in summer, which holds also for the reanalysis data. A course of decreasing amounts can not be depicted in winter, but for some models in summer, e.g. ECHAM5. For precipitation, the biases between the reanalysis data in the regional means are noteworthy, which cover about the half range of the spread of the models. Still, the multi-model mean shows some overestimation in the precipitation means, while the strength of a prevailing negative trend is generally underestimated by the models concerning the reanalysis. Despite the overall decrease of precipitation, the northern boundaries of the area of investigation are supposed to experience higher amounts in future. A general seasonal tendency for a reduction is not distinguishable out of the models (neither for the reference nor future periods), while for reanalysis the strongest drying is commonly situated in winter, enforcing drying trends in yearly assessments. Concerning relative amounts, GIORGI & LIONELLO (2008) identify a more pronounced reduction of precipitation in the warmer season accompanied by the warming trends, where water supply is typically short and temperatures are naturally hottest.

According to the variabilities and dispersions the same findings hold for sea-level pressure, where no distinct trend superimposes variability in both seasons. In contrast to precipitation the reanalysis data are close to each other and, as already seen, according to precipitation, strongly overestimated by the models. The closest one, following the reanalysis, is MIROC3.2 medres closely followed by ECHAM5. For precipitation and sea-level pressure, the spatial trends differ remarkable between the models and the reanalysis. Also considerable biases in the spatial distribution of the trend magnitudes, particularly for sea-level pressure, are found between the reanalysis data. Thus, the applied analyses definitely show the necessity of spatially detailed investigations, as also reanalysis data still show significant differences complicating evaluation or even verification methods with models. Still they depict a common signal in the regional averages, suggesting deceptive conclusions.

The multi-model ensemble represents the observed climate data quite well, which holds for both precipitation and temperature. Although for precipitation and sea-level pressure the multi-model-ensemble slightly underestimates the observed values, as the mean smoothes out variabilities, which confirms the findings of GIORGI & LIONELLO (2008).

Finally, there is no model fitting best to the reanalysis dataset, regarding all seasons and variables (also stated by e.g. GIORGI & FRANCISCO 2000a), which could furthermore be shown in the regional maps in specific grid-cells. This is a general finding within the analyses of different climate models, which justifies and confirms the use of multi-model ensembles, as today one climate model cannot cover all periods, locations and variables with a satisfying accuracy.

Anyway, the goodness of fitting of the GCMs to the reanalysis data does not imply any quantitative rating of models, nor a quantitative measurement of the future reliability of one model (REIFEN & TUOMI 2009). Although the idea of a model-rating is picked up by many studies, it is not given that a model, which

behaves well in the past, also will behave well in the future. But this topic will be discussed e.g. in chapter 5.4.

For the overall year a scenario-separated illustration according to the specific variable is given additionally (figure 4.44).
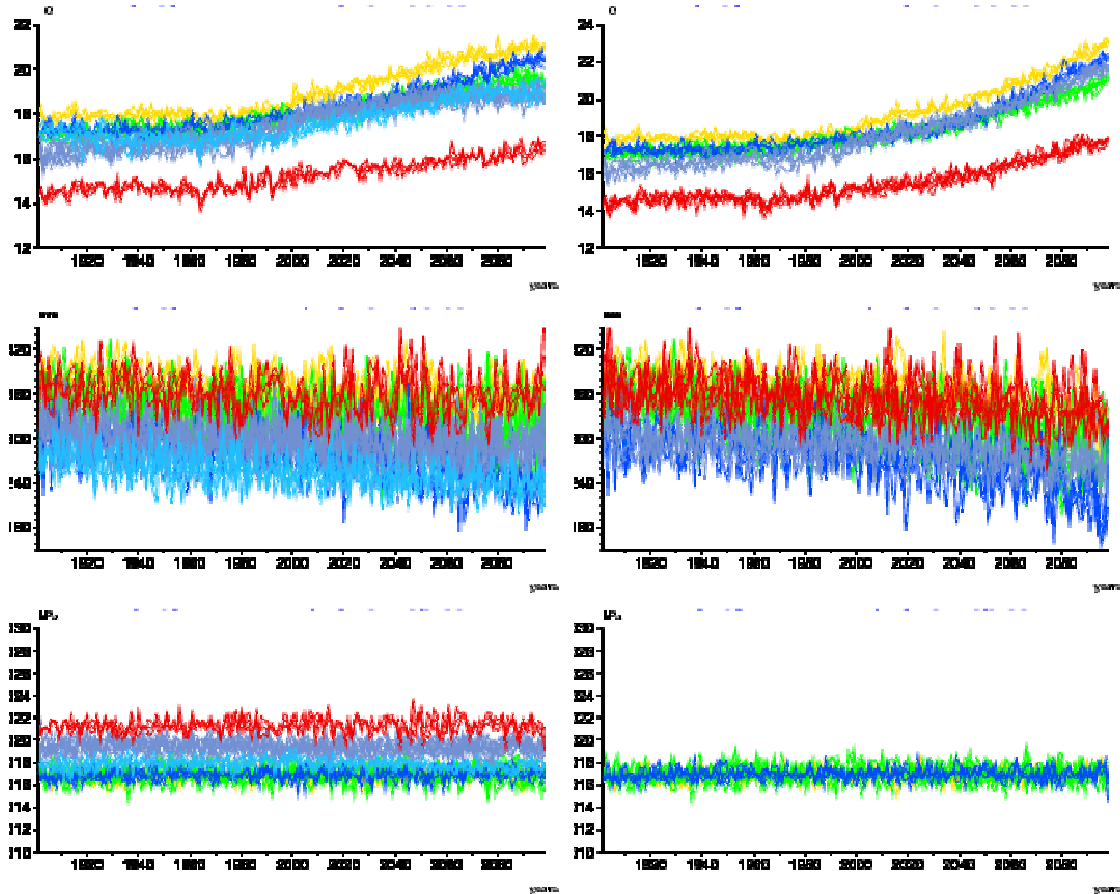
Figure 4.44: Temporal courses in the yearly averages of temperature [°C] upper row, precipitation [mm] middle row and sea-level pressure [hPa] lower row for the realizations of the models providing ensembles. For colours of the models see legend of the e.g. figure 4.42. Left column: B1 scenario, right column: A2 scenario.

At first, the reader is kindly advised to the different scales, pretending a stronger trend for the B1 scenario for temperature than within the A2 scenario, though at least for temperature and precipitation the opposite holds true. Again for precipitation, the dispersion of the models becomes lower with the enforcement of the scenario, accompanied with a slight increase of the variability within the realizations of one specific model. For sea-level pressure also in the A2 scenario a distinct trend becomes not evident. Here it must be emphasized, that only three models are applied for the analysis, as indicated in table 3.2.

But when considering temperature and precipitation, the illustrated projections are very robust across the different scenarios, whereupon the intensity of the trends is dependant from the specific scenario. Furthermore, the models and their related realizations mainly agree on the direction of the trends (with a decrease of the reliability of the trends by a shortening of time periods), with the exception of sea-level pressure. Thus, the warming and the precipitation,

illustrated in the right columns of the spatial maps in this chapter, are considered as representative for latest climate development. GIORGI & LIONELLO (2008) illustrate similar findings, in addition to the persistence of trends over different periods.

Consecutively, the affirmation of these findings by several studies (irrespective of their different assessments) provides a certain grade of reliability, indicating the MA being subject to intense changes in future. Again it must be emphasized, that the MA is a highly vulnerable region to climate change (chapter 1.2.4).

Concerning climatologic sciences, it is thus inevitably to assess and identify the genesis of these trends and the elements steering the climate variability, which modifies the observed trends by mitigation or enforcements (TRIGO et al. 2006).

From a statistical view, the relative strong regional trends, in combination with rather small interannual and natural variabilities (compare variables in figures 4.43 and 4.44), may facilitate a detection of an anthropogenic climate change by GHG forcing in terms of a signal-to-noise ratio. This can be compared with other global regions, where interannual and natural variability is relatively high and trends are low (e.g. Central Northern America (GIORGI 2002a)). STOTT & TETT (1998) analysed the probability of detection of climate change dependant on scales and the length of temporal periods. Likewise the figures 4.43 and 4.44 conduce to the following chapter, which is dealing with the quantification of the individual distributions of variability and thus giving quantitative values of certainty. The implemented GCMs provide some measurements of induced trends, eventually superimposing the other contributions of variability assigned to the differences of modelling or initial conditions. Furthermore, the position of the individual models and realizations to the reanalysis data will be subject in the following chapter. Further considerations of future climate conditions deal with an investigation in extreme events, as it is also done in chapter 6 in the underlying study.

5 Signal Analysis

As highlighted in the precedent chapter, partially strong trends are simulated by the different scenarios and their realizations. These are superimposed by natural variability, by differences inherent to the various realizations of one model with the specific initial conditions and last but not least to characteristic modelling techniques of the considered GCMs. The underlying chapter attempts to quantify the trend inherent to a climate change with respect to the other variabilities. The analysis of a common signal is fundamental for stakeholders and policymakers, as it defines the confidence one can have in the projections of climate models.

5.1 Motivation

A fundamental question arises from the precedent chapters, which is particularly important for policy makers:

How trustful are the simulations?

Irrespective of the capability of GCMs to reproduce natural climate conditions and climatic changes, one consecutively has to ask, how strong the simulated trends arise across all the models and superpose further aspects of variability inherent to the modelled results.

A powerful statistical tool to assess for this uncertainty is the **An**alysis **o**f **Va**riance (ANOVA) (VON STORCH & ZWIERS 1999, PAETH & HENSE 2002).

To encounter the problem of the unknown initial conditions (chapter 2.3.2) every model is realized several times with perturbed physical initial conditions. This leads to a diagnostic approach comprising a specific amount of uncertainty which tries to enhance the authenticity of long term predictions. Furthermore, several GCMs are used to gain a better understanding of the impact of discretizations and parametrizations, which are unique for specific GCMs (chapter 2.3.1).

Finally, these three questions develop with the use of GCMs in a signal analysis:

1) Estimate one GCM with two or more ensemble members for a certain scenario: What is the range of the simulated values within all of these different simulations for this scenario? And how representative is one simulation in comparison to the ensemble-mean?
2) Estimate several GCMs with a mean value for each ensemble-mean for one scenario: What is the range of the simulated values within all of these different GCMs for this scenario? And how representative is one GCM in comparison to the multi-model mean?
3) What is the range of simulated climate features to different forcing scenarios?

Consecutively, one can define the uncertainty of climate projections as intra-model variability, as inter-model variability or as inter-scenario variability. The latter one is not involved in these quantitative approaches, due to nonlinear rising complexity of these analyses. One has still to keep in mind that the results are dependant on time. An ANOVA is a technique to challenge the returned averages from different sets of influencing factors (VON STORCH & ZWIERS 1999). Thus, with the 1-way ANOVA and the 2-way ANOVA the fractions of the internal-model variability, the inter-model variability and external forced impact (i.e. the forcing of GHG emissions) on the total variability are analysed. Furthermore, the different response of all models with respect to time to a certain scenario is given, which is referred to climate sensitivity (PAETH 2007).

An ANOVA has been proven its applicability in many different scientific disciplines to divide the total amount of variability of an experiment to its partitions associated with the independent variables of this experiment. Introduced by SCHEFFE (1959) this tool has been applied e.g. by VON STORCH & ZWIERS (1999), HODSON & SUTTON (2008), PAETH & HENSE (2002) or by CONIL & LI (2003) in the science of statistical climatology. Nevertheless, up to now, it only has been utilized to investigate on global or hemispheric views but never to analyse smaller regions like the MA.

5.2 1-way ANOVA

The ANOVA accounts for the problem of the influence of classified factors belonging to a certain agglomeration of data on a quantitative variable on a continuous scale being displayed by all the different factors (VON STORCH & ZWIERS (1999), SCHÖNWIESE 2006). The "classified factors" or experimental units are GCMs or relating to the application of the 1-way ANOVA, simulations by GCMs. These individual realizations influence values (e.g. temperature) developed out of the agglomeration of all simulations. For this investigation a) the total collective of samples is considered, while also the derivation of the individual samples is accounted for and thus b) a distinction of the different individual groups, which are independent from each other but affect the total collective of samples, is conducted. Generally, the ANOVA requires a high number of these different affecting groups (e.g. >3) and a number of samples for each partition group of at least 30 (SCHÖNWIESE 2006). As this study is subordinated to the availability of data provided by the CMIP3 database, it was

not possible to account for this restriction by increasing the number of samples. Still, affecting groups less than 3 have not been investigated, e.g. NCAR-PCM in B1 (see 3.1). Dependant on the number of the different experimental units (=classified factors) one applies the 1-, 2-, 3-,…, n-way ANOVA. Though, it should be emphasized, that the complexity of the calculation of the different parts of variances, arising from each data collective, becomes rapidly complex and elaborate, which restricts this work to an application of a 2-way ANOVA and prohibits the quantitative investigation of the impact of a change of scenarios, as mentioned above. Still, the different scenarios A1B, B1 and A2 are analysed separately to gain an estimation of the freedom in applied mitigation strategies.

5.2.1 Method

In this chapter attention is turned to question 1) in 5.1, when one distinguishes between intra-model variability and external forcing, each as a fraction of the amount of total variability. For each coordinate in the MA the data Y_{ij} is defined by realizations j=1,…,J, i.e. different simulations with their specific initial conditions of one certain GCM. Each realization has the timesteps i=1,…,I. As the sizes of the different samples (i.e. the number of the timesteps in the different realizations) are equal, the total number of values is defined by formula (10).

10) $\qquad n = IJ$

The 1-way ANOVA will be calculated each time for the different models and different scenarios and different climate variables which all stay the same during one application. As a precondition normal distribution of the data must be approximately given, which is assumed in this applications, as climate data derived from models are very likely behaving this way (SCHÖNWIESE 2006, VON STORCH & ZWIERS 1999).

Formula (11) denotes the expected mean value for all realizations, holding for each time-step i.

11) $\qquad E(x_{ji}) = \mu_i \, ,$

being an equivalent to formula (12), where μ is the overall mean over all realizations and all time-steps (formula (13))

12) $\qquad E(x_{ji}) = \mu + \alpha_i \, .$

13) $\qquad \mu = \dfrac{1}{JI} \sum_{j=1}^{J} \sum_{i=1}^{I} \mu_{ji} \, .$

Thus the value α_i is established as the treatment effect, as it is the difference between the sample-mean and the total mean (formula (14)), being dependant from time, but common to all runs of the model:

14) $\alpha_i = \mu_i - \mu$.

The following linear statistical model (formula (15)) calculates every single value out of the overall mean, the treatment to a sample mean α_i and the errors ε_{ji}, which represent the unpredictable residual. This is due to the varying initial conditions and the nonlinearity of natural climate relationships and their reproduction within the model. The errors are independent identically distributed and are zero in their mean, while α_i result in zero by their sum. Formula (15) reflects some sort of a regression. Though, a regression is not desirable in this case, as the aim of the analysis is not the relationship of the single effects to the result or their specific coefficients, but the amount of variation of the specific effects to the total amount of variance. This is the case as firstly, one cannot change the model and its contributing factor in this study and secondly, the factors have no direct or quantitative connection to each other (VON STORCH & ZWIERS 1999).

15) $x_{ji} = \mu + \alpha_i + \varepsilon_{ji}$.

It is assumed that the single samples simulated by a specific realization are representative and completely randomized. To receive some idea of the percentage of these treatments and errors the Sum-of-Squares (SS) are calculated. To calculate the total SS the unbiased estimators X_{00} for the overall mean μ and X_{0i} for $\mu + \alpha_i$ are introduced (formulae (16) and (17)), which leads to the estimator X_{0i}-X_{00} for α_i (VON STORCH & ZWIERS 1999).

16) $\overline{x}_{00} = \frac{1}{JI} \sum_{j=1}^{J} \sum_{i=1}^{I} x_{ji}$,

17) $\overline{x}_{0i} = \frac{1}{J} \sum_{j=1}^{J} x_{ji}$,

where the $_0$ indicates the average determination of the absent subscript. The total sum-of-squares is defined as follows (formula (18)):

18) $SST = \sum_{j=1}^{J} \sum_{i=1}^{I} (x_{ji} - \overline{x}_{00})^2$.

The fundament of an ANOVA is the mathematical theorem of the additivity of variances to the total variance. Applying this assumption to the sums of squares associated with their specific category, one receives:

19) $SST = \sum_{j=1}^{J} \sum_{i=1}^{I} ((x_{ji} - \overline{x}_{0i}) + (\overline{x}_{0i} - \overline{x}_{00}))^2$.

Now, one can solve this term binomially, where following formula (20) is received:

20) $$SST = J\sum_{i=1}^{I}(\bar{x}_{0i} - \bar{x}_{00})^2 + \sum_{j=1}^{J}\sum_{i=1}^{I}(x_{ji} - \bar{x}_{0i})^2 - 2\sum_{j=1}^{J}\sum_{i=1}^{I}((x_{0i} - \bar{x}_{00})(\bar{x}_{ji} - \bar{x}_{0i}))^2 .$$

The last term can be neglected, as it will result in zero, as it is constituted, that the sum of the errors, indicated in the second bracket of the last term, are zero itself (see above). So the total SS is dedicated to the two first terms (formula (21))

21) $$SST = J\sum_{i=1}^{I}(\bar{x}_{0i} - \bar{x}_{00})^2 + \sum_{j=1}^{J}\sum_{i=1}^{I}(x_{ji} - \bar{x}_{0i})^2 \qquad df : IJ - 1 .$$

Formula (22) firstly indicates the treatment sum-of-squares with SSα, collecting the variance between the groups, i.e. the ensemble members and secondly the error sum-of-squares with SSε, capturing the added variance within each group (formula (22-24)) (SCHÖNWIESE 2006).

22) $$SST = SS\alpha + SS\varepsilon .$$

23) $$SS\alpha = J\sum_{i=1}^{I}(\bar{x}_{0i} - \bar{x}_{00})^2 \qquad df : I - 1 .$$

24) $$SS\varepsilon = \sum_{j=1}^{J}\sum_{i=1}^{I}(x_{ji} - \bar{x}_{0i})^2 \qquad df : I(J - 1) .$$

The degrees of freedom are shown behind each formula. Finally, it is now possible to compute the specific amounts partitioning the total sum-of-squares (formula 25).

25) $$\hat{R}_{\alpha}^2 = \frac{SS\alpha - \dfrac{(I-1)}{I(J-1)}SS\varepsilon}{SST} .$$

Furthermore, it is also possible to derive R_{ε}^2 analogously to formula (25)), which was not necessary in this study, as the partition of unexplained noise is defined as the difference of R_{α}^2 and the total amount, which is 1 (formula (26)). In the figures, the results will be depicted as percentage, as they are multiplied by 100.

26) $$\hat{R}_{\varepsilon}^2 = 1 - \hat{R}_{\alpha}^2 .$$

This shows also an estimate of the expressiveness of the developed model regarding the formula as a signal-to-noise ratio. It is referred to the treatment partition as explained variance.

The aim of an ANOVA is to check whether there is significant impact from the individual samples on the total mean and thus whether the samples are uniform to each other.

To test whether there is a treatment effect, the 0-Hypothesis neglects in formula (27) any treatment effect with:

27) $H_0 : \alpha_1 = ... = \alpha_i = 0$,

which can also be shown with formula (28):

28) $H_0 : \sum_{i=1}^{I} \alpha_i^2 = 0$.

A treatment effect can be stated, when at least one of the coefficients is not equal to zero (formula (29)):

29) $H_1 : \sum_{i=1}^{I} \alpha_i^2 > 0$.

After applying upper formulas and definitions, formula (30) is derived, which provides the critical value for the test statistics. In this study, it was decided to test the 0-Hypothesis with formula (30) to account for the degrees of freedom. However it is also possible to use tests with the variances associated with SSα and SSε (VON STORCH & ZWIERS 1999).

For closer reading on the deduction of the test, the reader is kindly referred to VON STORCH & ZWIERS (1999, pp.176-177).

30) $\hat{F} = \dfrac{1 + \dfrac{I(J-1)}{I-1}\hat{R}_{\alpha}^2}{1 - \hat{R}_{\alpha}^2}$ $df : I-1, (J-1)I$.

Formula (30) shows thus a relationship between R_{α}^2 and F. As F is only used to account for the significance, its specific values are not illustrated in the figures. R_{α}^2 and probable significance is shown.

One still has to keep in mind, that in this study the sampling sizes were equal over all the samples. In the case the sizes are unequal, the analysis of variances is still useful with the constraint, that the tests are limited to the smallest samples and thus less powerful, as they are not accounting for the larger samples. Furthermore, it is obvious that the total number of values n needs to be calculated by the sum of all the sample sizes depending each time on the specific sample size i. This is reflected in many of the formulas described above. For further reading on the utilization of a 1-way ANOVA, the reader is kindly referred to (VON STORCH & ZWIERS 1999 and SCHÖNWIESE 2006).

The introduced method has been applied in two different approaches. First of all, every grid-cell has been subordinated to this analysis in a specific time

period, like they have been determined in 3.1.2, which will be referred to as spatial approach. Afterwards, the same analysis is conducted for the average mean in consecutive periods of equal length, which will be denoted as temporal approach. This second approach incorporates further statistical effort, which will be described in more detail in the beginning of chapter 5.2.2.2, as these applications neither affect the formulae described above, nor belong to the accomplishment techniques of the ANOVA itself.

5.2.2 Results of the 1-way ANOVA

In this study the 1-way ANOVA is applied for all the models, where several runs are provided by the CMIP 3 database with the exception of NCAR-PCM, where errors occurred for A2 and B1, see 3.1. The analyses are conducted on the basis of monthly means in a seasonal context, as indicated in chapter 3.1.2, and for yearly aspects. This is done for temperature, sea-level pressure and precipitation. Again, particular respect is due to ECHAM5.

The following analyses of variances have been calculated in two different ways. At first, every grid-cell in the defined MA has been conducted to the analyses with respect to the three time-slices 1961-2000, 1961-2050, 2001-2098 and the whole time period from 1901-2098. This gives insight in the spatial pattern of the specific distribution of the partitions of the Sum-of-Squares.

In the second application, for the whole time-slice in a moving time window of 30 years/60 years the spatial averages over the MA have been investigated to show the temporal behaviour of the contributors to the total Sum-of-Squares.

5.2.2.1 Spatial approach

In figure 5.1, the results of the 1-way ANOVA for ECHAM5 are shown for temperature in the A1B scenario for run 1-4 in the time period 2001-2098. In the left panel the known partition of the amount of the total variance is highlighted, while the right panel describes the unknown partition [%]. Together they aggregate to 100% of the total variability, which is inherent to the different runs within the time at each specific grid-cell. Black dots in the figures, illustrating the known parts, document significance at a confidence level of 95%.

One can easily conclude, that there are few differences between the different seasons, though the partition of the known variability reduces in the northern areas of the Mediterranean region in winter and spring in particular. The explained variance reaches relatively high values with about 51.4-93.7% over most regions in the warmer seasons. This develops out of the proportion of the long term trends in the period on hand. Highest values of the known partition of variance can be reached over the year and in summer, where particularly strong trends are evident in figure 4.19. The remarkable meridional stripe of a low known partition in the west of the Iberian Peninsula in the right column is also reflected in figure 4.19 by lower trends, particularly in summer. Lowest values of known variability can be found in winter, where variability between the simulations is high. This holds generally for the northern and western areas,

being subordinated to Atlantic storms and cyclones predominantly in winter and thus to a high variability of atmospheric conditions.
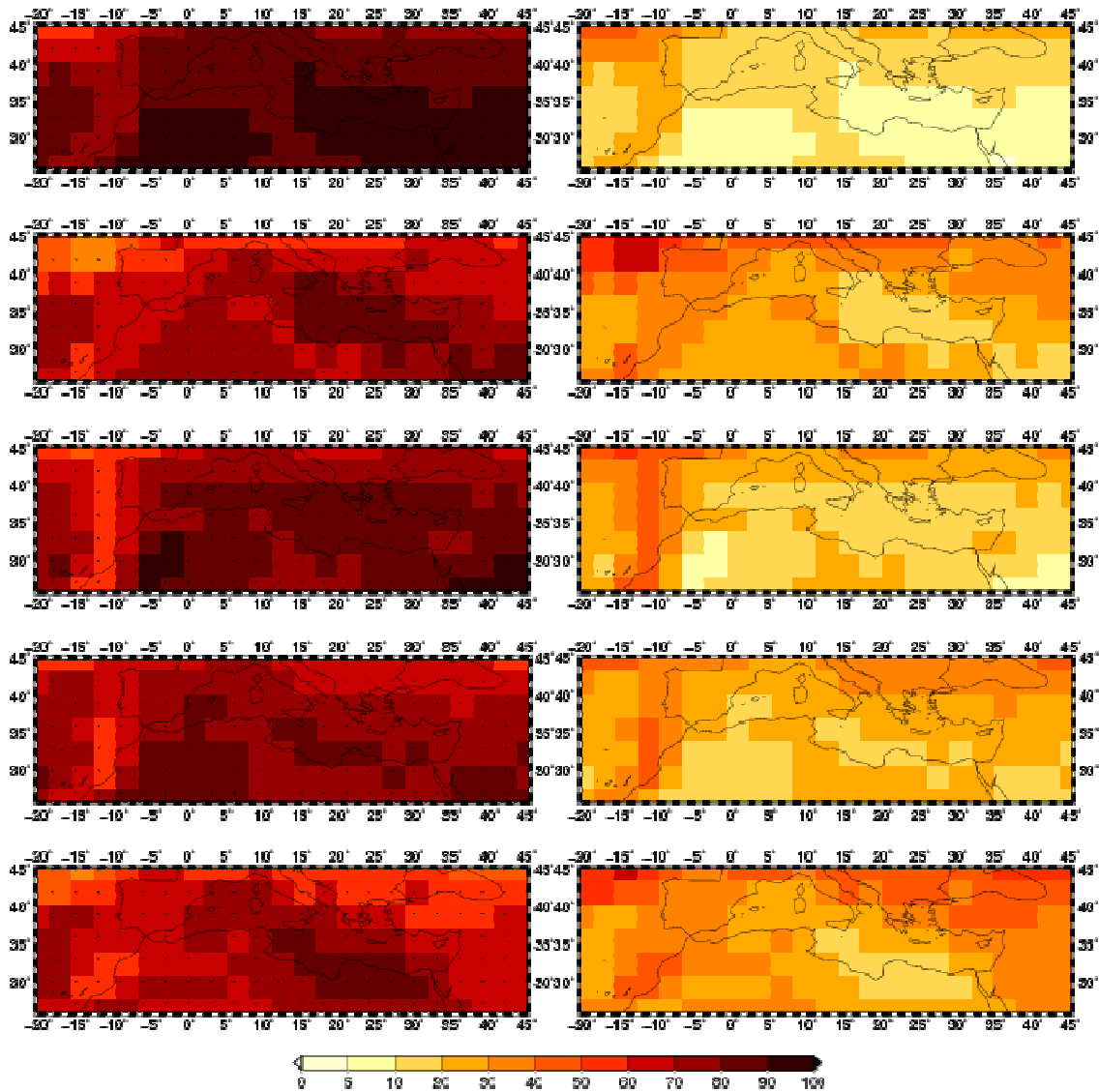
Figure 5.1: 1-way Analyses of variance with runs 1,2,3 and 4 of Echam5 in the scenario A1B for temperature for 2001-2098. The left panel describes the known variability and the right panel the partition of the unknown variability in percentage. Rows indicate the season from top to the bottom year, spring, summer, autumn, winter. Black dots in the left panel describe significance for the specific grid-cell on a level of α=5%.

Over the Mediterranean Sea the low variability of the simulations counteracts the low trends in figure 4.19 leading consecutively to high amounts of treatment variability.

For precipitation, figure 5.2 shows much lower values of known variability, which indicates a stronger variability over the individual runs, which can be stated by figure 4.44. Certainly, precipitation is a spatially and temporarily very heterogeneous variable, being therefore harder to model than temperature. However, the pattern of known/unknown variability over the MA is more homogeneous than that for temperature, indicating a) a spatially equally distribution of differences between the individual simulations and b) a spatially

homogeneous trend. This also holds for winter, where strongest reductions of precipitation are depicted (figure 4.27). Though, for the overall year, where also a strong trend is evident, the distribution of the trends is roughly reflected. A seasonal difference is hard to detect.
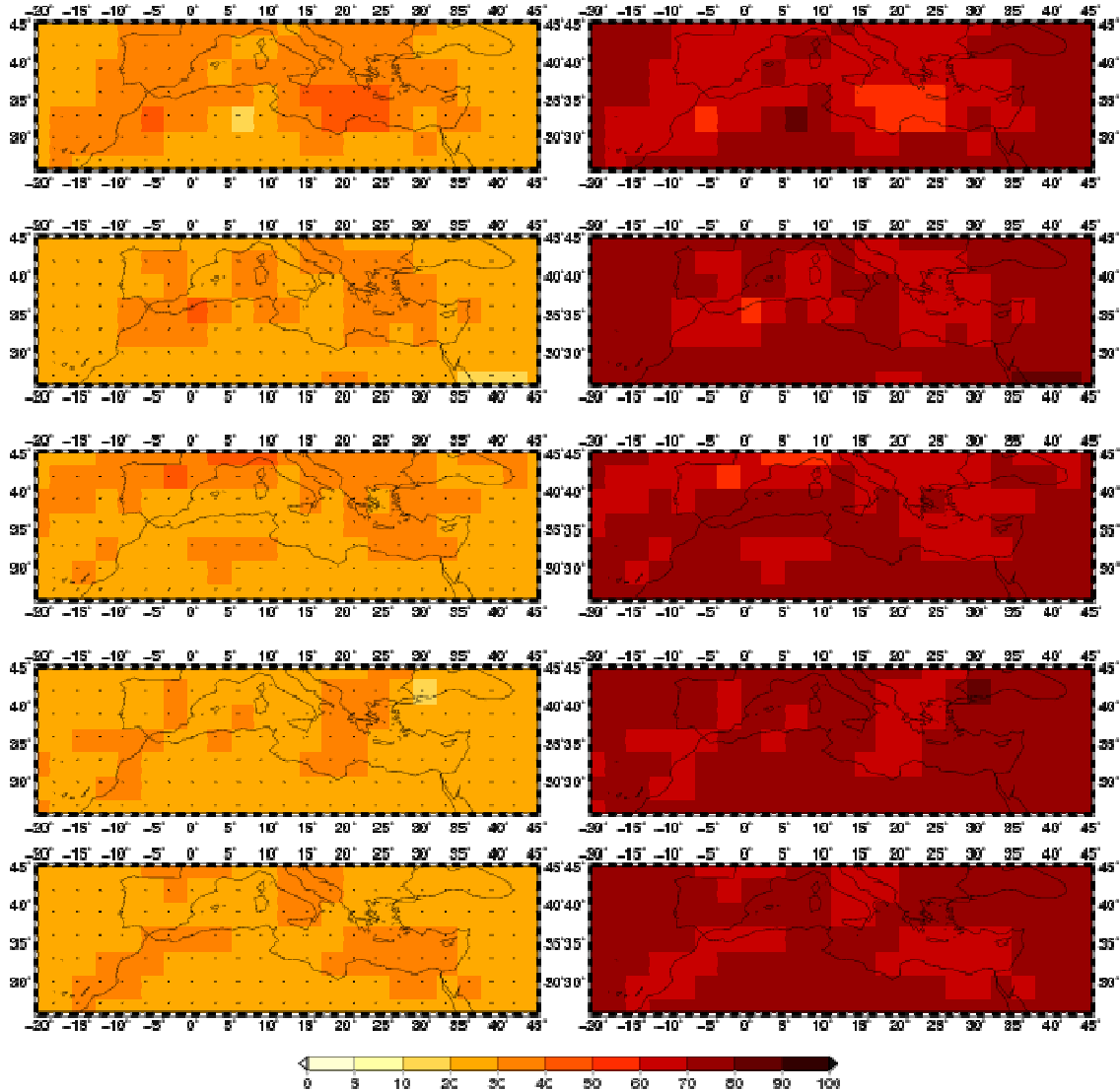
Figure 5.2: As Figure 5.1 but for precipitation.

Also a homogeneous pattern is depicted by figure 5.3, for the four runs of ECHAM5, when sea-level pressure is conducted to an ANOVA again for the same period in the A1B scenario. Here one can clearly distinguish the different seasons, as e.g. highest values are reached in summer, when the MA is mainly unaffected by Atlantic stormtracks leading to a high agreement within the different runs and reflecting a common trend within the time. Furthermore, in the eastern basin the strong negative trend is expressed by more than 43.5% of known variance in the total year. Still, also the patterns for winter and summer confirm the trend patterns illustrated in figure 4.35. Overall, the sea-level pressure analysis expresses known partitions at the magnitude of precipitation, while they are also far lower than that for temperature.

116

In figure 5.4 different integration periods have been chosen for temperature, within the ANOVAs are applied. With the B1 scenario on the left side and the A2 scenario on the right side, in this figure two different scenarios are illustrated. The upper row shows the total time period from 1901-2098 and thus the longest time period, which is available for this study. Here, the common signal expands to the highest amounts in the study, being affected by a strong trend over this relative long period and becoming more dominant within a longer time. This leads to the conclusion, that the longer the period is, the higher is the partition of the treatment effect to the total variability, while the known variability declines with the shortening of the time period within the analyses are conducted.
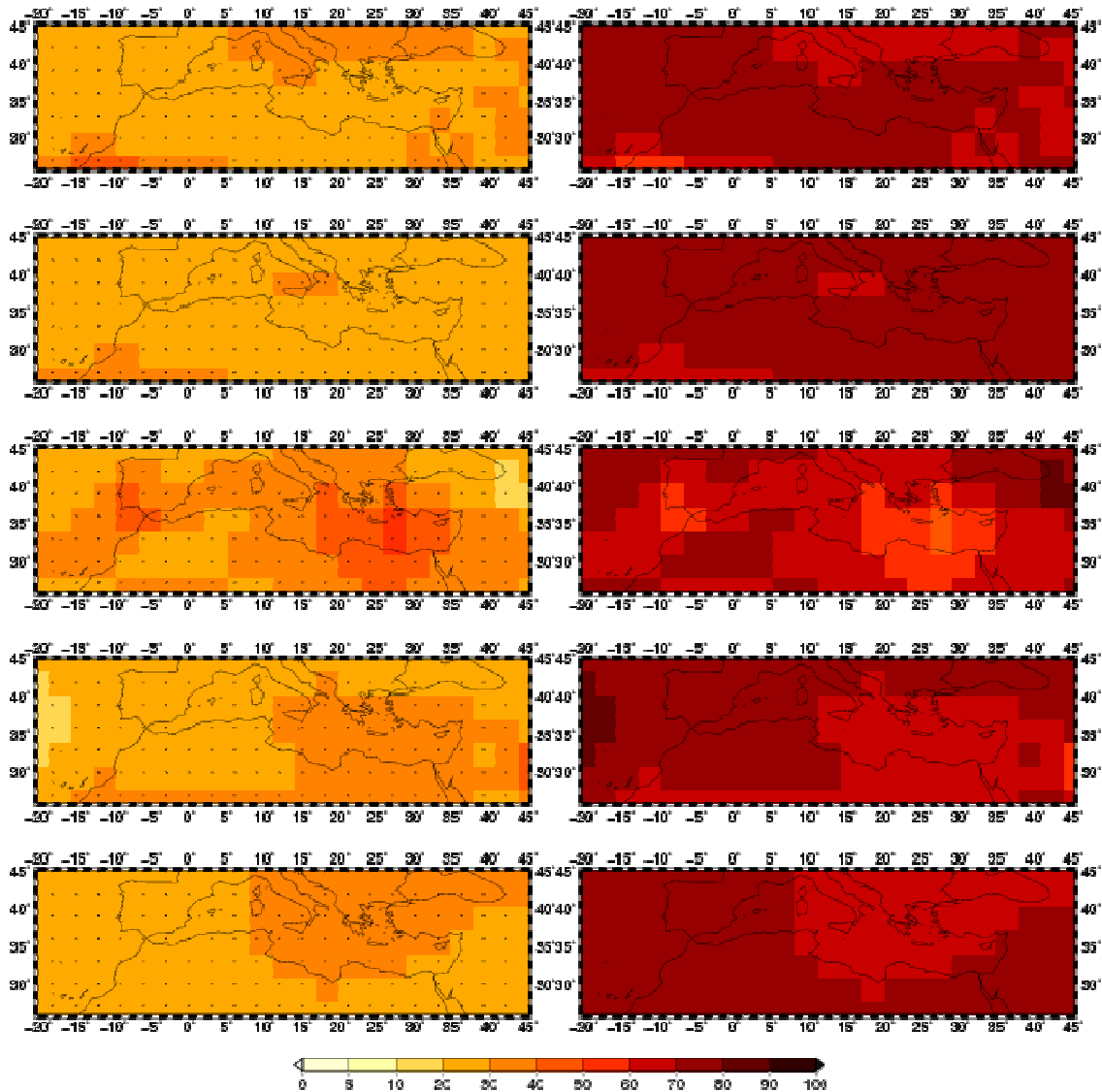
Figure 5.3: As Figure 5.1 but for sea-level pressure.

Please note, that this phenomenon is confirmed for the shortest period from 1961-2000, when the partition of the unknown variability is highest. The period from 1961-2000 is deliberately not shown, since at this time no separating courses of climatic development reflected in the SRES scenarios are enabled. Thus, this period is solely depicted by the 20c3m scenario affiliating the groundwork for the subsequent process of the SRES scenarios. This effect of the partition of variabilities is also stated for precipitation and sea-level pressure.

Whereat, for precipitation and sea-level pressure, there is hardly a difference in the magnitude for the periods of 1961-2050 and 2001-2098 (figures 5.5 and 5.6 middle and lower rows). Concerning temperature, the trend is highest in the A2 scenario, when temperature rises of about 6.5°C over the nearly 200 years at some regions in the overall year (compare figure 4.21 with a period from 2001-2098). For the B1 scenario the trend is much lower, although in this ecologic scenario a trend is detectable leading to a strong signal of the known variability still. Consecutively, the known partition of the A2 scenario is exceeding the B1 scenario (figure 5.4). Comparing the results from 2001-2098 (in the middle row of figures 5.5-5.6 on the right and the upper left figure in figures 5.2-5.3) also the signal in the A2 scenario exceeds the A1B scenario for precipitation and sea-level pressure. An unexpected phenomenon is depicted by sea-level pressure and precipitation, where the known partition of the B1 scenario exceeds the other scenarios. This becomes explainable by a closer investigation of the time-series, where particularly for the A2 scenario a higher variability between the simulations is evident. It cannot be excluded that natural variability is independent of climate change. Rather opposite considerations are plausible. E.g. GIORGI & LIONELLO (2008) or GIORGI & FRANCISCO (2008) discuss the increasing variability of precipitation with a progress of time and an enforcement of a scenario. Also variability of precipitation becomes stronger in the warmer seasons than in the cold seasons. This is consistent with an expected intensification of the hydrologic cycle under warmer conditions. Besides, it must be highlighted, that for the B1 and the A2 scenario only 3 simulations had been available compared to the A1B scenario, where 4 simulations have been used (see e.g. figure 3.1). This might also have impacts on the signal (see below).
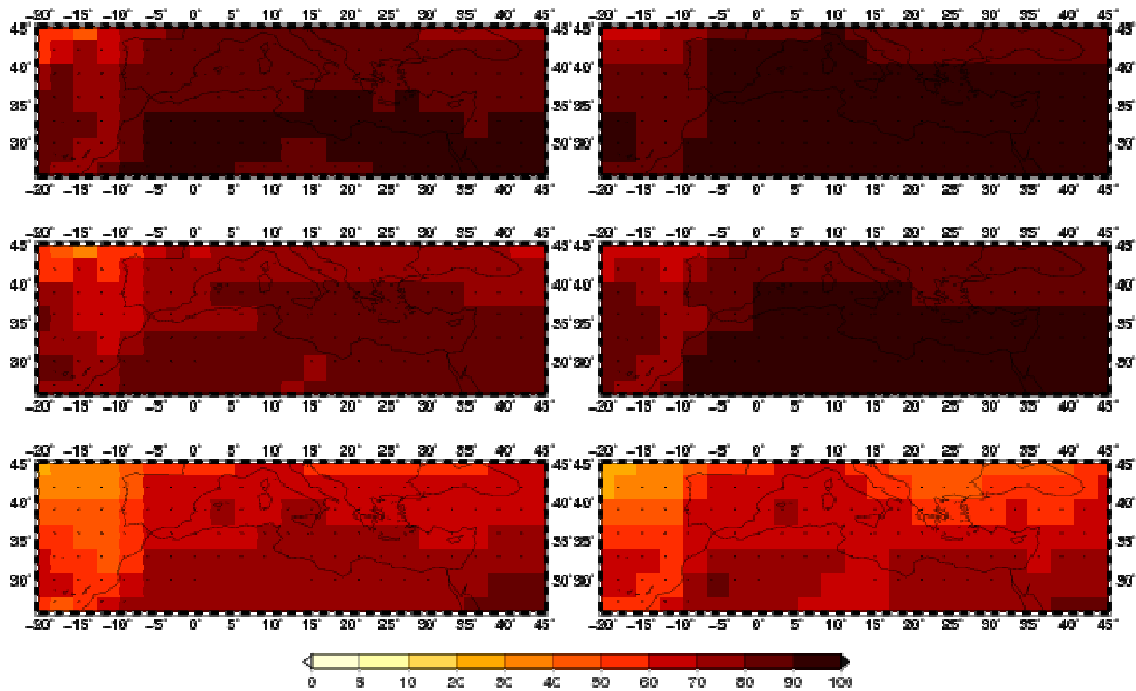
Figure 5.4: Comparison of the yearly partitions of the known variances of temperature. For the scenarios B1 (left side) and A2 (right side) the simulations 1,2 and 3 of Echam5 have been used. Different time periods have been calculated, i. e. from the top to the bottom 1901-2098, 2001-2098 and 1961-2050. Black dots describe significance for the specific grid-cell on a level of α=5%.

This gives insight, that the strong impact of the partition of the external forcing, still is dependant on the magnitude of the internal variability, which may outbalance the enforcements of trends by the change of scenarios in some cases. Apart from these exceptions, the expected results of an enhancement of the known partition by an enforcement of the scenario and thus an enforcement of the trends, is conventional. Thus, the partition of the known variability rises from B1 to A1B to A2.

For ECHAM5 and its respective simulations, one can conclude a high agreement concerning temperature, being only lowly disturbed by changing assumptions like scenarios or preconditions. The rise of temperature, projected by ECHAM5, holds complete confidence over different uncertainties. This is not granted for precipitation or sea-level pressure as the differences between the runs are relatively high. This analysis has been conducted for all the models displayed in chapter 3.1 with several realizations, where the finding concerning the impact of the length of the period can be stated throughout all models and all seasons, and shows the main differences concerning these analyses.

For brevity it is proceeded as accustomed by giving a fast overview of the results of the spatially means developed out of the MA by different models, where the results of the model NCAR-CCSM3 are withdrawn from this analysis, as the high number of simulations (e.g 7 in A1B and 8 in B1 see table 3.2) and the accompanied high amount of variability represses the known partition and adulterates the appearance of the following figures. Furthermore, it does only show a relatively low increase of temperature (e.g. figure 4.24), giving a further explanation on the low known partition. At this point the reader is kindly referred to compare the results shown here with the means and trends of the ensemble-means in chapter 4.2.
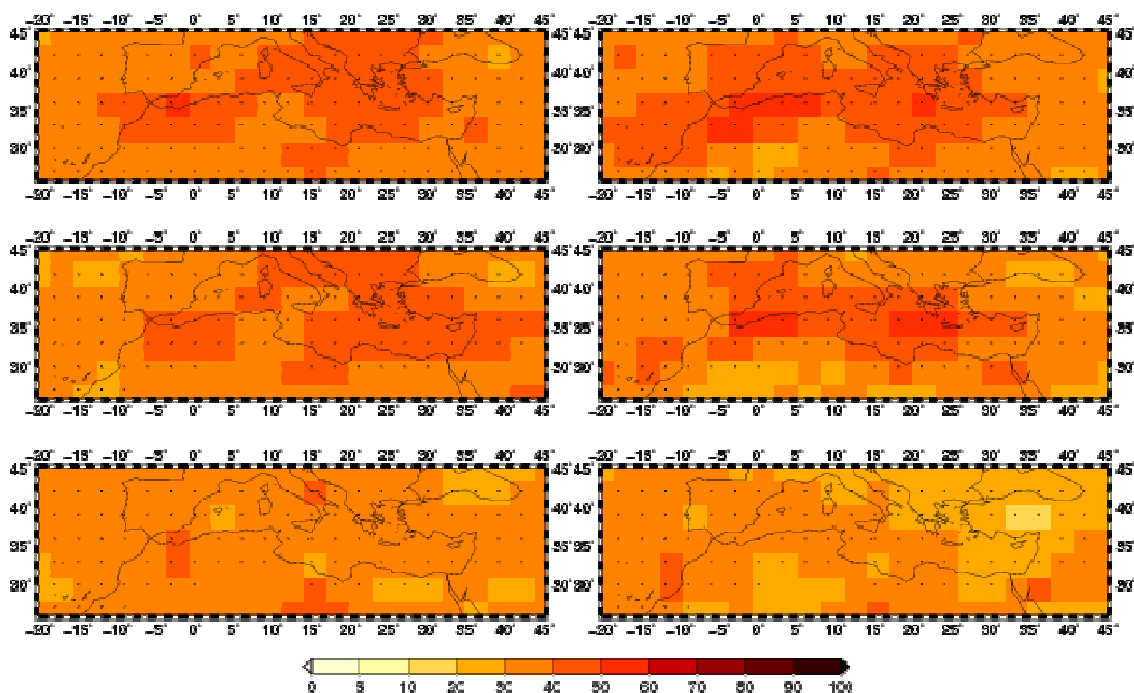
Figure 5.5: As Figure 5.4 but for precipitation.
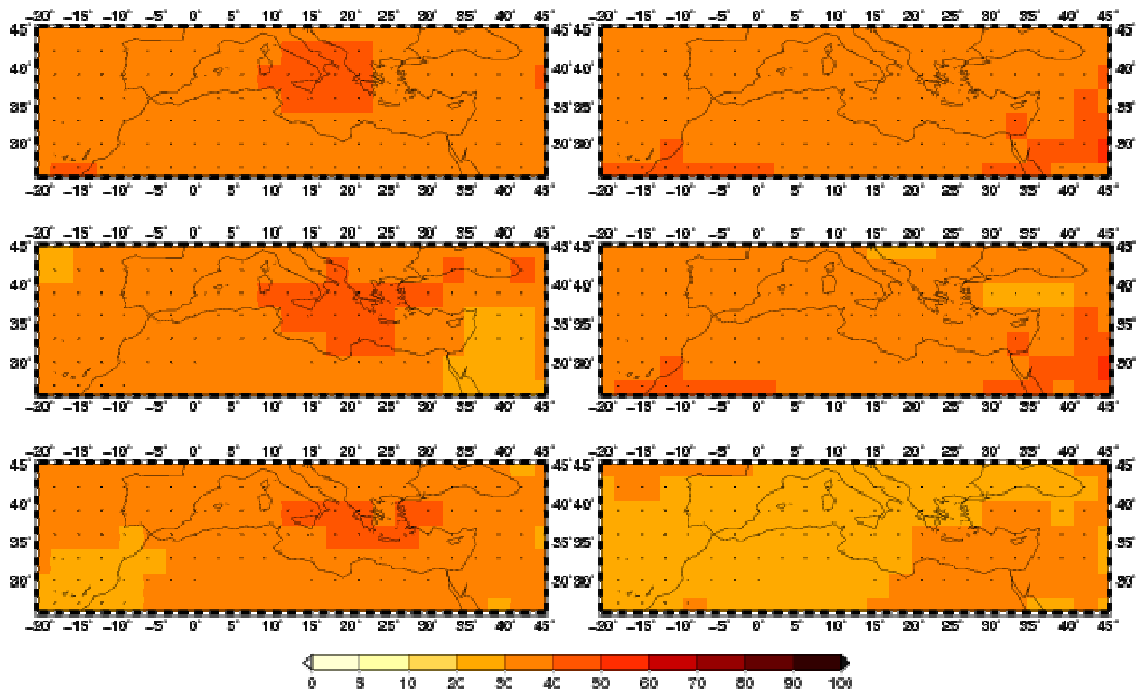
Figure 5.6: As Figure 5.4 but for sea-level pressure.

For temperature, the means of the known partition are shown in figure 5.7, where different models are displayed with respect to the specific season for A1B. For all of the five remaining models the values of spring and winter are the lowest. Summer is the season, where lowest discrepancies can be found between the simulations. Furthermore, it is the season with the most impressive trend, leading again to these high results. Comparing the trends of the individual models in figure 4.24, the highest signals are found by the models with the most distinct trends. Total year values are even higher than seasonal variabilities.
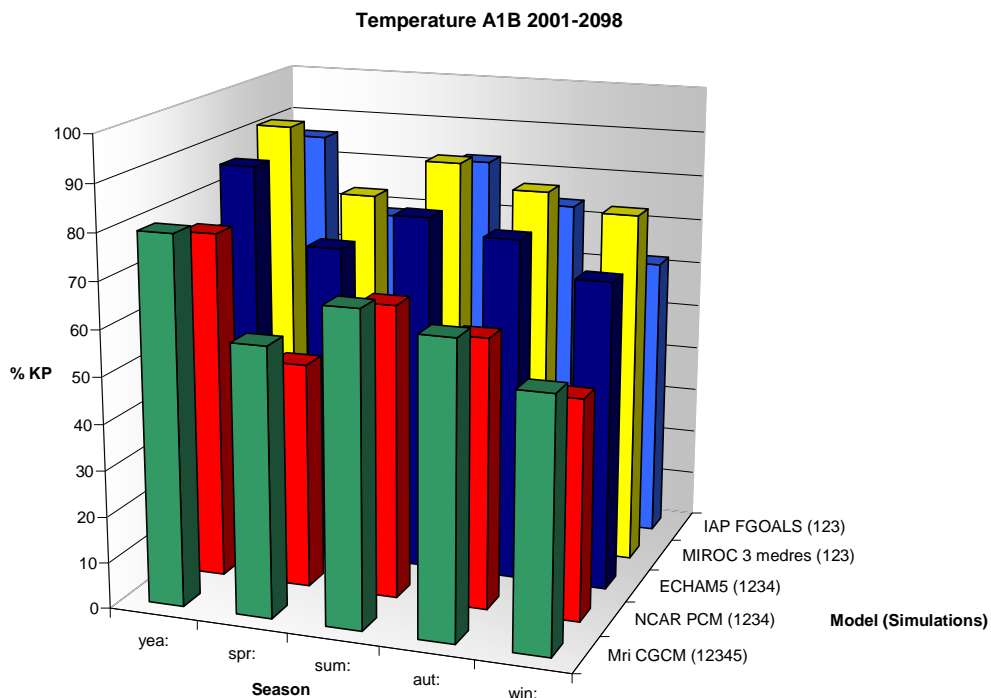
Figure5.7: Spatially averages in the MA of the partition of the known variability. Shown are the analyses of temperature for 2001-2098 for different seasons and the total year depending on the specific model with its numbers of simulations in brackets.

It is an interesting feature, that the high difference of the 4 runs of the NCAR PCM leads to the lowest partitions of known variability in all seasons. This does not hold for precipitation, as could be seen in figure 5.8, where the NCAR PCM reaches approximately the level of ECHAM5. Please note the changing values at the ordinate, as the amounts for precipitation are generally lower than those for temperature, as already shown above for ECHAM5. With an exception to MIROC3.2 medres, where the known partition in winter is higher than in summer, the other models depict highest partitions of known variabilities in summer, which counteracts the theories concerning the amplitudes of the trends, as shown in figure 4.32, where summer exhibits lowest trends for e.g. ECHAM5. Still one should keep in mind, that summer precipitation is low anyway (figure 4.31), causing a strong relative decrease. Furthermore, the variability between the simulations is lower than in winter, which is reflected in figure 4.44.

Models with fewer simulations have a smaller inherent unknown variability leading to higher values of the opponent dimension. Partitions of known variances for sea-level pressure values (figure 5.9) are lower than those for temperature and range at nearly the same level like precipitation. Nevertheless, the models are veritably illustrating the signal of sea-level pressure. While MRI CGCM is at lowest scales it has the biggest group of simulations. On the other hand, IAP FGOALS and MIROC3.2 medres, both having only 3 members, depict a higher agreement of the different simulations, which results in a relatively high amount of the known partition. Furthermore, both models indicate a strong trend, while it is noteworthy that, though the individual realizations of the specific models confirm each other, the models depict different courses of the trends in winter. This is a negative trend for IAP FGOALS and a slight positive one for MIROC3.2 medres (figure 4.40). Again, this highlights the necessity of the analysis of different models, though one model can pretend relative high certainty concerning the agreement of its realizations. The negative trend in summer is common to all models and also common to all simulations, which is reflected in the highest amplitudes of known variability in this season.

Precipitation A1B 2001-2098
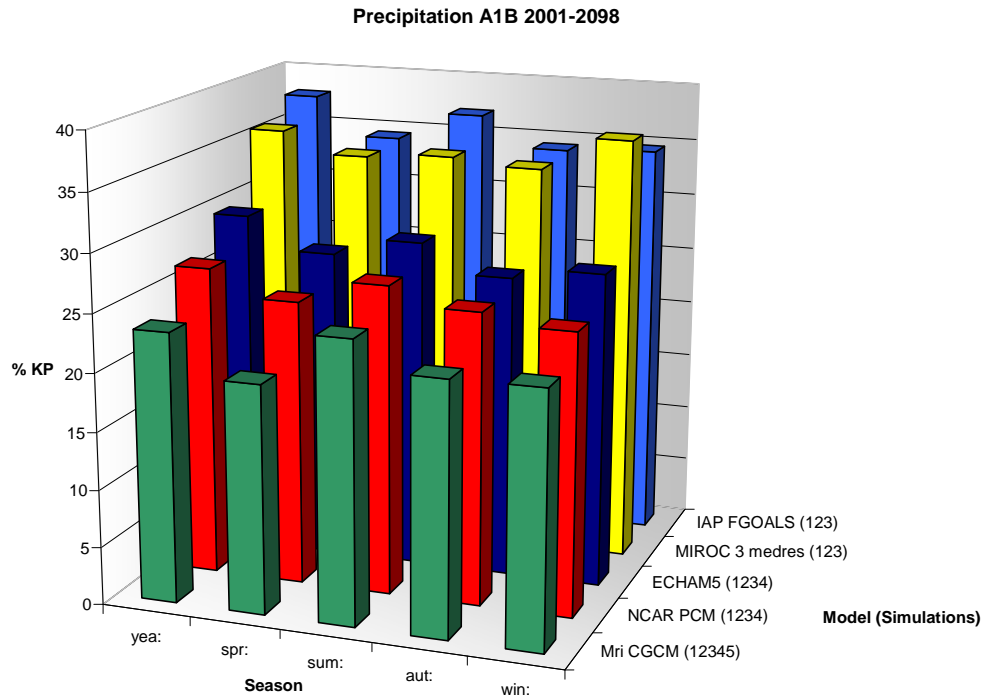
Figure5.8: Same as figure 5.7 but for precipitation.

Sea-level pressure A1B 2001-2098
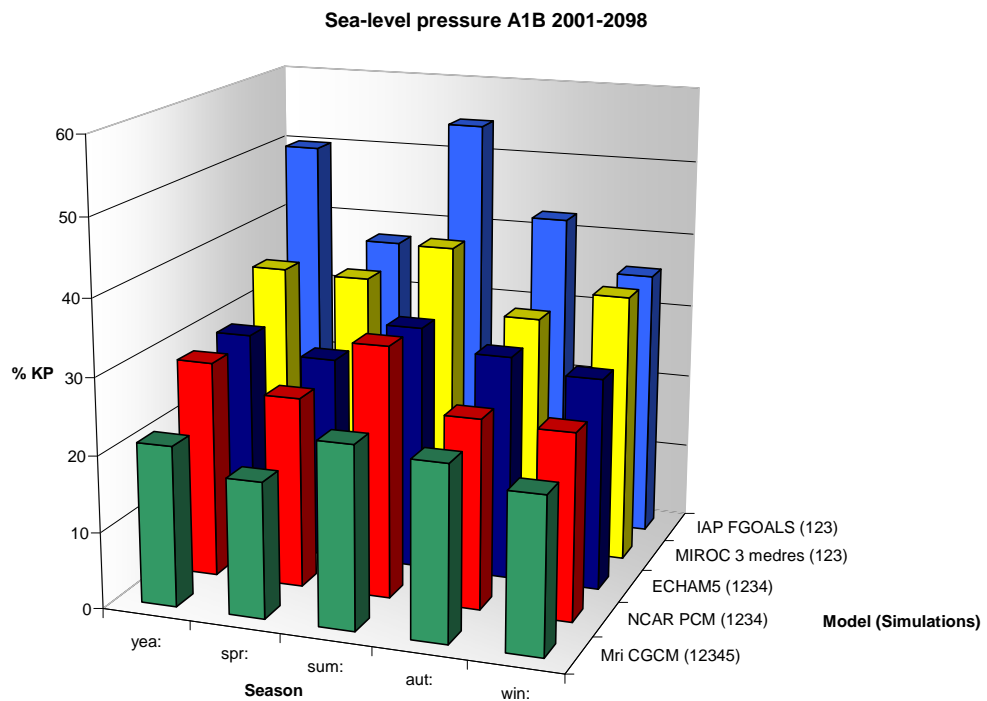
Figure5.9: Same as figure 5.7 but for sea-level pressure.

5.2.2.2 Temporal approach

The role of the magnitude of the trends in relation to the internal variability leads to the inevitable question about the amplitude of a trend affecting the ANOVA, and then, when it starts to affect the analysis. The latter question will be addressed now. Consecutively, one is necessarily interested in the point in time, when the signal of the external forcing becomes dominant. That is why the ANOVA is conducted again with respect to the temporal evolution of the specific signals this time. This second approach will be denoted as temporal approach additionally to the already shown spatial approach.

For the temporal approach the gridded values of the specific variable, e.g. temperature, sea-level pressure and precipitation, of the MA are averaged, which is simply done by 5) in the "cooking recipe". For this regional mean value the ANOVA is calculated for each time period z comprising a certain length N, which is 30 years and 60 years in this work. The length of the time period is chosen to smooth out natural variability on the one hand, which at least should be true for the integration period of 60 years and to provide a relatively high signal of an external forcing on the other hand. The applied period is shifted by yearly steps throughout the maximum integration period, which is 1901-2098 (see 3.1.2), while the ANOVA is calculated for each period z. In case of an 1-way approach, the ANOVA is computed by the temporal average value within this period of the ensemble-mean, the individual yearly values of the ensemble-mean and the individual yearly values of each specific realization. The mean values X_{jz} depicting a value of a specific realization and a specifically shifted time window with the length of N, projected on year I, is given within formula (31).

$$31) \qquad X_{jz} = \frac{1}{N} \sum_{i=z}^{N+z} X_{ji}$$

The 2-way ANOVA (see below) is calculated analogously. The resulting partitions of variance are projected on the middle year of this period, which is the 15th or the 30th year for the associated integration period of 30 years or 60 years respectively. That is why the first value is given at 1915 or 1930 and the last value in 2083 and 2068. Consecutively, the whole period is shortened to 169 years and to 139 years respectively. Thus, the temporal approach works analogously to the spatial approach, while it is not done for every grid-cell in the maps, but for the average mean of a certain period, as it e.g. has been already done for the selected periods in figure 5.4. This time the periods of equal length are in a sequence directly following each other. Consecutively, they are not completely independent, as additionally two ensuing periods overly each other with 29 and 59 years respectively. This has an elevating impact on the statistical significance associated to a temporal memory inherent to the subsequent periods. To account for this problem the overall mean, which is in case of the 1-way ANOVA the ensemble-mean and in the case of the 2-way ANOVA the multi-model mean (see below), calculated out of the ensemble-means, is subject to an analysis of autocorrelation (formulae (32-34)). For this procedure the trend is calculated with the application of the trend formulae in the "cooking recipe" with b as the slope or the regression coefficient by formula (5) and a as the intercept

of the axis by (formula 6). The calculated trend is subtracted from the original values. The received series of residuals, which does not offer any trend now, is processed by correlating it with itself. Each correlation is done with a shift by yearly steps q=1,2,…,Q. The temporal shift is confined to 169 steps defining Q for the 30-year approach and to 139 for the 60-year approach. Analogous to formula (7) the coefficient of correlation can be calculated by formula (32).

$$32) \qquad r_q = \frac{\sum\limits_{z=1}^{z-q} \left(X_z - \overline{X_z} \right)\left(x_{z+q} - \overline{x_{z+q}} \right)}{\sqrt{\sum\limits_{z=1}^{z-q} \left(X_z - \overline{X_z} \right)^2 \sum\limits_{z=1}^{z-q} \left(x_{z+q} - \overline{x_{z+q}} \right)^2}} \quad,$$

with the declared mean values of the specific neighboured time periods.

With the specific coefficients of correlation r_q the standard error SE can be estimated by formula (33).

$$33) \qquad SE_q = \frac{\sqrt{1 + 2\sum\limits_{q}^{Q} r_q^{\,2}}}{\sqrt{N}} \;.$$

Consecutively, a t-Test is used to estimate significance for the individual correlation coefficients (formula (34)).

$$34) \qquad g(q) = \frac{\left| r_q \right|}{\left| SE_q \right|} \;.$$

The autocorrelation defines the temporal memory inherent to the dataset. The number of periods Z is divided by the number of years this temporal memory is sustained in. This reduces the degrees of freedom concerning the statistical test.

In figure 5.10 the temporal approach of the 1-way ANOVA is displayed for temperature and the different seasons for the A1B scenario. The left column illustrates the course of the explained variability within a 30-year time window, which is shifted through the integration period. The received percentages of variability are focused on the middle year of this 30-year period. This is analogously done for the 60-year accomplishment (right column), whereat the investigated period is furtherly shortened as the first value cannot be displayed before the year 1930, after 30years from the beginning in 1901. For the 30year period the initial year is 1915. The levels of significance are indicated with green lines, where the upper one accounts for α=5% and the lower one for α=10%.

Though the periods are shorter than the period from 2001-2098 with its nearly 90 years, still long term variability is conserved in the sliding 30-year and 60-year low-pass filter. The 30-year approach indicates evident higher variability in

the signal, which is due to the lower power of the low-pass filter applied on the original series compared to the 60-year low-pass filter. In all graphs an increase of the known partition is displayed, which starts in the late 1980s for the 30-year approach with the exception of autumn, where it starts earlier. The starting point is shifted to the past by the 60-year approach, which is due that the 60-year integration period includes former times with its extended length up to times where GHG emission start affecting the atmosphere. As expected, the highest parts of the known variability are experienced in summer (see above), where, besides the overall year, the 5% level of significance is reached. Winter exhibits lowest partitions of known variability with highest variability between the realizations and shows weakest trends. Still, highest values are obtained by the 60-year integration period, revealing again the higher values of the known partition, which depends on the longer period, where trends are developed in. Consecutively, the levels of significance are trespassed easily in the 60-year approach. At the end of the investigation period one detects a decrease in the overall year, spring and summer, leading to the assumption of a diminished trend by reduced forcing power of the A1B scenario (chapter 2.4). The warming trend and thus the rising known partition in the 20th century is preliminary due to its first and to its last decades (GIORGI 2002b, PAETH 2007). Besides natural forcings, like volcanic eruptions or variations of solar irradiance, this can possibly be explained by the enhancement of industrial filter techniques, particularly in the middle of the 20th century, leading onward to a reduction of sulphate aerosols with their specific cooling effect, finally evoking an increased warming of the atmosphere again (HEGERL et al. 2007, TETT et al. 1999).

On the other hand, an enforced disagreement over the 4 realizations is also possible. This phenomenon is also noticed in the 60-year period in spring. Particularly in the 30-year approach small minima and maxima are evident, which are hard to interpret, as they are dependent on the force of the scenario but also on the individual realizations, where each of them is subject to the chaotic projection of natural climate variability (see 2.2).

Finally, it is noteworthy, that these results confirm the findings above, out of figures 5.1, 5.4, 5.7, as the temporal values need to be consistent with the spatial approaches, considering the specific episodes in the temporal approach. The only constraint, prohibiting a direct comparison, is the different length of the period defining the amount of the trend and the calculation of the regional mean.
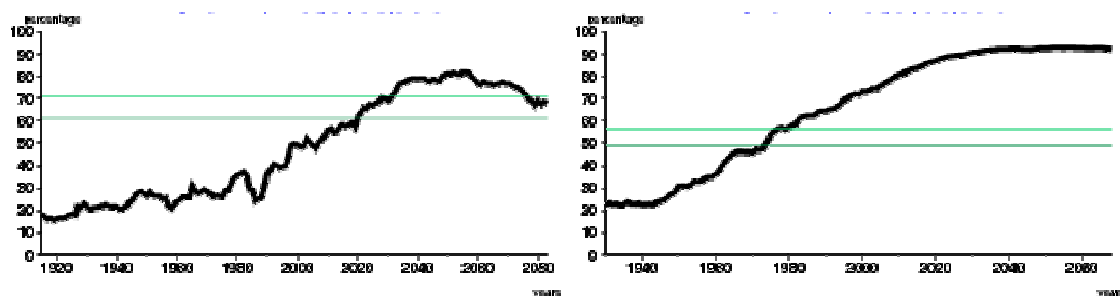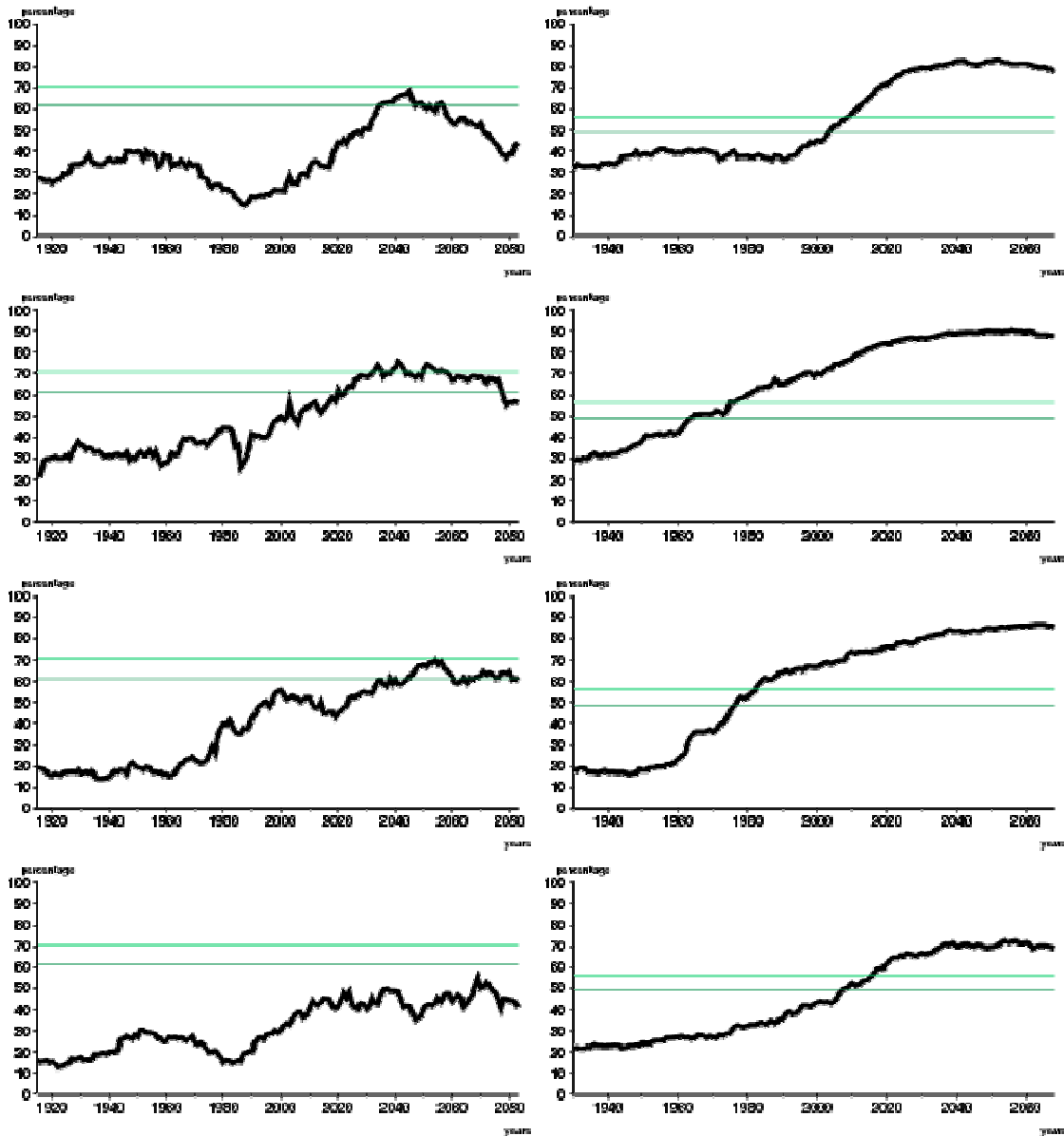
Figure 5.10: Known partition (left 30y/right 60y) of the temporal approach of the 1-way ANOVA for ECHAM5 for temperature in the A1B scenario for the runs 1,2,3 and 4. Green lines indicate levels of significance (brighter line 5%, darker and lower line 10%). From top to bottom: year, spring, summer, autumn and winter.

As the 60year approach receives a higher percentage of known variability, as stated for temperature, in figure 5.11 the 60year approach is also shown for precipitation (left column) and sea-level pressure (right column). Here, the variables are assigned by a general lower percentage of known partition. In none of the four seasons, nor in the overall year significance is reached by neither sea-level pressure nor precipitation. This clearly must be attributed to the relative short period, compared to the periods in figure 5.2 or figure 5.3, where significance is reached. Furthermore, a distinct offset of the known partition evoked by the forcing is not evident. At least for precipitation in summer an increase from about 2010 persisting until 2040 is noticeable. Contrary to the missing maximum signal in summer for sea-level pressure, which is shifted into winter, the outlined behaviour of precipitation is confirmed by longer time series, see above. Still the course of the known variability for sea-level pressure in

winter is reasonable by a closer investigation of the time series, as the signal is quite low in the last decades, diminishing the average value for the 21st century, which is roughly depicted in figures 5.3 and 5.7.
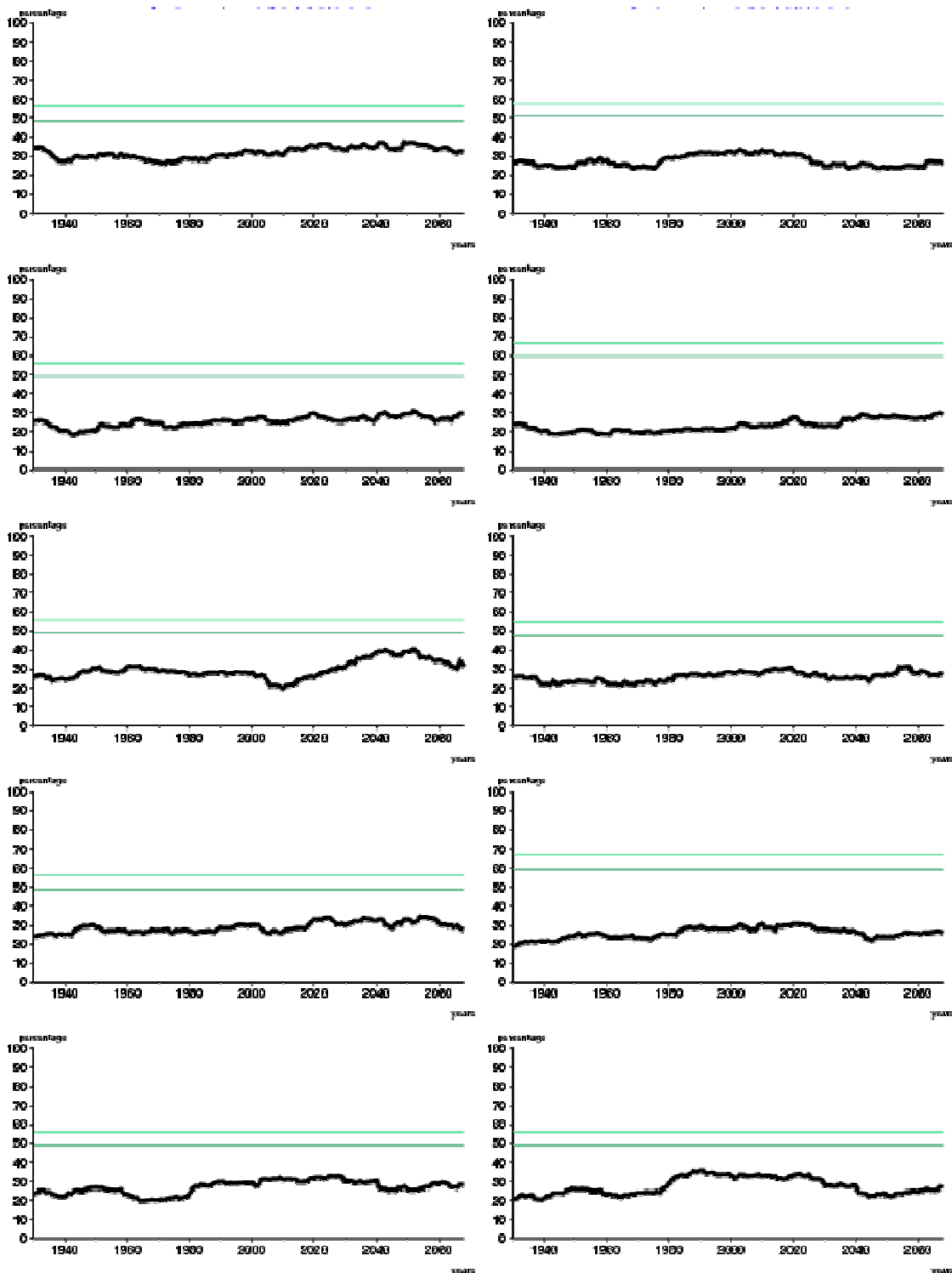
Figure 5.11: Known partition (left precipitation/right sea-level pressure) of the temporal approach of the 1-way ANOVA for ECHAM5 for 60y in the A1B scenario for the runs 1,2,3 and 4. Green lines indicate levels of significance (brighter line 5%, darker and lower line 10%). From top to bottom: year, spring, summer, autumn and winter.

An already mentioned question deals with the enhancement of the signal by an enforcement of the scenario. Figure 5.12 shows the yearly results for the three variables temperature, precipitation and sea-level pressure from top to bottom, dependent on the different scenarios B1 on the left side and A2 on the right side. Concerning temperature the signal reaches significance earlier in A2 and finally continues on a higher level than in B1 and A1B (in figure 5.12). For precipitation and sea-level pressure again no significance can be stated. Again it is noteworthy that in B1 higher values can be reached than in the other scenarios. These results confirm the already gained insights, derived by the spatial approaches.
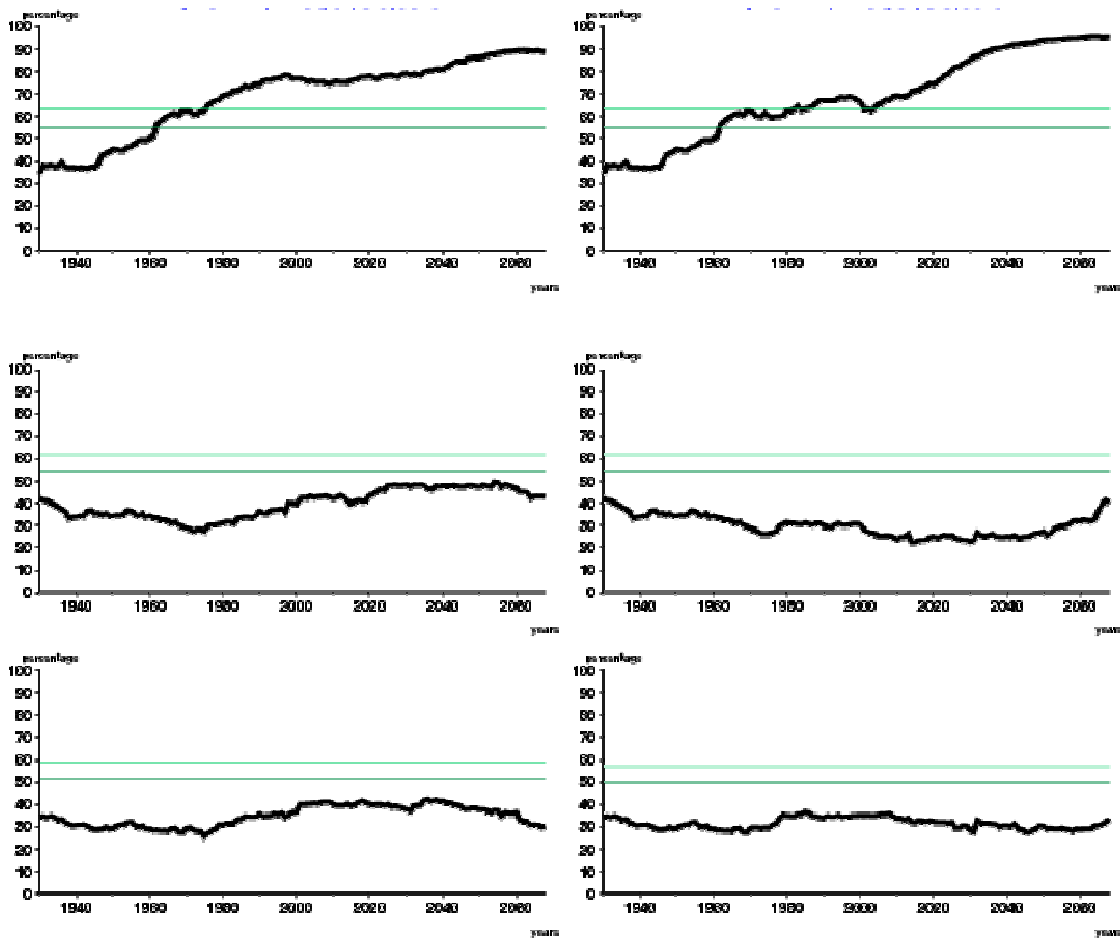
Figure 5.12: Yearly known partition (left B1/right A2) of the temporal approach of the 1-way ANOVA for ECHAM5 for 60y for the runs 1,2 and 3. Green lines indicate levels of significance (brighter line 5%, darker and lower line 10%). From top to bottom: temperature, precipitation and sea-level pressure.

5.3   2-way ANOVA

The classical tool to separate inter-model variability from intra-model variability and from external forcings is the 2-way ANOVA. For this purpose it is necessary to use an identical external forcing for each application. Otherwise the amounts of intra-model and inter-model variability will be disturbed.

Please note, that only these models are subordinated to a 2-way ANOVA, which offer several realizations within an ensemble. Combined with the constraints, discussed in chapter 3.1, this constricts the number of the models used to 6 in the A1B and B1 scenarios (FGOALS-g1.0, MIROC3.2 medres, MRI-CGCM2.3.2, ECHAM5, NCAR CCSM3 and NCAR PCM). In the A2 scenario FGOALS-g1.0 has no realization, why for this scenario the analyses are done with 5 models. For sea-level pressure, this number is even reduced to 3 models, as some problems occurred with the processing of the NCAR models in the A2 scenario, which could not be solved (see table 3.2).

5.3.1 Method

For the following analysis, the experiments consist of random variables X_{kji}, which are independent from each other. The data are normally distributed with $i=1,\ldots,I$ timesteps, $j=1,\ldots,J$ realizations in $k=1,\ldots,K$ models. The total amount of the sampling elements cannot be assessed by a simple multiplication, as it has been done for the 1-way ANOVA (see formula 10). Here, the number of realizations is different across the models and thus dependant on the model k, as it has been e.g. shown in table 3.2. That is why the number of elements is calculated by formula (35), where the number of time-steps I is the same for each individual realization j.

$$35) \qquad n = I \sum_{k=1}^{K} J_{(k)} \ .$$

Analogous to the 1-way ANOVA again a linear model for the 2-way ANOVA is established (formula (36)):

$$36) \qquad x_{ijk} = \mu + \alpha_k + \beta_i + \gamma_{ki} + \varepsilon_{ijk} \ ,$$

with:

- μ = overall mean of all data of the multi-model mean

- α_k = adjustment for the GCM k

- β_i = adjustment for the time-steps

- γ_{ki} = time specific adjustment for the GCM k

- ε_{ijk} = residual effect over the variability of runs.

Where α_k reflects the ensemble-mean of one specific model over the time. Thus, the term α_k can be interpreted as the systematic bias of all climate models to each other and will be defined as block effect. Consecutively, β_i describes the temporal change of the multi-model mean, which will be interpreted as the treatment effect, as it expresses the trend within the time, inherent in all the models. The term γ_{ki} is dependant by time and the specific model and thus shows the different response of the climate models within the time, e.g. how fast

the runs react to a scenario. The reader is again kindly reminded that the scenario will always stay the same in one specific analysis. It will be referred on γ_{ki} as the so-called interaction coefficient. The unpredictable residual is given by ε_{ijk}, which depicts the intra-model uncertainty by means of the variability over the ensemble-members concerning their different initial conditions. Again the errors are independent identically distributed and are zero in their mean. The assumption is given, that the mentioned effects are additive.

Again, one is particularly interested in the relative magnitudes of the variance components SS_α, SS_β, SS_γ and SS_ε to the total variance SS_{tot}, which again can be determined by the decomposition of the total SS (formula 37).

$$37) \qquad SS_{tot} = SS_\alpha + SS_\beta + SS_\gamma + SS_\varepsilon$$

Where analogously to the foregoing paragraph, SS_α is the relative amount of the variability, which is due to all models and SS_β is the relative amount of the variability, which is due to the time and thus is a general signal of climate change. SS_γ is the relative amount of the variability from the response of one model within time and thus an indication of the models´ specific response to a certain scenario. SS_ε is the relative amount of the variability due to the different ensemble-members.

The different SS are calculated as follows in formulae (38-41):

$$38) \qquad SS_\alpha = I \sum_{k=1}^{K} \left(J_{(k)} \left(\overline{x}_{k00} - \overline{x}_{000} \right)^2 \right),$$

where the number of realizations J again depends on the specific model k. The SS representing the treatment effect is given in formula (39):

$$39) \qquad SS_\beta = \sum_{k=1}^{K} J_{(k)} \left(\sum_{i=1}^{I} \left(\overline{x}_{00i} - \overline{x}_{000} \right)^2 \right),$$

here, again specific attention has to be paid because of J. The SS of the interaction coefficient is displayed in formula (40):

$$40) \qquad SS_\gamma = \sum_{k=1}^{K} \left(J_{(k)} \sum_{i=1}^{I} \left(\overline{x}_{k0i} - \overline{x}_{00i} - \overline{x}_{k00} + \overline{x}_{000} \right)^2 \right),$$

while the residual can be computed with formula (41):

$$41) \qquad SS_\varepsilon = \sum_{k=1}^{K} \sum_{j_{(k)}=1}^{J_{(k)}} \sum_{i=1}^{I} \left(x_{kji} - \overline{x}_{k0i} \right)^2 .$$

Finally, the assumption of additivity leads to formula (42), declaring the total SS:

42) $$SS_{tot} = \sum_{k=1}^{K} \sum_{j_{(k)}=1}^{J_{(k)}} \sum_{i=1}^{I} \left(x_{kji} - \overline{x}_{000} \right)^{2} .$$

Needless to say, that the applied models are again subordinated to the calculation of the means (formula (43-46)), as they are introduced into the procedure of the ANOVA (formulae (38-42)). Again, $_0$ denotes the mean value of the group of the replaced subscript.

43) $$\overline{x}_{000} = \frac{1}{n} \sum_{k=1}^{K} \sum_{j_{(k)}=1}^{J_{(k)}} \sum_{i=1}^{I} x_{kji} ,$$

44) $$\overline{x}_{k00} = \frac{1}{J_{(k)} I} \sum_{j_{(k)}=1}^{J_{(k)}} \sum_{i=1}^{I} x_{kji} ,$$

45) $$\overline{x}_{00i} = \frac{1}{K J_{(k)}} \sum_{k=1}^{K} \sum_{j_{(k)}=1}^{J_{(k)}} x_{kji}$$

and

46) $$\overline{x}_{k0i} = \frac{1}{J_{(k)}} \sum_{j_{(k)}=1}^{J_{(k)}} x_{kji} .$$

The SS allow the computations of the specific partitions relative to the total amount of variance, which is inherent to the universe dataset. This is done with the consecutive formulae (47-50).

47) $$\hat{R}_{\alpha}^{2} = \frac{SS_{\alpha} - \dfrac{K-1}{n-KI} SS_{\varepsilon}}{SS_{tot}} ,$$

48) $$\hat{R}_{\beta}^{2} = \frac{SS_{\beta} - \dfrac{I-1}{n-KI} SS_{\varepsilon}}{SS_{tot}} ,$$

49) $$\hat{R}_{\gamma}^{2} = \frac{SS_{\gamma} - \dfrac{(K-1)\cdot(I-1)}{n-KI} SS_{\varepsilon}}{SS_{tot}}$$

and

50) $$R_{\varepsilon}^{2} = \frac{\dfrac{n-1}{n-KI} SS_{\varepsilon}}{SS_{tot}} .$$

131

The 4 received partitions again aggregate to 1 at each grid-cell or at each time-step, which depends on the approach. In the following figures, they are depicted in percentage, that is why the partitions are multiplied with 100.

To test their significance, a two-sided F-test is applied, with the confidence level of 95%. For the derivation of the tests, the reader is kindly referred to VON STORCH & ZWIERS 1999.

The specific tests are given in formulae (51-53) with its degrees of freedom:

51)
$$\hat{F}_{\alpha} = \frac{\frac{1}{K-1}SS_{\alpha}}{\frac{1}{n-KI}SS_{\varepsilon}} \qquad df : K-1, n-KI \; ,$$

52)
$$\hat{F}_{\beta} = \frac{\frac{1}{I-1}SS_{\beta}}{\frac{1}{n-KI}SS_{\varepsilon}} \qquad df : I-1, n-KI$$

and

53)
$$\hat{F}_{\gamma} = \frac{\frac{1}{KI-K-I+1}SS_{\alpha}}{\frac{1}{n-KI}SS_{\varepsilon}} \qquad df : KI-K-I+1, n-KI \; .$$

5.3.2 Results of the 2-way ANOVA

Analogously to the 1-way ANOVA, now results are presented for the 2-way ANOVA. Again, a spatial and a temporal approach have been fulfilled.

As the treatment effect β_i is the temporal adjustment of all of the models, the multi-model trends, displayed in chapter 4, provide an indispensable illustration for the interpretation of the results of the ANOVA. However, as only models with several realizations have been used for the 2-way ANOVA (see above) the means calculated by the formulae (43 and 45) for the 2-way ANOVA (with the lower number of models) differ slightly from the means, which partially have been illustrated in 4. The accompanied trends in the figures of chapter 4 were calculated by all of the models, indicated in table 3.2, as well. Nevertheless, the differences of the means and trends of these distinct inputs are extremely small. That is why the new means and trends are not displayed in the following. Furthermore, the application of the means and trends in chapter 4 for the interpretation of the results of the 2-way ANOVA is considered as satisfying.

5.3.2.1 Spatial Approach

In figure 5.13 the temperature simulations of all models and their realizations in the A1B scenario have been subordinated to the 2-way ANOVA. The left column illustrates the α-partition, representing the discrepancy between the models, while the right column depicts the impact of a common trend on the total variability over the time, the models and their realizations. The familiar sequence of seasons is maintained. One recognizes a higher block effect than the treatment is in the β partition. Particularly the discrepancy over the models rises from northwest to the southeast of the MA from about 40% to up to nearly 90%, being a clue of uncertainty. This is possibly emerged by a lack of climatologic time series and knowledge in this area, as it is sparsely populated and has a low coverage of observing stations, which is also depicted in the high discrepancy between the means of the reanalyses (illustrated in figures 4.1 – 4.4). Furthermore, regions with high α terms indicate high spatial variability, which again challenges the reliability of the reanalysis datasets. Hence, the impact of the agreement considering a temporal trend is decreasing to the southeast. Generally the reasons for these biases are manifold and can neither be defined nor distinguished from each other in the approach of this study. However, some reasons may also be dedicated to the different spatial resolutions of the models, while others also might be associated with the models´ specifications, as e.g. different planetary boundary schemes, which provide the basics for vertical transport of heat, energy or moisture and thus again control the surface temperature (see 2.3.1.1).

Highest values of the treatment effect are distributed over the Mediterranean Sea with some extension to the northwest parts. Particularly over the total year this effect gains highest values with up to 60%, dominating the amount of the total variability at some grid-cells. The lesser amount of treatment in the specific seasons, compared to the overall year, indicates the higher unsteadiness of the models within the seasons, as this is a more detailed investigation than a simple assessment concerning the yearly average. By a precise study of the distribution of the specific values over the seasons, it is surprising, that there is no distinct follow up to the multi-model trend of figure 4.20. For instance the summer is not endued with the highest amounts of β on average, compared to the transition seasons. Nevertheless, winter shows lowest partitions of the β partition, where also the smallest trends are found in figure 4.20. The highest warming trend over surfaces and thus a possible high impact of the trends is not reflected, as highest partitions of the β partition are found over the sea, which has also been found by PAETH & HENSE (2002). Their study focuses on a global analysis with a fewer number of models, depicting highest values of β in subtropical and midlatitudinal regions. The block effect α, concerning temperature, is particularly high in summer. The study by PAETH & HENSE (2002) also describes a lower impact of the β partition over mountain ridges, where different parametrization schemes obtain a higher impact of the α-term, i.e. the inter-model variability. Here, the mountain ranges in the MA are rather small, compared to the Andes or the Himalaya and are possibly a subscale phenomenon. This information might also be lost during the interpolation procedure. However, on global scales the inter-model differences are still predominant over regions with possible sea-ice coverage, one of the biggest shortcomings of GCMs, and areas of extratropical cyclogenesis. Reasonably,

the first cannot be depicted in this work and also for the latter regions, i.e. here the eastern Atlantic with the NAO, there is no approval in the underlying study. However, in the study of PAETH & HENSE (2002) the α-term is relatively weak in areas in which the NAO takes place. Finally, the amounts of the resulting values in the underlying study, with the precise analysis of the MA and with a higher number of models, confirm the former study by PAETH & HENSE (2002).
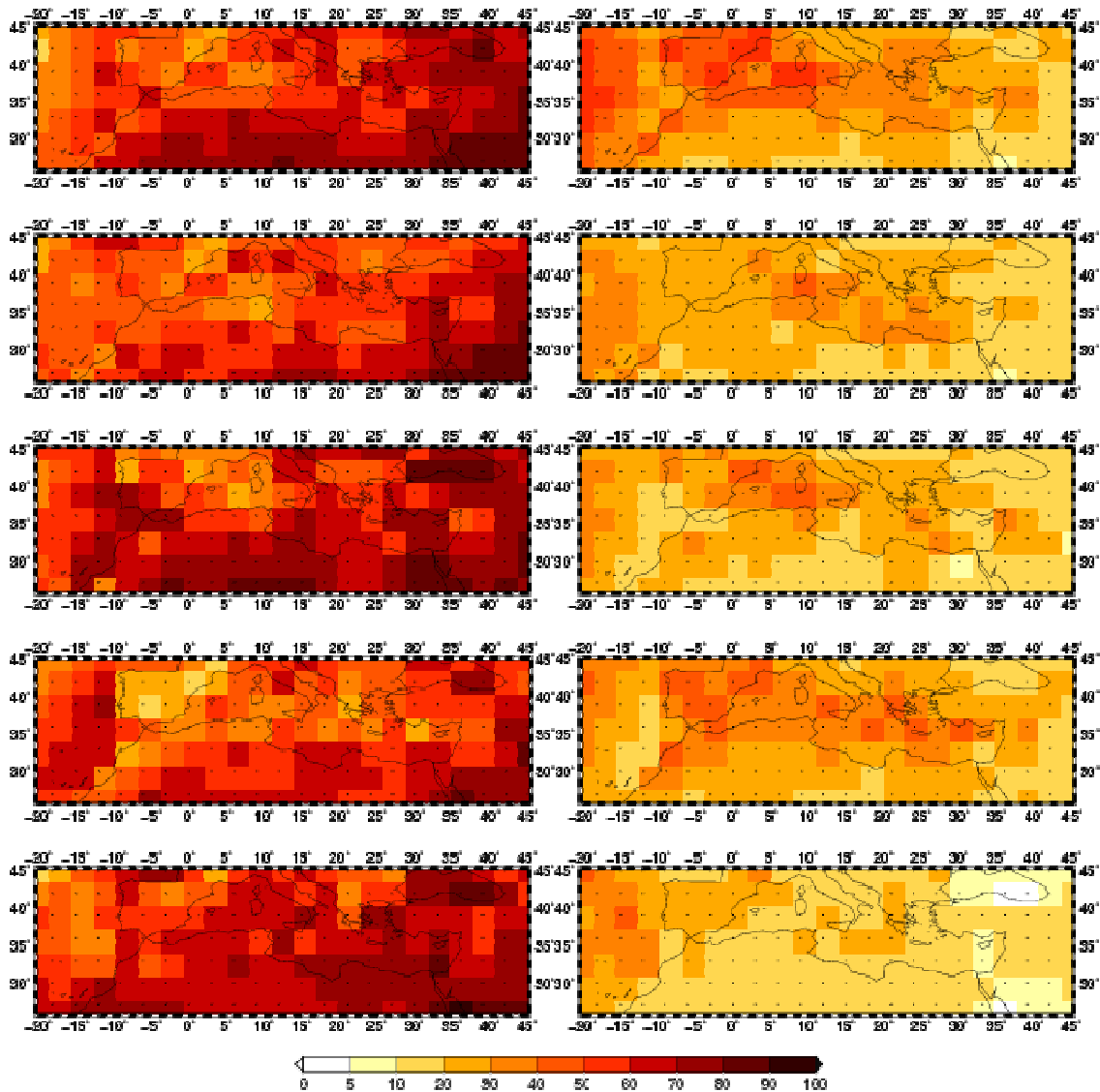
Figure 5.13: 2-way ANOVA partitions of model discrepancies α (left column) and the treatment amount β (right column) in the A1B scenario for temperature for the time period 2001-2098. Rows indicate the season from top to bottom year, spring, summer, autumn and winter. Black dots describe significance for the specific grid-cell on a level of α=5%.

In figure 5.14 one realizes a low impact of the interaction coefficient. This is due to the fact, that the scenario stays the same for all models over each step of the analysis. The interaction coefficient informs about difference in the time of reaction on the scenario by different GCMs. Thus, differences in general climate sensitivity and thus the difference of the sensitivity on the forcing are low over the models. Particularly over the northern part in the area of investigation the contribution of ε becomes more influential. Its increase, principally in colder

seasons, is possibly an impact evoked by the NAO and the impinging western winds. In summer, the temperature in the south is very stable over all realizations. Overall, for spring, summer and autumn low contributions of ε are accompanied with stronger trends in figure 4.20, again referring to the interplay of trends and internal variability. Generally, the regions of cyclogenesis are subordinated to a high amount of internal variability, which is here e.g. the lee of the Atlas ridge (see 1.2.2). Again, this region is furthermore one with the lowest trend of warming, as depicted in the multi-model trend of figure 4.20.
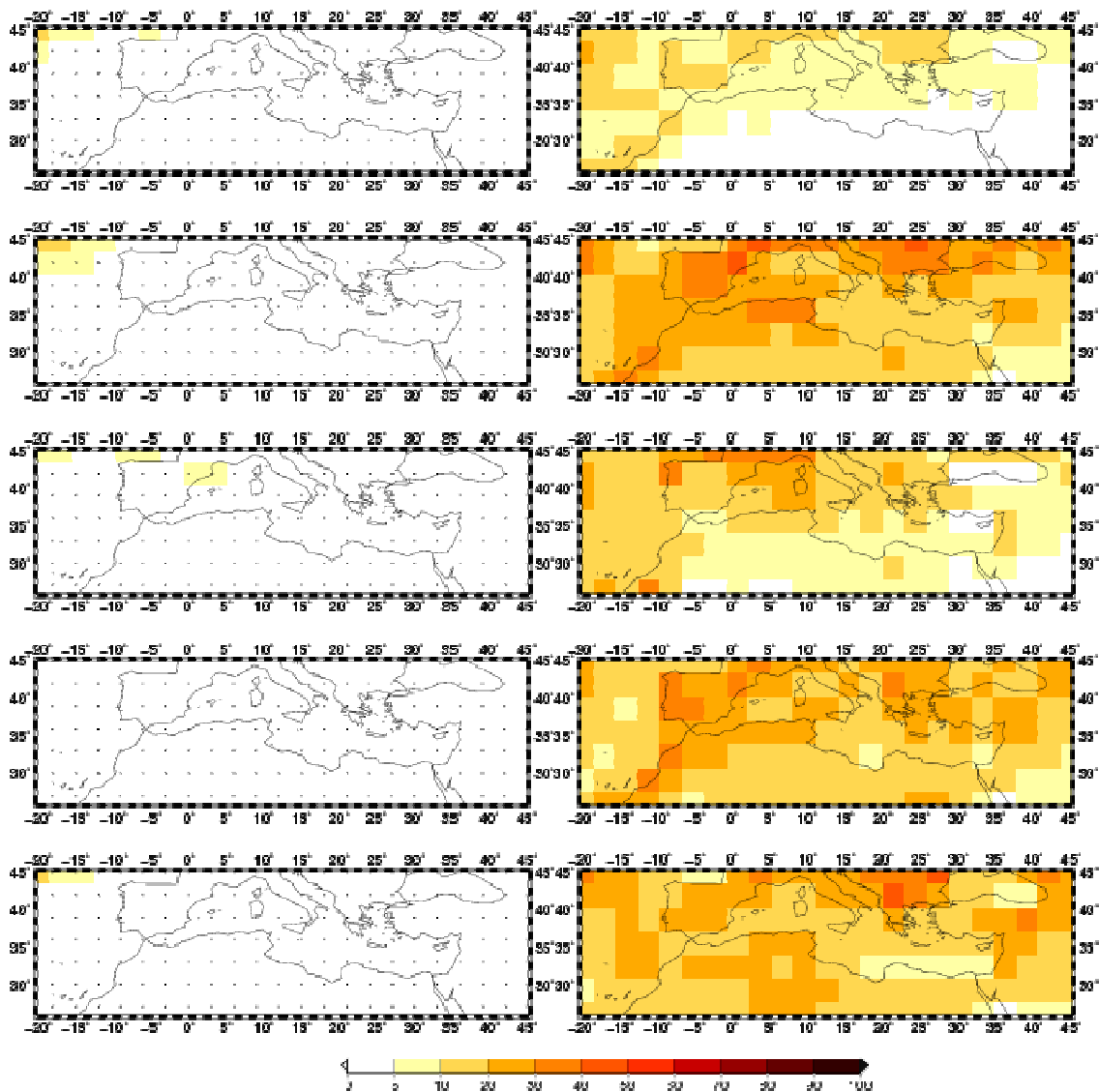
Figure 5.14: 2-way ANOVA partitions of interaction coefficient γ (left column) and the unknown amount ε (right column) in the A1B scenario for temperature for the time period 2001-2098. Rows indicate the season from top to bottom year, spring, summer, autumn and winter. Black dots describe significance for the specific grid-cell on a level of α=5%.

Analogously this analysis has been conducted for precipitation, which is illustrated in figures 5.15 and 5.16. The agreement in a common trend (β) is beneath 5% in relation to the total amount of variability. Concerning individual seasons, highest values are reached in summer (only visible northwest of the Iberian Peninsula). The low amount of β is furthermore affected by a relatively

high impact of the initial conditions and thus the internal variability, i.e. the ε-term. Particularly in winter the residual becomes predominant, when the precipitation regime is closely related to the winter storms, being mainly evoked by the interplay of the Icelandic low and the Azores high among others. The projection of these storms by the models is rather difficult and strongly dependent on the individual simulation. Consecutively, the initial conditions and thus the different realizations account for the main part of variability in winter and to a minor, but in most cases still dominant part in the transitional seasons. In summer the overall amount of precipitation is low, leading to relative high amounts of variability by the α-partition, where weak differences between the models have relative high impact. In contrast to the colder seasons the impact of teleconnections is rather low (see 1.2.2). The geographical pattern is very heterogeneous. For the total year, analogously to temperature, the α-term rises over sparsely observed regions where climatologic expertise is relative low, which might also apply for the Alps and their lee-sided regions. An interesting fact is the east-west distribution of partitions for α and ε, where in the colder seasons the α-term is repressed in the west, where storms from the Atlantic have stronger impact, than in the east. Towards the colder seasons one might depict a shift of low ε -values to the south, when the predominant storm tracks are also latitudinally altered.
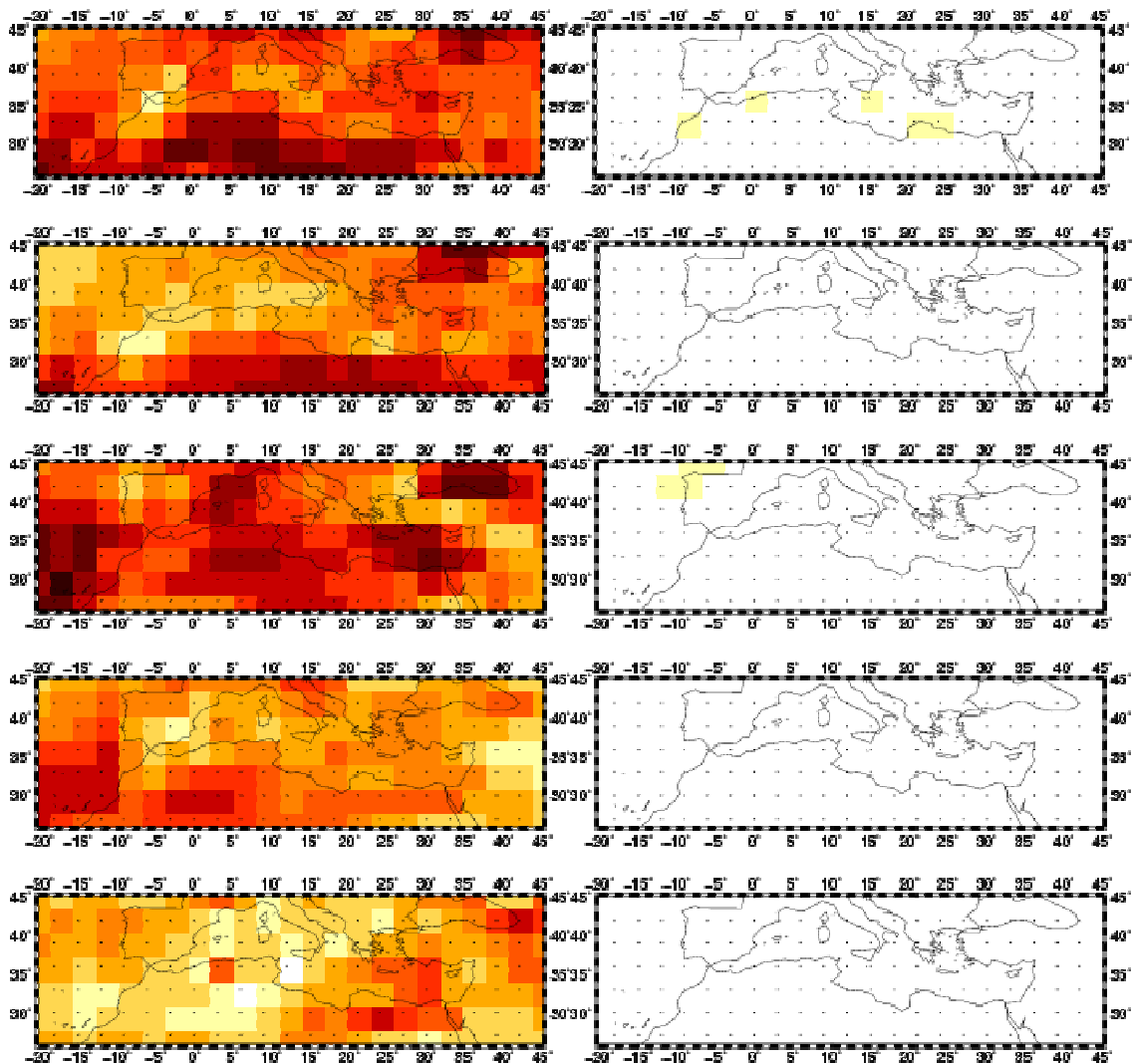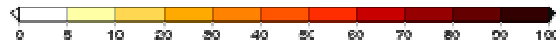
Figure 5.15: As figure 5.13 but for precipitation
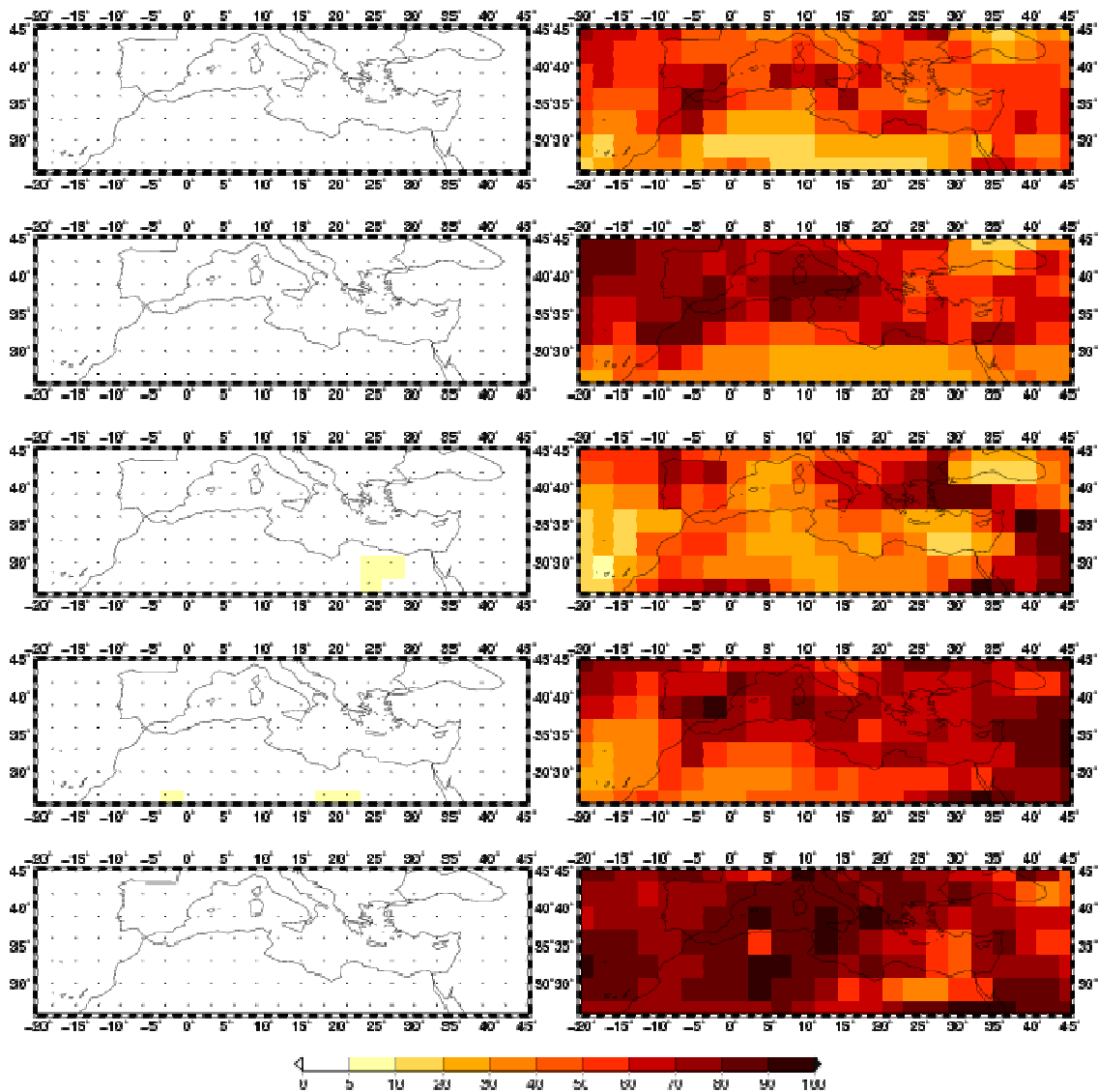
Figure 5.16: As figure 5.14 but for precipitation.

For sea-level pressure, illustrated in figure 5.17, higher values of the treatment partition β are depicted, which becomes visible in summer, concerning the decrease of hPa mentioned in chapter 4.2.3. Nevertheless, the overall increasing trend is not depicted by the β-term. Apart from the detailed regional distribution in the A1B scenario the trend of the multi-model mean in summer is more pronounced than the one in winter. Furthermore, in the southwestern corner of the area of investigation, also some slight partitions of a common course of the models are evident. Considering the α and ε terms, one must note, that these yellow shaded areas in the β-column are rather due to a minor disagreement of the models, with respect to the other regions, than it is evoked by substandard variability between the realizations. This highlights the agreement over the models, concerning this region and the season, while still the treatment partitions (β) are not that high. The spatial patterns are not as

137

heterogeneous as for precipitation, as sea-level pressure has not got comparable high spatial variability. Furthermore, a more distinct pattern is detectable describing a meridional gradient of percentages with rising/decreasing α-/ε-terms from north to the south (figure 5.17 and 5.18). This pattern is dependant on the season, where (similar to precipitation) the NAO may account for this phenomenon, with its rising impact during the colder part of the year, when its impact is progressively shifted to the south and to the east with the resultant values of α- and ε-terms. Overall the discrepancies between the models, shown in the α-term, are still highest related to the overall variance. Again the γ-term is low and close to 0%, indicating the low lag in the reaction time within the different models on one chosen scenario of sea-level pressure. The study by HODSON & SUTTON in 2008 also applies 4 models for the application of a 2-way ANOVA for sea-level pressure. Though their results are limited to the control period in general their results can be confirmed, as also α and ε are the main contributors. The reader is kindly advised that HODSON & SUTTON (2008) used α to describe the treatment partition in their study, while in the study at hand, it will be continued to use β for this partition and α for the block contribution. Consecutively, the appellation of HODSON & SUTTON (2008) is transferred into the denomination of the study at hand. Though, only winter is illustrated in their study, in this season roughly a similar pattern can be depicted. Finally, it is evident that these results are hard to compare, as their analyses are configured of a different model ensemble in 1951-1994. A closer comparison is furthermore not meaningful, as the legend of their former study is not approximately as detailed as the underlying ones, prohibiting a more distinct determination of values. Nevertheless, as their study considers global characteristics, focus is given to most influential features. Here it is confirmed that the residual term is predominant in regions with strong baroclinic instability and regions favoured by cyclogenesis and crossed by stormtracks, and thus in particular in the extratropics. Generally, for sea-level pressure a high percentage of α and thus variability can be found over the oceans in lower latitudes, which is associated with the mismatch of the models. This also is depicted for Antarctica, which represents the strong uncertainty considering sea-ice coverage and the future development of Antarctic conditions (PAETH & HENSE 2002), and over areas with strong orography like the Andes or the Himalaya, indicating uncertainty because of the excelling spatial heterogeneity. While the treatment shows highest percentage over southeastern Asia, the Indian Ocean and the Pacific, the interaction coefficient γ shows lowest values, though in the mentioned study, the GCMs have been forced by scenarios, which represent slightly diverse observed emissions (HODSON & SUTTON 2008).
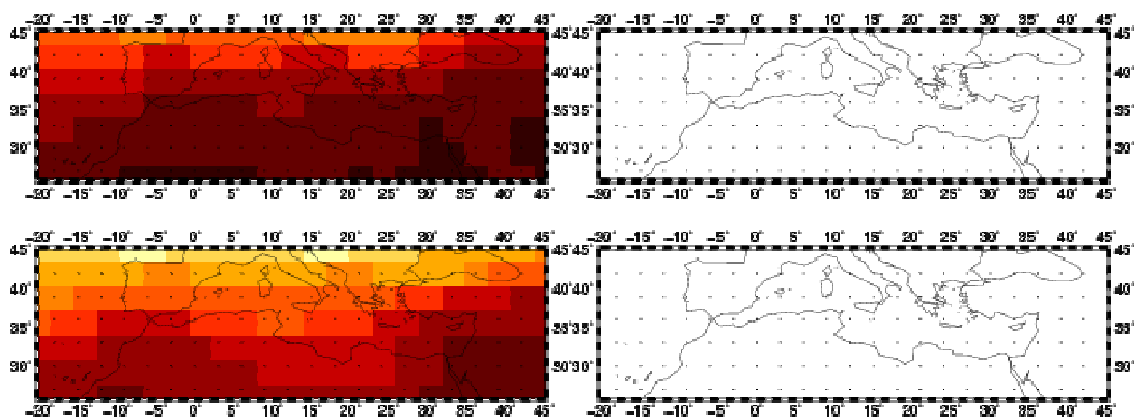
Figure 5.17: As figure 5.13 but for sea-level pressure.
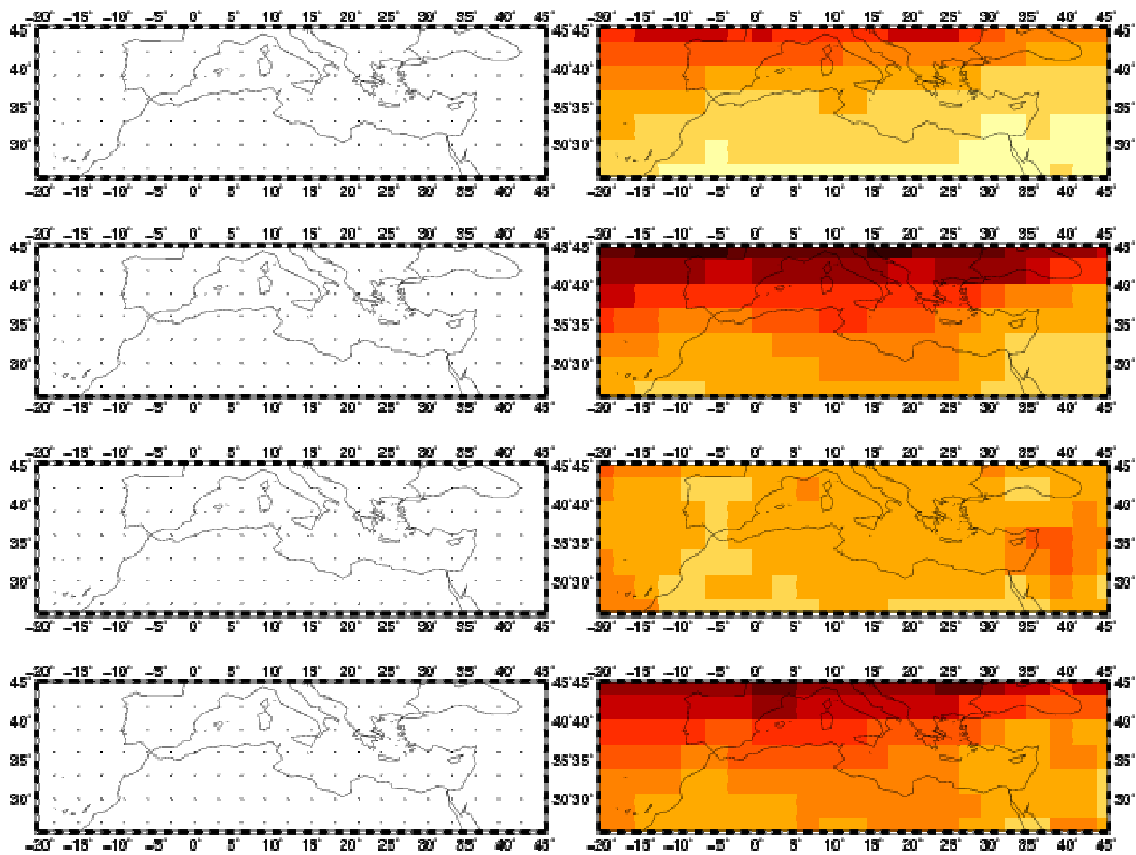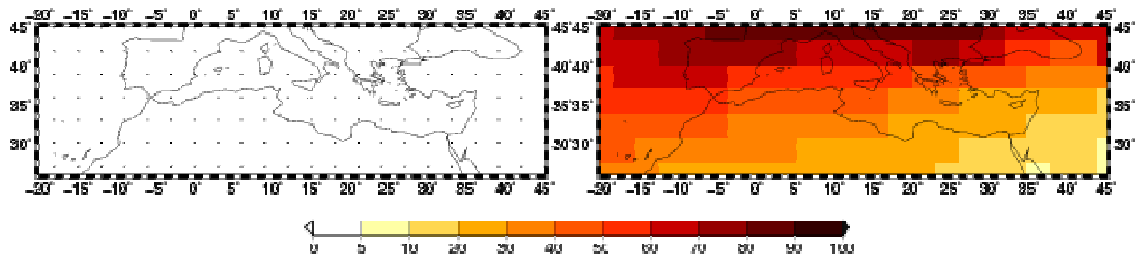
Figure 5.18: As figure 5.14 but for sea-level pressure.

Again it is investigated, how the usage of different scenarios alters the results, which is shown for temperature in figure 5.19. It shows the four partitions from top to bottom for the block partition, the treatment partition, the interaction partition and in the last row the residuals. The left column depicts the B1 scenario, while the right column shows the A2 scenario in contrast. All maps are based on yearly averages. The insight of the strengthening of the β contribution by an enforcement of the emissions gained by the 1-way ANOVA with ECHAM5 can also be confirmed for the 2-way ANOVA. All scenarios detect the Iberian Peninsula and the Eastern Atlantic Ocean as a hot spot of anthropogenic warming (figure 4.22). With the intensification of the emissions, the anthropogenic impact rises and the treatment pattern expands from the Iberian Peninsula to the whole western MA and finally into the Eastern basin. Vice versa the block partition and the contribution of the residuals are declining. For the A2 scenario the treatment contribution reaches its maximum with 66.1% in some regions, where the western parts of the MA in particular offer a high reliability over the models. Apart from the magnitudes, the differences between the spatial patterns over all the scenarios are low. For the interpretation of the patterns within one scenario the reader is kindly referred to the discussion of figures 5.13 and 5.14. Also the other scenarios do not depict any evident matching to the multi-model trends represented in figure 4.22.
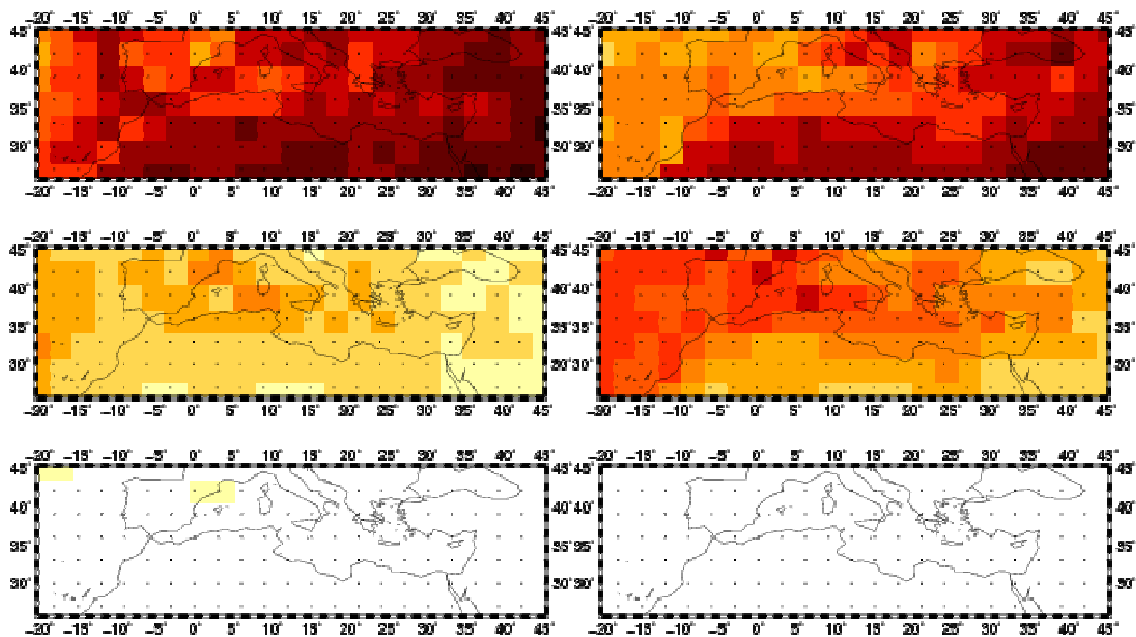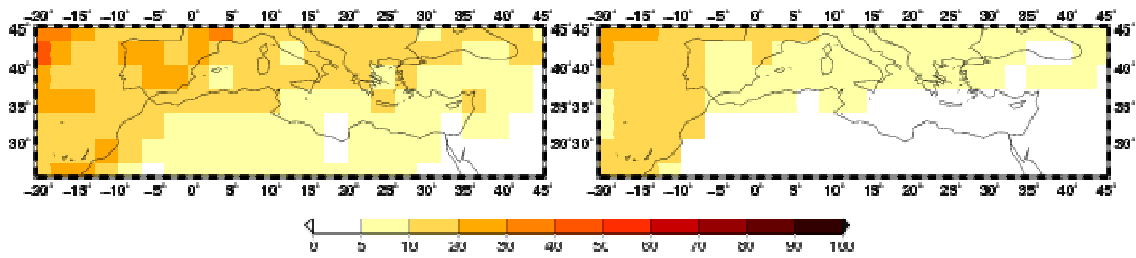
Figure 5.19: Yearly 2-way ANOVA partitions of B1 (left column) and A2 (right column) of temperature for the time period 2001-2098. Rows indicate the partitions from top to bottom α, β, γ and ε. Black dots describe significance for the specific grid-cell on a level of α=5%.

Analogously, in figure 5.20, the two further scenarios are displayed for precipitation. Again, one detects a higher contribution of β by an enforcement of the scenario, located at least between nearly 0 and 12%. At few locations there is some temporal delay in the reaction on the A2 scenario within the different models, which is reflected in the γ coefficient, while in the other scenarios its contribution does not reach the 5% threshold. Consecutively, the block partition is lowest in the A2 scenario. In the B1 scenario it reaches its maxima accompanied by A1B. This implies that the disagreement of the models is highest within the A1B and the B1 scenario, where the first one is prevalently utilized frequently for scientific assessments, as it is supposed to be in the middle range of projected emission scenarios (see 2.4). A phenomenon already encountered by the 1-way ANOVA for ECHAM5, concerning the magnitude of the residual contribution over the scenarios (see above), is experienced here again, when in the A2 scenario the partitions of the residuals are highest, implying an enhanced natural variability by the enforcement of the scenarios.
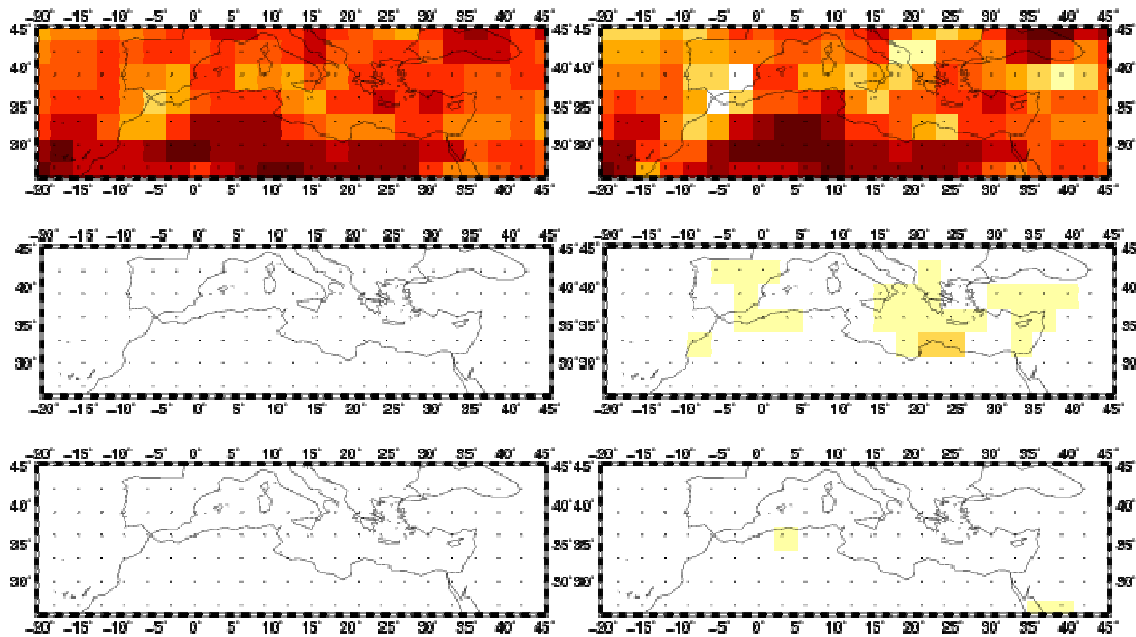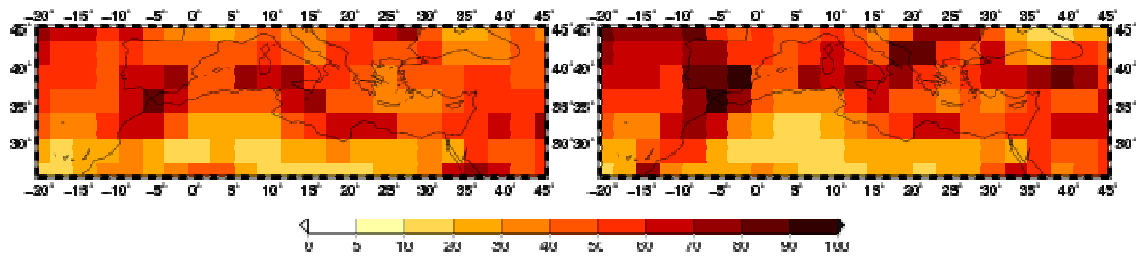
Figure 5.20: As figure 5.19 but for precipitation.

Still to come is the comparison of the different scenarios and their affection of sea-level pressure (figure 5.21). Here, the latter phenomenon described for precipitation becomes more evident, where the residuals become the highest contributor in the A2 scenario. Unfortunately it must be admitted, that only 3 models (see above and table 3.2) contribute to this analysis for A2, while in A1B and B1 6 models have been utilized. This may have a serious impact on the distribution of the individual magnitudes of the different contributors. Though, the problems evoked by providing a comprehensive analysis, the results are shown nevertheless. At least an above board comparison can be drawn by A1B and B1, where a higher block contribution (α) is attributed to A1B than to B1. As no great amounts of other contributors, like β or γ, are detectable, the difference of the α-contributor can inversely be explained by a change of the ε-term. Still the differences between the scenarios are extremely low. Considering the A2 scenario it should be emphasized that particularly the neglected NCAR models show highest deviance to the other models, which indirectly may be a hint accounting for the extreme low/high α-contributor/ε-contributor. It is furthermore pointed out, that the number of samples obviously enhances the residual fraction, when one reminds of the different numbers of the individual realizations (see above). At least the β-term reaches some values of nearly 20% in the south of the area of investigation, describing the negative trend of figure 4.38.
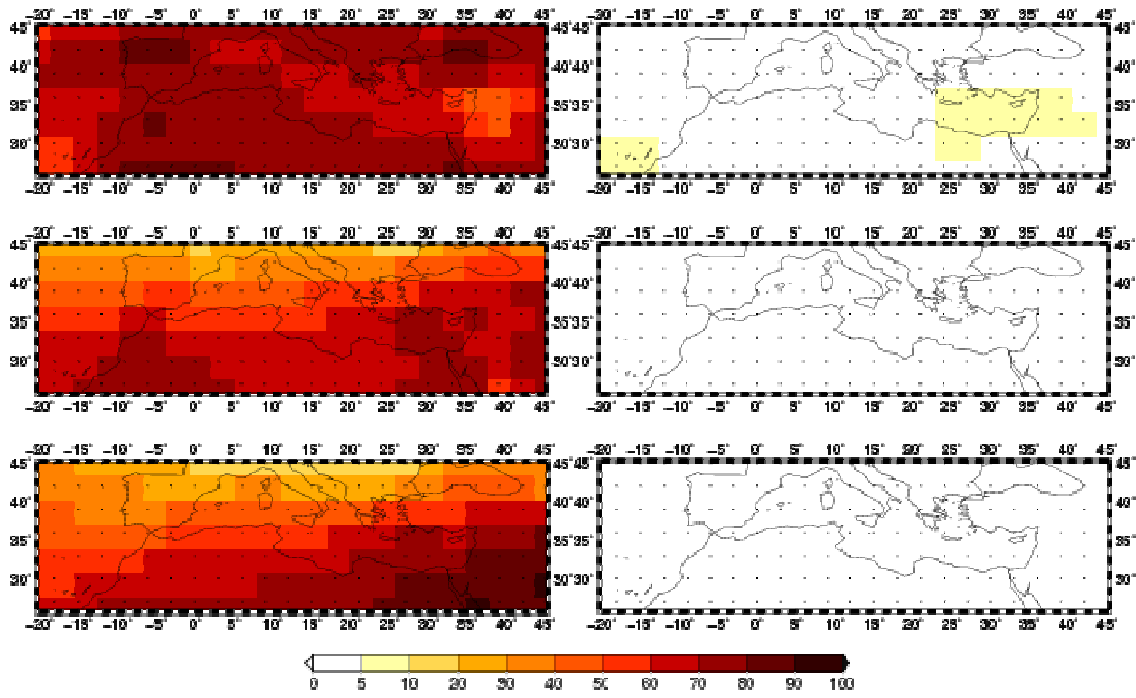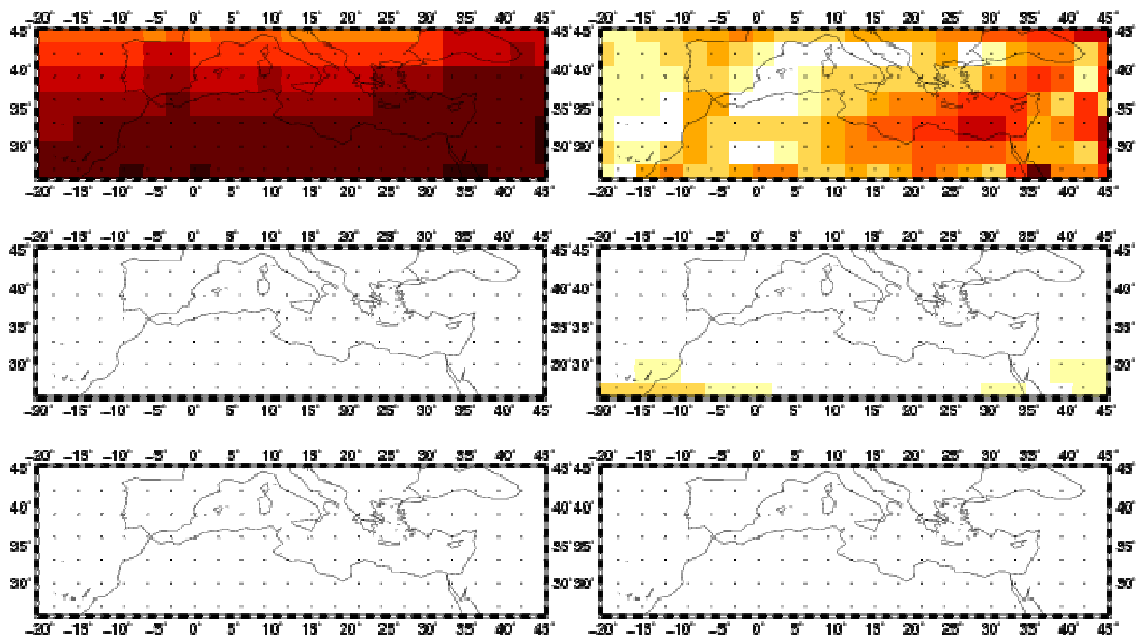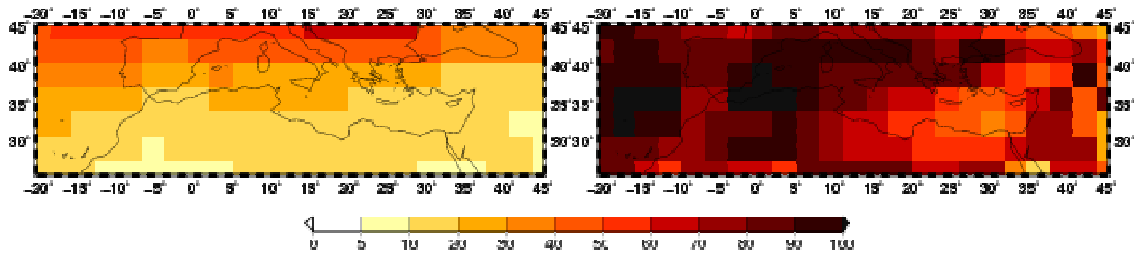
Figure 5.21: As figure 5.19 but for sea-level pressure.

The results of figures 5.13 -5.21 confirm generally the findings of GIORGI & FRANCISCO (2000a) quantitatively, who conducted a qualitative comparison of mean values of different GCMs and their specific realizations for equal variables. So, they conclude that the uncertainty due to the internal variability by several realizations of one model is relatively low for all scenarios in relation to the variability by means of different climate models concerning temperature and sea-level pressure. The results of this study deviate only in the A2 scenario, when for sea-level pressure (and precipitation) the ε-contributor becomes at least equally influential like the discrepancy of the different models. Also, GIORGI & FRANCISCO (2000a/b) find that for precipitation the internal variability is more pronounced, which also is evident in figure 5.16 and 5.20 in some seasons, although the discrepancy between the individual realizations of one specific model is still beneath the spread over the models over the total year, which holds particularly for temperature and sea-level pressure.

Following the procedure of the 1-way ANOVA, dependant on the A1B scenario, the specific time-slices with their characteristic impact of their contributors are investigated in the following, whereupon figure 5.22 highlights the results for temperature averaged for the whole MA. For at least temperature, it is distinct, that a prolonged time period enhances the contribution of the treatment effect. Furthermore, in the future period from 2001-2098 the β-contribution is developed higher, compared to the period of 1961-2050. This is reasonable, as the firstly mentioned slice comprises a period, where GHG forcing becomes effective. For this periods, this phenomenon is accompanied by a shrinking block effect. The same holds for the fraction of the residuals, while it might still be repressed by an enforced model diversity, i.e. the α-contribution in the future period. Anyway for precipitation and sea-level pressure (not shown) no explicit shifting of the contributions is evident over various time periods (though analogously to temperature the β-partition is enhanced by a prolonged time period), where the α-contribution earns the major partition with about up to 55% for precipitation and 78% for sea-level pressure. The treatment contributions account roughly 4% for precipitation and analogously to figure 5.17, less for sea-level pressure. As the interaction coefficient is close to zero, the rest can be attributed to the ε-contribution, which is about 42% for precipitation and around 20% for sea-level pressure.

T2m A1B
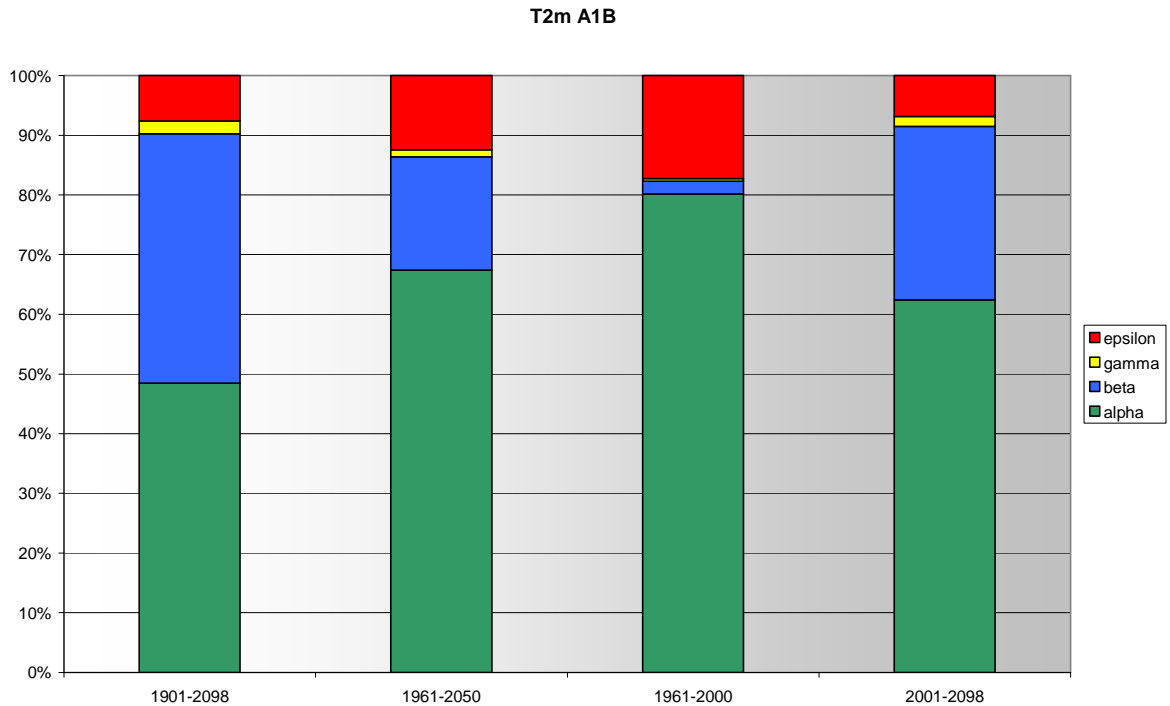
Figure 5.22: Partitions of the contributors dependant on the time in the A1B scenario for temperature for the overall year approach in the Mediterranean average.

5.3.2.2 Temporal approach

The temporal approach of the 2-way ANOVA works analogously to the one for the 1-way ANOVA, but with the specific calculations of chapter 5.3.2.1. Consecutively, again the spatial means for yearly steps have been computed for all the input data on the base of seasons or years. Afterwards, 30year and 60year periods have been shifted by yearly steps throughout the period, while for every yearly step the 2-way ANOVA is calculated on the averages of this period and later projected and illustrated on the median year of this specific period. Figure 5.23 depicts the temporal approach of the 2-way ANOVA for temperature in the A1B scenario. The colours of the different contributors, which accumulate to 100%, are analogously chosen to the former figures, where green refers to the block partition, blue to the treatment effect, yellow to the interaction coefficient and red to the residual partition. The left column represents an integration period of 30 years, where the signal or the treatment contribution is relatively low, as it is repressed by the strong impact by the disagreement of the models. The common treatment effect is highest in the warmest seasons, i.e. summer and autumn, following the strongest warming with a maximum at about 2050. The residuals are lowest over the whole year while they decease with ongoing temporal course. Again a prolongation of the period of acquisition strengthens the impact of the forcing and thus the trend, which evokes nearly 30% of the β partition in summer and even more in autumn. The exceeding of summer by autumn is considered as being accidentally. With further extension, the α-coefficient loses percentages to the

144

common treatment, until it rises again towards the end of the temporal course. The contribution of the residuals again decreases apart from winter. The interaction is close to zero, as it is supposed to be. Again, one recognizes a stronger smoothing by the 60year period of acquisition.
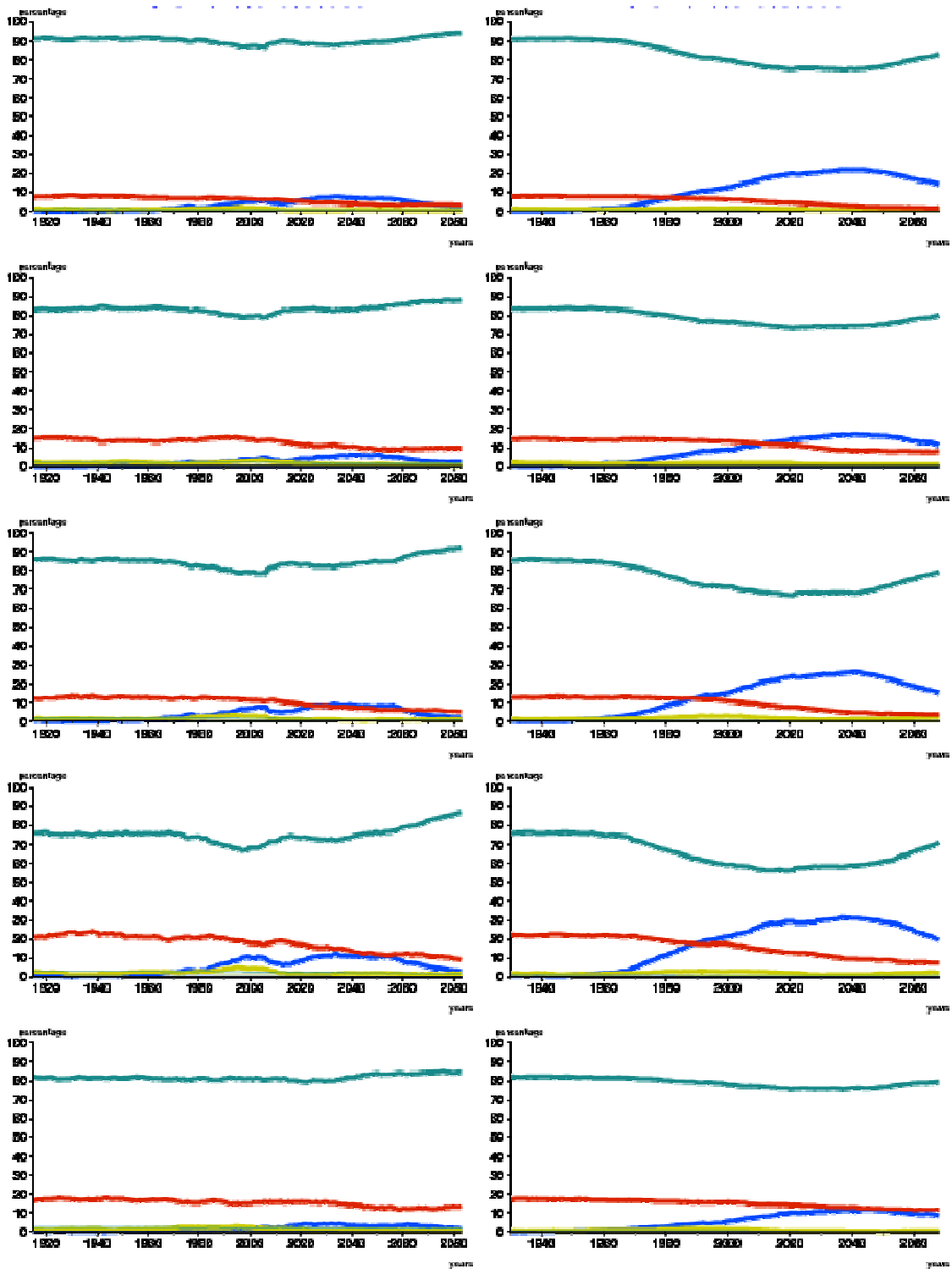
Figure 5.23: Temporal approach of the 2-way ANOVA (left 30y/right 60y) for temperature in the A1B scenario. α=green, β=blue, γ=yellow and ε=red. From top to bottom: year, spring, summer, autumn and winter. 5% levels of significance are indicated in the specific colour for each partition in thin lines.

145

Such clear signals cannot be reproduced for precipitation or sea-level pressure in figure 5.24. Here, the partitions of ε and α dominate the appearance. When one has a closer view on the reciprocal behaviour of the two fractions one at first realizes a minor difference for precipitation than for sea-level pressure. Though, the overall year cannot be considered as the average of all the seasons (see 3.1.2), this smaller difference is due to seasons like spring and winter, where for precipitation the contribution of the residuals on the total variability becomes even higher than the contribution of the block partition. Meanwhile, the phenomenon of a stronger variability for the individual realizations for precipitation is well known in winter. For this interesting behaviour a seasonal cycle can be derived, indirectly inducing that in the colder seasons the uncertainty, which is inherent to the individual realizations, is higher than the disagreement between the models, while in the warmer seasons the disagreement between the models dominates. Related to the sources of uncertainty defined in chapter 2.3, the differences of parametrizations and discretizations become more demanding in summer, while the initial conditions require more attention in winter bearing in mind the necessity of reduction of uncertainties. This seasonal cycle is repeated with minor extreme outcomes for sea-level pressure. Here, in every season the disagreement contribution α between the models, is the highest partition in the total amount of variability, which leads to the stronger impact of the different modelling approaches, GCMs are constructed with, on the total uncertainty. The deterministic chaos evoked by different initial conditions (chapter 2.3.2.1) again becomes relatively more essential in the colder seasons. All these findings confirm the increasing impact of natural climate variability during winter as it is illuminated in chapter 1.2.2. Though this finding, the impact of an agreeing course of the models is rather small and the small treatment somehow disappointing, apart from the fact that a more pronounced trend would lead to a stronger signal in the β-partition. Though, no one can be interested in enforced trends of climate variables, the A2 and the B1 scenarios offer this situation of modulating trends, becoming at least evident for precipitation regarding the regional multi-model trends (see 4.2.2).
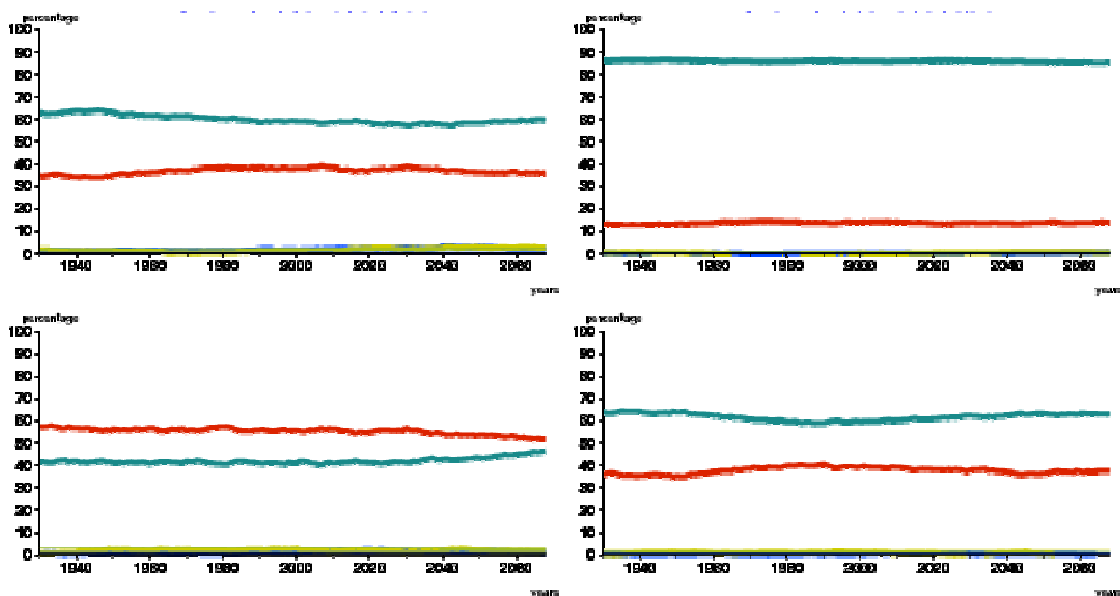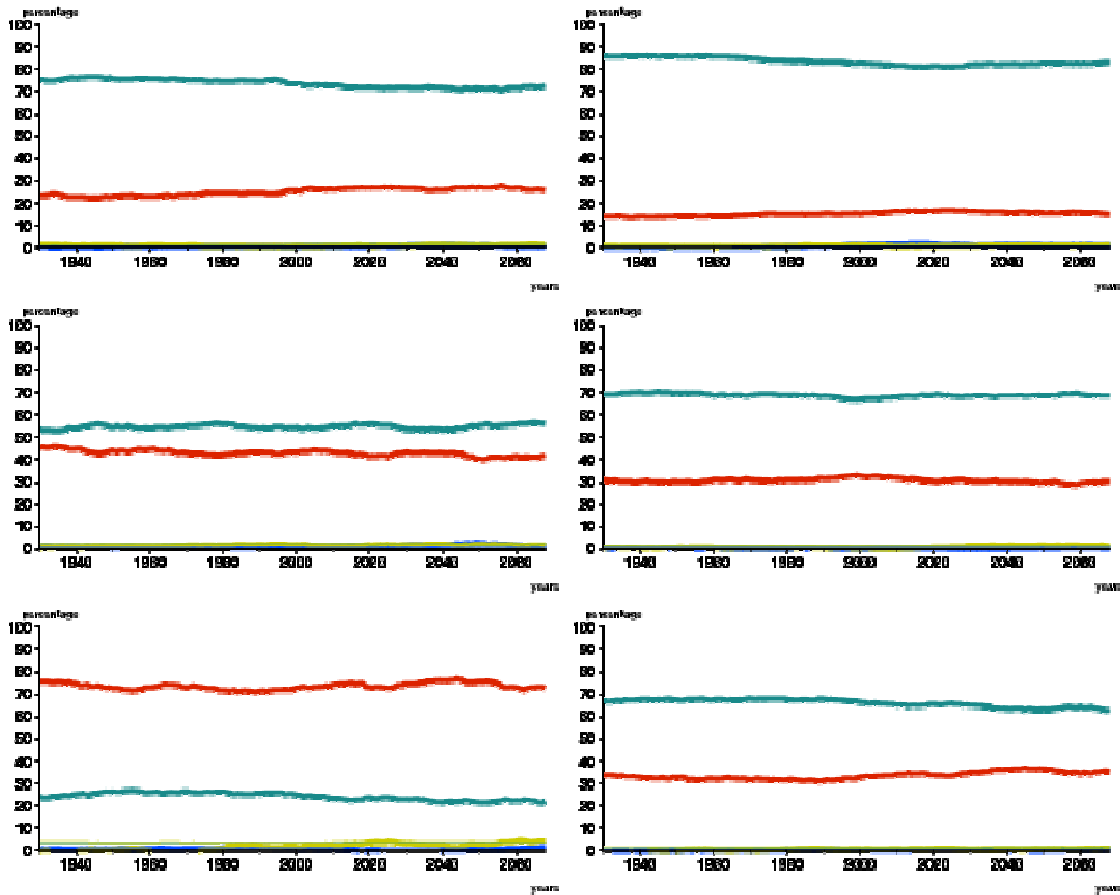
Figure 5.24: Temporal approach of the 2-way ANOVA (left precipitation/right sea-level pressure) in the A1B scenario for a 60-year acquisition period. α=green, β=blue, γ=yellow and ε=red. From top to bottom: year, spring, summer, autumn and winter. 5% levels of significance are indicated in the specific colour for each partition in thin lines.

Former contemplations of an increase of the signal by the treatment, associated with a more pronounced forcing, are attested by figure 5.25 for at least temperature. In the B1 scenario the warming impact of the GHG emissions declines with the further temporal progress in the 21st century. The impact of the initial conditions declines as well, which consecutively leads to an increase of the inter-model variability. This diminution of the treatment effect is not evident for the A2 scenario, as it reaches its maximum with 23.1% (with the maximum of 21.9% in the A1B scenario) not before the end of the period of investigation. The A1B scenario, where the trend and thus the effect of the GHG are temporally confined (in figure 5.23), can be classified as being somewhere between the B1 and the A2 scenario. For precipitation, the impact of the scenarios is smaller, particularly when comparing the A1B and the B1 scenario. In the A2 scenario the residuals become more influential, nearly reaching the amount of the α-contributor in 2007, when the α-contribution/ε-contribution reaches 50.2%/48.0%, as the interaction coefficient stays close to zero as usual and still a common treatment becomes not identifiable. However, the increase of the contribution by the residuals by an enforced scenario indicates an accompanied fortification of natural variability, being reflected in a higher amount of variance dedicated to the specific realizations of one GCM (see 5.2.2.1) (GIORGI & LIONELLO 2008). This is finally not evident in the A2 scenario for sea-level pressure, as the block partition outperforms over all the other models in the B1 scenario. For the A2 scenario for sea-level pressure only

three models have been consulted, which may evoke this superimposing impact of the ε-residuals, while in the B1 scenario the adulterating NCAR models concerning the overall behaviour of the remaining models still have been considered. This issue encourages to conduct a "bootstrapping" approach with a concerted discard of one model per analysis.
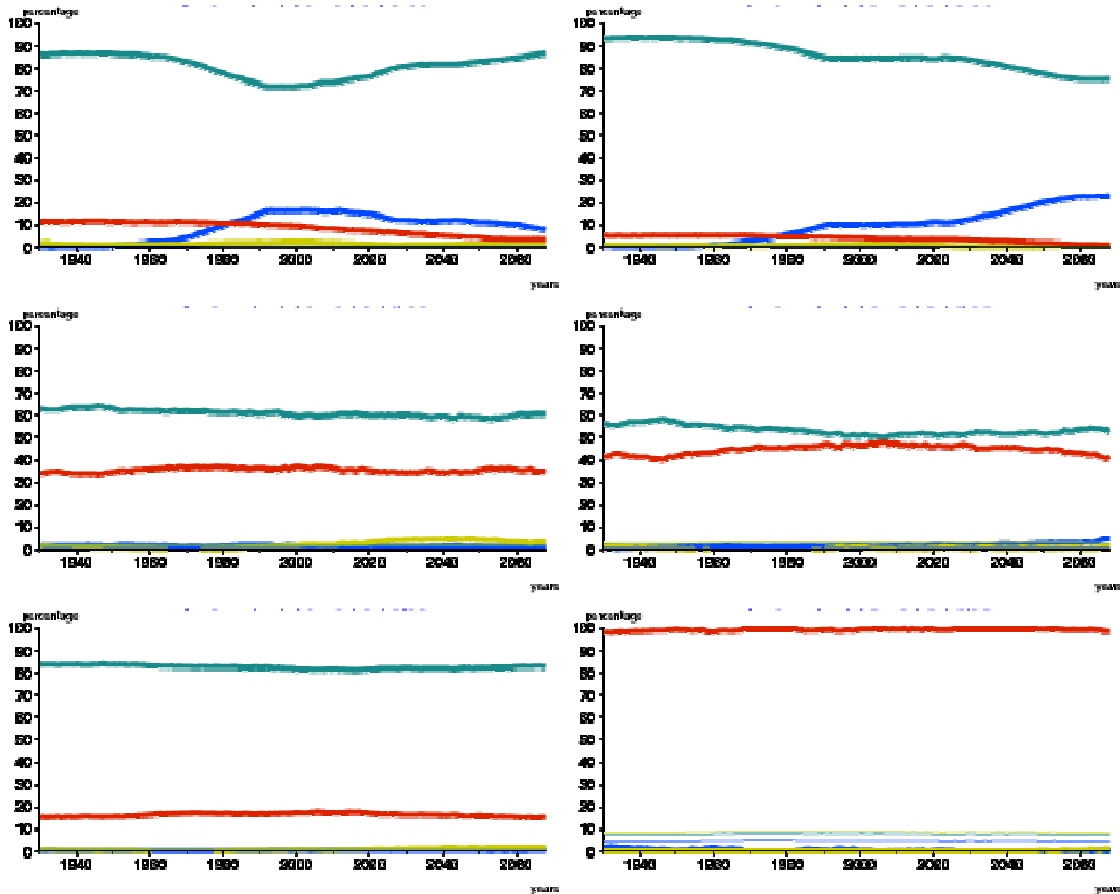
Figure 5.25: Yearly temporal approach of the 2-way ANOVA (left B1/right A2) for a 60year acquisition period. α=green, β=blue, γ=yellow and ε=red. From top to bottom: temperature, precipitation and sea-level pressure. 5% levels of significance are indicated in the specific colour for each partition in thin lines.

5.4 Bootstrapping

As it has already been done, by disregarding the NCAR models, the result of the 2-way ANOVA changes by an alteration of the participating models. Furthermore, it becomes evident in chapter 4.1, that there may be a remarkable discrepancy between some models and observations. However, within this approach, there is no other feasibility to account for the accuracy of models (REIFEN & TUOMI 2009). Still, the 2-way ANOVA accounts for the degree of coinciding variability of the different datasets, i.e. the models and the realizations within the time. As one still would like to receive a maximum contribution by the β-coefficients, at least to underline the veritableness of climate change, being projected in high agreement among the models, the

question arises, whether to neglect one model with the intention to achieve even higher treatment effects. The most desirable case would be a shift to a higher β-contribution by the disregard of the model fitting worst with the reanalysis data. On the other hand, this procedure diminishes the sample sizes and consecutively the range of certainty is decreased. Following the principle "the more the merrier", the more models one uses, the higher is the probability to match with the future climate adequately and the higher is the expressiveness concerning a common trend. Thus, also REIFEN & TUOMI (2009) recommend a maximum amount of models. Again, the analyses are accomplished in figure 5.26-5.28 for all variables in the A1B scenario over the whole period of investigation in order to give some idea of the change of the different contributions by an alteration of the model set up. For each column in the following diagrams one model is left aside, which name is denoted at the abscissa. For interpretation, this means, that the stronger the treatment coefficient becomes, the stronger is the discrepancy of the neglected model to the remaining models. Consecutively, for temperature and sea-level pressure it becomes evident, that NCAR-PCM strongly deviates from the others, while at least for temperature, the opposite holds for NCAR-CCSM3. For ECHAM5 changes seem to be minor, confirming that ECHAM5 is one model being close to the mean of the other models. However, with disregarding NCAR PCM apart from temperature, the contribution of the treatment is not strengthened, as contrary to the decrease of the block partition the residuals gain impact on the total variability. This also holds for MIROC 3.2 medres, but for a lower portion. It indicates that, apart of the artificial reduction of the α-partition for precipitation and sea-level pressure, the major part of variability still derives from different initial conditions and natural climate variability. It is noteworthy, that the disregard of NCAR CCSM3 reduces the partition of the residuals, as many realizations have been applied for this model (see table 3.2).
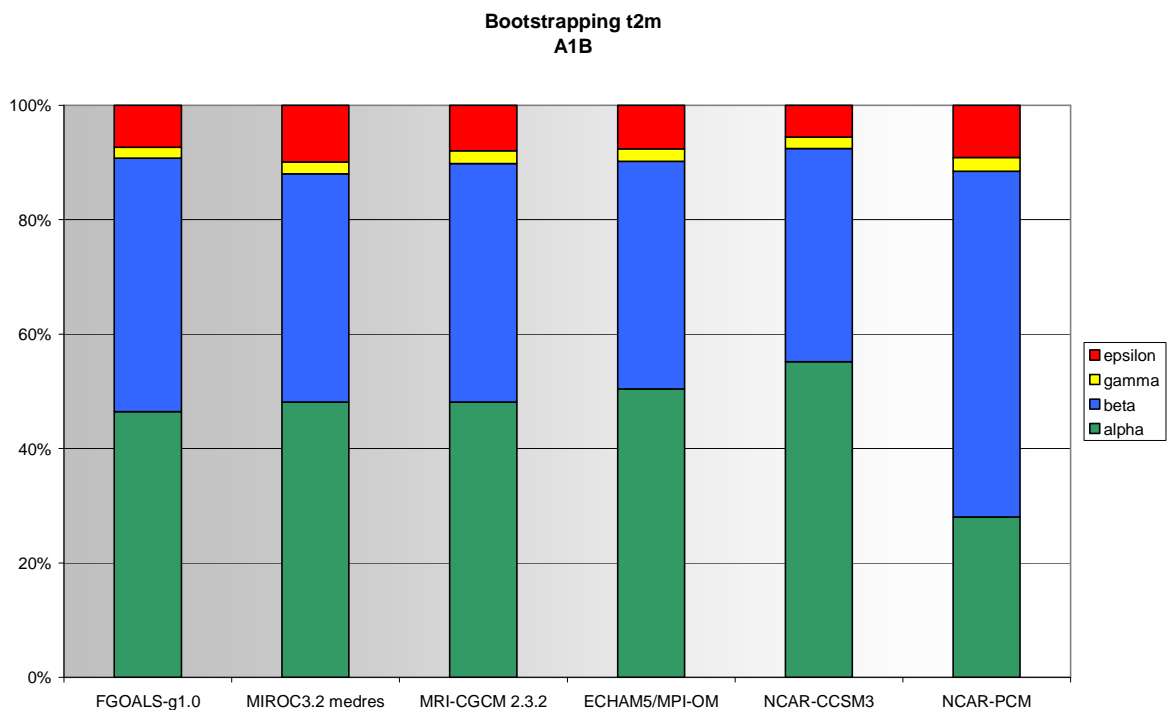
Figure 5.26: Changes of the contributors by neglecting the indicated model in the

analyses of the overall year in the period from 1901-2098 in the A1B scenario for temperature.
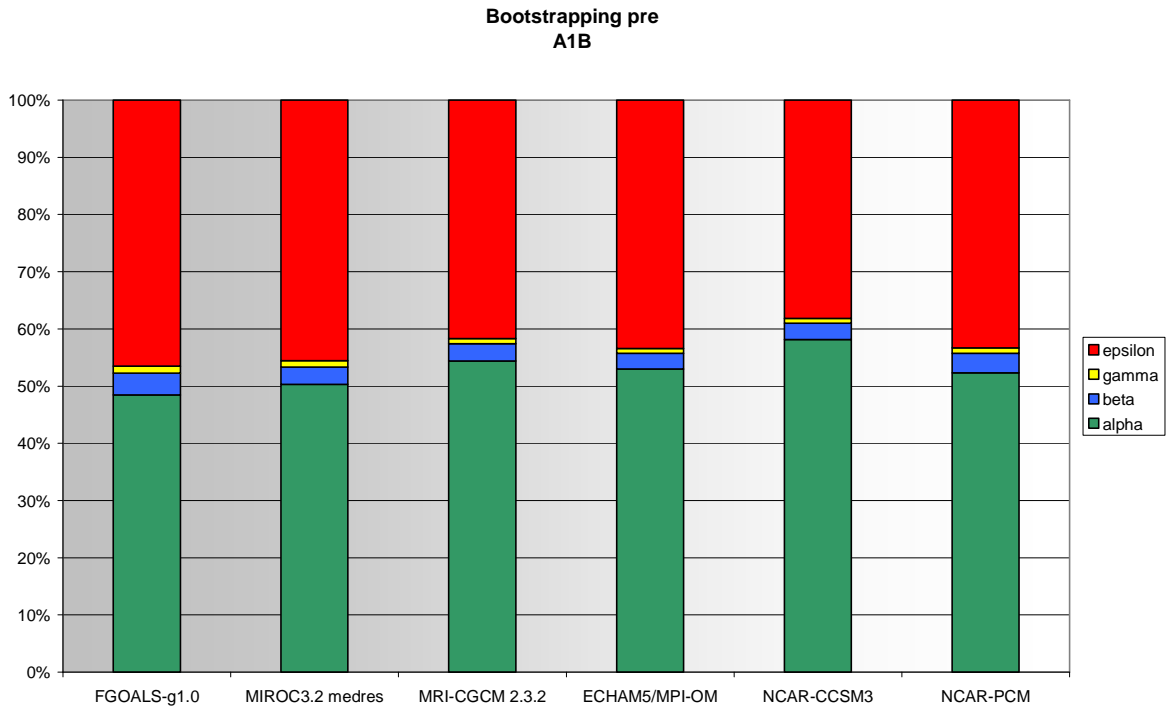
Figure 5.27: As figure 5.26 but for precipitation.
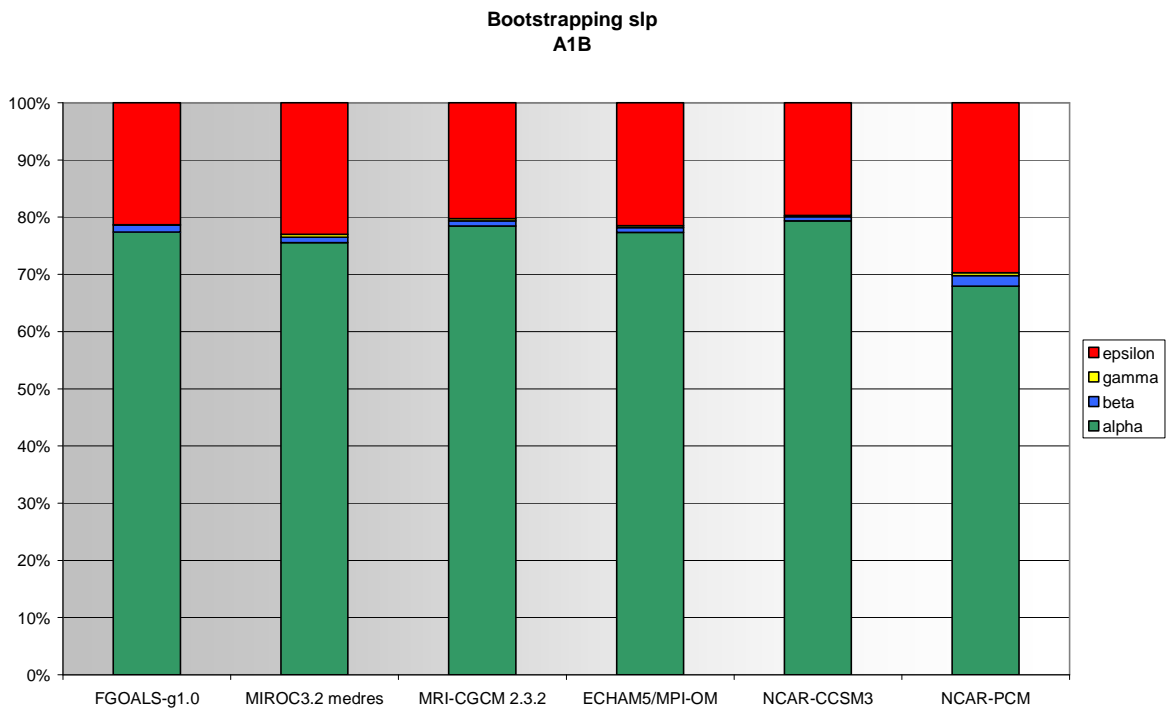
Figure 5.28: As figure 5.26 but for sea-level pressure.

5.5   Normalized temporal approach

As depicted e.g. in figures 5.13, 5.15. or 5.17 and 5.23, 5.24 or 5.25 a high partition of the block effect is evident. This indicates a relatively strong bias between the models (compare figures 4.43 and 4.44).

In chapter 2.3.1, it was outlined that this bias is an indication of independently developed GCMs and therefore a measure of uncertainty. The higher the spread of these realizations is, the higher is the security in the incidence of the projected climate. Nevertheless, it should be the aim to minimize the spread while sustaining the reliability of these projections. This leads to the consideration to normalize the individual GCMs on each other at a certain time (period) to minimize the linear bias between them. It can be done with the help of the reanalysis dataset introduced in chapter 3.3, as it is assumed to reflect climate reality. With this normalization all of the GCMs are assimilated to a specific level. This new initial level is calculated in the control period from 1961-1990. From there onward the simulations of the individual models take their specific normalized course, e.g. each with its characteristic intra-model variability, its characteristic reaction on external forcing, etc… . Anyway, the high bias resulting in a large partition of the α-term in the 2-way ANOVA is eliminated. This holds at least for the normalization period, while afterwards the bias may rise again. As already mentioned, this removal is permitted as only one climate condition has been observed by the reanalysis data. Unfortunately these reanalysis datasets do not inspire much confidence among the comparison to the models and among the relatively huge bias to each other (see figure 4.43). Anyway, this normalization is firstly done to detect a higher signal, i.e. the β-term, with respect to a common level in the control time. That is why it makes no difference, which reanalysis dataset is chosen, which is the ERA40 dataset in this case. Still, the bias term β gives information about the consistency between the different climate models, but gives no estimate about the agreement to observation data.

The normalization procedure has been applied for 30-year and 60-year approaches. Sea-level pressure is neglected here, as agreements of the different models have been poor, whilst models already have been dismissed in the preceding analyses and secondly the predominant term has been the ε-partition, which results from short term variability between the individual realizations (see e.g. figure 5.25). For this normalization, the bias within the common time period, i.e. 1961-1990, is calculated by a simple subtraction of the mean values given by the observation dataset and the simulation j. The observations are denoted in the first bracket and the individual run j given by one specific model k in the second bracket of formula (54):

$$
54) \qquad \Delta_{(X_{kj}-obs)} = \left(\frac{\sum\limits_{p}^{P} A_p}{P} \right) - \left(\frac{\sum\limits_{p}^{P} X_{kjp}}{P} \right),
$$

where A is simply chosen to be the regional mean value of temperature or precipitation of the the ERA40 dataset. The variable p indicates the timestep of the year 1961, while the summation is done until 1990 referring to 30 years by P. The next step is the yearly addition of the bias, which is resulting out of formula (54) to the original values of the simulated data. This is done for the course of precipitation or temperature given by the considered simulation onward from 1961 (formula (55)).

55) $\qquad Xnorm_{kji} = \Delta_{(X_{kj}-obs)} + X_{kji}$.

This procedure is repeated for all seasons and the overall year and again for every run in every model of the chosen models (table 3.2). Afterwards the "cooking recipe", described in chapter 3.1.3, is applied again to compute ensembles and multimodel-means in the sliding time windows of 30 years and 60 years. The 2-way ANOVA is now applied again on these normalized dataset. Nevertheless, one should keep in mind, that there is no possibility to assess future model accuracy with former observations.

Figure 5.29 illustrates the results of the latter application on temperature for a 30-year (left column) and a 60-year (right column) shifted computation window in the A1B scenario. Again, the seasons and the overall year are depicted in the individual rows. In the beginning of each temporal course the α-partition is close to zero, as the models are normalized onto the observations and thus consecutively normalized in a certain amount onto each other. This enhances the contributions of the other coefficients, when even the interaction coefficient becomes identifiable. Also the treatment effect is much higher than it is in the non-normalized applications. Particularly in the 30-year approach the residuals are the main contributor, also promoted by the low block effect and the diminished discrepancies among the models. After this beginning, the block partition is growing again, implying the common deflection of the specific models in the further course. This holds again for the warmer seasons, where the individual realizations are close to each other, which also has become evident for precipitation and sea-level pressure (figure 5.24). Contrary to that finding, the residuals become again predominant in winter, where the natural climate variability and thus the different initial conditions play the main part. This confirms the findings above, though in figure 5.23 the block effect is higher, as the data is not adjusted on a common fix point, i.e. the ERA40 data. Again, the A1B scenario is supposed to have maximum effect on temperature in the middle of the 21st century, when the β-partition reaches highest percentages. With a prolongation of the period, where the 2-way ANOVA is computed in, a well known effect appears (right column of figure 5.29): The contribution of the variability, which is accompanied with a common trend of rising temperature, becomes predominant over all other involvements (reaching about 64.7% in summer in 2041 and above 73.0% over the total year in 2043). An exception is winter, where the residuals are controlling the main part of variability again. It is also noteworthy, that in all seasons, at every time the treatment contribution reaches significance at the 5% level of error. As the integration period of 60years is longer than the period of the normalization, in the right column the block partition lifts evidently from zero already at the beginning. One still has to be aware, that the different contributions are strongly affected by the diminishment of the α-coefficient, prohibiting a pristine comparison to the non-

normalized approaches. The reader is kindly encouraged to compare the results illustrated in figure 5.29 and the two following figures with the figures 4.43 and 4.44, as it will be evident that, as already depicted in the interpretation of figures compiled by the non-normalized 2-way ANOVA, the maximum β-contributions follow the magnitudes of the trends.

Figure 5.29: Normalized temporal approach of the 2-way ANOVA (left 30y/right 60y) for temperature in the A1B scenario. α=green, β=blue, γ=yellow and ε=red. From top to bottom: year, spring, summer, autumn and winter. 5% levels of significance are indicated in the specific colour for each partition in thin lines.

In figure 5.30, again temperature is depicted for the 60year approach for the B1 (left column) and the A2 scenario (right side). Concerning the comparison to figure 5.29, the A2 scenario does not become conspicuous in exhibiting even higher partitions of the treatments, but depicts a later increase of the latter one. Even in winter, the β-contribution becomes predominant in A2. Furthermore, it does not seem likely, that the α-contribution will overcome the treatment effects in further future, as the differences between the models are rather persistent, though a little increase of the discrepancies is evident. Though, they are not at the expense of the β-contribution. For B1, the treatment is lower than the one in the other scenarios and with the exception of the overall year and some sequences in summer and autumn it does not become predominant at all. Furthermore, no clear rising sequences are apparent. Still, it must be noted, that significance is reached in all seasons but winter, where again the residual component is at its maximum.
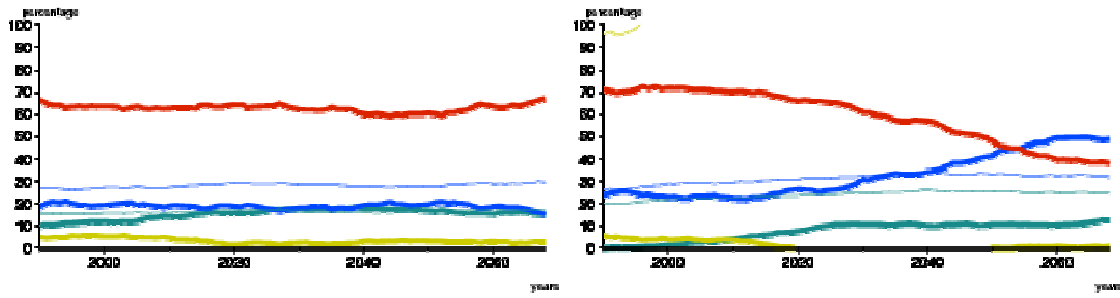
Figure 5.30: Normalized temporal approach of the 2-way ANOVA (left B1/right A2) for a 60y acquisition period for temperature. α=green, β=blue, γ=yellow and ε=red. From top to bottom: year, spring, summer, autumn and winter. 5% levels of significance are indicated in the specific colour for each partition in thin lines.

As already mentioned before, the same analysis concerning the normalization has been conducted for precipitation. The courses of the according partitions for the overall years are figured in 5.31. Though, the normalization causes a decrease of the block partition, a distinct signal of the β-contribution cannot be depicted. This holds for every scenario and is due to the high impact of the discrepancies and the variability within the individual realizations. Only towards the end of the whole period the residual partition is slightly decreasing, which is due to rising discrepancy among the models. These results are persistent over the specific seasons without any strong variation among them (not shown). Surely, it is disillusioning to be unable to elucidate a common treatment, though, still the commentarial behaviour of the high variability of precipitation within the time and realizations is pointed out. Again, this confirms the high uncertainty evoked by the complexity of precipitation in its immaculate simulation.
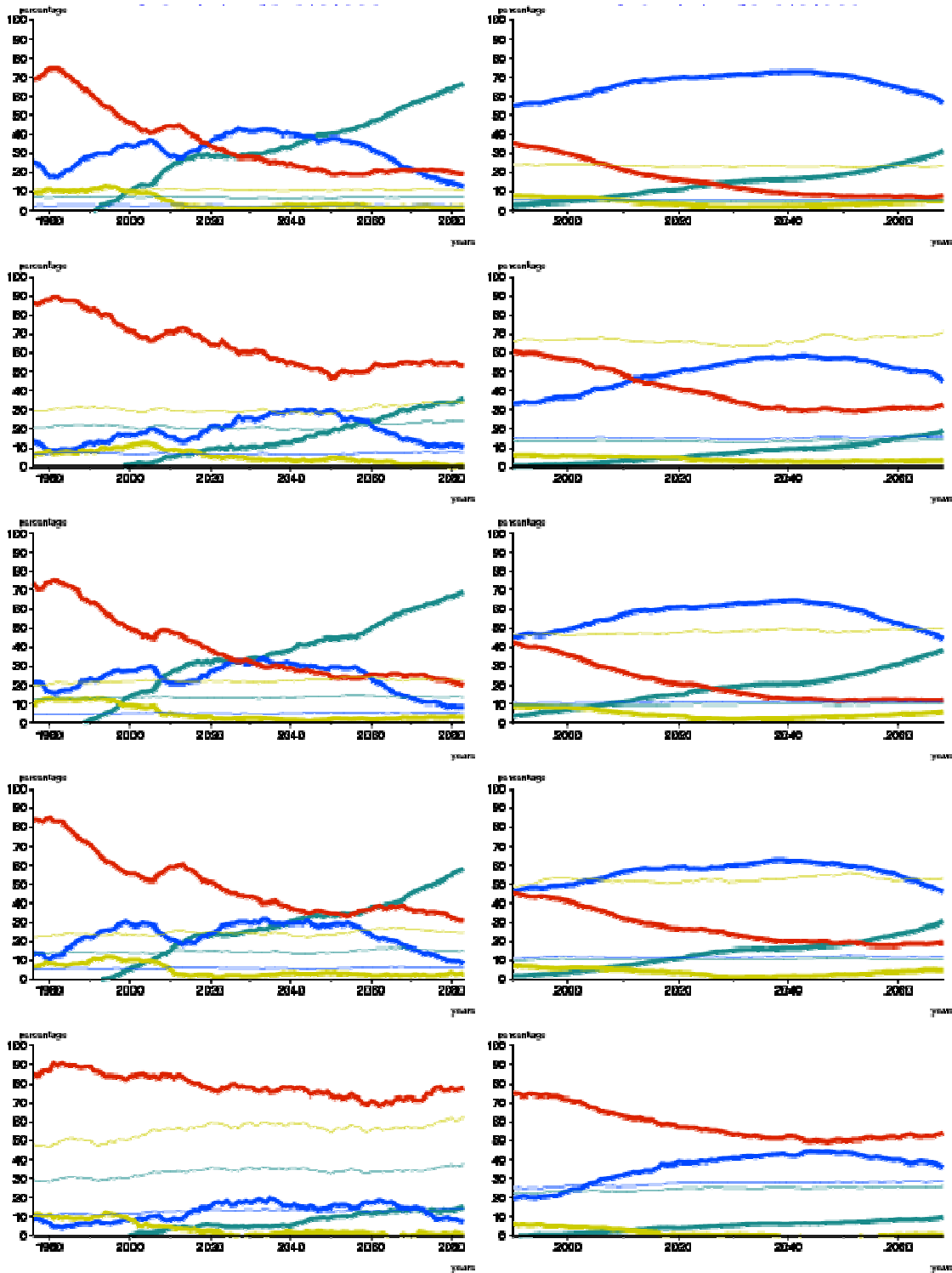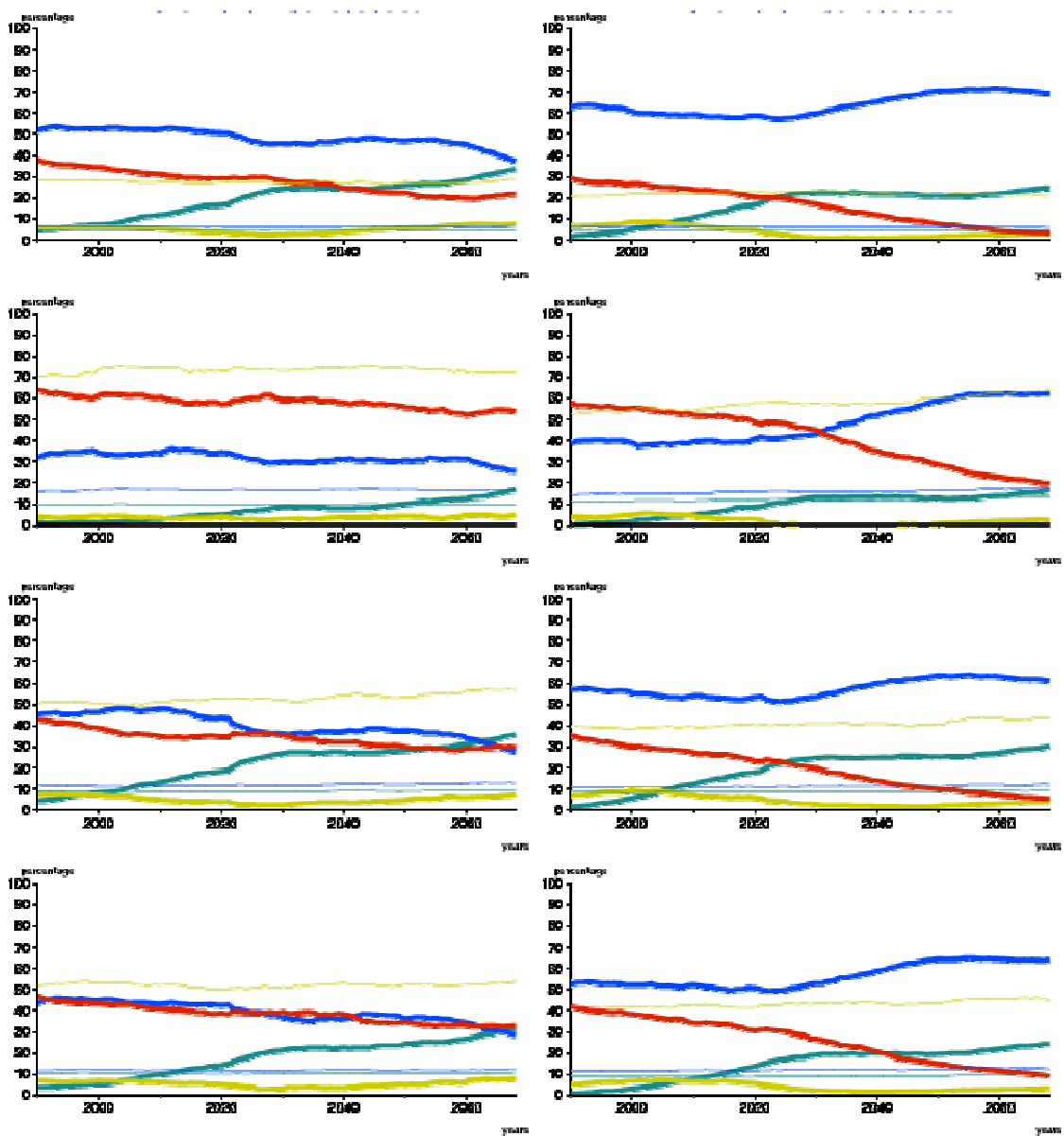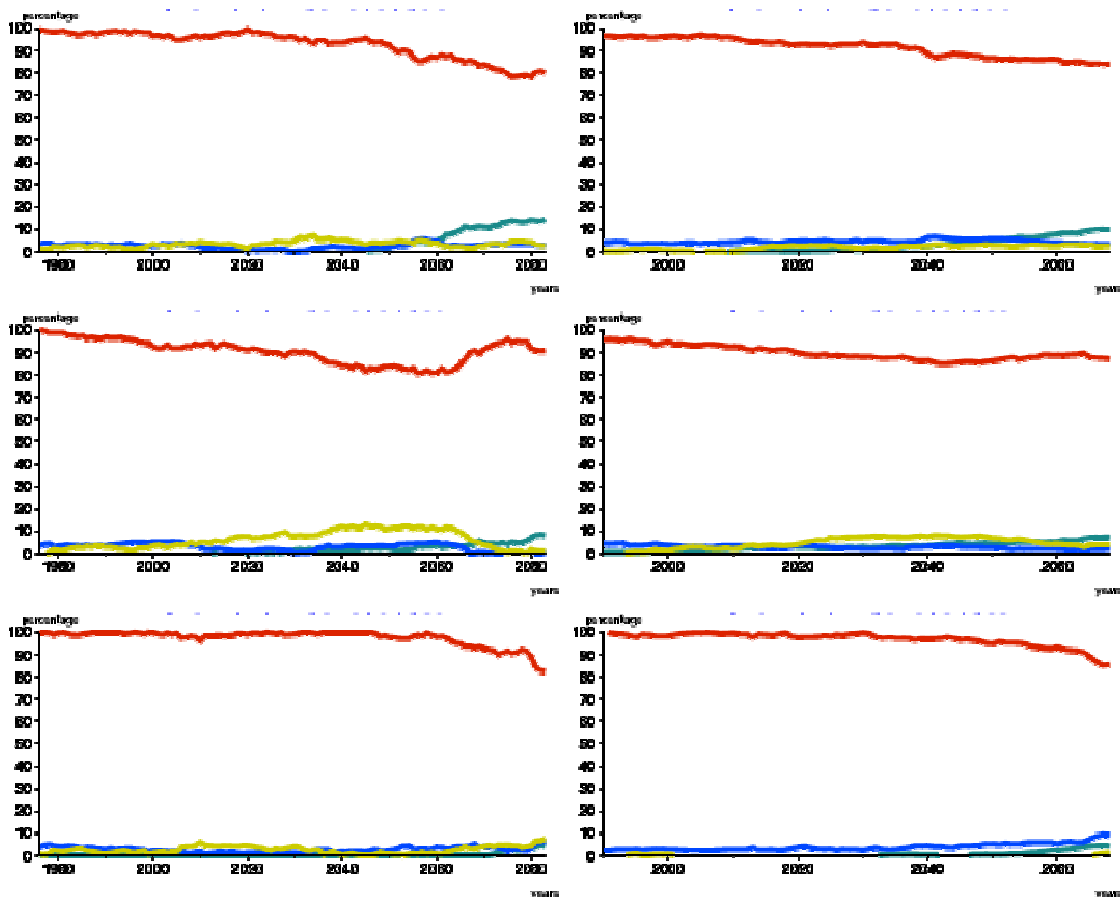
Figure 5.31: Normalized temporal approach of the 2-way ANOVA (left 30y/right 60y) for precipitation for the whole year. α=green, β=blue, γ=yellow and ε=red. From top to bottom: A1B, B1 and A2. 5% levels of significance are indicated in the specific colour for each partition in thin lines.

5.6   Conclusion

The chapter at hand highlights the different contributions of the total variability, being inherent in climate projections of individual models and of the total assembly of models. This is done with respect to spatial and temporal characteristics. Furthermore, different scenarios have been taken into account. The application of the ANOVA increases profundity by the alteration of the assembly of models and the detailed seasonal investigation. The variables analysed are temperature, precipitation and sea-level pressure.

Concerning these different computations, dependant on the chosen parameters, the results obtained evidently vary. Consecutively, the composition of the variance and thus the contribution of GCMs, its individual realizations and the GHG forcing within a specific time interval, strongly depends on the region, the variable, the time slice and the season. This is a result, which is also found by NORTHROP 2010.

Considering the different climatologic fields, for nearly all cases the discrepancy between the models is the strongest contribution on the total variance. While for temperature a strong impact of GHG forcing reveals a strong contribution of a common trend inherent to all realizations and models, for precipitation the partition developed by the variability within the realizations and/or models prevails in the total amount of variability. For sea-level pressure, the main contribution develops out of the discrepancy between the models. Reasons for this are the homogeneous reaction of surface temperatures by the forcing, while precipitation is spatially and temporally a highly variable field, strongly subordinated to natural variability and thus to initiating conditions. Consecutively, these residuals overcome the discrepancies of the models for precipitation. The future development of sea-level pressure is generally associated with great uncertainty, as models demonstrate different courses in their trends, with negative and positive directions as well. Still, the impact on the total inherent variability by the residuals and the discrepancies between the individual ensemble-members/realizations is relatively high. The other contributions of the specific variables are extenuated by their characteristic dominant partitions. These findings can be confirmed by other studies, as e.g. NORTHROP shows 2010, that the main amount of variability is associated with the different GCMs, followed by the contribution of the different ensemble members. Also KITTEL, GIORGI & MEEHL (1998), who investigate precipitation and temperature of 9 GCMs, experience a high inter-model variability. The interaction coefficient, indicating the difference of the sensitivity of the models to a certain forcing, is comparatively weak and constantly close to zero. This is due to the unchanged forcing scenario.

Though the presumption of an atmospheric equally distribution of emitted GHGs, there are strong differences in the spatial affection of the climate

variables, justifying the spatially detailed investigation. Consecutively, the detection of anthropogenic warming cannot be given equally on the MA. Particularly temperature exhibits reasonable patterns of treatment contributions, e.g. associated with land-sea distributions, while for precipitation no distinct collocation is detectable. At least, one can interpret a rising contribution of discrepancies over the models in areas with low observation station density and accompanied lack of climatologic knowledge. Sea-level pressure exhibits latitudinal gradients, predominantly for the contribution of model discrepancies and the residuals. Still, trend patterns are partially reproduced by strong signals, which e.g. also holds for sea-level pressure in summer for the 1-way ANOVA.

Seasonal differences can also be distinguished for all variables. Particularly, seasons with strongest trends exhibit high signals of treatment effects, e.g. temperature or sea-level pressure in summer. Concerning the 2-way ANOVA, seasonal alterations of the three main contributors, i.e. α, β and ϵ, are established, as e.g. α, which denotes individual model specifics, becomes predominant in summer, where natural variability by hemispheric steering is rather small and a local phenomenon and thus parametrizations come to the fore. These maximum differences in summer are also described by GIORGI, BI & PAL (2004a). The residuals become more influential in winter, where e.g. temperature and precipitation is highly subordinated to hemispheric steering and thus to natural variability. For sea-level pressure and precipitation, a latitudinal alteration of the ϵ-contribution becomes evident within the seasons, as it is shifted to the south during the colder parts of the year.

The longer the time periods are defined, in which the analyses are conducted in, the longer and higher may be the development of meaningful trends, which at least holds for the underlying study. Strong trends naturally enforce common signals, as they underlie several realizations and models.

To exhibit a potential alteration in the contribution of variabilities a bootstrapping approach has been conducted. The resulting shifts are only of low extent by neglecting specific models. By discarding NCAR-PCM, one experiences a slight increase of the β-contribution for temperature, indicating the high singularity of the mentioned model. A rather common model, well aligned to the overall results of all the models is ECHAM5, as only slight alterations are depicted in the partitions of variability, when the MPI model is neglected.

An adaption of all the realizations of the individual models to a common initial position, i.e. the ERA40 reanalysis dataset, diminishes the block partition α, as the model discrepancies are reduced. Consequently, the other partitions are enhanced, which leads to a high contribution of the residuals in the case of precipitation. Still, for temperature strong treatment effects are evident, which are even pronounced by a longer period of integration and nearly reach 72% in the A2 scenario.

A qualitative investigation of the results of independently computed ANOVAs with exchanged forcings exhibits an alteration of the arrangement of the different contributors. As expected, the common trend, i.e. the treatment effect, is enhanced by the strengthening of the forcing and the GHG emissions. This

holds particularly for temperature, while for the other variables an enforcement of the scenarios may enhance natural variability, which is an already assumed phenomenon (GIORGI & LIONELLO 2008, GIORGI & FRANCISCO 2008a/b) in climate sciences, though it cannot be proven finally in this study.

To expand the research on uncertainty and to receive quantitative findings on the impact of the scenarios, one could comprise the variability of different scenarios into the statistical analysis, as in the underlying study in each application of the ANOVAs the forcing remains the same. It should be noted, as an aside, that this would boost the partitions of the interactions. At least, this would provide a more detailed approach concerning the overall range of uncertainty, climate research is connected with by providing future projections. On the other side, there is no quantitative order of the scenarios, and as mentioned in chapter 2.4 they are treated as equally possible, which finally will enhance the discussion about the validity of the range of these results. GIORGI & FRANCISCO (2000b), who also combined different scenarios in their analysis, conclude that the major partition of uncertainty is still concerned with different models. Although, their comparison of the models is qualitatively, as in the underlying study it is done in the consideration of various forcing impacts. Anyway, NORTHROP (2010) confirmed this also quantitatively. Especially in the northern hemisphere for the mid of the 21st century, NORTHROP (2010) shows a greater variance of the GCMs, than the different scenarios exhibit. Though, NORTHROP (2010) recognizes a growing influence on the variability by the scenarios with a later time slice to the end of the 21st century. Then, the variability associated with the scenarios is even greater than the amount of the different GCMs to the total variance. However, with the choice of the depicted time-slices in the underlying study, a clear separation of the different influences of the scenarios within the 21st century is not possible.

An extension of the introduced temporal approach is a spectral approach, by a continuous stretching of the period of computation by yearly steps. By this advancing prolongation, one can clearly detect the threshold concerning the length of the period, when a potential trend on a variable becomes predominant in overall variability. An example of this application is given by PAETH & POLLINGER (2010).

6   EXTREMES

A central tendency of climate means and trends might give an overall overview of the future development in climate. Though, this general assessment gives no hints about the future occurrence of extreme events (HEGERL et al. 2004), as even in regions with decreasing amounts of precipitation an enforced effect of extremes is possible (GAO, PAL & GIORGI 2006). Thus, ALPERT et al. (2006) conclude, that the daily amounts of extreme precipitation are rising, whilst the yearly sums are declining in the observation period from 1951-1995. Compared to this findings, also GAO, PAL & GIORGI (2006) note, that the occurrence of extremes is not directly deducible from the changing in the mean, as they could depict longer dry spells in regions of increasing precipitation amounts or an increase of 5days precipitation maxima in regions with a reduction of precipitation amounts. This identifies a broadening of the distribution of precipitation with a probable higher occurrence of damaging events. While the antecedent chapters of this study deal with a reduction of precipitation, extremes are expected to increase (KHARIN & ZWIERS 2004), which is supposed to be evoked by a rise of average temperatures and the accompanied amplified capacity of atmospheric water vapour and increased alterations of synoptic patterns (MEEHL, ARBLASTER & TEBALDI 2005).

Still, as one can easily follow, the question about a changing climate is closely related with that aspect (TRENBERTH et al. 2007). Consecutively, in recent projects stronger attention has been directed to extreme events by the community of climate research (e.g. FREI et al. 2006, HERTIG et al. 2013a/2012), as they can strongly affect socio, natural and economic systems within short time scales and small regions. In fact, they have a large potential of high damage (e.g. eroded fertile soils, landslides, yield losses, flooding, forest fires, portable water availability, agricultural productivity, fatalities due to heat waves, etc.).

As indicated in chapter 1.2.4, the MA is a highly vulnerable region. Particularly at the change of the millennium, extreme events occurred in a very frequent and dramatic matter, which was related to an optional changing climate in the upcoming century in conclusion (BOLLE 2003).

For instance, the heat wave occurring over Europe in 2003, directly caused almost 15,000 fatalities solely in France in the first half of August (POUMADERE et al. 2005). Recent estimates suggest it as the warmest summer in the last 500 years with a temperature exceeding the 1961-1990 mean of about 2.3°C over land surface. The question arises, whether these extremes will indeed become more frequent as STOTT, STONE & ALLEN (2004) discuss, when they postulate a doubling of the possibility of such events in the last years. They furthermore consider human contribution to this doubling as very likely with a level of confidence of 90%.

Before, in 1999, Portugal, Spain and Italy suffered new temperature records in summer and heavy precipitation amounts in spring and autumn. In Valladolid precipitation exceeds the highest monthly record since 130 years and on a

single day it rained about 230 mm in the northeast of Italy (BOLLE 2003). Sicily recorded the highest locally ever measured temperature of 45°C in August. On the other side, the Sicilians experienced snowing – for the first time for 18 years in winter. Also, in the eastern parts of the MA extremes occurred in 1999. In Greece landslides, evoked by heavy precipitation, caused loss of agricultural land, harvest losses and fatalities. The temperature on eight consecutive days exceeded the normal by 5°C in Israel. In contrast, in 2000 dry periods lasted in Spain, southern France and Italy. After that, in winter 2000/2001 this dry period has been replaced again by torrential precipitation and its dramatic consequences (BOLLE 2003). LIBERATO et al. 2011 analysed the winter storm Klaus in 2009, causing damage of about 6 billion dollars only in France and Spain with its accompanied torrential rainfall. Based on the normalization on 2009, BARREDO established 122 extreme flood events occurring from 1970-2006 and occasioning a loss of 140 billion dollars. These are only few instances of the appearances of extremes in the last years, and highly justify the consideration of extremes in the study at hand. In the mentioned examples, it already becomes evident that these occurrences of extreme events are not spatially unique or temporal dependant.

With the alternation of the hygric conditions with the seasons, also the number of rainy days is affected, accounting about 40 days in winter and approximately the half in the transition seasons, whereat summer exhibits lowest amounts with one quarter of the frequency in winter (WEISCHET & ENDLICHER 2000).

A frequently cited study concerning extremes has been fulfilled by MOBERG et al. 2006, who analysed temperature and extremes over Europe by stationary series from 1901-2000. They find e.g. an intensification of precipitation over Europe. Similar results are depicted by GROISMAN et al. (2005) for the USA and more generally in the extratropics. Further studies also confirm an upward occurrence of temperature extremes, following different approaches (e.g. NOGAJ et al. 2006 or SIMOLO et al. 2010 analysing moderate extremes) and investigating different fields, e.g. duration of hot spells (DELLA-MARTA et al. 2007) or the occurrence of day and night extremes over different regions of the MA (KIOUTSIOUKIS, MELAS & ZERFOS 2010 (Greece), RODRIGUEZ-PUEBLA et al. 2010 (Iberian Peninsula), SIMOLO et al. 2010 (Italy)). The different sources and their relative importance for temperature extremes e.g. have been investigated by YIOU & NOGAJ (2004), who suggest the NAO as the leading contributor in winter for northern Europe. Also remarkable contribution is provided by short scale characteristics, like SSTs and soil moisture, which also account for heat extremes in summer, besides synoptic steerings like the blocking actions and a northward shift of the ITCZ (**I**ntertropical **C**onvergence **Z**one) over the Atlantic (CARRIL et al. 2008, CASSOU, TERRAY & PHILLIPS 2005).

In general, the IPCC report reminds, that extreme precipitation events have not only increased recently in their frequency and strength (TRENBERTH et al. 2007) but also are projected to increase in their intensity future (MEEHL et al. 2007).

Thus, an intercomparison for the projection of precipitation extremes is accomplished in the antecedent chapter, as the results for multiple realizations are analysed for different GCMs of the CMIP3 database. The fields, which are investigated, are R95N, R95AM, R95T and SDII95p.

For this purpose, at first means and trends, i.e. sensitivities, are figured, closely following the overall structure of this study, while afterwards a signal analysis is conducted.

6.1   Calculation of extremes

Though extremes occur in short time periods in spatially small locations, it is attempted to account for them with the application of GCMs, in order to conserve the methodology of this study. Furthermore, approaches within the overall scientific project - where the underlying study is also embedded in - have been conducted with the regional climate model REMO (PAXIAN et al. 2011) and statistical downscaling (e.g. HERTIG & JACOBEIT 2008a, HERTIG et al. 2013a/2012), providing a more spatially and temporal detailed consideration. Nevertheless, the input, which drives these more detailed investigations, is supplied by the GCMs, i.e. in most cases ECHAM5. Thus, besides the analogous treatment for GCMs, ECHAM5 is consequently highlighted specifically in the consecutive analyses by a description of the means, sensitivities and again a potential investigation of uncertainties concerning extremes. Hence, the advantage of a signal analysis is sustained within this approach. Again, this contribution is a proposal for quantitative climate sciences to depict the inherent uncertainties with the intention to accommodate decision-makers, stake-holders and policymakers in order to adapt and mitigate on incidents in response to climate change.

There are different approaches of the calculation of extremes with specific advantages and disadvantages (COLES 2001), like the alignment of generalized extreme value distributions (GEVs) on the occurring extremes, e.g. the General Pareto Distribution with its shape, scale and location parameters (PAXIAN et al. 2013, TORETI et al. 2010, NOGAJ et al. 2006) or the estimation of the return values, with e.g. the block maximum effect (FREI et al. 2006). Despite the applied method the problem of the few values, defined as extremes and the evoked affliction by the weak robustness of the analyses and the low degrees of freedom persists. Remedy could be given by the application of a Bayesian prior for the shape parameter (FREI et al 2006), the utilization of L-moments (PAXIAN et al. 2013) or the assessment of frequency analyses (FREI et al. 2006). The severity of an extreme event defines the location in the probability distribution, while the strongest extremes occur relatively scarcely. The lower the frequency of extremes is, the lower is the ability to obtain the correct statistical result about the description of its future characteristics (KLEIN TANK & KÖNNEN 2003). Please note, that particularly for summer an interpretation of percentiles and their changes is difficult, as the rare amount of wet days weakens the robustness and the information value (MOBERG et al. 2006).

In the underlying study, a definition of percentiles is utilized. This implies the definition of a certain threshold, in order to show, whether in future the fields occur more or less frequent above or beneath this threshold.

A general constraint of extremes is the usage, as the applicable values only consist of a low percentage of the total amount of data. To account for the problem of the calculation of only very few data, naturally those referring as extremes, the upper five percent of all the data are used and thus defined as extreme. This is a compromise conserving at least one twenty of all the values. On the other hand, the calculation of percentiles is relatively easy and thus often applied on future climate projections and observation data (RODRIGO 2010; ALEXANDER et al. 2006; FRICH et al. 2002). Furthermore, one has to admit that the interpolation procedure, which is also applied on the extremes, smoothes the intensity of the extreme events, which holds for all extremes above the 75th percentile (HAYLOCK et al. 2008). Still, as the modelling and the measurement of extremes is still affected by high uncertainties (PAETH 2007) the analysis of extremes is always accompanied with strong uncertainties and thus should be treated with care.

For this purpose, daily data of the GCMs from the CMIP3 database have been consulted (see 3.2). First of all, due to the huge amount of data and the consecutive reduced supply of data by the CMIP3 database (see 3.1), the time periods of 1981-2000 as reference period and 2046-2065 and 2081-2100 as future periods have been chosen, as within these slices most models are provided. The procedure considering the building of means is conducted analogously to the analyses of the monthly datasets. The models with their realizations can be obtained from table 3.3. Percentiles are calculated by equation (56).

$$56) \qquad M_{95} = \frac{(100 - 95)\,x_k + 95 x_{k+1}}{100} \,,$$

where M_{95} depicts the value of the 95th percentile and x_k are the sorted elements with its number n, i.e. $x_1 > x_2 > \ldots > x_n$. k is defined by formula (57):

$$57) \qquad k = \frac{n \cdot 95}{100} \,,$$

where $\qquad k \in Z$

and n is amount of elements, i.e. days of precipitation within the specific period.

The fields of percentiles, which have been applied in the underlying study, are chosen according to MOBERG et al. 2006 and HERTIG et al. 2013a/2012. The variables are the number of events exceeding the 95th percentile of daily precipitation (i.e. R95N) describing the frequency of these events, the percentage of the percentiles to the total amount of precipitation (R95T), the total amount of precipitation above the 95th percentile (R95AM) and the mean daily intensity of precipitation of events exceeding the 95th percentile (simple

daily intensity index = SDII95p) (as indicated in table 6.1). Particularly R95T supplies crucial information, as it is directly linked to the results of the average precipitation trends, analysed in chapter 4, while SDII95p is the ratio of R95AM and R95N. The universe amount (100%) is defined as the number of events, i.e. days with at least 0.1mm precipitation.

R95AM	total amount of precipitation from events exceeding the 95th percentile
R95N	frequency of events exceeding the 95th percentile of daily precipitation
R95T	percentage of the rainfall from events exceeding the 95th percentile to the total rainfall
SDII95p	mean daily intensity from events exceeding the 95th percentile

Table 6.1: Precipitation variables of extremes used in this study.

The indices in table 6.1 are chosen, because of their widely spread application in the scientific community, which eases the comparison to other findings (e.g. HERTIG et al. 2013a/2012) and because of their different perspectives on extremes, providing a comprehensive view on modelled and observed conditions. Though the total amount of precipitation may decrease, the intensity may rise instead, resulting in a lower frequency but heavier rainfall. So, the extreme variables are interrelated to each other. All of them are derivated from the upper tail of the probabilistic density function and thus, can be called wet extremes.

The resulting percentiles have been yearly averaged for every season. The outcomes are the seasonal extremes for every year in the mentioned periods for every realization of every available model for every scenario. Again, these analyses are conducted for all of the grid-cells defined in chapter 3.1.1. Dependant on these grid-cells, models, realizations, scenarios and seasons, the averages are computed over the specific periods, followed by the calculation of the trends. These are simply derived by the difference from one of the two future periods and the reference period and thus in the following referred to "sensitivities". Out of the sensitivities and the individual means the ensemble-means and the ensemble sensitivities are developed, by averaging the incorporated data. The ensemble-means and ensemble sensitivities are the groundwork for the calculation of the multi-model means and multi-model sensitivities by averaging. This is done analogously to section 3) and 4) in the "cooking recipe" in chapter 3.1.3. Still, the dependency to grid-cells, periods, seasons and scenarios are sustained within the multi-model datasets.

6.2   Means and sensitivities

Pertaining the sequence of chapter 4, at first the results of the ensemble of ECHAM5 are presented, followed by the results derived from a multi-model approach.

6.2.1 ECHAM5/MPI-OM

For the ensemble of ECHAM5, the results of R95AM, i.e. the total amount of precipitation exceeding the 95th percentile, for the A1B scenario are illustrated in

figure 6.1. The left panel shows the sensitivities calculated by the difference from the average of the two time slices 2046-2065 and 1981-2000, while the right panel depicts the average of R95AM in the future period. The pattern of the maps in the right panel exhibits a bimodal distribution of R95AM, with maxima in the northeast and the northwest of the MA. To the southern central, the amount of heavy precipitation is at its minimum. In summer, the amounts of extreme precipitation reaches highest values, with up to 155.8mm. In the colder seasons the amounts of extreme precipitation are less hazardous. Compared to other approaches, like statistical downscaling assessments or REMO, the extremes of ECHAM5 are relatively low (HERTIG et al. 2012).

Considering the sensitivities, one can identify a heterogeneous pattern of its distribution with only minor alterations concerning the seasons. In the warmer section R95AM increases in most parts with general higher amounts in the northwest of the MA and maximum differences in summer in the northeastern area. With the colder period in the year, a decrease of these extremes becomes evident in the south and here particularly in the southeastern sections. HERTIG et al. (2013a) found a decrease in spring, predominantly over the western regions, which can not be confirmed by this study. However, over most parts the changes in figure 6.1 are only small. Still, concordant are the findings for Greece. In summer the results of figure 6.1 and even more distinct in figure 6.2, denoting sensitivities towards the later period of 2081-2100, are in contrast to HERTIG et al. (2013a), who describe a reduction of R95AM, particularly in the north, and slight increases above the Greek coasts and vicinal to the Tyrrhenian Sea. In autumn the reductions of the southern part, again more distinct in figure 6.2, are in line with the findings of HERTIG et al. (2013a) exhibiting a decrease southwest - northeast diagonal. Also, increases in autumn over the Gulf of Lyons, northern Italy and the southern coast of Turkey are depicted in downscaling assessments (HERTIG et al. 2012) and ECHAM5. Still deflections can be found over Greece and Spain. For winter, the increases of R95AM over western areas of the Iberian Peninsula and southern France and decreases in southeastern areas of Italy are similar to the study of HERTIG et al. (2013a).

Again, it must be emphasized, that a comparison between the studies is only feasible by keeping the constraints in mind they are conducted with. I.e. the interpolation procedure and the coarse resolution ECHAM5 is subordinated to in the underlying study, while the study of HERTIG et al. (2012) attempts to depict high resolved spatial characteristics. It shall be noted, that HERTIG et al. (2012) also applied an interpolation on results of downscaling assessments and experienced an overall smoothing of these extremes. Furthermore, changes are computed by slightly differing time periods, which e.g. justifies the difference to the means of 1961-1990 and to the sensitivities calculated by the difference to 2021-2050 in the study of HERTIG et al. (2012). Consulting further studies, the differences in the results become rapidly evident, as e.g. FREI et al. (2006) detect only minor changes in extremes for winter with an overall tendency towards a decrease, while others analyse increases in winter e.g. for Italy (NIKULIN et al. 2011).
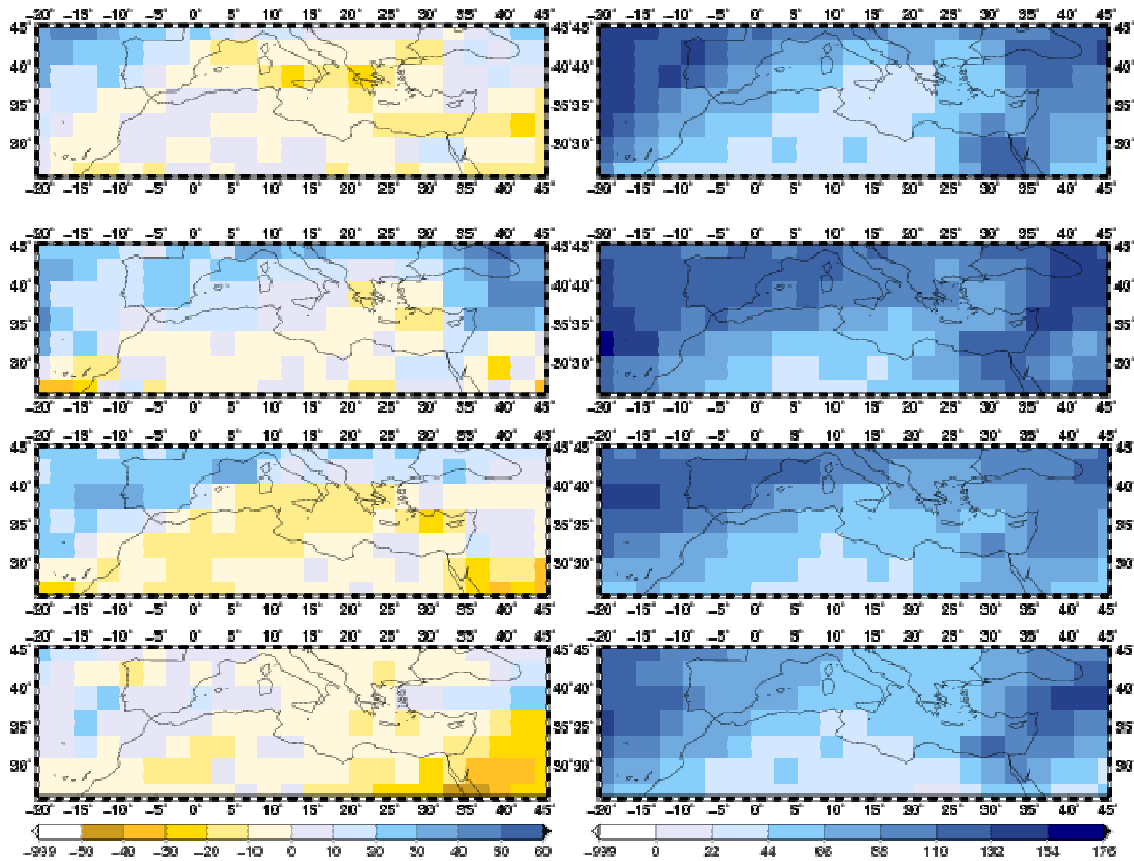
Figure 6.1: ECHAM5 runs 1,2,3 of R95AM [mm] in the A1B scenario. Left panel: Differences of the means of (2046_2065)-(1981_2000). Right panel: Mean percentiles in the period of 2046_2065. From top to bottom: Spring, Summer, Autumn, Winter.

Taking into account the time period of 2081-2100, for the mean values of R95AM the gradients in the spatial distribution are pronounced, while the overall pattern remains (figure 6.2). Thus, the northerly eastern and western areas become more affected by an increase of heavy precipitation amounts. Consecutively, the general results, displayed in figure 6.1, are more pronounced in the differences to the 2081-2100 period (figure 6.2). The reduction of extremes in winter in the east is diminished and shifted into summer, where the increase over minor Asia (already depicted in figure 6.1) is even enforced evoking a strong gradient in the east. Consecutively, summer is the season, which exhibits the greatest changes between the two illustrated future periods. Finally, in the drier seasons heavy precipitation is reduced in the southern central areas. This also becomes evident in the colder seasons. The increase of extreme precipitation in spring is hardly to interpret, but it is still noteworthy, that this pattern is already indicated in figure 6.1.
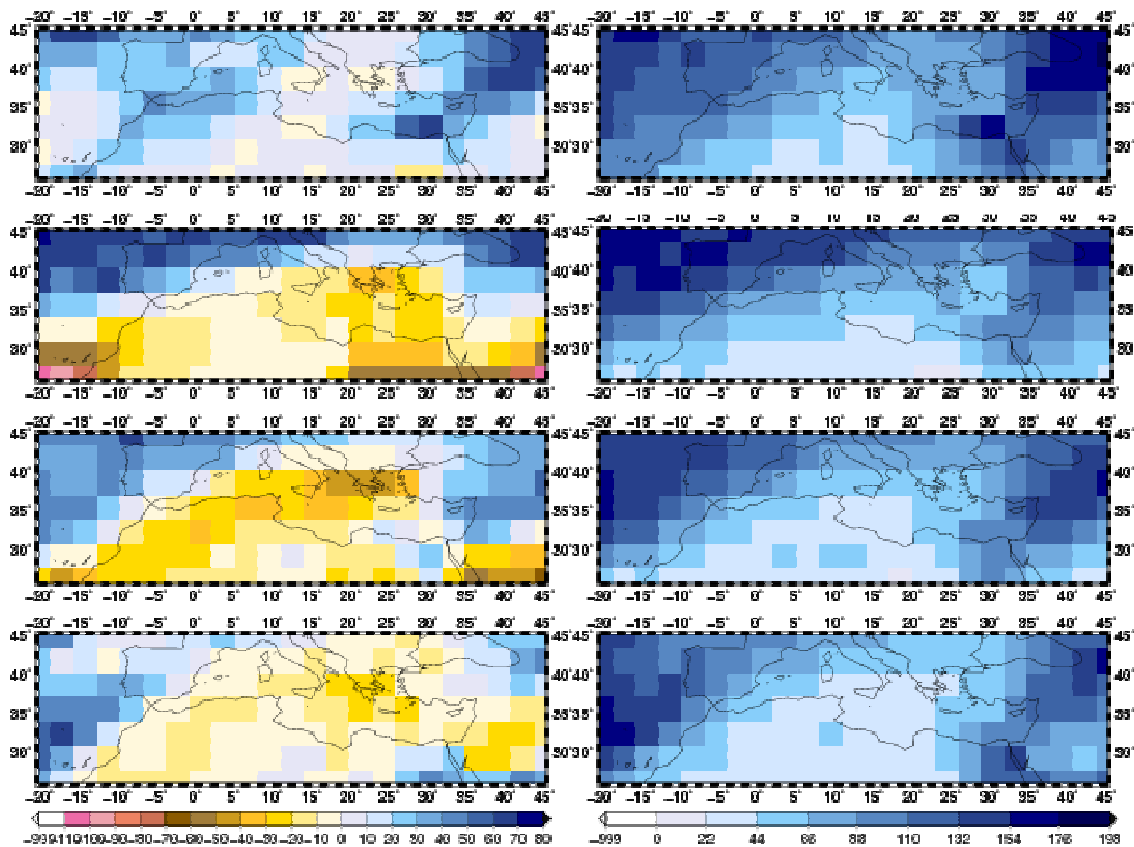
Figure 6.2: ECHAM5 runs 1,2,3 of R95AM [mm] in the A1B scenario. Left panel: Differences of the means of (2081_2100)-(1981_2000). Right panel: Mean percentiles in the period of 2081_2100. From top to bottom: Spring, Summer, Autumn, Winter.

For brevity, only summer and winter are depicted for the following fields. This procedure is applied, as the climatic conditions exhibit maximum differences (TRIGO et al. 2006, compare chapter 4). The overall means of the percentage of the precipitation occurring above the 95th percentile to the total amount show only minor differences between the different seasons (figure 6.3). The values reach from 18.2% to 32.8% representing the bimodal structure with maxima in the eastern and western regions again. HERTIG et al. (2012) describe higher amounts of R95T out of modelled databases compared to data from reanalysis or statistical downscaling. This may depend on the individual representation of R95N and SDII95p. As the total amount of precipitation of ECHAM5 is relatively low, as one can also see in figure 4.11, where ECHAM5 is one of the driest models, it heightens the percentage in R95T. R95T does not solely get its high amounts from SDII95p (see below), but also from the low number of wet days.

While the total amount of extreme precipitation is decreasing in some regions, the percentage of the amounts evoked by these extreme events to the total amount of precipitation is increasing over vast areas identifying the overall trend of decreasing precipitation, which is indicated in figure 4.32. This holds mainly for summer in the northern areas, closely following the trends in figure 4.27 . Still, decreases can be found, while the reduction in winter must be dedicated to a decrease of R95AM, as the south of the MA is affected to a lower amount on decreasing overall sums. Both holds for the reduction of R95T in summer in the south until 2081-2100, being again explained by figures 6.2 and 4.27. The projected growing of R95T in eastern and western regions in winter by

166

ECHAM5 is also discovered by HERTIG et al. 2012, which also holds for REMO, but can not be reproduced by statistical downscaling.

Figure 6.3: ECHAM5 runs 1,2,3 of R95T [%] in the A1B scenario. Uppest row: Means for 1981-2000. Middle row: Differences of the means of (2046_2065)-(1981_2000). Lowest row: Differences of the means of (2081_2100)-(1981_2000). Left: Summer; Right: Winter.

Figure 6.4 illustrates in its upper row the average pattern of the number of events, whereupon precipitation exceeds the 95th percentile. Although the pattern gives no hint of any allegeable spatial distributions, one realizes a higher number of these events in summer (left column). Overall, these numbers of events are relatively high, compared to other assessments in analysing extremes with percentiles (HERTIG et al. 2012), which induce low values in the intensity (see below). For the future, a decrease of these events is depicted, where at least for summer, stronger sensitivities can be found for the reference to period 2081-2100 in the lower row. In summer, also a spatially bipartite distribution is pictured, as the north of the investigated area experiences an increase, while the southern areas show a decrease of the number of these extreme events. Particularly in the southern-east the decrease is also apparent in both of the depicted seasons. REMO depicts analogous results for winter (HERTIG et al. 2012), while statistical downscaling approaches identify lower values in their trend amplitudes (HERTIG et al. 2013b). GIORGI, BI & PAL (2004b) find a general reduction of rainy days, which also holds for the days with rain amounts above the 95th percentile, as shown in figure 6.4. This is partially in contradiction to FREI et al. (1998), who found an increase of heavy precipitation days in the south for October.
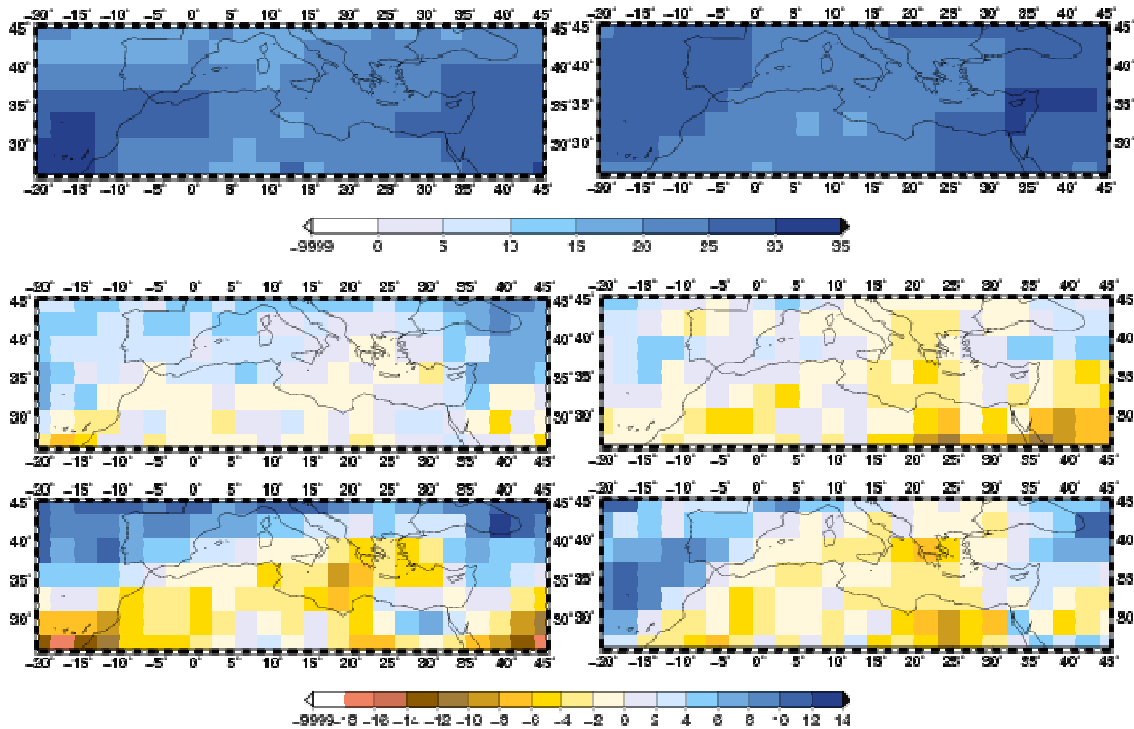
Figure 6.4: ECHAM5 runs 1,2,3 of R95N [d] in the A1B scenario. Uppest row: Means for 1981-2000. Middle row: Differences of the means of (2046_2065)-(1981_2000). Lowest row: Differences of the means of (2081_2100)-(1981_2000). Left: Summer; Right: Winter.

As already suggested in chapter 4, higher variability is expected to be linked with an intensification of the hydrologic cycle in the case of general warming (Clausius-Clapeyron relation, e.g. FREI et al. 1998, DEQUE, MARQUET & JONES 1998). Thus, precipitation in general may be shifted to extreme events, because of the higher moisture holding-capacity of warm air masses (FREI et al. 2006), while the periods between these precipitation days may become longer (MEEHL et al. 2007), due to feedback with generally drier landscapes (ROWELL & JONES 2006).

Consecutively, a further field analysed, is the intensity of extreme precipitation, i.e. the amount of heavy precipitation within an event, as figured in 6.5. The dipole structure of the means strongly resembles the means of R95AM. HERTIG et al. 2012, who illustrated SDII95p for ECHAM5 for the period of 1961-1990 within its original spatial resolution of 1.875° for winter and autumn, found results, which can be verified here. In winter highest intensities can be located in the western of the Iberian Peninsula, the eastern Atlantic and over vast regions of the eastern MA (map in the upper right of figure 6.5). This east-west bimodal distribution of highest values is linked by a transition of higher values in the north of the area of investigation. From the southern centre, a tongue of lower intensities expands to the north, which is apparent in winter and summer. Overall, vast parts of the MA suffer higher intensities in summer than in winter. Comparing these results with other models (e.g. in the multi-model mean, see below or NCAR-CCSM3, MRI-CGCM2.3.2, both not shown), one will experience higher intensities for ECHAM5, which is in contrast to the findings debated in SILLMANN & ROECKNER 2008, who report an underrating

of extreme precipitation above the 95th with up to 50mm related to observations. Neglecting the low intensities and the missing of orographic details, which are dissolved by the coarse resolution, as e.g. height, proximity to the sea or exposition, ECHAM5 still follows the gridded dataset of E-OBS (HAYLOCK et al. 2008) – shown by HERTIG et al. 2012. However, as SDII95p describes the ratio between R95AM and R95N, it is diminished by the comparatively high amount of R95N, relative to other extreme approaches (HERTIG et al. 2012). Considering the changes, illustrated in the lower rows of figure 6.5, one only recognizes small differences, which again evidently change with a further progression of time (lowest row). Thus, in the sensitivities to the period of 2081-2100, the south of the MA and here particularly Egypt and the Atlantic coast of Africa, exhibit distinct reductions of intensities in summer. Roughly the opposite picture is described in winter, where the Atlantic Ocean and the southeastern areas experience an increase of intensities with up to 13.9mm/d. In the first future period, at 2046-2065, these differences are not identifiable. Also evident discrepancies cannot be depicted between summer and winter. With the constraints of a disturbing interpolation to 3x3° and slightly differing time periods, the winter for the later period in future is resembling in pattern and amounts to the findings of HERTIG et al. 2012. GIORGI, BI & PAL 2004b indicated a reduction in daily rainfall intensity with RCMs in summer, while the intensity increases in autumn and spring, where the latter is well reproduced by ECHAM5 indeed (not shown). Higher resolved approaches, e.g. REMO, detect increase of intensities in uplift regions of luv areas of orographic barriers (HERTIG et al. 2012, GAO, PAL & GIORGI 2006). Maybe the smaller changes in central areas can be related to a an overall increase of pressure, which is depicted by figures 4.37 for ECHAM5, providing increased atmospheric stability and being unfavourable for storms and associated high precipitation intensities (GIORGI & LIONELLO 2008). Nevertheless, generally the intensity of precipitation is supposed to become higher, though the projected reduction of overall precipitation (MEEHL et al., 2007 p.750) in the MA.
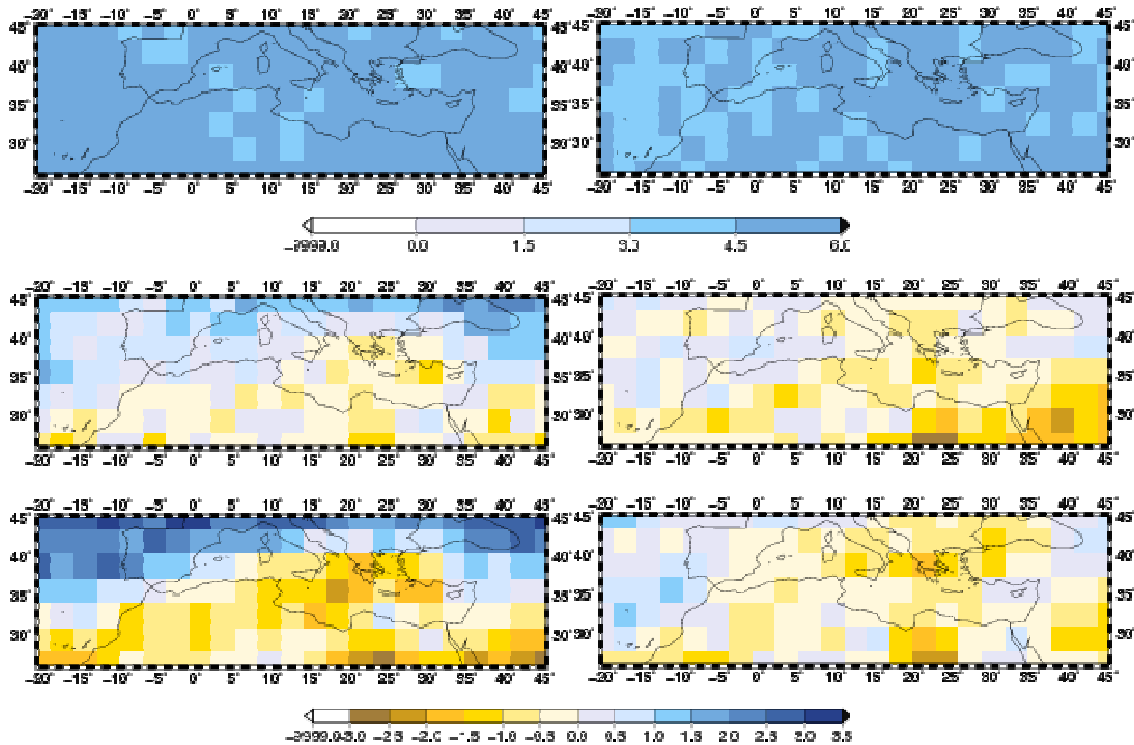
Figure 6.5: ECHAM5 runs 1,2,3 of SDII95p [mm/d] in the A1B scenario. Uppest row: Means for 1981-2000. Middle row: Differences of the means of (2046_2065)-(1981_2000). Lowest row: Differences of the means of (2081_2100)-(1981_2000). Left: Summer; Right: Winter.

6.2.2 Multi-Model Approach

All applied models (see table 3.3) exhibit means with an evidently smoothed pattern, where a distinct spatial distribution is lost and cannot be interpreted (figure 6.6). Evidently, ECHAM5 shows higher values of extreme precipitation. The bimodal distribution of strong extremes, with the expanding tongue of lower extremes to the north, can hardly be distinguished. At least, a north-south gradient becomes evident, which is particularly pronounced in winter. In contrast to ECHAM5, all models in average (including ECHAM5) bear resemblance to nearly no change, except for some minor increases. These increases are strongest in the north in winter, which is also not reproduced by ECHAM5.
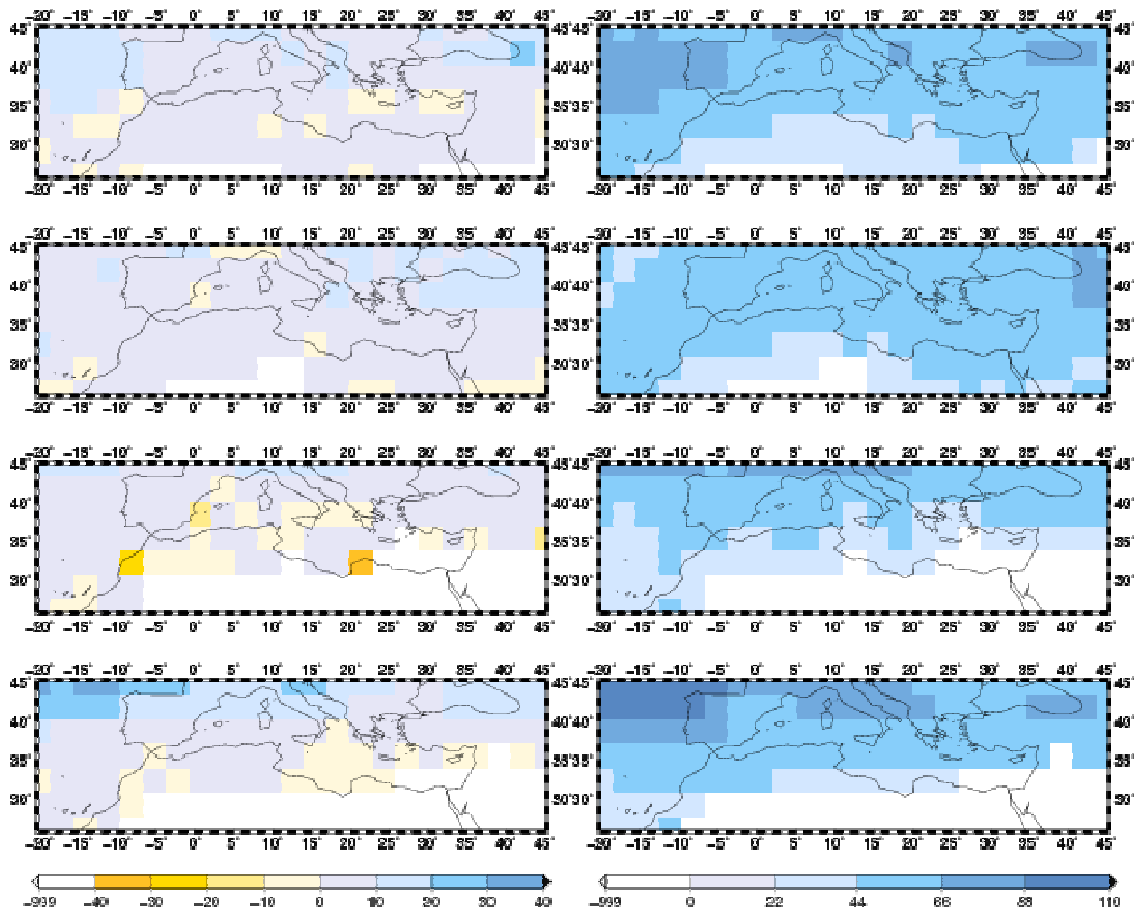
Figure 6.6: Multi-model mean of R95AM [mm] in the A1B scenario. Left panel: Differences of the means of (2046_2065)-(1981_2000). Right panel: Mean percentiles in the period of 2046_2065. From top to bottom: Spring, Summer, Autumn, Winter.

Considering figure 6.7, it becomes evident, that the differences between the two different future periods is low, indicating the small changes to happen in the first half of the 21st century. At this point, the reader is kindly advised, that grid-cells with missing values, associated by to few data exceeding the 95th

percentile, are illustrated in white. This only exhibits within some models, e.g. ECHAM5 has always a sufficient amount of values satisfying the requirements. Still, this missing values occur, e.g. within MRI-CGCM2.3.2. In the occurrence of a missing value in any case, i.e. for any realization of any model in any time period, the considered grid-cell of a subsequent mean or sensitivity, e.g. ensembles-mean or multi-model mean (see cooking recipe), is described by -9999 and consecutively shaded in white. Thus, the number of cells with missing values increases with the utilization of more models. Hence, in a resulting multi-model sensitivity, missing values are accumulated by the subordination to all missing values derived from all utilized models and the means of both time slices, namely 1981-2000 and 2046-2065 or 1981-2000 and 2081-2100.
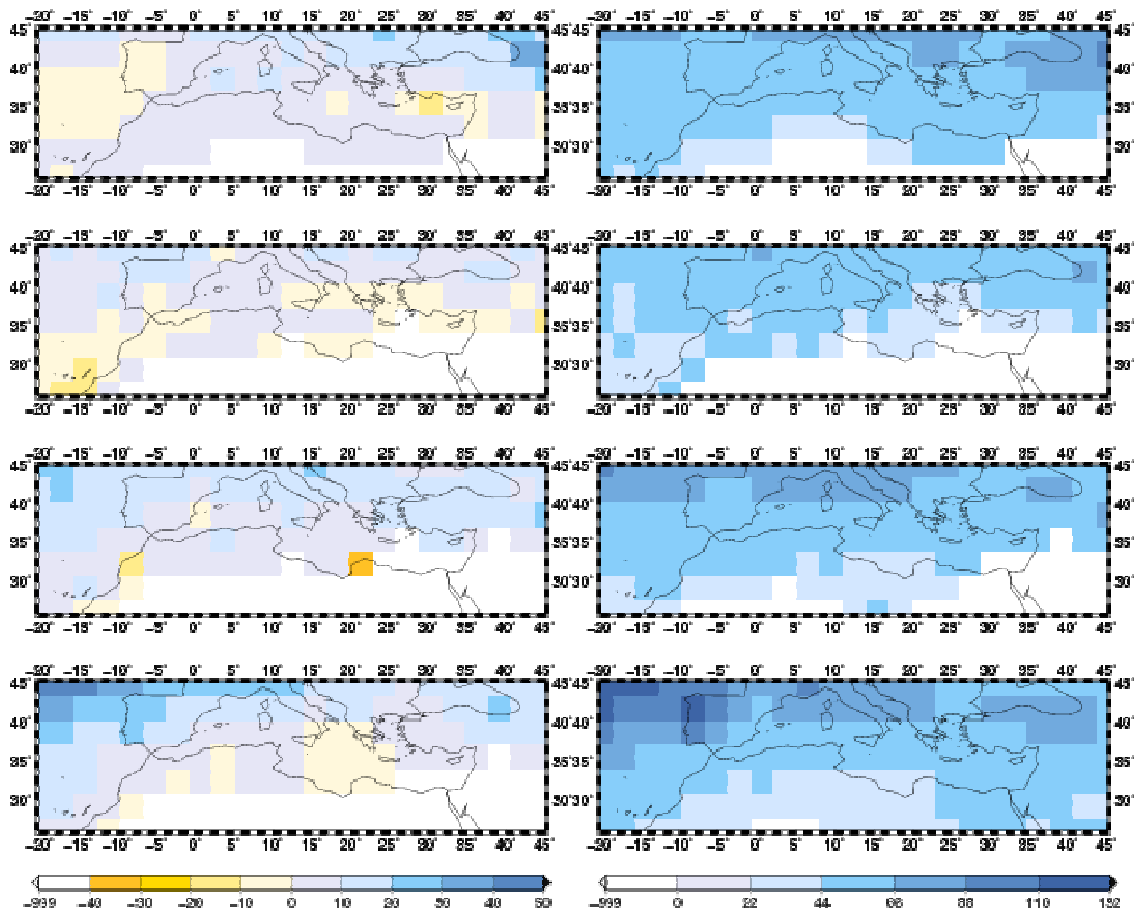
Figure 6.7: Multi-model mean of R95AM [mm] in the A1B scenario. Left panel: Differences of the means of (2081_2100)-(1981_2000). Right panel: Mean percentiles in the period of 2081_2100. From top to bottom: Spring, Summer, Autumn, Winter.

Compared to ECHAM5, the multi-model mean does not exhibit similar high percentages of mm of precipitation according to extremes (upper row of figure 6.8). This indicates a more moderate distribution of average precipitation. In summer high percentage is found over the Atlantic Ocean, while in winter these higher percentages are expanded into the central area of investigation. Both patterns do hardly resemble to the one projected by ECHAM5. The sensitivities, depicted by the multi-model mean, illustrate small increases and thus a shift to pronounced extreme precipitation, which becomes most evident in summer over the western regions over the Atlantic and in winter over the northern boundaries of the area of investigation. Despite the results for R95AM a specific sensitivity

between the two future periods becomes definite by stronger increase towards the period of 2081-2100. The increase over Minor Asia, illustrated in summer for 2046-2065, vanishes in further future. Again, these findings are in contrast to ECHAM5, which illustrates opposite signals considering season and spatial distribution. This cannot be identified by the means illustrated in figures 4.27 and 4.28, which confirms the statement of the disproportionate behaviour of precipitation mentioned by HEGERL et al. (2004) (see above) and shifts responsibility to a strong discrepancy of modelling of extreme amounts, as already depicted by figures 6.1 and 6.7.

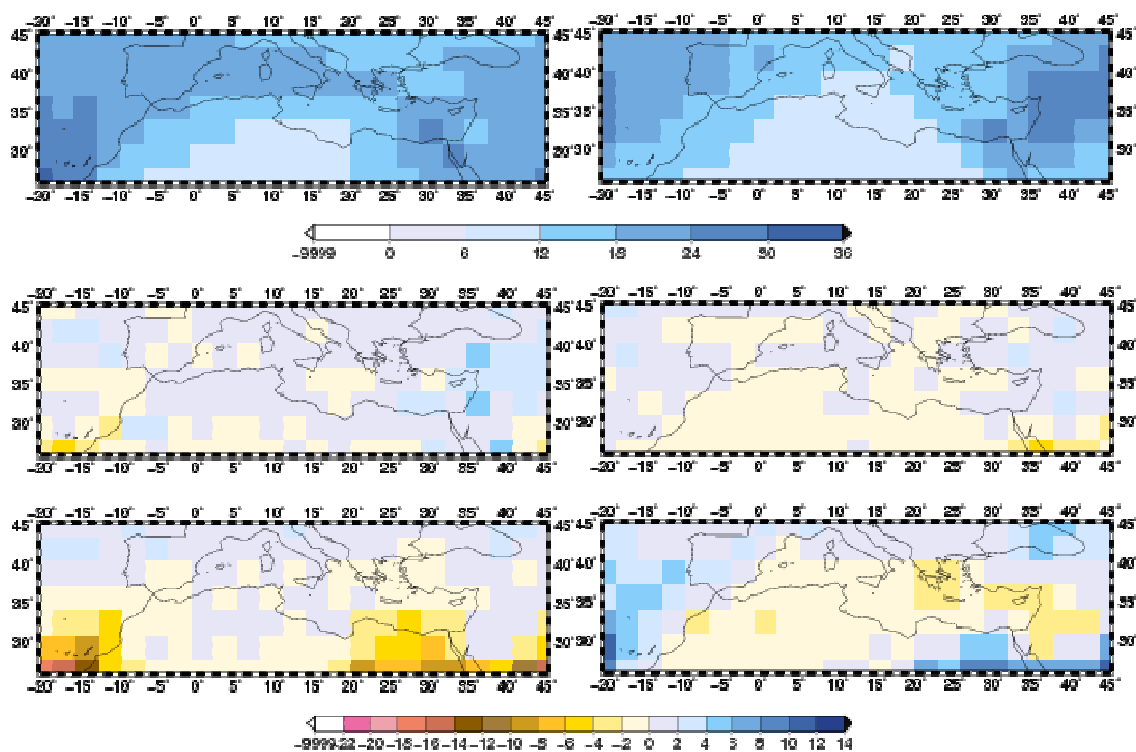*Figure 6.8: Multi-model mean of R95T [%] in the A1B scenario. Uppest row: Means for 1981-2000. Middle row: Differences of the means of (2046_2065)-(1981_2000). Lowest row: Differences of the means of (2081_2100)-(1981_2000). Left: Summer; Right: Winter.*

Considering R95N, in the multi-model mean, a spatially more specified pattern becomes evident (figure 6.9) comparing the pattern given by the ECHAM5 ensemble in figure 6.4. Irrespective of the correctness of this projection, the application of several models exhibits a more reasonable spatial distribution with respect of the nearly randomly scattering of one model. Obviously, over all the utilized models, some grid-cells are more or less sensitive to the number of extreme events becoming apparent in the multi-model average. Furthermore, some regions, offering between 3 and 4.5 events, are also depicted by REMO as regions with less events in winter, i.e. North Africa or the southeastern coast of the Iberian Peninsula (HERTIG et al. 2012). Again, the multi-model mean contrasts ECHAM5 within the typical spatial distributions specific to seasons, as they seemed to be changed. Furthermore, an increase of days with heavy precipitation amounts is projected, while ECHAM5 models decreases. Also the sensitivity between these two seasons is rather pronounced in winter for the multi-model mean, showing transient growing of R95N.
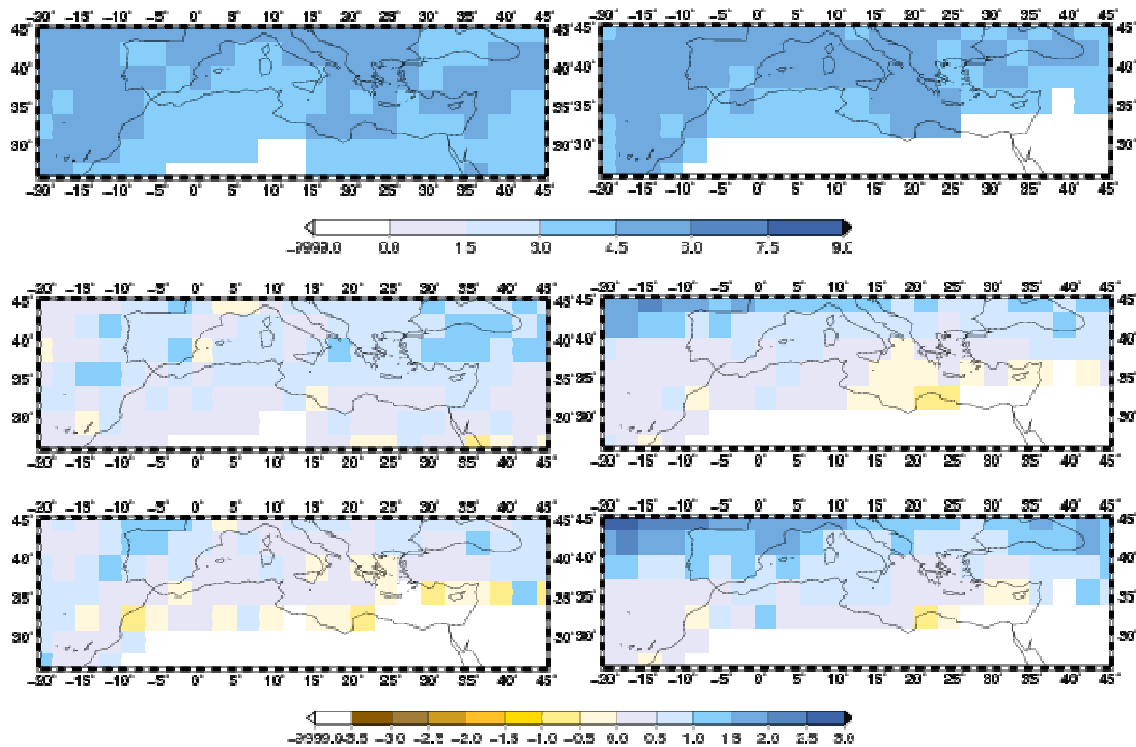
Figure 6.9: Multi-model mean of R95N [d] in the A1B scenario. Uppest row: Means for 1981-2000. Middle row: Differences of the means of (2046_2065)-(1981_2000). Lowest row: Differences of the means of (2081_2100)-(1981_2000). Left: Summer; Right: Winter.

As already mentioned above, the intensities exhibited by the multi-model mean (figure 6.10) are less than the intensities by ECHAM5. The reasons for this are manifold, as interpolation procedure diminishes extremes. Furthermore, the computation of averages smoothes the extremes. Also the dipole structure is dissolved. This is in contrast to R95N, where a more illuminative pattern is produced by the multi-model mean. The projections of lower amounts and higher number of days by the multi-model mean, compared to ECHAM5, justify the smooth results. The sensitivities show intensity changes of few mm in both directions, where particularly for summer an interpretable pattern is neither obtained for 2046-2065, nor for 2081-2100 in the specific relation to 1981-2000. Possibly, in winter one can derive an increase of the intensity for the land surface surrounding the Mediterranean Sea and in the north of the area of investigation, whereas the differences are low and might deceive this interpretation.
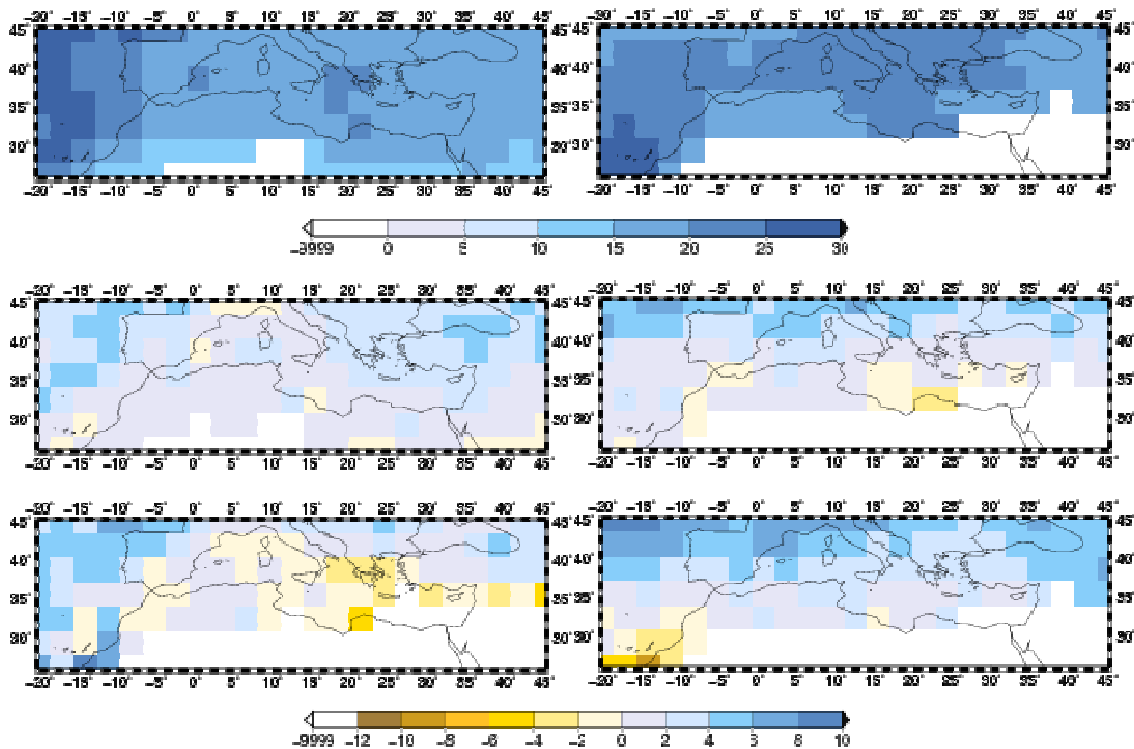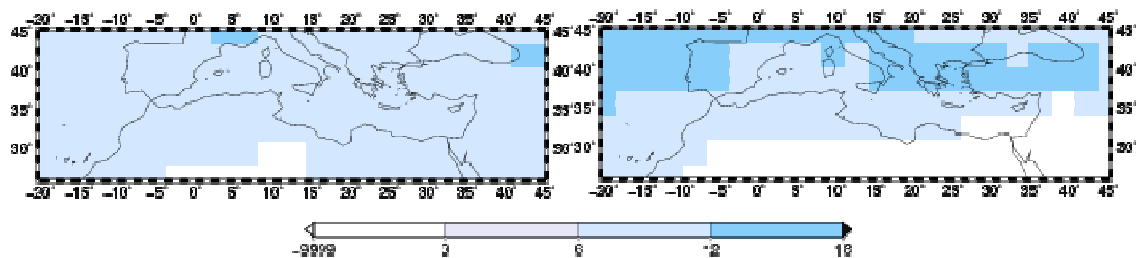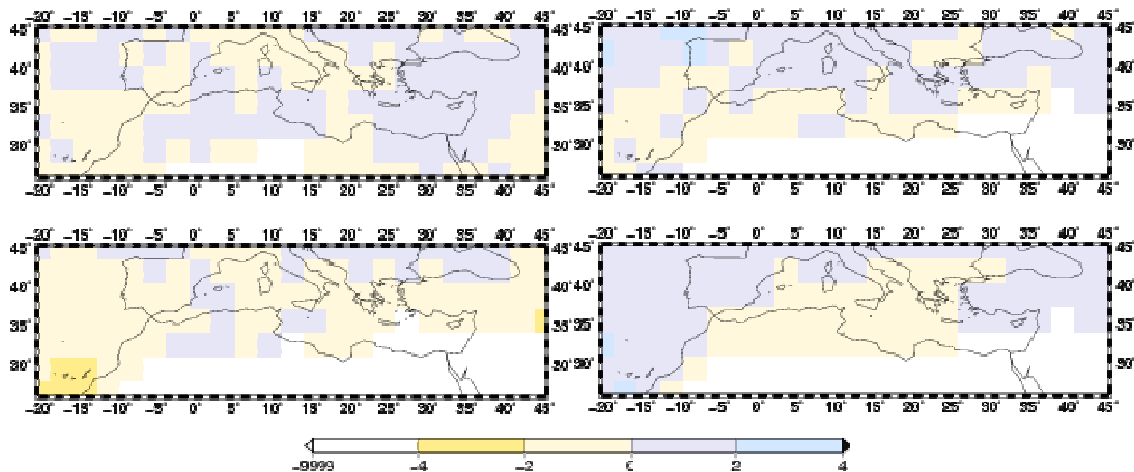
Figure 6.10: Multimodel mean of SDII95p [mm/d] in the A1B scenario. Uppest row: Means for 1981-2000. Middle row: Differences of the means of (2046_2065)-(1981_2000). Lowest row: Differences of the means of (2081_2100)-(1981_2000). Left: Summer; Right: Winter.

6.2.3 Conclusion

Due to the smooth resulting values of the multi-model mean, the model discrepancies play a prominent role. Still, a detailed investigation of the frequency of wet days and of their intensity on rainy days by GCMs is recommended, with the intention to get a closer insight of the specific projection of precipitation by the models in general. These discrepancies also clearly affect the extremes. As chapter 4.2.2 is already implying, the future projections of precipitation are quite heterogeneous across the models. This holds for all seasons, but particularly for winter, where large-scale steering is predominant, while in summer again the impact of the parametrization schemes, resolving small scale processes like convection, may prevail. Particularly the latter finding justifies the consideration of the multi-model approach.

ECHAM5 shows an east–west dipole of R95AM in future means. Considering sensitivities for R95AM, ECHAM5 shows decreases in the regional average, whereupon the highest reductions in autumn can be confirmed by former studies (HERTIG et al. 2012). Strongest effects become evident in the eastern MA, with seasonal alterations of the prefix. Most of these results are pronounced in the differences to the later future period, besides summer, when a slight local increase of heavy precipitation is substituted by an overall strong decrease. Arranging ECHAM5 into the multi-model mean, the MPI model is overruled by the other models, which agree on slight increasing values with no characteristic spatial patterns, neither in means, nor in sensitivities, besides some small north-south differences. Also sensitivities between the two different future periods can hardly be depicted. In recent literature, results are divergent as well. In the western MA results of extreme-value analyses have been very contradictorily. On the one hand, ALPERT et al. (2002) reported a significant upward/downward trend of heavy/moderate precipitation, using the threshold method, particularly for Italy. These results are confirmed for the eastern MA by NORRANT & DOUGUEDROIT (2006). Using percentiles, RODRIGO (2010),

NIKULIN et al. (2011), LOPEZ-MORENO et al. 2010 found opposite results in historical datasets over the Iberian Peninsula for all seasons. This rather resembles to the results, which are found within the underlying study.

While the total amount of precipitation is reduced, R95T, which depicts the percentage of the extreme precipitation to the total precipitation, is only affected to a lower amount. In summer ECHAM5 also exhibits increases, which particularly holds for the north. Concerning ECHAM5, the high percentages of the amount of extreme precipitation are due to a low number of rainy days, accompanied by general low precipitation amounts and high overall intensities. Particularly these values are in a sharp contrast to the multi-model mean in both, seasonal and spatial pattern, which is not reflected by differences in the trends of the overall precipitation amounts as they behave relative similar.

For the number of days (R95N), which show heavy precipitation, the geographic pattern is more diverse for the multi-model mean, compared to ECHAM5. In contrast to the amount of extreme precipitation, the projection seems to become more sharpened. Again, ECHAM5 is placed aside the overall projection of the models, though their spread is relatively high (not shown), resulting in small changes in average towards future periods.

Considering the intensities (SDII95p) of heavy precipitation, ECHAM5 can be assigned to models, which project higher intensities. This is also reflected by the lower intensities of the multi-model mean, whereupon the spatial distribution is less meaningful due to the smoothing of extremes. One still has to concern the ratio intensities are calculated with, i.e. R95AM and the number of days extreme precipitation occurs, where the higher amount of R95N across the majority of models (in contrast to ECHAM5) gives some reasonable explanation.

While ECHAM5 shows mainly a reduction of extreme events in the MA, the multi-model mean exhibits slight increases, particularly for the number of days and the precipitation associated with high amounts (R95T). For SDII95p changes can hardly be detected by neither ECHAM5, nor by the multi-model mean associated with the different projections of the involved fields.

6.3   Application of an Anova on extremes

In the following chapter a spatial ANOVA of the mean percentiles has been conducted. For this application a persistent slice of time is not available, as discussed in chapter 3.2. This prohibits the application of the ANOVA in the already described method (chapter 5.3.1). Concerning extremes, it is decided to account for the variability between and within the specific time periods. Consecutively, this is done once for the variability of 1981-2000 and 2046-2065 and secondly for 1981-2000 and 2081-2100. As the formulae in theory are the same as described in chapter 5.3.1, they are not repeated here. Yet, the inputs are substituted, leading to another approach, which is explained in the following passage.

First of all, the multi-model means have been calculated. As it is not the purpose to compute for the variability within the individual realizations of different models, all realizations, independent of their model and its ensemble size, are averaged, instead of the procedure concerning the ensemble-means, as it has been done above. The number of realizations depends on the model. Thus, models with several members now have a higher impact on this weighted mean. It will be referred to this mean as multi-realization mean to contrast it from the former denotations. This mean is furthermore averaged over the specific yearly steps, which are 20 years for each period. Afterwards, the reference period and the future period is averaged again, building up an average value for once 1981-2000 and 2046-2065 (period1) and secondly 1981-2000 and 2081-2100 (period2). The following procedure is then fulfilled in dependence of the specific grid-cells, period1 and period2, the considered season and the demanded field. In this case the number of runs i are 1,…,I, where I is 22 (table 3.3), with j time-steps from 1,…,J, where J is 20 and the 2 periods K.

SSα shows the square sums, which are calculated out of the differences of the realization mean of one specific time period, e.g. at first 1981-2000 and secondly 2081-2100, and the realization mean over both periods, which is in this case the mean over period2. Consecutively, the α-partition describes the amount of variability, which is dedicated to the differences between these two temporal slides. SSβ is computed out of each realization, which is denoting the average over period1 or period2 minus the multi-realization mean over the considered period. Finally, the β-partitions inform about the amount of the discrepancies of the realizations to the overall mean. The formerly denoted temporal lag of reaction of the different models (SSγ), is now substituted by the information of the amount of temporal alteration of the specific realizations to the overall variability. This is rather complicated and consecutively provides statements on how strong the specific realizations alter between each other over two different periods. The formula is derived analogously to formula (40), whereat here, the multi-realization mean of one individual period and the mean of period1 or period2 of the considered realization are subtracted from each specific realization mean in one of both sub-periods. Finally, the multi-realization-mean of period1 or period2 is added. SSε is calculated by the difference of the individual realization means over each of the considered periods and the original data, which is dependant on one of both of the comprising slices, the realization and the individual years inherent to this specific period. This is again synonymic for the partition of variability, which cannot be explained, as the individual yearly steps are involved. Thus with SSε, the temporally short variations are computed within each period and each realization. With these sums of squares, again the percentage of the contributing partition is analogously calculated to the formulae (47-50). Overall, all of these mentioned partitions again aggregate to 100% of the total inherent amount of variability. Afterwards, tests of significances are applied with methods described in chapter 5.3.1 in formulae (51-53).

6.3.1 Results

In figure 6.11 the percentages of the individual contributions of the variance to the total variance are displayed for R95AM. As one can depict, the partitions given by the variability within the periods are close to zero. A seasonal alteration is not given. This low temporal variation can be identified by the low differences between the means in figures 6.6 and 6.7, whereat in the latter figures the multi-model-means have been calculated instead of the multi-realization means. For the β-partition, in some areas the 50% threshold is nearly reached, which holds particularly for the warmer half of the overall year. In spring and winter this contribution declines and here, particularly over the central regions, while highest partitions are found over the Atlantic Ocean and the southeastern areas. This defines the discrepancy of the individual realizations to each other, being particular high in summer and here over areas with a sparse distribution of a spatial observation network. Thus figure 6.11 reminds of figure 5.15 and its α-contribution, highlighting that the found discrepancies of the models concerning average precipitation also apply for the amounts of extreme precipitation. It must be emphasized, that information of a probably evident signal of forcing impact is divided into the α- and the β-partition, as β comprises the averages of the reference period and the future period. Consecutively, the sum of both partitions provides advices of changing climate concerning extremes due to anthropogenic emissions.

Figure 6.11: 2-way ANOVA of R95AM for pre in the A1B scenario between the two slices 1981_2000 and 2046_2065. From top to bottom: Spring, Summer, Autumn,

Winter. Left: α-partition Right: β-partition.

The interaction coefficient in the γ-partition intermittently shows values up to 30%, defining the yearly temporal variation of the different realizations to each other with respect to the overall time (left column in figure 6.12). In autumn some grid-cells with high percentages can be found, where no distinct explanation can be provided. As these grid-cells are isolated, this may be dedicated to random effects. The residuals, which are depicted in the right column of figure 6.12, contribute the majority of the total variability, which is dedicated to the specific yearly temporal steps. Concerning the amount of extreme precipitation, the individual yearly variation is more influential in spring and winter.

Figure 6.12: 2-way ANOVA of R95AM for pre in the A1B scenario between the two slices 1981_2000 and 2046_2065. From top to bottom: Spring, Summer, Autumn, Winter. Left: γ-partition Right: ε-partition.

To give insight of probable changes considering further future periods, analogous figures are presented for period2 (figures 6.13 and 6.14). Again, the α-partition is relatively weak, but this time a few spots up to 15.7% are exhibited, which depict a quantitative measurement of changes of the extreme amount of precipitation within the two periods of 1981-2000 and 2081-2100. Still their distribution is not regular across the seasons. The β-partition again is considerable, whereat the amounts are less than in the first period, identifying the higher agreement over the individual realizations. At least, this holds for all seasons except for summer, where highest values are reached over the Atlantic

178

Ocean in the northwestern corner of the area of investigation with up to 62.8%. Consecutively, the challenge of parametrizations and initial conditions abates with respect to a pronounced change of climate conditions until the end of the 21st century, while the difficulty in the projection of sparse summer precipitation and the extremes aggravates.
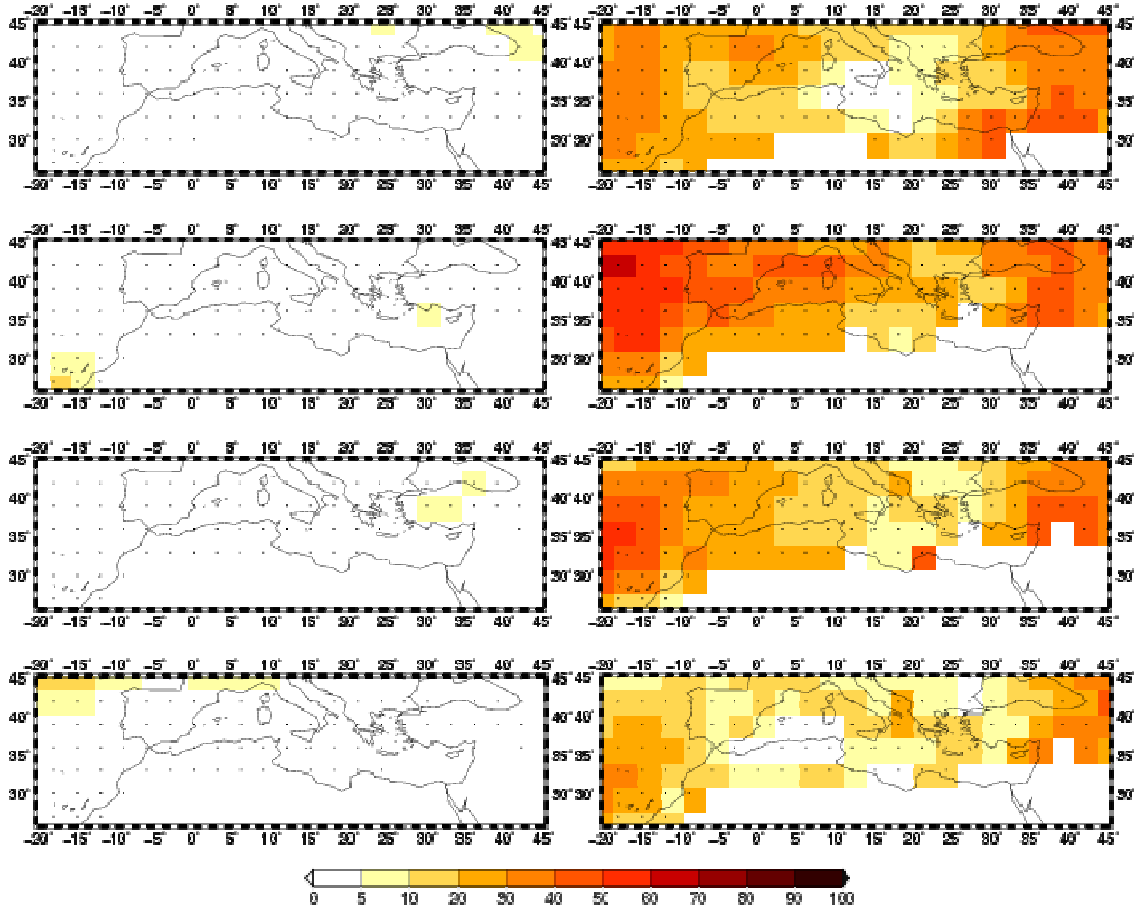
Figure 6.13: 2-way ANOVA of R95AM for pre in the A1B scenario between the two slices 1981_2000 and 2081_2100. From top to bottom: Spring, Summer, Autumn, Winter. Left: α-partition Right: β-partition.

Besides summer, the contribution within the ε-partition dedicated to the annual variability is supposed to be diminished in the later period. This is established by a particular increase of the γ-partition. Consecutively, the interannual variability is projected to decrease for extreme precipitation. Still, it must be emphasized, that the comparisons between the analyses are conducted qualitatively and only exhibit small differences. The temporal variation between the realizations within the time is increasing, which reveals a different reaction on changes for extreme precipitation.
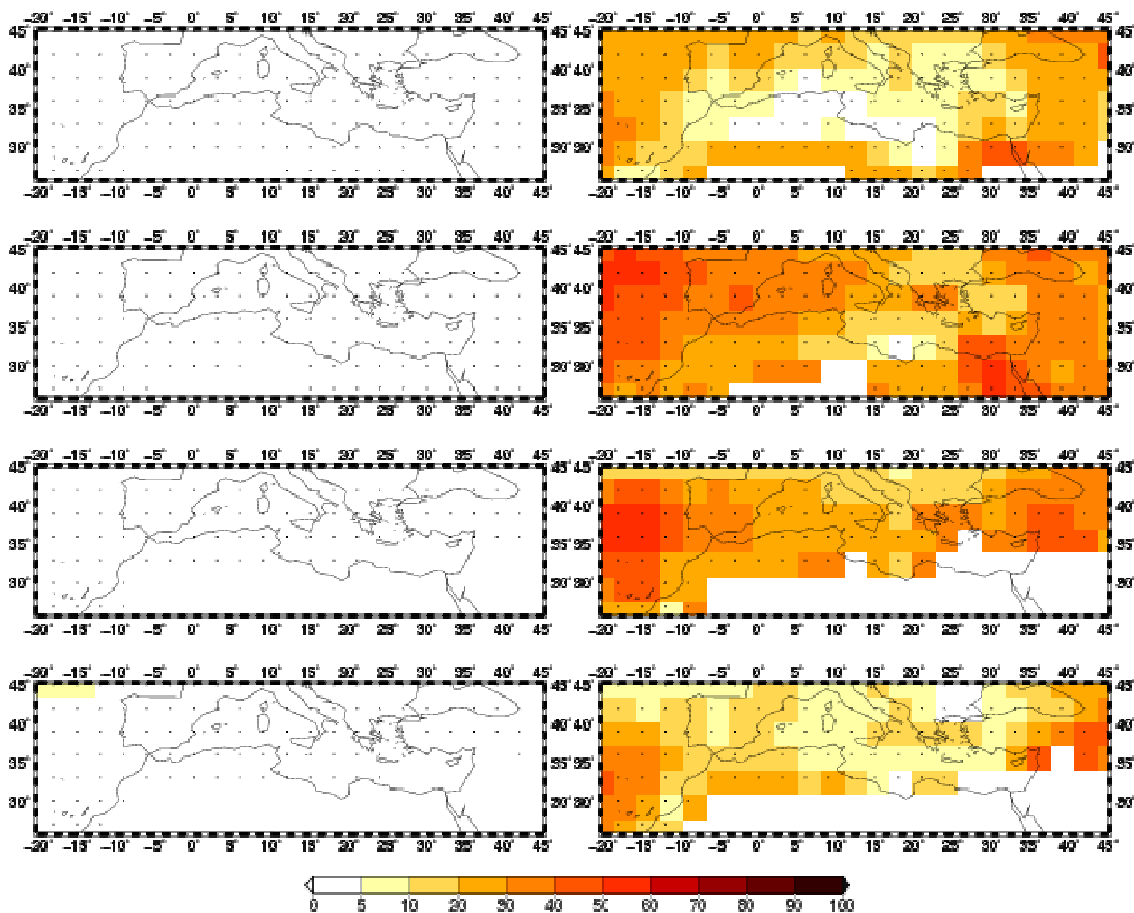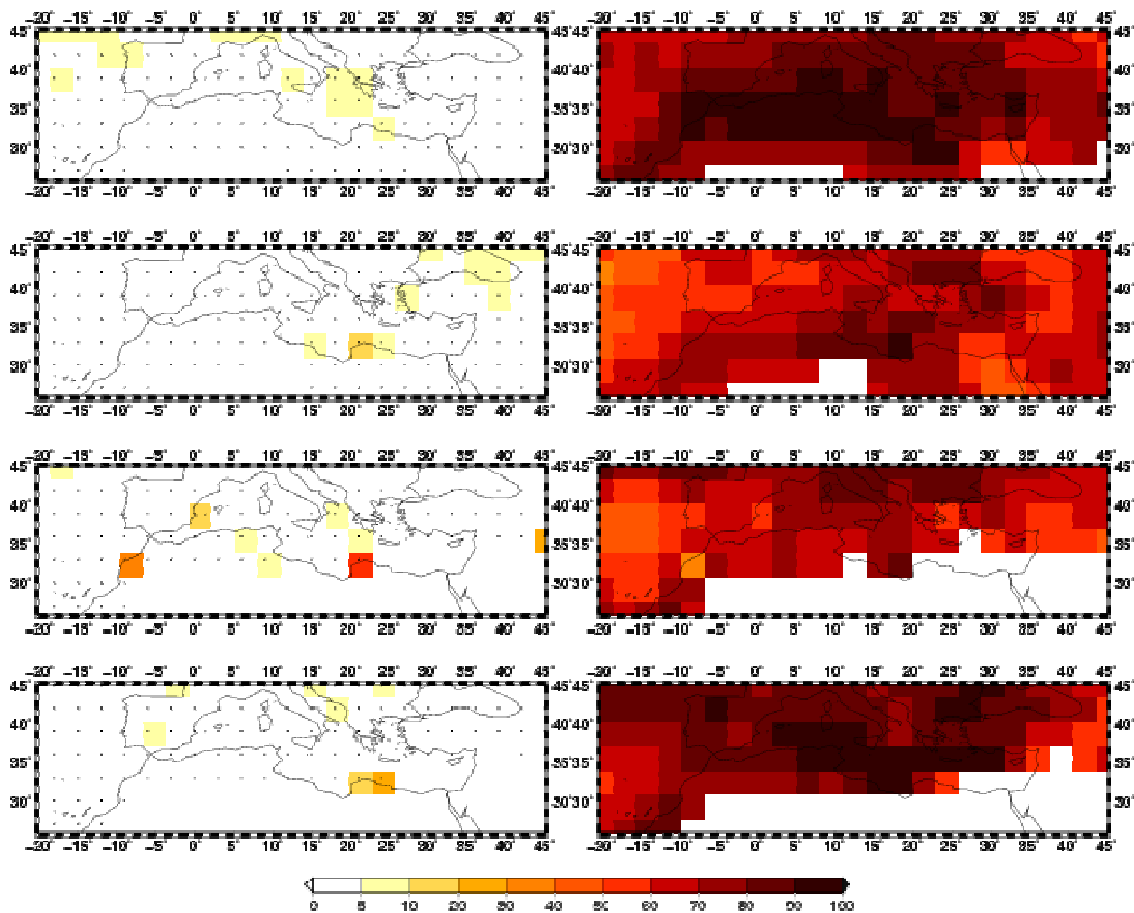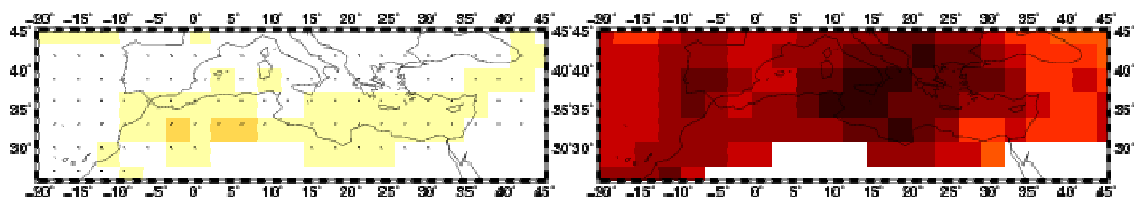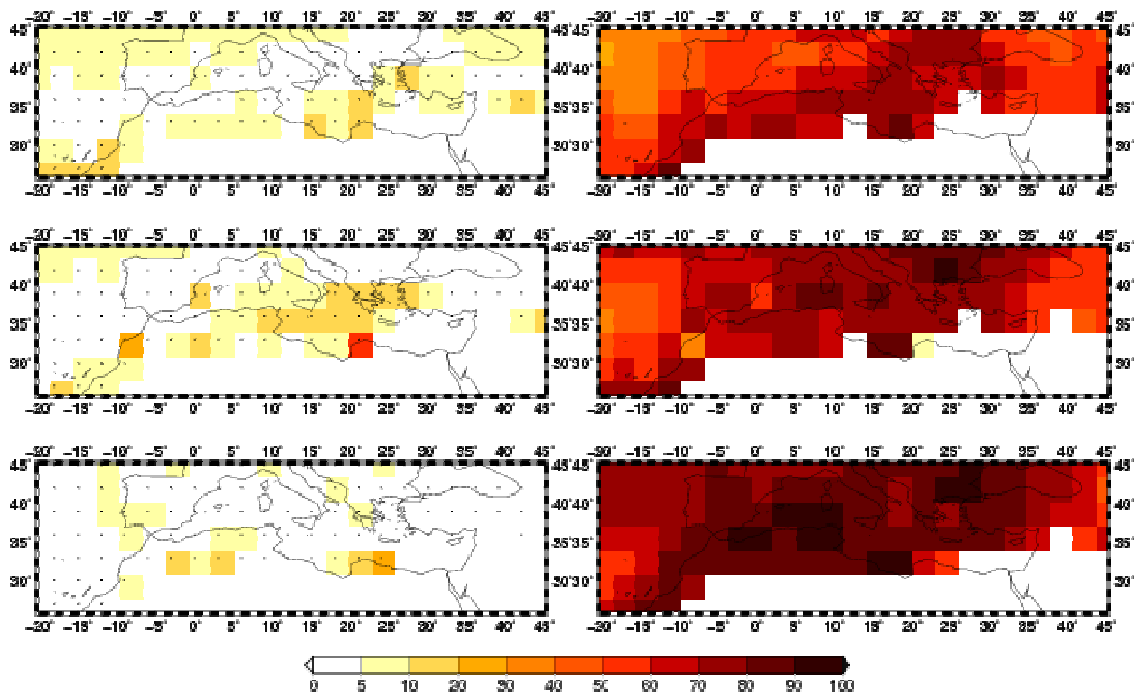
Figure 6.14: 2-way ANOVA of R95AM for pre in the A1B scenario between the two slices 1981_2000 and 2081_2100. From top to bottom: Spring, Summer, Autumn, Winter. Left: γ-partition Right: ε-partition.

The spatial pattern is hard to interpret, whereat one should not forget, that the spatial distribution of the extreme fields is not distinct within the results of the means and the sensitivies for individual models (e.g. ECHAM5) or the multi-model mean in chapter 6.2. Furthermore, as already discussed, spatially innate results of future courses of extremes could not be found by former times, when different studies are compared. These uncertainties are even aggravated by the investigation of extremes, which are simulated by GCMs. Consecutively, the ANOVA accomplished for the other three variables of extreme precipitation (R95T, R95N and SDII95p) are depicted for regional averages.

But first of all, the comprising regional averages for R95AM of the four individual contributions of variability are displayed by figure 6.15. The two analyses, assigned to the two periods of 1981-2000 with 2046-2065 and 1981-2000 with 2081-2100 are shortly described as 2046-2065 and 2081-2100 respectively. The predominant partition of the ε-contributor particularly becomes evident in winter. The increasing percentage of the β-partition in summer conducts to a higher impact of individual parametrizations. These are dedicated to the diverse models, which are inherent in this approach, as they are represented by their realizations. In contrary the different initial conditions, reflected in the ε-contributor, are more emphasized in winter. Again, it must be noted, that these results are derived from sparse data and depict the changes in extreme precipitation. A change in extreme precipitation is particularly exhibited in summer, as the common signal, derived by the sum of the α- and β-contributions, accounts up to 35.4% in summer in the combined period of 1981-2000 and 2081-2100.

180

Figure 6.15: Regional averages of the contributors in the 2-way ANOVA for summer and winter for the different periods of R95AM.

Figure 6.16 highlights the regional ANOVA results of the number of days, where precipitation amounts above the 95th percentile are occurring (R95N). The ε-partition again is predominant, showing much higher impact on the total variability than for R95AM. Thus in the A1B scenario, the variability of the individual years on the days with heavy precipitation superimposes the signal of an anthropogenic change of extremes, as this impact is depicted by the α- and β-partition summing up to almost 10%. Here, the impact of different periods is higher than that of the season. Still, the discrepancy between the individual realizations with its various models is higher in summer, while a temporal treatment, as indicated by the α-partition, becomes higher in the colder season.

Figure 6.16: Regional averages of the contributors in the 2-way ANOVA for summer and winter for the different periods of R95N.

The percentage of amounts dedicated to extreme precipitation to the overall precipitation sum and the variability in the multi-realization approach over different time periods can be extracted from figure 6.17. Consecutively, the changes of this field again are displayed by means of percentages to the total variability by the α-partition. Again, this partition is the lowest contributor. Accompanied with the β-partition, an overall signal of at least 10% can be derived for nearly all seasons, except for winter for 1981-2000 combined with 2046-2065. As the multi-model mean describes in figure 6.8, this signal is subdued by a shift of the overall precipitation amounts towards extreme events. Again, the signal is enforced towards the end of the 21st century. The γ-partition is considerable again, denoting the increasing temporal spread of the individual realizations within their different time periods towards the later future.

For SDII95p the model discrepancy becomes the predominant factor (figure 6.18). This is an interesting result, as it is due to the different parametrization schemes of the models, though, one must not forget, that this approach is not conducted by different models, but by different realizations, which at least are associated with various models. Consecutively, the parametrization has more impact on the intensity of heavy precipitation, than on the number of events with heavy precipitation (R95N). For the latter the ε-partition is predominant, which might depict the interannual variability and thus e.g. the NAO. In contrast, precipitation intensity is rather steered by local characteristics and hence reproduced by parametrizations, which are specific for the individual models. The signal again becomes more distinct in the later period. Despite the lack of the ability to reproduce small-scale features by the GCMs, the presented results clearly indicate, that also GCMs, besides RCMs and statistical downscaling

assessments, differ in the reproduction of the steering factors, i.e. the interannual synoptic variability and local effects.
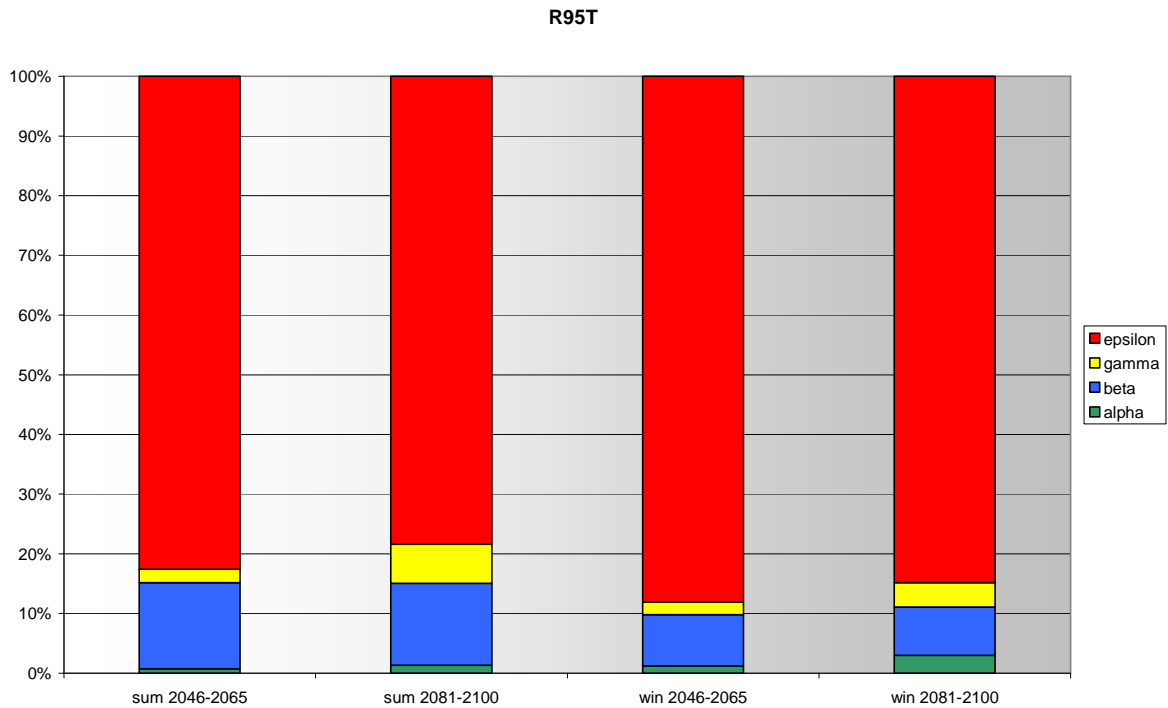
R95T

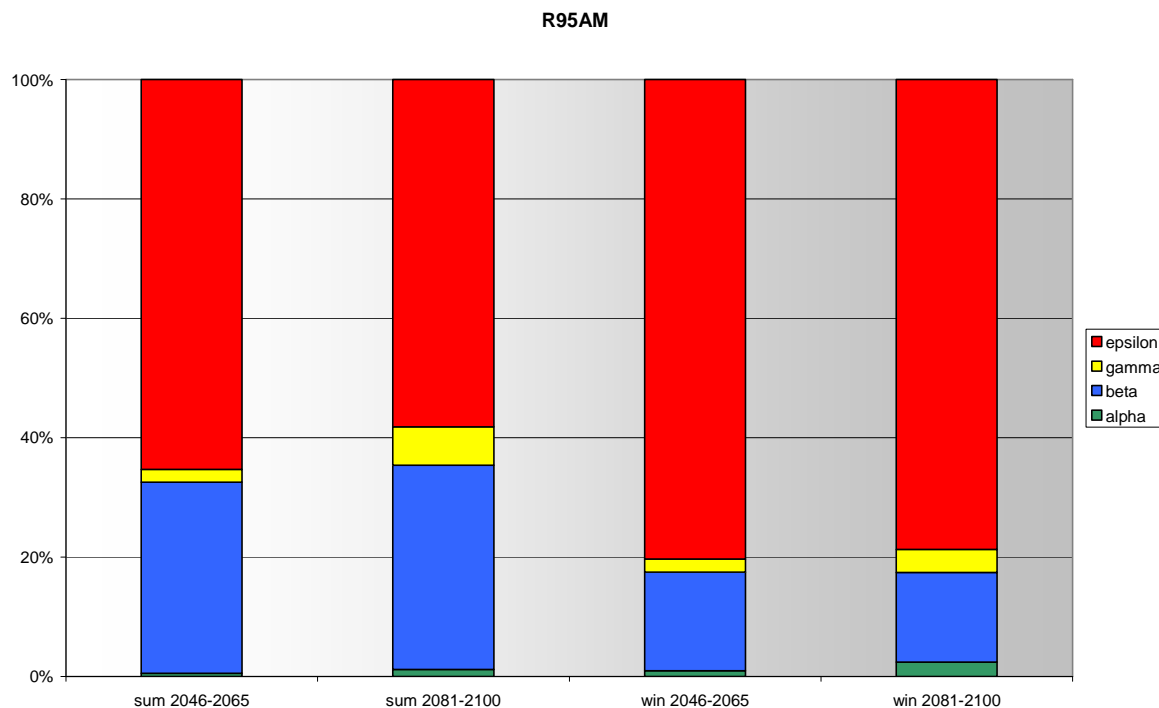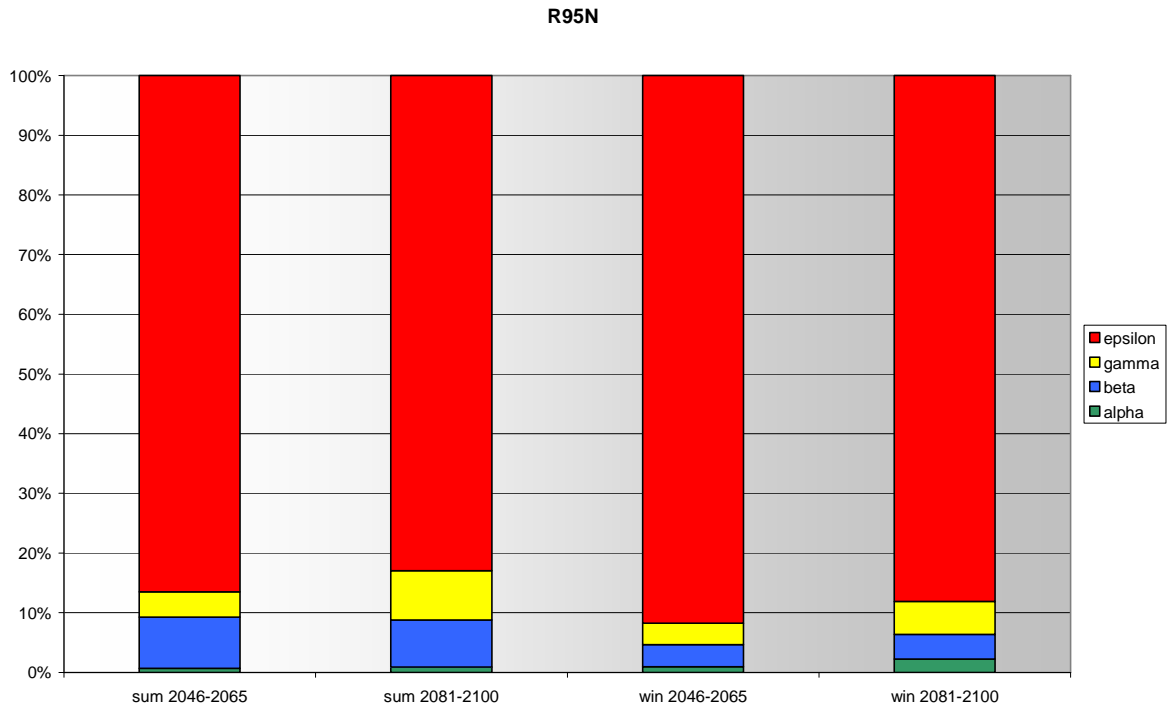*Figure 6.17: Regional averages of the contributors in the 2-way ANOVA for summer and winter for the different periods of R95T.*
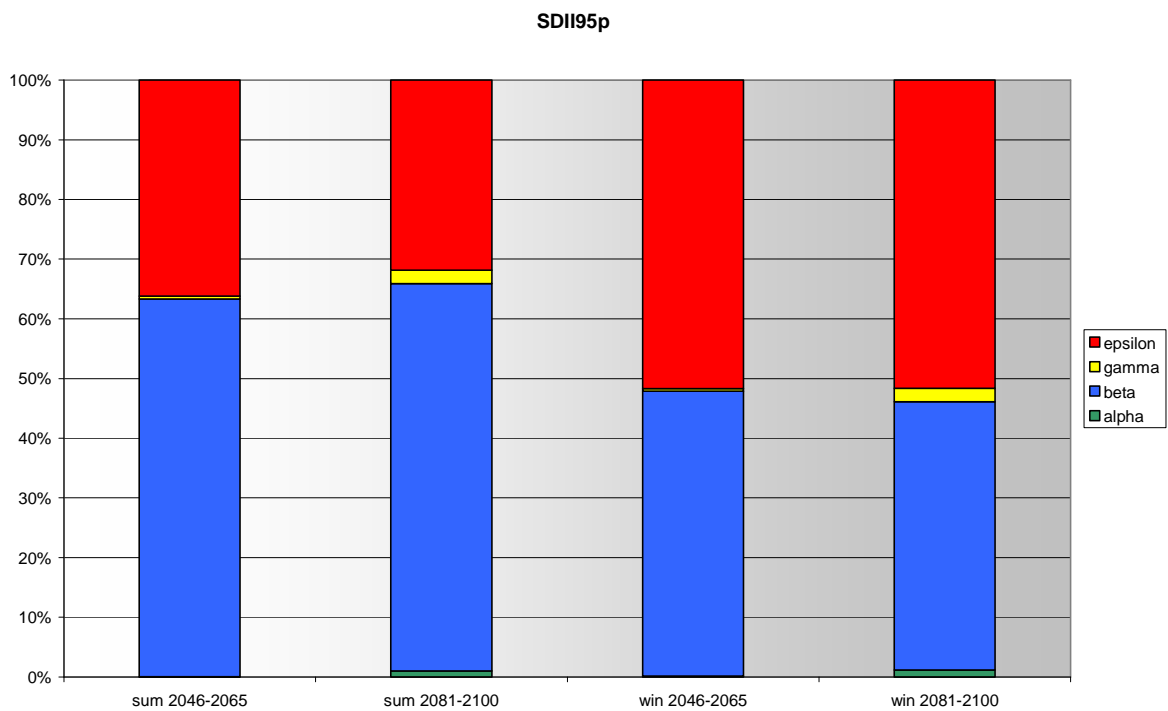
SDII95p

Figure 6.18: Regional averages of the contributors in the 2-way ANOVA for summer and winter for the different periods of SDII95p.

183

6.3.2 Conclusion of the Signal Analysis on Extremes

The underlying chapter describes one of the first attempts to quantify changes in precipitation extremes, which are induced by climate change. For this, several GCMs have been subordinated to the investigation with a 2-way ANOVA. Though, the constraints of the simulation of extremes by GCMs, e.g. by their coarse spatial resolution, are kept in mind and have been discussed in the former chapters, GCMs also should be involved to analogous investigations of extremes, which have come more and more to the centre of attention in the last years in climate sciences, as GCMs provide the groundwork of future climate assessments. Still further constraints, like non-transient data-series, prohibit an application like it was demonstrated in chapter 5. Also in the mean values, GCMs show a small common course, which even cannot be accentuated with a normalization procedure of the models onto a common level. Concerning these constraints, the results provide only remote insights, though a few conclusions can be drawn, which are not inconsiderable.

For nearly all of the variables, the ε-contribution is highest, followed by the β-partition. The only exception is given by the intensity of heavy precipitation, denoted by SDII95p, where the model discrepancy (β) accounts for the highest amount of variability. Still, this is only the case for summer, while in winter the residuals overcome the β-partition. Completion is given by the following γ-contribution and α-contribution, where the latter denotes, besides the β-contributor, the signal evoked by external forcing and a shift in the future characteristics of extremes. Generally, for the alterations of seasons, variations in the different partitions of variance are discernable, though the sequence of the participating factors is not changing, despite the mentioned case for SDII95p. This latter result implies the conclusion of a stronger impact of model discrepancies in summer, while in winter the residuals have stronger impact. Again, this confirms the results from the ANOVA on the monthly means, e.g. figure 5.24, where precipitation also exhibits a seasonal alteration of the different contributors. Again, individual parametrizations of the models, e.g. convections schemes, may determine these contributions. So, one has to be aware, that in the approach of the chapter at hand no separation of the models in designed categories has been fulfilled. Still, various models are involved by the utilization of the multi-realization mean. While interannual variability is effective for winter extremes, the parametrizations come to the fore in the rather dry summer. Furthermore, a general signal, which is also expressed by the α-contribution, is higher for the warmer season, which cannot directly be dedicated to the reaction on an external forcing, as the sensitivities displayed in chapter 6.2 do not exhibit a stronger effect by changes in summer time. Taking the later future into consideration, one experiences a decrease of the impact of the biases between the realizations and a decrease of the residual partition, while the α-partition and the formerly denoted interaction coefficient gain more influence. Considering the α-partition solely, a common signal, as a reaction on external forcing is still low, though increased. Still, such a signal is also hidden within the β-contribution. Finally, the signal indicating overall change cannot be clearly distinguished within this approach. A spatial distinct pattern is not cognoscible, which is not remarkable, as already the means and sensitivities do not offer reasonable distributions of values overall (chapter 6.2.2).

Again, it must be stated, that this is one of the first quantitative attempts of detecting uncertainties of extremes simulated by GCMs, which consecutively requires several follow up studies dealing with this issue again in order to disapprove or confirm these first findings.

7   Conclusion

The following chapter concludes the underlying work by recapitulating the mentioned premises about climate models and the area of investigation and by summarizing the presented results. Afterwards, a final discussion is constituted, which combines the information reflected in the depicted results, embraces the mentioned abiding questions and provides recommendations on future climate investigations.

7.1   Results

The underlying chapter summarizes the considerations, results and findings made in this study.

The study is fulfilled in the Mediterranean Area, as this sub-continental region provides strong heterogeneities concerning its physical geographic conditions, which have complex effects on the local climate conditions. This complex climate recommends to subordinate the climate variables temperature, precipitation and sea-level pressure to the research, which is done here. Furthermore, the MA is located in a transitional region between subtropical high pressure zones and mid-latitude dynamics with the impinging west winds. Additionally, the impact of these two steering factors alternates within the seasons, advising a detailed seasonal approach. Also, preliminary considerations raise expectations of strong trends with low natural variability. This is accompanied by comparatively low model uncertainties, because of the relatively high knowledge about atmospheric realities, which is provided by the observational station density. Finally, the high vulnerability, e.g. given by the high population density or by the naturally limited availability of water, requires a focus of climate studies in the MA.

Being the fundamental data source of comprehensive future climate studies, General Circulation Models have been chosen to be consulted regarding the issue of a designated climate change in the MA. The strong benefits of GCMs, e.g. the potential to assess for climate variability and the opportunity to distinguish different individual processes being effective on the entire climate system and the supply of continuous data series, justify and recommend their application. Still, the uncertainties inherent to the projections have to be considered. These uncertainties develop from unsufficient model physics and parametrizations, discrete resolutions, model adjustments, unknown initial conditions and different forcing scenarios. The mentioned handicaps are delivered to statistical and dynamical downscaling methods, which demands an elaborate precedent investigation and quantification of these uncertainties inherent to GCMs. Following this aim, the results of the individual realizations of the GCMs have been interpolated to a concerted 3x3° grid to facilitate quantitative comparisons.

Furthermore, consistently interpolated reanalysis datasets have been involved and put into context to the results of the models in the reference period from 1961-2000, where models are forced by observed greenhouse gas emissions by the 20c3m scenario. It is shown, that the spread between two reanalysis datasets is at evidence, which holds particularly for precipitation. Nevertheless, the bias between the most extreme models is superior, whereat still many models perform between the gap of the reanalysis datasets. This finding at least holds for regional averages of the whole MA, whereat for more detailed research, e.g. spatially resolved values or trend analyses, the results are partially altered. Also with an exchange of the simulated variables, the modelled values might be out of the range of the reanalysis data, as e.g. for sea-level pressure all models overestimate the reanalysis data in the regional mean and underestimate the regional averaged trend. Still, all the models exhibit reliable averages in their mean values concerning the reference period with an authentic seasonal dependency. Applying a spatially detailed investigation on the mentioned grid, the models show reasonable distributions of projected values, i.e. a decrease/increase of precipitation/temperature from the north towards the south. Also for sea-level pressure the models exhibit meaningful local arrangements of zones of lower and higher pressure, which is e.g. displayed by the depressions in the southeastern MA in summer. Also the distribution of temperature and precipitation values is altered latitudinally within the sequence of the seasons. One also recognizes a slower seasonal reaction of temperature values over sea-surfaces, which are warmer in winter and cooler in summer than land-surfaces. To tie in with aligned studies, ECHAM5 plays a crucial role in this work. Besides the investigation of the other models, it can be stated that ECHAM5 behaves somewhere in the middle of their projected values, which holds for most cases. By the computation of the average of all models the multi-model mean is investigated. As expected, particular results of specific models are vanished by this smoothing process. Still, the multi-model mean combines the information presented by all the models and thus, it is a crucial indicator of modelled climate projections.

Concerning trends in the reference period, all models and reanalysis exhibit an overall warming, while the spatial diversity is very heterogeneous and also exhibits local and seasonal cooling particularly in the reanalysis data. For precipitation a slight drying is prevailing in winter, which is reflected by many models but only can be spatially allocated within the reanalysis data. No definite signal can be assigned to the models for sea-level pressure, while the reanalysis data show distinct increases and here mainly in the cooler seasons. To maintain the comprising approach, the behaviour of the models on different scenarios, i.e. the B1, the A1B and the A2 scenario, have been analysed for future assessments. For 2001-2098 the models show distinct changes to the mean values depicted in the reference period, whereat seasonal and latitudinal distributions remain reasonable. Meaningful trends superimposing the enduring perturbation by natural climate variability, which is naturally also reflected in the simulations, come to the fore in future, whereat these trends are governed by the strength of the underlying forcing scenarios. The characteristic of these future trends also strongly depends on the variable, whereat temperature exhibits the most expressive trends, as temperature is one of the most crucial and homogeneous variables. Here, all analysed models project warming, while for sea-level pressure the models even show a different prefix. Seasonal

analyses illustrate amplified or diminished trends, with e.g. strongest warming in summer, while the season with the strongest amplitude of the trend for precipitation depends on the model. Generally, models´ projections exhibit an overall decrease of precipitation with no clear seasonal tendency. Still, the belt of prevailing drying is latitudinally shifted over the seasons. Strongest drying is projected over the Iberian Peninsula. For temperature spatially differences are mainly due to land areas and sea-surfaces, whereat in the latter warming trends are lower. To obtain meaningful spatial distributions for sea-level pressure, one has to investigate seasonal patterns, as the prefixes of the trend for the warm and the cool period are opposite and extinguish each other for investigations of the overall year. This again justifies the seasonal investigation. Other parameters defining the trends are the time periods and their length. E.g. in the reference period from 1961-2000 trends of temperature are relatively low, compared to the strong signals, which e.g. are reflected for the future period of 2001-2098 in the A2 scenario. Considering these findings in general, it becomes obvious that the different aspects may lead to very different results justifying this comprehensive investigation. Only a detailed approach, as it is done, can highlight the specifics of the considered aspects like spatial heterogeneity, the seasonal alterations, the different scenarios, the different models and datasets, the time period and its length these analyses are conducted in and the differences in the behaviour of the variables. Naturally, these different aspects of investigation alter each other and may be weakened or enforced in specific combinations.

Supporting decisions-makers, stakeholders and policymakers and to have determined expectations on what is to come, uncertainties have to be accounted for, to provide at least some kind of probability of error. Though, by simple qualitative comparisons many of these sources can be determined, e.g. all models exhibit equal developments of trends for temperature or e.g. the dispersion of average precipitation over all models is very high, sources of uncertainties are still manifold and need to be quantified. A possibility is provided by an analysis of variance. It calculates individual contributions of variability and sets them into context to the total amount of variability. This method has been conducted on individual GCMs and the assembly of all the models in spatially and temporal approaches. Again, results depend strongly on the different aspects of investigation, which is also stated by seasonal and yearly applications for individual variables and an alteration of the forcing scenarios, prohibiting general conclusions. Still, the bias between the models, denoted as α-contribution, has strong effects as a part of the total amount of variability, whereat for precipitation the component of the residuals becomes more influential, as it is a temporally and spatially variable field and furthermore strongly affected by natural variability and initiating conditions. For temperature the contribution of a common signal is highest. As for each specific analysis the scenario has not been exchanged, the contribution of a temporal lag between the responses of the individual models, denoted as the interaction contribution, is constantly low.

The contribution of the individual sources of variability alter spatially, where patterns follow the trends depicted earlier and their spatial distribution or show differences of sea-surfaces and land-surfaces, e.g. for temperature. Regions with lower knowledge about climatic characteristics are indicated by higher

contributions of the block partitions. For sea-level pressure the contribution of the block partition and the contribution of the residuals alternate within the change of latitude, indicating the predominance of residuals in the north, e.g. evoked by different initial conditions, and the huge bias between the models in the south. This impact on the contribution is also shifted within the seasons, as not only seasonally amplified trends are figured out more clearly, but also the interaction between the block contribution and the residuals is involved. This is one of the key findings, as the residuals represent the affection of the total variability by individual realizations and thus their specific initial conditions, as they are nonlinearly altered by natural variability. The latter one is repressed during the warmer seasons, when local processes come to the fore, being implemented in the individual model physics and parametrizations, which enforces the block partition. Particularly, this can be extracted from the results of precipitation. Some intentional neglection of individual models within this analysis unmask models diverging from the overall model group and confirm the qualitative postulation of ECHAM5 being a "well-aligned" model in the multi-model mean. A fundamental criterion of the strength of the common signal is the strength of the integrated trend, whereat the trend again is affected by the length and the temporal location of the applied period and the forcing of the chosen scenario.

At this point it shall be stated, that at least the signal of temperature, shown by the individual models on the one hand, which is investigated by the 1-way ANOVA, and across all models on the second hand has strong contributions. It depicts at least above 70% of the total variability for each individual model in A1B and still more than 30% over all models. This signal still can be enhanced by an enforcement of the steering scenario or a prolongation of the time period.

Another attempt to strengthen the signal has been conducted by a normalization of the individual models onto the values of the ERA40 reanalysis data, which at first diminishes the biases between the models but conserves the individual model physics. After the correction of the initial biases, the common signal is risen up leading to more than 50% at any time in the 21st century in A1B. While precipitation is still subordinated to highly variable natural steering, the information about future courses of temperature again warns the highly vulnerable Mediterranean Area of severe future climate conditions.

The occurrence of extremes is not deducible directly from the changing in the mean, as the trend of average precipitation is e.g. not necessarily accompanied by increasing frequencies of heavy precipitation events or increasing intensities. This describes a broadening of the distribution of precipitation with probable higher occurrence of damaging events (GAO, PAL & GIORGI 2006). The investigation of extremes has been limited to precipitation in the A1B scenario on the one side, as this save of computational efforts enables the capacities to conduct research on different extreme variables, i.e. the amount of heavy precipitation, the percentage of extreme precipitation to total precipitation, the number of extreme precipitation events and the daily intensities of extreme precipitation, in three different periods.

The crude resolution of GCMs prohibits spatially detailed analyses. Consecutively, local characteristics as orographic features, land-sea contrasts

or exposition peculiarities are omitted (GAO, PAL & GIORGI 2006). Furthermore, HAYLOCK et al. (2008) note, that extremes are smoothed by spatial grids and only project mean values over the gridded cells, while point data may show much higher values. Nevertheless, in order to maintain a comprehensive set of analyses, the interpolation on the 3x3° grid is applied again.

For extremes it is hard to detect meaningful projections for future periods, which holds particularly for the multi-model mean, as discrepancies between the models are high. This finding can be extended for seasonal and spatial differences. Generally, individual models show more structured patterns in sensitivities and means, which still are hard to interpret. An exception is figured by the projection of the number of extreme events, whereat the multi-model mean obviously shows spatially more reasonable distributions. Furthermore, the directions of the general trends may be completely different for individual models. Here, the analysis of these extreme fields gives more insight on the differences between the models and the multi-model mean, whereat e.g. possible consensus of overall decreases of precipitation is not reproduced for extreme intensities, caused by e.g. a varying number of wet days. This also can be expressed by an application of an ANOVA. Furthermore, the ANOVA clearly discovers the stronger biases over the models in summer, which confirms mentioned results for precipitation means and extends them onto extremes.

For many variables these patterns are meaningful altered by either a strengthening of the values or a complete change of the prefix in a further future period. This is also reproduced in the ANOVA. Overall, it is very hard to draw meaningful conclusions, which holds particularly for the future development of extreme precipitation intensities.

Still, in the consideration of extremes, many general findings of enforced extreme precipitation in regions characterized by few precipitation amounts are not definitely confirmed here (e.g. GAO, PAL & GIORGI 2006). Consecutively, the general assumption of a globally increase of extreme precipitation by increased supply of air humidity (Clausius Clapeyron relation, e.g. FREI et al. 1998, DEQUE, MARQUET & JONES 1998) is hard to apply on the MA, as smaller local peculiarities, like orography, subtropical circulation patterns (FREI et al. 1998) and other typical characteristics of the MA, with its affection by the Mediterranean Sea and its steering sea-surface temperatures overly synoptic features.

7.2   Discussion

Considering the final results, one must not forget the antecedent suppositions and generalizations, which have been conducted to provide the feasibility of this investigation. Some of them develop during the propagation of the analyses to serious shortcomings demanding a closer view in probable connecting studies.

A generally discussed famous instance for this is the spatial resolution, as it is also mentioned several times in this study. Depending on the available data and

the applied statistical method, it is crucial for an explicit investigation of local circumstances. This holds particularly for the MA, as the spatial heterogeneity and thus the diversity of the small scale steerings is large. The local steering peculiarities like convection, upslope air movement on sides of mountain barriers, etc., are hard to handle by GCMs. Thus, it is a tenuous undertaking to conclude on local characteristics by the application on GCMs. The interpolation procedure exacerbates this aim. Still, as the application of different GCMs exhibits both, spatially discrepancies and high agreements on the other side, one is able to extract regions with more or less predictability or even enhanced knowledge about future conditions and finally an increased knowledge about uncertainty. This logical finding must not be underrated, as meanwhile huge databases, containing several GCMs, are available and their analysis is relatively facile regarding computational efforts. Also, former results of dynamical downscaling analyses are at the same magnitude as in the underlying study, with temperature trends at 6°C over land areas in the MA for the A2 scenario in summer and 3-4°C in winter in nearly corresponding periods (RÄISÄNEN et al. 2004).

The benefits of regional projection methods are still evident. Then, the question arises to what amount the mentioned processes can be captured by downscaling methods. Besides the ability of a more detailed view on future climate conditions, downscaling promises continuing progress in a deeper comprehension of climate processes. The output, derived by GCMs, can then be altered strongly by downscaling methods, e.g. when one considers the parallel studies fulfilled in the underlying project. But, although for reference periods the passed errors from GCMs to RCMs are supposed to be relatively low (FREI et al. 2006; FREI et al. 2003), the uncertainty inherent to GCMs generally overly the uncertainty of the dynamical downscaling. The analysis of uncertainties meanwhile must be extended to the application of subsequent downscaling methods (HERTIG & JACOBEIT 2008a). Consecutively, downscaling methods should be done not only with the implementation of the assessment of different methods and ensembles, e.g. to account for nonstationarities, the choice of predictors, etc., but also with the subordination of the different assessments to various GCMs and various initial conditions (HERTIG & JACOBEIT 2008b). Finally, this enhances exponentially the number of independent contributors of variability, as different RCMs may be implemented in different GCMs. One has to strike a balance between gaining higher experience about complex temporal and spatial relations and the restraint of associated lower accuracy and higher uncertainty.

A study dealing with the assessments of different GCMs and RCMs and the according development of uncertainty is the one of DEQUE et al. (2005) embedded in the PRUDENCE project (CHRISTENSEN, CARTER & GIORGI 2002). Another study is fulfilled by RÄISÄNEN et al. (2004). Recently, the application of several RCMs or high-resolution models has become very frequent in scientific investigations (FREI et al. 2006, CHRISTENSEN & CHRISTENSEN 2003).

For temperature, DEQUE et al. (2005) also stated, that behind the choice of the GCM the specific scenario is the second most important source of uncertainty, as it is dominant over the choice of the RCM, which is subdued by

the boundary conditions of the GCM and its forcing scenario. Although, the choice of RCMs matters more for precipitation particularly in summer, when the simulation of small convective features and regional circulation is clearly assigned to the specific RCMs, the contribution of the RCMs is about the amount of uncertainty of GCMs or of the scenario.

Thus, an analysis of the uncertainties given by different GCMs for means and overall trends is quite important, as this provides fundamental insight of first assessments about future climate change and gains synoptic information on overall modelling sciences. And finally, GCMs still provide the groundwork for the application of downscaling techniques by including globally acting steering phenomenona and teleconnections. Particularly, this becomes fundamental concerning first definitions of uncertainties, discrepancies and well proved appearances, followed-up by the conductions of downscaling approaches with the intention to resolve smaller features. As different sources of uncertainty concerning the projections of future climate exist, it is inevitable to pay attention to these uncertainties, as the handling of these uncertainties enhances confidence in the applied models and strengthens the robustness of the information.

Different results can be obtained by different studies as e.g. former studies show increases of winter precipitation over the Iberian Peninsula (TRIGO & PALUTIKOF 2001, GONZALEZ-ROUCO et al. 2000), while also decreases are indicated in spring and autumn. Other studies found an annual decrease over major parts of Spain (SUMNER et al. 2003). But, relating the results of the underlying study to other approaches with GCMs reveals still agreements in many situations (TEBALDI et al. 2006).

The investigation of the impact of anthropogenic emissions on the occurrence of extremes is still challenging (HEGERL et al. 2004). Thus, a low amount of concordant results have been obtained by many studies according to the excelling inherent uncertainties, though the methodical divergence of the accomplished assessments is encouraging (e.g. FREI et al. 2006, HERTIG et al. 2013a). Also, besides extremes, an antecedent approach with the application of multiple GCMs is a small step in this direction.

Following GIORGI & FRANCISCO (2000b), a low number of ensemble-members is sufficient to have a reliable assessment of future climate, as the differences within one ensemble are lower than the impact of the discrepancies over the individual models, which is for the MA also stated by NORTHROP (2010). This is also reflected in the trends of single simulations having only a low discrepancy to the ensemble-mean (compare figures 4.43 and 4.44). Consecutively, GIORGI & FRANCISCO (2000b) recommend 3-4 individual realizations for each GCM. This is confirmed with partially strong common signals within selected GCMs in this study. Irrespective of the low contribution of the residuals and the individual realizations, they represent the internal uncertainty of one model evoked by the different initial conditions and the nonlinearity of climate. Thus, natural climate variability is reflected in the individual realizations, which becomes e.g. highly effective in winter for precipitation by means of the steering of the NAO.

192

Thus, natural variability still must receive full attention in research of climate change and climate research in general, as it provides further insight in the interaction of climate processes and might amplify changes of climate conditions. Apart that, a closer definition of frequency, phase and amplitude of the natural variability may allow statistical progress in the application of regionalization techniques (GIORGI 2002a). Furthermore, its decomposition may allow the unmasking of external forcing. Also, it is stated, that GCMs generally underestimate natural climate variability, as excessive external steering factors are not implemented (PAETH & HENSE 2002, GIORGI 2002b). To capture this natural variability and to enhance climatologic knowledge about this issue with the help of GCMs, the implementation of several realizations still is recommended. Furthermore, statistical considerations recommend a far higher number of simulations realized by one GCM in order to provide adequate statistical distributions accounting for the total potential of uncertainty (WEHNER 1998).

Aside from the utilization of multiple members for one GCM, also several GCMs should be utilized, as one has to admit, that one single model may pretend a strong signal among its different members, though the overall treatment partition may be relatively weak and not even significant when considering several models with the 2-way ANOVA. This particularly holds for sea-level pressure, which is already depicted of the trend figures in chapter 4 and highlights the superimposing effect of different modelling approaches concerning parametrizations and discretizations. These effects overcome the effects of the residuals, which show natural variability and the effect of different initial conditions. Finally, this result strengthens the recommendation to derive values out of various GCMs to cover at least some amount of variability. Though, the multi-model mean may result in weak information concerning future trends, because of smoothing the individual extreme values of one model, at least the idea of handling the huge amount of uncertainty is forwarded. This is also stated by REIFEN & TUOMI (2009), who recommend a maximum number of GCMs and who ascribe highest information about future climate to the multi-model mean, as the different feedbacks and skills of the models are combined and at least provide the best estimation of uncertainty, e.g. reflected in the model spread.

Overall, there is always need to handle these amounts of uncertainty to gain results with maximum precision, which finally leads to a balance of contributing datasets. Given the case, that highest variability is dedicated to the residuals, the number of realizations should be maximized, whilst the number of independent GCMs can be diminished. By this strategic planning, resources are saved by time and cost effectivity (NORTHROP 2010).

Still one has to keep in mind that climate sensitivity, i.e. the amount of the reaction of a GCM on a defined GHG emission scenario, may be under- or overestimated, where the latter effect evokes a higher treatment signal in contrast to natural variability.

Additional improvements should be aspired in the simulating procedures and the numerics itself, where the modelling groups may obtain improvements by challenging parametrization schemes, models physics, boundary layers and the

definition of sensitivities of the model to likewise treatment. It may be the case, that in this region the results of trends in precipitation of several GCMs are more consistent than in their simulation of atmospheric sources like large-scale patterns. This is reflected in a relatively poor consistency within sea-level pressure but a high consistency according precipitation and temperature in this study. Now, it should be in focus to quantify the dependency of the modelled results on large-scale activities and their ability to reproduce this teleconnections. Thus, it also is indispensable to gain better representations of variables like solar radiation variability or (tropical) sea-surface temperatures, as they are important driving factors of natural variability and thus of atmospheric modes. An enhanced representation of the NAO and ENSO and their interplay would elucidate their affection of the Mediterranean Area (KODERA 2003). Whereat case studies about changed specifications are quite expensive and elaborate, though also executable with an ANOVA (VON STORCH & ZWIERS 1999). Additionally nesting and transfer functions from data of GCMs to RCMs still show potential in enhancing accuracies. Also the approach of double-nesting of the RCMs in the GCM sounds promising, as GCMs might have a learning effect on the feedback provided by the RCM, i.e. derived from small scaled processes. For this working point, further optimizing of nesting and nudging is required.

Further advances in modelling and in forcings can be achieved by a successive implementation of surface coverages and their changes, as it is e.g. done for REMO (PAETH et al. 2009). Regarding to vegetation and surface feedbacks, still astucious research is necessary.

Regardless of the problem to choose the correct models or the models with the highest ability, one can surely make the assumption, that the higher the variability over the models is, the more the prudent choice of the most reliable GCMs matters. Besides the fact, that neither GCMs can be verified for future periods nor their quality can be proved by data derived from observations, a foregoing selection of GCMs is still impossible antecedent to any analyses. However, the dispute whether to make a pre-selection of GCMs or not and which arguments to use in the case of a foregoing choice or weighting, is a topic receiving highest attention in current scientific debates in the community of statistical climatology. At least for a comprehensive and quantitative investigation on distinct consequences of climate change for specific regions it will be inevitable to process the science about an adequate choice of models, particularly in the consideration of the advantages and constraints of specific models concerning different variables and regions. A possible approach for this research may be the application of Bayesian statistics, as it is done by NORTHROP (2010), or an overall investigation of the ability of specific models to account for natural variability, e.g. atmospheric modes.

Besides the disciplines of the statistical processing of the output, which is in the main focus of this work, detailed illustrations of future means and trends have been depicted. Despite the recent controversy about climate change, the models clearly indicate that it is taking place. Furthermore, for temperature definite signals arouse out of various models and realizations. It should be mentioned again, that this progress is analysed in the very vulnerable Mediterranean Area. One must not forget, that this warming will be

accompanied by e.g. changes of the hydrologic cycle, extreme weather conditions or alterations of the sea level. These and other impacts imperil the nature and the economic and social life. Therefore, scientific interdisciplinary work has to be done on climate impact research to develop adaption and mitigation strategies in an integrative way. Still, natural positive and negative feedbacks will complicate the determination of the final effects, as e.g. also geographic interactions will play a crucial role. Thus, a special issue, which is not discussed in this project, is the affection of the global change by the future conditions in the Mediterranean Area. So, it must not be forgotten, that the Mediterranean Sea is one of the most important sources of salt for the Atlantic Ocean. Consecutively, the changing Mediterranean climate may affect the global climate itself, for instance in terms of heat and moisture transfers (BIGG et al. 2003).

Bibliography

ABRANTES, F., VOELKER, A., SIERRO, F.J., NAUGHTON, F., RODRIGUES, T., CACHO, I., ARIZTEGUI, D., BRAYSHAW, D., SICRE, M.-A. & BATISTA, L. (2012): Paleoclimate Variability in the Mediterranean Region. In: LIONELLO, P. (eds.): *The Climate of the Mediterranean Region.* Elsevier, Amsterdam, pp. 1-51.

AHRENS, D. (2000): Meteorology Today. An introduction to Weather, Climate and the Environment. Brooks/Cole, Pacific Grove, USA, pp.528.

ALEKSEEV, V., VOLODIN, E., GALIN, V., DYMNIKOV, V. & LYKOSSOV, V. (1998): Modelling of the present-day climate by the atmospheric model of INM RAS "DNM GCM". Description of the model version A5421 (1997 year) and the results of AMIP II simulations. INM reportN2086-B98. Available by request from the address: Volodin E.M., Institute of numerical Mathematics, Gubkina 8, Moscow 117951, Russia.

ALEXANDER, L. et al. (2006): Global observed changes in daily climate extremes of temperature and precipitation. In: *Journal of Geophysical Research*, vol. 111.

ALPERT, P. et al. (2002): The paradoxical increase of Mediterranean extreme daily rainfall in spite of decrease in total values. In: *Geophysical Research Letters*, vol. 29.

ALPERT, P. et al. (2006): Relations between climate variability in the Mediterranean Region and the Tropics: ENSO, South Asian and African Monsoons, Hurricanes and Saharan Dust. In: LIONELLO, P. MALANOTTE-RIZZOLI, P. & BOSCOLO, R. (eds.): *Mediterranean Climate Variability.* Elsevier, Amsterdam, pp. 149-188.

ANDRONOVA, N. & SCHLESINGER, M. (2000): Causes of global temperature changes during the 19th and 20th centuries. In: *Geophysical Research Letters*, vol. 27, pp. 2137-2140.

AVILA, A., QUERALT-MITJANS, I. & ALARCON, M. (1997): Mineralogical composition of African dust delivered by red rains over northeastern Spain. In: *Journal of Geophysical Research*, vol. 102, pp. 21977-21996.

BALDI, M., MENEGUEZZO, f., DALU, G., MARACCHI, G., PASQUI, M., CAPECCHI, V., CRISCI, A. & PIANI, F. (2006): Guinea Gulf SST and Mediterranean Summer Climate: Analysis of interannual Variability. http://cnr-it.academia.edu/MarinaBaldi

BARREDO, J. (2009): Normalised flood losses in Europe: 1970-2006. In: *Natural Hazards and Earth System Sciences*, vol. 9, pp. 97-104.

BARNSTON, A. & LIVEZEY, R. (1987): Classification, seasonality and persistence of low frequency atmospheric circulation patterns. In: *Monthly Weather Review*, vol. 115, pp. 1825-1850.

BARRIOPEDRO, D., GARCIA-HERRERA, R., LUPO, A. & HERNANDEZ, E. (2006): A Climatology of Northern Hemisphere Blocking. In: *Journal of Climate*, vol. 19, pp. 1042-1063.

BIGG, G., JICKELLS, T., LISS, P. & OSBORN, T. (2003): The Role of the oceans in climate. In: *International Journal of Climatology*, vol. 23, pp. 1127-1159.

BOLLE, H.-J. (2003): Climate, Climate Variability, and Impacts in the Mediterranean Area: An Overview. In: BOLLE, H.-J. (ed.): *Mediterranean Climate - Variability and Trends*. Springer Verlag, Berlin, Heidelberg.

CARRIL, A., GUALDI, S., CHERCHI, A. & NAVARRA, A. (2008): Heatwaves in Europe: areas of homogeneous variability and links with the regional to large-scale atmospheric and SSTs anomalies. In: *Climate Dynamics*, vol. 30, pp. 77-98.

CASSOU, C., TERRAY, L. & PHILLIPS, A. (2005): Tropical Atlantic Influence on European Heat Waves. In: *Journal of Climate*, vol. 18, pp. 2805-2811

CHRISTENSEN, J. & CHRISTENSEN, O. (2003): Climate modelling: Severe summertime flooding in Europe. In: *Nature*, vol. 421, pp. 805-806.

CHRISTENSEN, J., CARTER, T. & GIORGI, F. (2002): PRUDENCE employs new methods to assess European climate change, In: *Eos, Transactions American Geophysical Union,* vol. 83.

CHRISTENSEN, J., CHRISTENSEN, O., LOPEZ, P., VAN MEIJGAARD, E. & BOTZET, M. (1996): The HIRHAM4 Regional Atmospheric Climate Model, In: *Scientific Report* 96-4, 51 pp., Danish Meteorologic Institute, Copenhagen (Denmark).

CLAUSSEN, M. (1998): On multiple solutions of the atmosphere-vegetation system in the present-day climate. In: *Global Change Biology*, vol.4, pp. 549-559.

COLES, S. (2001): An Introduction to Statistical Modeling of Extreme Values. Springer, London, GB.

COLLINS, W. et al. (2006): The Community Climate System Model Version 3 (CCSM3). In: *American Meteorological Society*, vol. 19, pp. 2122-2143.

CONIL, S. & LI, Z. (2003): Influence of the North Atlantic on simulated atmospheric variability. In: *Annals of Geophysics*, vol. 46, pp. 57-70.

CONTE, M., GIUFFRIDA, A. & TEDESCO, S. (1989): The Mediterranean Oscillation. Impact on precipitation and hydrology in Italy. In: *Conference on: Climate Water. Publications of the Academy of Finland*, Helsinki. 11–15 September 1989, 121–137.

COSTA, A., SANTOS, J. & PINTO, J. (2012): Climate change scenarios for precipitation extremes in Portugal. In: *Theoretical and Applied Climatology*, vol. 108, pp. 217-234.

CSMD (2005): An introduction to The First-generation Operational Climate Model at National Climate Center, Advances in Climate System Modeling, vol. 1, pp. 1-14

CUBASCH, U. & KASANG, D. (2000): Anthropogener Klimawandel. Klett-Perthes Verlag, Gotha und Stuttgart.

CUBASCH, U., WASZKEWITZ, J., HEGERL, G. & PERLWITZ, J. (1995): Regional climate changes as simulated in time-slice experiments. In: *Climate Change*, vol. 31, pp. 273-304.

CUBASCH, U., VOSS, R., HEGERL, G., WASZKEWITZ, J. & CROWLEY, T. (1997): Simulation of the influence of solar radiation variations on the global climate with an ocean-atmosphere general circulation model. In: *Climate Dynamics*, vol. 13, pp. 757-767.

DEQUE, M. et al. (2005): Global high resolution versus Limited Area Model climate change projections over Europe: quantifying confidence level from PRUDENCE results. In: *Climate Dynamics*, 25, pp. 653-670.

DEQUE, M., MARQUET, P. & JONES, R. (1998): Simulation of climate change over Europe using a global variable resolution general circulation model. In: *Climate Dynamics*, vol. 14, pp. 173-189.

DELLA-MARTA, P., HAYLOCK, M., LUTERBACHER, J. & WANNER, H. (2007): Doubled length of western European summer heat waves since 1880. In: *Journal of Geophysical Research*, vol. 112.

DÜMENIL GATES, L. & LIESS, S. (2001): Impacts of deforestation and afforestation in the Mediterranean region as simulated by the mPI atmospheric GCM. In: *Global and Planetary Change*, vol. 30, pp. 309-328.

DÜNKELOH, A. & JACOBEIT, J. (2003): Circulation Dynamics of Mediterranean Precipitation Variability 1948-1998. In: *International Journal of Climatology*, vol. 23, pp. 1843-1866.

FERNANDEZ, J., SAENZ, J. & ZORITA, E. (2003): Analysis of wintertime atmospheric moisture transport and its variability over southern Europe in the NCEP Reanalysis. In: *Climate Research*, vol. 23, pp. 195-215.

FOLEY, J., LEVIS, S., PRENTICE, C., POLLARD, D. & THOMPSON, S. (1998): Coupling dynamic models of climate and vegetation. In: *Global Change Biology*, vol. 4, pp. 561-579.

FREI, C. SCHÄR, C., LÜTHI, D. & DAVIES, H. (1998): Heavy precipitation processes in a warmer climate. In: *Geophysical Research Letters*, vol. 25, pp. 1431-1434.

FREI, C., SCHÖLL, R., FUKUTOME, S., SCHMIDLI, J. & VIDALE, P. (2006): Future change of precipitation extremes in Europe: intercomparison of scenarios from regional climate models. In: *Journal of Geophysical Research: Atmospheres*, vol. 111.

FREI, C., CHRISTENSEN, J., DEQUE, M., JACOB, D., JONES, R. & VIDALE, P. (2003): Daily precipitation statistics in regional climate models: Evaluation and intercomparison fort he European Alps. In: *Journal of Geophysical Research*, vol. 108.

FRICH, P., ALEXANDER, L., DELLA-MARTA, P., GLEASON, B., HAYLOCK, M., KLEIN TANK, A. & PETERSON, T. (2002): Observed coherent changes in climatic extremes during the second half of the twentieth century. In: *Climate Research*, vol. 19, pp. 193-212.

FUREVIK, T., BENTSEN, M., DRANGE, H., KINDEM, I., KVAMTSÖ, N. & SORTEBERG, A. (2003): Description and evaluation of the bergen climate model: ARPEGE coupled with MICOM. In: *Climate Dynamics*, vol. 21, pp. 27-51.

GANOPOLSKI, A., KUBATZKI, C., CLAUSSEN, M., BROVKIN, V. & PETOUKHOV, V. (1998): The influence of vegetation-atmosphere-ocean

interaction on climate during the mid-Holocene. In: *Sciene*, vol. 280, pp. 1916-1919.

GARNAUT, R., HOWES, S., JOTZO, F. & SHEEHAN, P. (2008): Emissions in the Platinum Age: the implications of rapid development for climate-change mitigation. In: *Oxford Review of Economic Policy*, vol. 24, pp. 377-401.

GAO, X., PAL, J. & GIORGI, F. (2006): Projected changes in mean and extreme precipitation over the Mediterranean region from high resolution double nested RCM simulations. In: *Geophysical Research Letters*, vol. 33.

GFDL GAMDT (2004): The New GFDL Global Atmosphere and Land Model AM2-LM2: Evaluation with Prescribed SSt Simulations. In: *American Meteorological Society*, vol. 17, pp. 4641-4673.

GIBELIN, A. & DEQUE, M. (2003): Anthropogenic climate change over the Mediterranean region simulated by a global variable resolution model. In: *Climate Dynamics*, vol. 20, pp. 327-339.

GIORGI, F. (2006): Climate change hot-spots. In: *Geophysical Research Letters*, vol. 33.

GIORGI, F. (2002a): Variability and trends of sub-continental scale surface climate in the twentieth century. Part I: observations. In: *Climate Dynamics*, vol. 18, pp. 675-691.

GIORGI, F. (2002b): Variability and trends of sub-continental scale surface climate in the twentieth century. Part II: AOGCM simulations. In: *Climate Dynamics*, vol. 18, pp. 693-708.

GIORGI, F. & FRANCISCO, R. (2000a): Evaluating uncertainties in the prediction of regional climate change. In: *Geophysical Research Letters*, vol. 27, pp. 1295-1298.

GIORGI, F. & FRANCISCO, R. (2000b): Uncertainties in regional climate change prediction: a regional analysis of ensemble simulations with the HadCM2 coupled AOGCM. In: *Climate Dynamics*, vol. 16, pp. 169-182.

GIORGI, F. & LIONELLO, P. (2008): Climate change projections for the Mediterranean region. In: *Global and Planetary Change*, vol. 63, pp. 90-104.

GIORGI, F. & MEARNS, L. (1991): Approaches to the simulation of regional climate change: A Review. In: *Reviews of Geophysics*, vol. 29, pp. 191-216.

GIORGI, F. & MEARNS, L. (1999): Introduction to special section: Regional climate modelling revisited. In: *Journal of Geophysical Research*, vol. 104, pp. 6335-6352.

GIORGI, F. & MEARNS, L. (2002): Calculation of Average, Uncertainty Range, and Reliability of Regional Climate Changes from AOGCM Simulations via the "Reliability Ensemble Averaging" (REA) Method. In: *Journal of Climate*, vol. 15, pp. 1141-1158.

GIORGI, F., BI, X. & PAL, J. (2004a): Mean, interannual variability and trends in a regional climate change experiment over Europe. I. Present-day climate (1961-1990). In: *Climate Dynamics*, vol. 22, pp. 733-756.

GIORGI, F., BI, X. & PAL, J. (2004b): Mean, interannual variability and trends in a regional climate change experiment over Europe. II: climate change scenarios (2071-2100). In: *Climate Dynamics*, vol. 23, pp. 839-858.

GLAHN, H. & LOWRY, D. (1972): The Use of Model Output Statistics (MOS) in Objective Weather Forecasting. In: *Journal of Applied Meteorology*, vol. 11, pp.1203-1211.

GONZALEZ-ROUCO, J., HEYEN, H., ZORITA, E. & VALERO, F. (2000): Agreement between Observed Rainfall Trends and climate Change Simulations in the Southwest of Europe. In: *Journal Of Climate*, vol. 13, pp. 3057-3065.

GORDON, C., COOPER, C., SENIOR, C., BANKS, H., GREGORY, J., JOHNS, T., MITCHELL, J. & WOOD, R. (2000): The simulation of SST, sea ice extents and ocean heat transports in a version of the Hadley Centre coupled model without flux adjustments. In: *Climate Dynamics*, vol. 16, pp. 147-168.

GORDON, H., O´FARRELL, COLLIER, M., DIX, M., ROTSTAYN, L., KOWALCZYK, E., HIRST, T. & WATTERSON, I. (2010): The CSIRO Mk3.5 Climate Model. CAWCR Technical Report No. 021, Centre for Australian Weather and Climate Research (Australia).

GORDON, H. et al. (2002): The CSIRO Mk3 Climate System Model. CSIRO Atmospheric Research Technical Paper No. 60, CSIRO Atmospheric Research (Australia).

GOUBANOVA, K., LI, L., YIOU, P. & CODRON, F. (2010): Relation between Large-Scale Circulation and European Winter Temperature: Does It Hold under Warmer Climate?. In: *Journal of Climate*, vol23, pp. 3752-3760.

GRISOGONO, B. & BELUSIC, D. (2009): A review of recent advantages in understanding the meso- and microscale properties of the severe Bora wind. In: *Tellus*, vol. 61A, pp. 1-16.

GROISMAN, P., KNIGHT, R., EASTERLING, D., KARL, T., HEGERL, G. & RAZUVAEV, V. (2005): Trends in Intense Precipitation in the Climate Record. In: *Journal of Climate*, vol. 18, pp. 1326-1350.

HALPERT, M. & ROPELEWSKI, C. (1992): Surface Temperature Patterns Associated with the Southern Oscillation. In: *Journal of Climate*, vol. 5, pp. 577-593.

HASSELMANN, K. (1997): Multi-pattern fingerprint method for detection and attribution of climate change. In: *Climate Dynamics*, vol. 13, pp. 601-612.

HATZAKI, M., FLOCAS, H., ASIMAKOPOULOS, D. & MAHERAS, P. (2007): The Eastern Mediterranean Teleconnection Pattern: Identification and Definition. In: *International Journal of Climatology*, vol. 27, pp. 727-737.

HAYLOCK, M., HOFSTRA, N., KLEIN TANK, A., KLOK, E., JONES, P. & NEW, M. (2008): A European daily high-resolution gridded dataset of surface temperature and precipitation. In: *Journal of Geophysical Research,* vol. 113.

HEGERL, G., ZWIERS, F., STOTT, P. & KHARIN, V. (2004): Detectability of Anthropogenic Changes in Annual Temperature and Precipitation Extremes. In: *Journal of Climate*, vol. 17, pp. 3683-3700.

HEGERL, G., ZWIERS, F., BRACONNOT, P., GILLET, N., LUO, Y., MARENGO ORSINI, J., NICHOLLS, N., PENNER, J. & STOTT, P. (2007): Understanding and Attributing Climate Change. In: SOLOMON, S., QIN, D., MANNING, M., CHEN, Z., MARQUIS, M., AVERYT, K., TIGNOR, M. & MILLER, H. (eds.): In: Climate Change 2007: The Physical Science Basis. Contribution of Working Group I to the Fourth Assessment Report of the Intergovernmental Panel on Climate Change. Cambridge University Press, Cambridge, Unitd Kingdom and New York, USA.

HERTIG, E. & JACOBEIT, J. (2008a): Assessments of Mediterranean precipitation changes fort he 21st century using statistical downscaling techniques. In: *International Journal of Climatology*, vol. 28, pp. 1025-1045.

HERTIG, E. & JACOBEIT, J. (2008b): Downscaling future climate change: Temperature scenarios for the Mediterranean area. In: *Global and Planetary Change*, vol. 63, pp. 127-131.

HERTIG, E., PAXIAN, A., VOGT, G., SEUBERT, S., PAETH, H. & JACOBEIT, J. (2012): Statistical and dynamical downscaling assessments of precipitation extremes in the Mediterranean area. In: *Meteorologische Zeitschrift*, vol. 21, pp. 61-77.

HERTIG, E., SEUBERT, S., PAXIAN, A., VOGT, G., PAETH, H. & JACOBEIT, J. (2013a): Changes of total versus extreme precipitation and dry periods until the end of the twenty-first century: statistical assessments for the Mediterranean area. In: *Theoretical and Applied Climatology*, vol. 111, pp.1-20

HERTIG, E., SEUBERT, S., PAXIAN, A., VOGT, G., PAETH, H. & JACOBEIT, J. (2013b): Statistical modeling of extreme precipitation fort he Mediterranean area under future climate change. In: *International Journal of Climatology*, vol. 33.

HEWITSON, B. & CRANE, R. (1996): Climate downscaling: techniques and application. In: *Climate Research*, vol. 7, pp. 85-95.

HODSON, D. & SUTTON, R. (2008): Exploring multi-model atmospheric GCM ensembles with ANOVA. *Climate Dynamics*, vol. 31, pp. 973-986.

HOURDIN, F. et al. (2006): The LMDZ4 general circulation model: climate performance and sensitivity to parametrized physics with emphasis on tropical convection. In: *Climate Dynamics*, vol. 27, pp. 787-813.

HURRELL, J. (1995): Decadal Trends in the North Atlantic Oscillation: Regional Temperature and Precipitation. In: *Science*, vol. 269, pp. 676-679.

IPCC (2007): Summary for Policymakers. In: Climate Change 2007: The Physical Science Basis. Contribution of Working Group I to the Fourth Assessment Report of the Intergovernmental Panel on Climate Change. In: SOLOMON, S., QIN, D., MANNING, M., CHEN, Z., MARQUIS, M., AVERYT, K., TIGNOR, M. & MILLER, H. (eds.). Cambridge University Press, Cambridge, United Kingdom and New York, NY, USA,

IPCC (2012): Summary for Policymakers. In: Managing the Risks of Extreme Events and Disasters to Advance Climate Change Adaptation In: FIELD, C. et al. (eds.): A Special Report of Working Groups I and II of the

Intergovernmental Panel on Climate Change. Cambridge University Press, Cambridge, UK, and New York, NY, USA, pp. 1-19.

JACOB, D. et al. (2001): A comprehensive model inter-comparison study investigating the water budget during the BALTEX-PIDCAP period. In: *Meteorology and Atmospheric Physics*, vol. 77, pp. 19-43.

JACOB, D. et al. (2007): An inter-comparison of regional climate models for Europe: model performance in present day climate. In: *Climate Change*, vol. 81, pp. 31-51.

JACOBEIT, J. (2007): Zusammenhänge und Wechselwirkungen im Klimasystem. In: ENDLICHER, W. & GERSTENGARBE, F.-W. (eds.): *Der Klimawandel – Einblicke, Rückblicke, Ausblicke*. Postdam-Institut für Klimafolgenforschung e.V., Berlin-Potsdam, pp. 1-16.

JACOBEIT, J., DÜNKELOH, A. & HERTIG, E. (2007): Mediterranean rainfall changes and their causes. In: LOZAN, J., GRAßL, H., HUPFER, P., MENZEL, L. & SCHÖNWIESE, C.-D. (eds.): *Global Change: Enough Water for all?* Wissenschaftliche Auswertungen/GEO, Hamburg, pp. 195-199.

JACOBEIT, J., JÖNSSON, P., BÄRRING, L. BECK, C. & EKSTRÖM, M. (2001): Zonal indices for Europe 1780-1995 and running correlations with temperature. In: *Climatic Change*, vol. 48, pp. 219-241.

JONES, P. & MANN, M. (2004): Climate over past millennia. In: *Review of Geophysics*, vol. 42, pp. 1-42.

JONES, P. & REID, P. (2001): Assessing future changes in extreme precipitation over Britain using regional climate model integrations. In: *International Journal of Climatology*, vol. 21, pp. 1337-1356.

K-1 Model Developers (2004): K-1 Coupled GCM (MIROC) Description. Technical Report. Center for Climate System Research, University of Tokyo (Japan).

KAHANA, R. ZIV, B., ENZEL, Y. & DAYAN, U. (2002): Synoptic climatology of major floods in the Negev desert, Israel. In: *International Journal of Climatolgy*, vol. 22, pp. 867-882.

KHARIN, V. & ZWIERS, F. (2004): Estimating Extremes in Transient Climate Change Simulations. In: *Journal of Climate*, vol. 18, pp.1156-1173.

KIOUTSIOUKIS, I., MELAS, D. & ZEREFOS, C. (2010): Statistical assessment of changes in climate extremes over Greece (1955-2002). In: *International Journal of Climatology*, vol. 30, pp. 1723-1737.

KISTLER, R. et al. (2001): The NCEP-NCAR 50-Year Reanalysis: Monthly Means CD-ROM and Documentation. In: *Bulletin of the American Meteorological Society*, vol. 82, pp. 247-267.

KITTEL, T., GIORGI, F. & MEEHL, G. (1998): Intercomparison of regional biases and doubled CO_2-sensitivity of coupled atmosphere-ocean general circulation model experiments. In: *Climate Dynamics*, vol. 14, pp.1-15.

KLEIN TANK, A. & KÖNNEN, G. (2003): Trends in Indices of Daily Temperature and Precipitation Extremes in Europe, 1946-99. In: *Journal of Climate*, vol. 16, pp. 3665-3680.

KNIPPERTZ, P., ULBRICH, U., MARQUES, F. & CORTE-REAL, J. (2003): Decadal Changes in the Link between El-Nino and Springtime North Atlantic Oscillation and European-North African Rainfall. In: *International Journal of Climatology*, vol. 23, pp. 1293-1311.

KODERA, K. (2003): Solar influence on the spatial structure of the NAO during the winter 1900-1999. In: *Geophysical Research Letters*, vol. 30.

KÖPPEN, W. (1931): Grundriß der Klimakunde. Walter de Gruyter & Co., Berlin.

KRICHAK, S. & ALPERT, P. (2005): Decadal Trends in the East-Atlantic-West Russia Pattern and Mediterranean Precipitation. In: *International Journal of Climatology*, vol. 25, pp. 183-192.

KUTIEL, H. & BENAROCH, Y. (2002): North Sea-Caspian Pattern (NCP) - An upper level atmospheric teleconnection affecting the eastern Mediterranean: identification and definitions. In: *Theoretical and Applied Climatology,* vol. 71, pp. 17–28.

LAITA, M. & GRIMALT, M. (1997): Vorticity and Pressure Anomalies in the western Mediterranean during El-Nino/Southern Oscillation Extremes. In: *International Journal of Climatology*, vol. 17, pp. 475-482.

LEGUTKE, S. & VOSS, R. (1999): The Hamburg Atmosphere-Ocean Coupled Circulation Model ECHO-G. Technical Report no.18. Deutsches Klimarechenzentrum Hamburg (Germany).

LIBERATO, M., PINTO, J., TRIGO, I. & TRIGO, R. (2011): Klaus – an exceptional winter storm over northern Iberia and southern France. In: *Weather*, vol. 66, pp. 330-334.

LIONELLO, P. et al. (2006a): The Mediterranean Climate: An Overview of the Main Characteristics and Issues. In: LIONELLO, P. MALANOTTE-RIZZOLI, P. & BOSCOLO, R. (eds.): *Mediterranean Climate* Variability. Elsevier, Amsterdam, pp. 1-26.

LIONELLO, P. et al. (2006b): Cyclones in the Mediterranean Region: Climatology and Effects on the Environment. In: LIONELLO, P. MALANOTTE-RIZZOLI, P. & BOSCOLO, R. (eds.): *Mediterranean Climate Variability*. Elsevier, Amsterdam, pp. 325-372.

LIONELLO, P., CAVALERI, L., NISSEN, K., PINO, RAICICH, F. & ULBRICH, U. (2012): Severe marine storms in the Northern Adriatic: Characteristics and trends. In: *Physics and Chemistry of the Earth*, vol. 40-41, pp. 93-105.

LOPEZ-MORENO, J., VICENTE-SERRANO, M., ANGULO-MARTINEZ, M., BEGUERIA, S. & KENAWY, A. (2010): Trends in daily precipitation on the northeastern Iberian Peninsula, 1955-2006. In: *International Journal of Climatology*, vol. 30, pp. 1026-1041.

LUTERBACHER, J. et al. (2006): Mediterranean Climate Variability over the Last Centuries: A Review. In: LIONELLO, P. MALANOTTE-RIZZOLI, P. & BOSCOLO, R. (eds.): *Mediterranean Climate Variability*. Elsevier, Amsterdam, pp. 27-148.

LUTGEN, F. & TARBUCK, E. (2007): The Atmosphere. Pearson Education, Upper Saddle River, USA.

MAHERAS, P. & KUTIEL, H. (1999): Spatial and temporal Variations in the Temperature Regime in the Mediterranean and their Relationship with Circulation during the last Century. In: *International Journal of Climatology*, vol. 19, pp. 745-764.

MAHERAS, P., XOPLAKI, E., DAVIES, T., MARTIN-VIDE, J., BARIENDOS, M. & ALCOFORADO, M. (1999): Warm and Cold Monthly Anomalies across the Mediterranean Basin and their Relationship with Circulation:1860-1990. In: *International Journal of Climatology*, vol. 19, pp. 1697-1715.

MARIOTTI, A., BALLABRERA-POY, J. & ZENG, N. (2005): Tropical Influence on Euro-Asian Autumn Rainfall Variability. In: *Climate Dynamics*, vol. 24, pp. 511-521.

MARIOTTI, A., ZENG, N. & LAU, K.-M. (2002): Euro-Mediterranean Rainfall and ENSO – a seasonally varying relationship. In: *Geophysical Research Letters*, vol. 29, no. 12.

MARIOTTI, A., STRUGLIA, M., ZENG, N. & LAU, K.-M. (2002): The Hydrological Cycle in the Mediterranean Region and Implications for the Water Budget of the Mediterranean Sea. In: *Journal of Climate*, vol. 15, pp. 1674-1690.

McFARLANE, N., SCINOCCA, J., LAZARE, M., HARVEY, R., VERSEGHY, D. & LI, J. (2005): The CCCma third generation atmospheric general circulation model. CCCma Internal Reports, Canadian Centre for climate Moelling and Analysis, University of Victoria (Canada).

MEEHL, G., ARBLASTER, J. & TEBALDI, C. (2005): Understanding future patterns of increased precipitation intensity in climate simulations. In: *Geophysical Research Letters*, vol. 32.

MEEHL, G., et al. (2007): Global Climate Projections. In: SOLOMON, S., QIN, D., MANNING, M., CHEN, Z., MARQUIS, M., AVERYT, K., TIGNOR, M. & MILLER, H. (eds.): In: Climate Change 2007: The Physical Science Basis. Contribution of Working Group I to the Fourth Assessment Report of the Intergovernmental Panel on Climate Change. Cambridge University Press, Cambridge, Unitd Kingdom and New York, USA.

MERKEL, U. & LATIF, M. (2002): A high resolution AGCM study of the El Nino impact on the Northern Atlantic/European sector. In: *Geophysical Research Letters*, vol. 29.

MOBERG, A. et al. (2006): Indices for daily temperature and precipitation extremes in Europe analyzed for the period 1901-2000. In: *Journal of Geophysical Research*, vol. 111.

NAKICENOVIC, N. et al. (2000): Special Report on Emission Scenarios: A Special Report of IPCC Working Group III. 599pp. Cambridge University Press, New York.

NEELIN, J, MÜNNICH, M., SU, H., MEYERSON, J. & HOLLOWAY, C. (2006): Tropical drying trends in global warming models and observations. In: *Proceedings of the National Academy of Sciences*, vol. 103, pp. 6110-6115.

NEW, M., HULME, M. & JONES, P. (1999): Representing twentieth-century space time climate variability. Part I: development of a 1961-1990 mean

monthly terrestrial climatology. In: *Journal of Climatology*, vol. 12, pp. 829-856.

NEW, M., HULME, M. & JONES, P. (2000): Representing twentieth-century space time climate fileds. Part II: development of a 1901-1996 mean monthly terrestrial climatology. In: *Journal of Climatology*, vol. 13, pp. 2217-2238.

NIKULIN, G., KJELLSTRÖM, E., HANSSON, U., STRANDBERG, G. & ULLERSTIG, A. (2011): Evaluation and future projections of temperature, precipitation and wind extremes over Europe in an ensemble of regional climate simulations. In: *Tellus*, vol. 63, pp. 41-55.

NISSEN, K., LECKEBUSCH, G., PINTO, J., RENGGLI, D., ULBRICH, S. & ULBRICH, U. (2010): Cyclones causing Wind Storms in the Mediterranean: Characteristics, Trends and Links to large-scale Patterns. In: *Natural Hazards and Earth System Sciences*, vol. 10, pp. 1379-1391.

NOGAJ, M., YIOU, P., PAREY, S., MALEK, F. & NAVEAU, P. (2006): Amplitude and frequency of temperature extremes over the North Atlantic region. In: *Geophysical Research Letters*, vol. 33.

NORRANT C. & DOUGUEDROIT, A. (2006): Monthly and daily precipitation trends in the Mediterranean (1950-2000). In: *Theoretical and Applied Climatology*, vol. 83, pp. 89-106.

NORTHROP, P (2010): Using statistics to assess climate uncertainty. Presentation, given on 15th of July 2010 at the IMSC (International Meetings on Statistical Climatology); Session1; Edinburgh.

OVERLAND, J. & WANG, M. (2005): The arctic climate paradox: The recent decrease of the Arctic Oscillation. In: *Geophysical Research Letters*, vol. 32.

PAETH, H. (2007): Klimamodellsimulationen. In: ENDLICHER, W. & GERSTENGARBE, F.-W. (eds.): *Der Klimawandel – Einblicke, Rückblicke, Ausblicke*. Potsdam-Institut für Klimafolgenforschung e.V., Berlin-Potsdam, pp. 1-16.

PAETH, H., BORN, K., GIRMES, R., PODZUN, R., JACOB, D. (2009): Regional climate change in tropical and northern Africa due to greenhouse forcing and land use changes. In: *Journal of Climatology*, vol. 11, pp. 114-132.

PAETH, H. & DIEDERICH, M. (2010): Postprocessing of simulated precipitation for impact research in West Africa. Part II: A weather generator for daily data. In: *Climate Dynamics*, vol. 36, pp. 1337-1348.

PAETH, H. & HENSE, A. (2001): Signal analysis of the atmospheric mean 500/1000hPa temperature north of 55°N between 1949 and 1994. In: *Climate Dynamics*, vol. 18, pp. 345-358.

PAETH, H. & HENSE, A. (2002): Sensitivity of climate change signals deduced from multi-model Monte Carlo experiments. In: *Climate Research*, vol. 22, pp. 189-202.

PAETH, H. & MANNIG, B. (2013): On the added value of regional climate modelling in climate change assessment. In: *Climate Dynamics*, accepted.

PAETH, H. & POLLINGER, F. (2010): Enhanced evidence in climate models for changes in extratropical atmospheric circulation. In: *Tellus*, vol. 62a, pp. 647-660.

PAETH, H., HENSE, A., GLOWIENKA-HENSE, R., VOSS, R. & CUBASCH, U. (1999): The North Atlantic Oscillation as an indicator for greenhouse-gas induced regional climate change. In: *Climate Dynamics*, vol. 15, pp. 953-960.

PAL, J., GIORGI, F. & BI, X. (2004): Consistency of recent European summer precipitation trends and extremes with future regional climate projections. In: *Geophysical Research Letters*, vol. 31.

PAREDES, D., TRIGO, R., GARCIA-HERRERA, R. & TRIGO, I. (2006): Understanding Precipitation Change in Iberia in Early Spring: Weather Typing and Storm-Tracking Approaches. In: *Journal of Hydrometeorology*, vol. 7, pp. 101-113.

PARRY, M. et al. (2000). Assessment of potential effects and adaptations for climate change in Europe. The Europe ACACIA project. Jackson Environment Institute, University of Norwich, UK, 320 pp.

PAXIAN, A., HERTIG, E., VOGT, G., SEUBERT, S., JACOBEIT, J. & PAETH, H. (2011): Greenhouse gas related predictability of regional climate model trends in the Mediterranean area. In*: International Journal of Climatology*, in press.

PAXIAN, A., HERTIG, E., SEUBERT, S., VOGT, G., JACOBEIT, J. & PAETH, H. (2013): Comparative methodical assessment of present-day and future Mediterranean precipitation extremes. In: *Climate Dynamics*, submitted.

PINO,C., LIONELLO, P. & GALATI, M. (2010): Characteristics and present Trends of Wave Extremes in the Mediterranean Sea. In: *Geophysical Research Abstracts*, vol.12, EGU 2010-5984-1.

POPE, V., GALLANI, M., ROWNTREE, P. & STRATTON, R. (2000): The impact of new physical paramtrizations in the Hadley Centre climate model: HadAM3. In: *Climate Dynamics*, vol. 16, pp. 123-146.

POUMADERE, M., MAYS, C., LE MER, S. & BLONG, R. (2005): The 2003 Heat wave in France: Dangerous Climate Change Here and Now. In: *Risk Analysis*, vol.25, no. 6, pp. 1483-1493.

POZO-VAZQUEZ, D., ESTEBAN-PARRA, M., RODRIGO, F. & CASTRO-DIEZ, Y. (2001): A study of NAO variability and its possible non-linear influences on European surface temperature. In: *Climate Dynamics*, vol. 17, pp. 701-715.

POZO-VAZQUEZ, D., GAMIZ-FORTIS, S., TOVAR-PESCADOR, J., ESTEBAN-PARRA, M. & CASTRO-DIEZ, Y. (2005): El Nino - Southern Oscillation Events and associated European Winter Precipitation Anomalies. In: *International Journal of Climatology*, vol. 25, pp. 17-31.

RAICICH, F., PINARDI, N. & NAVARRA, A. (2003): Teleconnections between Indian Monsoon and Sahel Rainfall and the Mediterranean. In: *International Journal of Climatology*, vol. 23, pp. 173- 186.

RANDALL, D. et al. (2007): Climate Models and their Evaluation. In: SOLOMON, S., QIN, D., MANNING, M., CHEN, Z., MARQUIS, M., AVERYT, K., TIGNOR, M. & MILLER, H. (eds.): In: Climate Change

2007: The Physical Science Basis. Contribution of Working Group I to the Fourth Assessment Report of the Intergovernmental Panel on Climate Change. Cambridge University Press, Cambridge, Unitd Kingdom and New York, USA.

RÄISÄNEN, J., HANSSON, U., ULLERSTIG, A., DÖSCHER, R., GRAHAM, L., JONES, C., MEIER, H., SAMUELSSON, P. & WILLEN, U. (2004): European climate in the late twenty-first century: regional simulations with two driving global models and two forcing scenarios. In: *Climate Dynamics*, vol. 22, pp. 13-31.

REIFEN, C. & TOUMI, R. (2009): Climate projections: Past performance no guarantee of future skill?. In: *Geophysical Research Letters*, vol. 36.

RODO, X. (2001): Reversal of three global atmospheric fields linking changes in SST anomalies in the Pacific, atlantic and Indian oceans at tropical latitudes and midlatitudes. In: *Climate Dynamics*, vol. 18, pp. 203-217.

RODRIGO, F. (2010): Changes in the probability of extreme daily precipitation observed from 1951 to 2002 in the Iberian Peninsula. In: *International Journal of Climatology*, vol. 30, pp. 1512-1525.

RODRIGUEZ-PUBLA, C., ENCINAS, A., GARCIA-CASADO, L. & NIETO, S. (2010): Trends in warm days and cold nights over the Iberian Peninsula: relationships to large-scale variables. In: *Climatic Change*, vol. 100, pp. 667-684.

ROECKNER, E. et al. (2003): The Atmospheric General Circulation Model ECHAM5. Technical Report. Max-Planck Institute für Meteorologie Hamburg (Germany).

ROTHER, K. (1993): Der Mittelmeerraum. B. G. Teubner, Stuttgart.

ROWELL, D. & JONES, R. (2006): Causes and uncertainty of future summer drying over Europe. In: *Climate Dynamics*, vol. 27, pp. 281-299.

RÖTTER, R., & VAN DE GEIJN, S. (1999): Climate change effects on plant growth, crop yield and livestock. In: *Climate Change*, vol. 43, pp. 651–681.

RUSSELL, G., MILLER, J. & RIND, D. (1995): A coupled atmosphere-ocean model for transient climate change studies, Atmosphere-Ocean, vol. 33, pp. 683-730.

SALAS-MELIA, D., CHAUVIN, F., DEQUE, M., DOUVILLE, H., GUEREMY, J., MARQUET, P., PLANTON, S., ROYER, J. & TYTECA, S. (2005): Description and validation of the CNRM-CM3 global coupled model. Centre National de Recherches Meteorologiques, Meteo-France, Toulouse.

SANCHEZ, E., GALLARDO, C., GAERTNER, M., ARRIBAS, A. & CASTRO, M. (2004): Future climate extreme events in the Mediterranean simulated by a regional climate model: a first approach. In: *Global and Planetary Change*, vol. 44, pp. 163-180.

SCHEFFE, H. (1959): The analysis of variance. John Wiley & Sons, New York.

SCHERRER, S., CROCI-MASPOLI, M., SCHWIERZ, C. & APPENZELLER, C. (2006): Two-dimensional Indices of Atmospheric Blocking and their

Statistical Relationship with Winter Climate Patterns in the Euro-Atlantic Region. In: *International Journal of Climatology*, vol. 26, pp. 233- 249.

SCHMIDT, G. et al. (2006): Present-Day Atmospheric Simulations Using GISS ModelE: Comparison to In Situ, Satellite, and Reanalysis Data. In: *Journal of Climate*, vol. 19, pp. 153-192.

SCHÖNWIESE, C.-D. (2006): Praktische Statistik für Meteorologen und Geowissenschaftler. Gebrüder Bornträger, Berlin-Stuttgart.

SCOCCIMARO, E., GUALDI, S., FOGLI, P., MANZINI, E., GREZIO, A. & NAVARRA, A. (2007): INGV-SXG: A Coupled Atmosphere Ocean Sea-Ice General Crculation Model. Technical Report. Centro Euro-Mediterranea Per I Cambiamenti Climatici (Italy).

SEUBERT, S. (2010): Telekonnektionen des Niederschlags im Mittelmeerraum zur Zirkulation in den Tropen. PhD Thesis, University of Augsburg (Germany).

SHINDELL, D., MILLER, R., SCHMIDT, G. & PANDOLFO, L. (1999): Simulation of recent northern winter climate trends by greenhous-gas forcing. In: *Nature*, vol. 399, pp. 452-455.

SILLMANN, J. & ROECKNER, E. (2008): Indices for extreme events in projections of anthropogenic climate change. In: *Climate Change*, vol. 86, pp. 83-104.

SIMOLO, C., BRUNETTI, M., MAUGERI, M., NANNI, T. & SPERANZA, A. (2010): Understanding climate change-induced variations in daily temperature distributions over Italy. In: *Journal of Geophysical Research*, vol. 115.

SOMOT, S. (2005): Modelisation Climatique Du Bassin Mediterraneen: Variabilite et Scenarios de Changement Climatique. PhD Thesis, University of Toulouse (France).

SON, S.-W., POLVANI, L., WAUGH, D., AKIYOSHI, H., GARCIA, R., KINNISON, D., PAWSON, S., ROZANOV, E., SHEPHERD, T. & SHIBATA, K. (2008): The impact of Stratospheric Ozone Recovery on the Southern Hemisphere Westerly Jet. In: *Science*, vol. 320, pp. 1486-1489.

STEPPELER, J., DOMS, G., SCHÄTTLER, U., BITZER, H., GASSMANN, A., DAMRATH, U. & GREGORIC G. (2003): Meso-gamma scale forecasts using the nonhydrostatic LM. In: *Meteorology and Atmospheric Physics*, vol. 82, pp.75-96.

STOTT, P. & TETT, S. (1998): Scale-Dependant Detection of Climate Change. In: *Journal of Climate*, vol. 11, pp. 3282-3294.

STOTT, P., STONE, D. & ALLEN, M. (2004): Human contribution to the European heatwave of 2003. In: *Nature*, vol. 432, pp. 610-614.

STOTT, P., TETT, S., JONES, G., ALLEN, M., MITCHELL, J. & JENKINS, G. (2000): External control of 20th century temperature by natural and anthropogenic forcings. In: *Science*, vol. 290, pp. 2133-2137.

STOTT, P., JONES, G., LOWE, J., THORNE, P, DURMAN, C., JOHNS, T. & THELEN, J.-C. (2006): Transient Climate Simulations with the HadGEM1 Climate Model: Causes of Past Warming and Future Climate Change. In: Journal of Climate, vol. 19, pp. 2763-2782.

SUMNER, G., ROMERO, R., HOMAR, V., RAMIS, C., ALONSO, S. & ZORITA, E. (2003): An estimate of the effects of climate change on the rainfall of Mediterranean Spain by the late twenty first century. In: *Climate Dynamics*, vol. 20, pp. 789-805.

TEBALDI, C., HAYHOE, K., ARBLASTER, J. & MEEHL, G. (2006): Going to the extremes – An intercomparison of model-simulated historical and future changes in extreme events. In: *Climate Change*, vol. 7, pp. 185-211.

TETT, S., STOTT, P., ALLEN, M., INGRAM, W. & MITCHELL, J. (1999): Causes of twentieth-century temperature change near the Earth´s surface. In: *Nature*, vol. 399, pp. 569-572.

TORETI, A., DESIATO, F., FIORAVANTI, G. & PERCONTI, W. (2010): Seasonal Temperatures over Italy and their Relationship with low-frequency atmospheric Circulation Patterns. In: *Climate Change*, vol. 99, pp. 211-227.

TRENBERTH, K. & HOAR, T. (1997): El nino and climate change. In: *Geophysical Research Letters*, vol. 24, pp. 3057-3060.

TRENBERTH, K. et al. (2007): Observations: Surface and Atmospheric Climate Change, In: SOLOMON, S., QIN, D., MANNING, M., CHEN, Z., MARQUIS, M., AVERYT, K., TIGNOR, M. & MILLER, H. (eds.): Climate Change 2007: The Physical Science Basis. Contribution of Working Group I to the Fourth Assessment Report of the Intergovernmental Panel on Climate Change. Cambridge University Press, Cambridge, United Kingdom and New York, USA.

TRIGO, R. et al. (2006): Relations between Variability in the Mediterranean region and Mid-Latitude Variablity. In: LIONELLO, P. MALANOTTE-RIZZOLI, P. & BOSCOLO, R. (eds.): Mediterranean Climate Variability. Elsevier, Amsterdam, pp. 179-226.

TRIGO, R. & PALUTIKOF, J. (2001): Precipitation Scenarios over Iberia: A Comparison between Direct GCM Output and Different Downscaling Techniques. In*: Journal of Climate*, vol. 14, pp. 4422-4446.

TRIGO, I., BIGG, G. & DAVIES, T. (2002). Climatology of cyclogenesis mechanisms in the Mediterranean. In: *Monthly Weather Review*, vol. 130, pp. 549–569.

TRIGO, R., OSBORN, T. & CORTE-REAL, J. (2002): The North Atlantic Oscillation Influence on Europe: Climate Impacts and Associated Physical Mechanisms. In: *Climate Research*, vol. 20, pp. 9-17.

TSIMPLS, M., & JOSEY, S. (2001): Forcing of the Mediterranean Sea by atmospheric oscillations over the North Atlantic. In: *Geophysical Research Letters*, vol. 28, pp. 803–806.

ULBRICH et al. (2012): Climate of the Mediterranean: Synoptic Patterns, Temperature, Precipitation, Winds and their Extremes. In: LIONELLO, P. (ed.): The climate of the Mediterranean Region. Elsevier, London, pp. 301-346.

ULBRICH, U., MAY, W., LI, L., LIONELLO, P., PINTO, J.G. & SOMOT, S. (2006): The Mediterranean Climate Change under Global Warming. In: LIONELLO, P. MALANOTTE-RIZZOLI, P. & BOSCOLO, R. (eds.): Mediterranean Climate Variability. Elsevier, Amsterdam, pp. 319-413.

UPPALA, S. et al. (2005): The ERA-40 re-analysis. In: *Quaterly Journal of the Royal Meteorological Society*, vol. 131, pp. 2961-3012.

VAN DEN BESSELAAR, E., KLEIN TANK, A. & VAN DER SCHRIER, G. (2010): Influence of circulation types on temperature extremes in Europe. In: *Theoretical and Applied Climatology*, vol. 99, pp. 431-439.

VON STORCH, H. & ZWIERS, F., W. (1999): Statistical Analysis in Climate Research. Cambridge University Press, Cambridge.

VON STORCH, H., GÜSS, S. & HEIMANN, M. (1999): Das Klimasystem und seine Modellierung – Eine Einführung. Springer Verlag, Berlin, Heidelberg

WANG, B., WAN, H., JI, Z., ZHANG, X., YU, R., Yu, Y. & LIU, H. (2004): Design of a new dynamical core for global atmospheric models based on some efficient numerical methods. In: *Science in China*, vol. 47, pp.4-27.

WASHINGTON et al. (2000): Parallel climate model (PCM) control and transient simulations. In: *Climate Dynamics*, vol. 16, pp. 755-774.

WEHNER, M. (1998): Determination of the Sampling Size of AGCM Ensemble Simulation. PCMDI Report No.47. University of California, Livermore, USA.

WEISCHET, W. & ENDLICHER, W. (2000): Regionale Klimatologie Teil 2 – Die Alte Welt. B. G. Teubner, Stuttgart, Leipzig.

WILBY, R., WIGLEY, M., CONWAY, D., JONES, P., HEWITSON, B., MAIN, J. & WILKS (1998): Statistical downscaling of general circulation model output: A comparison of methods. In: *Water Resources Research*, vol. 34, no.11, pp. 2995-3008.

XOPLAKI, E. (2002): Climate variability over the Mediterranean. PhD Thesis, University of Bern (Switzerland).

XOPLAKI, E., MAHERAS, P. & LUTERBACHER, J. (2001): Variability of climate in meridional balkans during the periods 1675–1715 and 1780–1830 and its impact on human life. In: *Climate Change*, vol. 48, pp. 581–615.

XOPLAKI, E., GONZALEZ-ROUCO, J., LUTERBACHER, J. & WANNER, H. (2004): Wet season Mediterranean precipitation variability: influence of large-scale dynamics and trends. In: *Climate Dynamics*, vol. 23, pp. 63-78.

YIOU, P. & NOGAJ, M. (2004): Extreme climatic events and weather regimes over the North Atlantic: When and where?. In: *Geophysical Research Letters*, vol. 31.

YUKIMOTO, S., NODA, A., UCHIYAMA, T., KUSUNOKI, S. & KITOH, A. (2006): Climate changes of the twentieth through twenty-first centuries simulated by the MRI-CGCM2.3. Technical Report. Meteorological Research Institute, Tsukuba (Japan).

ZIV, B. (2001): A subtropical rainstorm associated with a tropical plume over Africa and the Middle-East. In: *Theoretical and Applied Climatology*, vol. 69, pp. 91-102.

ZIV, B., SAARONI, H. & ALPERT, P. (2004): The Factors Governing the Summer Regime of the Eastern Mediterranean. In: *International Journal of Climatology*, vol. 24, pp. 1859- 1871.

Acknowledgements

Danksagung

Ein großer Dank gebührt vor allem meinem Doktorvater Prof. Heiko Paeth, dem keine Frage zu schwierig war und der immer eine Idee hatte, auftretenden Problemen zu begegnen. Ich danke Dir Heiko, dass Du auch immer eine schützende Hand über unsere Arbeitsgruppe gehalten hast und auch kameradschaftlich ein super Chef warst. Ich hoffe, dass sich die Geduld (dazu gehört auch das Bereitstellen eines Arbeitsplatzes nach der Vertragslaufzeit – was nicht selbstverständlich ist), die Du mir entgegengebracht hast, sich auszahlt.

Weiteren Dank möchte ich meinem Zweitprüfer an Herrn Prof. Jacobeit an der Universität Augsburg richten, dem mindestens die gleiche Geduld zu bescheinigen ist, und ohne den das ganze Projekt überhaupt nie entstanden wäre und auch nicht funktioniert hätte.

Im selben Projekt führte Dr. Andreas Paxian eine parallel laufende Arbeit durch. Lieber Andy, ich habe die Zeit der Zusammenarbeit mit Dir in unserem Projekt sehr genossen. Es war mir eine Freude den langen gemeinsamen Werdegang von der LMU bis über die Universität Würzburg mit Konferenz- und Tagungsreisen mit Dir zu teilen. Auch privat warst und bleibst Du ein guter Freund.

Ein anderer Teil des Projekts wurde an der Universität Augsburg von Dr. Elke Hertig und Dr. Stefanie Seubert durchgeführt. Auch bei Euch möchte ich mich für die angenehme Atmosphäre und den aufmunternden sowie fachlichen Ratschlägen herzlich bedanken! Ich wünsche Euch weiterhin alles Gute. Auf dass wir weiterhin in Kontakt bleiben.

Als einer der „ewigen" Zimmernachbarn auch Dir ein herzliches Dankeschön, lieber Sebastian. Gerne denke ich an die Zeiten des Unfugs zurück, den wir veranstaltet haben. Als sehr guter Freund bleibst Du mir erhalten!

Weiterhin möchte ich der Klimagruppe an der Universität Würzburg meinen Dank aussprechen.

Felix: danke für Deine Hilfen und Deiner Freundschaft. Ich kann mit Sicherheit sagen, dass ohne Deine fachlichen Hinweise das alles überhaupt nicht funktioniert hätte.

Birgit: als beste Freundin in Würzburg; Dir an dieser Stelle ein ganz besonderes Dankeschön!

Desweiteren vielen Dank auch an die restlichen Kollegen der Würzburger Truppe: Christian Steger (für die genialen Abende), Daniel Schwindt (für die Musik), Doro Schill (für die IT), Daniel Jäger (fürs Fußballspielen und das Fachsimpeln). Und schließlich sind da noch Fritschi, Jens, Anja, Christian Büdel, Angela, Tobi Ullmann und Tobi Rödder, Jürgen, Sabine, Christopher, Michael, Julian, Günni, Chrischne, Sylvia, Cornelius, Ferdi, Patrick, Marius, Julius, Clemens und Katharina, Christina, Rike, Melli, George und Lorenz. Danke für die tolle Zeit!!! Ich werde Euch vermissen.

Und auch wenn am Ende alles relativ übergangslos von statten ging, so kann ich doch mit reinem Gewissen behaupten, dass diese Arbeit zu einem Teil meines Lebens geworden ist und auch einen geraumen Teil davon eingenommen hat. Hierbei möchte ich mich besonders bei meinen Liebsten bedanken, die mich auf diesem Weg begleitet haben. Allen voran stehen da meine lieben Eltern Marianne und Klaus Vogt, die nicht nur an mich glaubten, sondern dies auch bezeugten, indem sie mich in schwierigen Phasen finanziell und aufmunternd unterstützten und eine Heimat für mich bereithielten und mich dort immer mit offenen Armen empfingen.

Außerdem meine Freundin Kathrin die mit einer Engelsgeduld auch die schwierigen Zeiten mit ertragen hat.

Dafür, dass die guten Zeiten in der heimatlichen Vergangenheit nicht verloren gegangen sind, möchte ich noch meinem Münchner Freundeskreis ein paar Zeilen widmen. Von den Freunden der Kindheit, über die Schulzeit, über den Sport wie Skifahren und Fußball bis zu den Kommilitonen an der LMU kann ich mit Freude behaupten, dass mir sehr viele erhalten geblieben sind, auch wenn viele Wege räumlich wie beruflich in unterschiedliche Richtungen gegangen sind. Schön, dass Ihr da seid!

Ihr alle(!) wart mehr als nur einfache Arbeitskollegen. Mein Versprechen Euch gegenüber, diese Arbeit zu machen, war eine wichtige Motivation für mich, dies

alles auch wirklich durchzuziehen und zu einem annehmbaren Ende zu bringen.

Euch allen ist diese Arbeit gewidmet.

Publikationen

HERTIG, E., PAXIAN, A., VOGT, G., SEUBERT, S., PAETH, H. & JACOBEIT, J. (2012): Statistical and dynamical downscaling assessments of precipitation extremes in the Mediterranean area. In: *Meteorologische Zeitschrift*, vol. 21, pp. 61-77.

HERTIG, E., SEUBERT, S., PAXIAN, A., VOGT, G., PAETH, H. & JACOBEIT, J. (2013a): Changes of total versus extreme precipitation and dry periods until the end of the twenty-first century: statistical assessments for the Mediterranean area. In: *Theoretical and Applied Climatology*, vol. 111, pp.1-20

HERTIG, E., SEUBERT, S., PAXIAN, A., VOGT, G., PAETH, H. & JACOBEIT, J. (2013b): Statistical modeling of extreme precipitation for the Mediterranean area under future climate change. In: *International Journal of Climatology*, vol. 33.

PAXIAN, A., HERTIG, E., VOGT, G., SEUBERT, S., JACOBEIT, J. & PAETH, H. (2011): Greenhouse gas related predictability of regional climate model trends in the Mediterranean area. In*: International Journal of Climatology*, in press.

PAXIAN, A., HERTIG, E., SEUBERT, S., VOGT, G., JACOBEIT, J. & PAETH, H. (2013): Comparative methodical assessment of present-day and future Mediterranean precipitation extremes. In: *Climate Dynamics*, submitted.

SEUBERT, S., FERNANDEZ-MONTES, S., PHILIPP, A., HERTIG, E., JACOBEIT, J., VOGT, G., PAXIAN, A. & PAETH, H. (2013): Mediterranean climate extremes in synoptic downscaling assessments. In: *Theoretical Applied Climatology*, (accepted).